Julius-Maximilians-Universität

Würzburg

Synthesis and Investigation of Borylene Complexes: from Borylene Transfer to Borylene Catenation

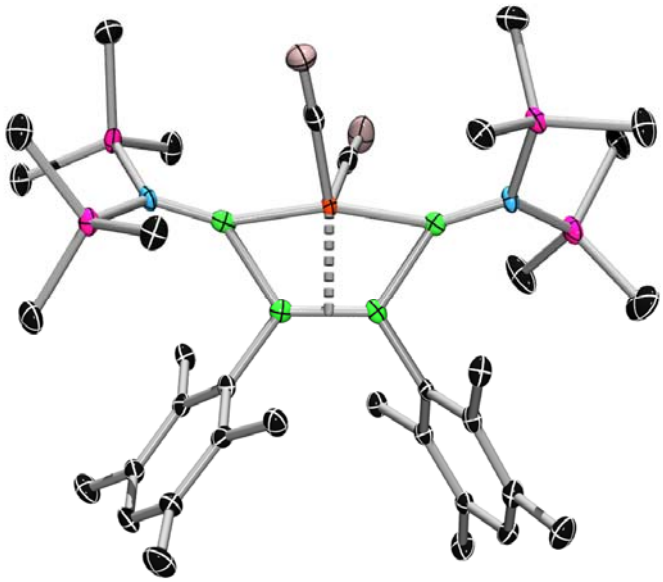

Dissertation zur Erlangung des naturwissenschaftlichen Doktorgrades

QING YE

Würzburg 2012

Synthesis and Investigation of Borylene Complexes: from Borylene Transfer to Borylene Catenation

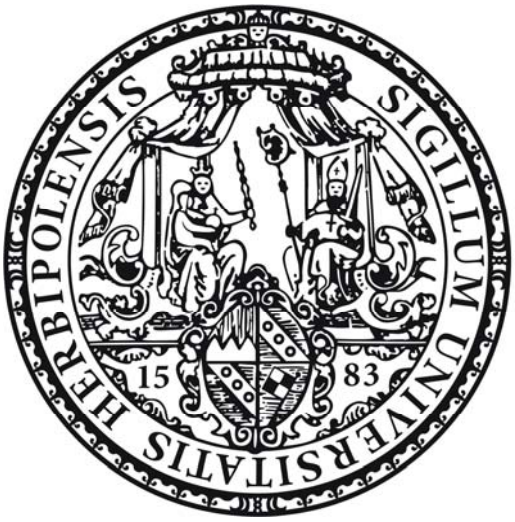

Dissertation zur Erlangung des
naturwissenschaftlichen Doktorgrades
der Julius-Maximilians-Universität Würzburg

vorgelegt von
Qing Ye
aus Jiangsu, China

Würzburg 2012

Eingereicht am: 29.03.2012
Bei der Fakultät für Chemie und Pharmazie.

1. Gutachter: Prof. Dr. Holger Braunschweig
2. Gutachter: Prof. Dr. Todd B. Marder
der Dissertation.

1. Prüfer: Prof. Dr. Holger Braunschweig
2. Prüfer: Prof. Dr. Todd B. Marder
3. Prüfer: Prof. Dr. Volker Engel
des öffentlichen Promotionskolloquiums.

Tag des öffentlichen Promotionskolloquiums: 11.06.2012

Doktorurkunde ausgehändigt am:

Meinen Eltern,
meiner lieben Frau Xiuyi,
und unserer süßen Tochter Jiaying.

"学而不思则罔，思而不学则殆。"

——孔子

To learn without thinking risks to be blind,

while to think without learning risks to be impractical.

CONFUCIUS

Die Experimente zur vorliegenden Arbeit wurden in der Zeit von April 2008 bis Dezember 2011 im Institut für Anorganische Chemie der Julius-Maximilians-Universität Würzburg unter Anleitung von Herrn Professor Dr. Holger Braunschweig durchgeführt.

Die vorliegende Arbeit wurde auszugsweise veröffentlicht unter:

- **Borylene-based functionalization of Pt-alkynyl complexes by photochemical borylene transfer from [$(OC)_5Cr=BN(SiMe_3)_2$]**

H. Braunschweig, Q. Ye, K. Radacki, *Chem. Commun.* **2009**, 6979–6981.

- **Borylene-based Functionalization of Iron-alkynyl-σ-complexes and Stepwise Reversible Metal-boryl-to-borirene Transformation: Synthesis, Characterization and DFT Studies**

H. Braunschweig, Q. Ye, K. Radacki, P. Brenner, G. Frenking, S. De, *Inorg. Chem.* **2011**, *50*, 62–71.

- **Reactivity of a Platinum-substituted Borirene**

H. Braunschweig, Q. Ye, K. Radacki, T. Kupfer, *Dalton Trans.* **2011**, *40*, 3666–3670.

- **Synthesis of 1-Aza-2-borabutatriene Rhodium Complexes by Thermal Borylene Transfer from [$(OC)_5Mo=BN(SiMe_3)_2$]**

H. Braunschweig, Q. Ye, A. Damme, K. Radacki, T. Kupfer, J. Wolf, *Angew. Chem.* **2011**, *123*, 9634–9638; *Angew. Chem. Int. Ed.* **2011**, *50*, 9462–9466.

- **High Yield Synthesis of a Neutral and Carbonyl-rich Terminal Arylborylene Complex**

H. Braunschweig, Q. Ye, K. Radacki, *Chem. Commun.* **2012**, *48*, 2701–2703.

- **Homocatenation of Boron on a Transition Metal – Towards One-Dimensional Polyboranes**

H. Braunschweig, Q. Ye, A. Vargas, R. D. Dewhurst, K. Radacki, A. Damme, *Nat. Chem.* **2012**, DOI: 10.1038/NCHEM.1379.

- **Borylene Transfer from an Iron-Bis(borylene) Complex: Synthesis of 1,4-Diboracyclohexadiene and 1,4-Dibora-1,3-Butadiene Complexes**

H. Braunschweig, Q. Ye, K. Radacki, A. Damme, *Angew. Chem.* **2012**, *124*; *Angew. Chem. Int. Ed.* **2012**, *51*, accepted.

Mein besonderer Dank gilt

Professor Dr. Holger Braunschweig nicht nur für sein bemerkenswertes Vertrauen, dass er mir ermöglichte, in seinem Arbeitskreis unter perfekten Bedingungen meine Doktorarbeit anzufertigen, sondern auch für die interessante Themenstellung, stets vorhandene Diskussionsbereitschaft und endlosen Vorrat an tollen Ideen. Was für ein Glück!

Prof. Dr. Sundargopal Ghosh und *Dr. Carly Anderson*, die mir die Grundlagen dieser Arbeit vermittelt haben.

Prof. Dr. Ching-wen Chiu, der sehr intelligenten Chemikerin, für die umfangreichen und anregenden Diskussionen sowohl bezüglich chemischen als auch privaten Angelegenheiten, die mir ein gutes Gespür für die Chemie vermittelt haben.

Dr. Krzysztof Radacki, nicht nur für die Durchführung der zahlreichen Röntgenstrukturexperimente und ihrer Auswertung, sondern auch für die Betreuung bei der selbständigen Durchführung von quantenmechanischen Rechnungen. Es hat auch viel Spass gemacht, mit dir auf die Tischtennisplatte zu "klopfen". Danke Kris!

Daniela Gamon, *Johannes Wahler* und *Christian Hörl* für die sehr schöne und lustige Atmosphäre, die tollen Arbeitsbedingungen im Labor 220 sowie die großartige Hilfsbereitschaft und Unterstützung bei allen Arten von Problemen. Danke für die wunderschöne Zeit in den letzten Jahren mit euch im 220!

Dr. Justin Wolf nicht nur für die ausgezeichnete Einführung in die Rh-Chemie und die vielen wertvollen Tipps, sondern auch für die Aufnahme der GC-MS-Spektren.

Dr. Carsten Kollann，*Dr. Rian Dewhurst* und *Dr. Ivo Krummenacher* für ihr stetiges Interesse und ihre Diskussionsbereitschaft.

Dr. Rian Dewhurst, *Dr. Ivo Krummenacher*, *Dr. Christopher Tate* und *Dr. Alfredo Vargas* für die kritische Durchsicht und zuverlässige Korrektur dieses Manuskripts.

Dr. Alfredo Vargas und *Alexander Damme* für die Durchführung quantenchemischer Rechnungen sowie deren lehrreiche Interpretation.

Prof. Dr. Gernot Frenking, *Dr. Susmita De* (Universität Marburg) für die theoretischen Untersuchungen zur reversiblen Umwandlung von Eisen-Boryl- in Eisen-Boriren-Komplexe.

Benedikt Wennemann und *Yang Shi*, die mich im Rahmen ihres F-Praktikums zuverlässig und erfolgreich unterstützt haben.

Dr. Thomas Kupfer, *Alexander Damme* und *Peter Brenner* für die Durchführung der Röntgenstrukturanalysen. *Sascha Stellwag* für die Aufnahme der IR-Spektren und *Daniela Gamon* für die Aufnahme der UV-Vis-Spektren.

Kai Hammond und *Sascha Stellwag* für die zuverlässige Synthese einiger Eduktverbindungen.

Dr. Rüdiger Bertermann und *Marie-Luise Schäfer* für den NMR-Service, *Liselotte Michels* und *Sabine Timmroth* für die Durchführung der Elementaranalysen sowie *Berthold Fertig* für die Anfertigung und Reparatur mancher Glasgeräte.

Den derzeitigen und ehemaligen Mitarbeitern des Arbeitskreises Braunschweig für die großartige Arbeitsatmosphäre und die stets sehr gute Zusammenarbeit in den letzten Jahren.

Ein besonderer Dank gilt meinen *Eltern*, die mir dieses Studium ermöglicht und mich immer unterstützt haben.

Abschließend möchte ich speziell meiner Frau *Xiuyi* danken. Sie hat mich während der gesamten Studien- und Promotionszeit, auch in den schwierigen Phasen meines Lebens immer liebevoll unterstützt und ermutigt. Ohne ihren Rückhalt wäre das Studium nicht möglich gewesen. Hierbei noch ein Küsschen für unsere süße Tochter *Jiaying*, die uns das Leben in Deutschland wunderschön gestaltet hat. Alles Liebe!

Abbreviations:

9-BBN	9-borabicyclo-[3.3.1]nonane
atm	atmospheres (pressure)
Ar^f_4	3,5-bis(triflurомethyl)phenyl-
bs	broad singlet
Bu	butyl
COD	1,5-cyclooctadiene
Cp	cyclopentadienyl
Cp*	pentamethylcyclopentadienyl
Cy	cyclohexyl
δ	chemical shift
d	doublet
d, h, min	day, hour, minute
DCC	*N,N′*-dicyclohexyl-carbodiimide
DFT	density functional theory
Dipp	2,6-diisopropylphenyl
dppm	bis(diphenylphosphino)methane
Dur	2,3,5,6-tetramethylphenyl
EI	electron ionization
equiv	molar equivalents
Et	ethyl
Fig.	figure
h	hour
hυ	photolysis
HOMO	highest occupied molecular orbital
*I*Me	*N,N′*-bis(methyl)imidazol-2-ylidene
*I*Mes	*N,N′*-bis(2,4,6-trimethylphenyl)imidazol-2-ylidene
*i*Pr	isopropyl
IR	infrared
J	coupling constant
L	ligand
LUMO	lowest unoccupied molecular orbital
m	multiplet

M	metal
$[M^+]$	molecule ion
Me	methyl
Mes	2,4,6-trimethylphenyl
MS	mass spectrometry
min	minute
NBO	natural bond order
NHC	N-heterocyclic carbene
NMR	nuclear magnetic resonance
OTf	trifluoromethanesulfonate
Ph	phenyl
pic	picoline
RT	room temperature
s	singlet
t	triplet
*t*Bu	*tert*-butyl
THF	tetrahydrofuran
TMP	2,2,6,6-tetramethyl-piperidine
UV-vis	ultraviolet-visible spectroscopy

1 Introduction

Prussian blue (or *Berliner Blau*) and the alkylzinc complexes prepared by Frankland in 1849 are considered the earliest known synthetic examples of complexes containing transition metal-carbon two-center bonds.[1,2] In addition to carbon, this classical bonding situation has been very well established for transition metal complexes of silicon or heavier Group 13 elements for decades.[3-7] In comparison, transition metal boryl complexes containing metal-boron two-center bonds were first proposed in 1963[8] and structurally confirmed in 1990 by Baker, Marder and Merola.[9,10] Since then, the number of compounds with electron-precise transition metal-boron single bonds has steadily increased. Due to the electrophilic character of boron, M-B bonds for the electron-poor transition metals of groups 3 and 4 (including lanthanides and actinides) were unknown until the very recent report of boryl complexes of Ti and Hf.[11]

Since the late 1990s, transition metal complexes of boron have been classified according to the coordination number of the boron atom and the number of metal-boron bonds. As a result, borane (**I**), boryl (**II**), bridging borylene (**III**) and terminal borylene (**IV**) complexes were defined (Fig. 1 above). Moreover, the high Lewis-acidity of the boron center allowed the synthesis of Lewis base adducts of boryl (**IIa**), bridging borylene (**IIIa**), and terminal borylene complexes (**IVa**) (Fig. 1 below).

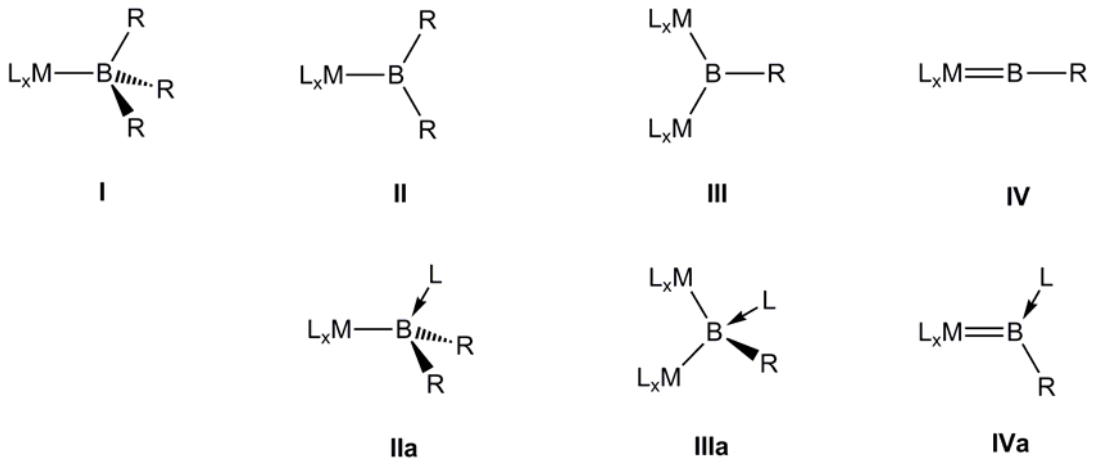

Fig. 1 Coordination modes of transition metal complexes of boron.

Borane complexes (**I**) can be described as Lewis acid–base adducts of acidic boranes BR_3 and basic transition-metal complexes resulting in a fourfold coordination of the boron atom. In

contrast, boryl transition metal complexes **II** contain a terminal σ-bound boryl group BR_2, and the coordination number of the boron atom is reduced to three. This class of complexes has attracted tremendous attention since the first description of catalytic hydroboration,[12] which was accomplished utilizing a rhodium catalyst. In the case of borylene transition metal complexes **III,** the borylene ligands :BR are either bridging between two metal centers (**III**) with three-coordinate boron, or terminal with formation of a metal-boron double bond (**IV**) and boron with the coordination number two. In the past decade, borylene chemistry has come into focus due to the close relationship to the isoelectronic carbonyl ligands in terms of bonding pattern and coordination modes.[13]

1.1 Borane complexes

In 1963 Shriver proposed a metal-boron dative bond in $[Cp_2WH_2(BF_3)]$ and $[Cp_2WH_2\{B(t\text{Bu})Cl_2\}]$, which were generated from the reaction between Lewis basic $[Cp_2WH_2]$ and Lewis acidic borane BF_3 or $t\text{BuBCl}_2$.[14] However, according to new investigations of these complexes around 30 years later by means of X-ray structure analysis and NMR spectroscopy, the presence of a W-B bond was refuted. Instead, the ionic complex $[Cp_2WH_3][BX_4]$ (X = F, Cl) or the zwitterionic complex $[\{\eta^5\text{-}C_5H_4\ (t\text{BuBCl}_2)\}CpWH_3]$ was generated.[15-17] Since the 1960s, a broad range of unsupported transition metal-borane complexes were reported.[18] However, the evidence for their chemical constitution was merely based on IR and NMR data. Among these, the reaction of $[NEt_4][CpFe(CO)_2]$ with BPh_3 provided the most plausible evidence for the formation of a M-B dative bond, i.e. the ^{11}B NMR signal at $\delta_B = -29$ is indicative of tetracoordinated boron.[19] In 1999, A. F. Hill *et al.* reported the first structurally characterized borane complex, $[(Ph_3P)Ru(CO)\{B(mt)_3\}]$ (**1**) (mt = methimazolyl) that is prepared according to Fig. 2. The tetrahedral arrangement at the boron center, as well as the short Ru-B separation of 2.16 Å confirmed the pronounced Ru-B interaction. The synthesis of osmium-analogue **2** was achieved a few years later.[20]

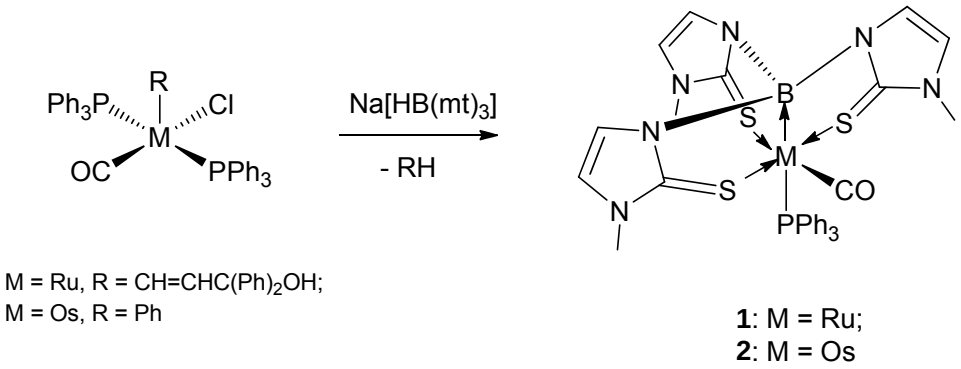

M = Ru, R = CH=CHC(Ph)$_2$OH;
M = Os, R = Ph

1: M = Ru;
2: M = Os

Fig. 2 Synthesis of the first structurally characterized borane complex $[(Ph_3P)Ru(CO)\{B(mt)_3\}]$ (**1**) and its osmium analogue **2**.

In the further studies, upon altering donor groups of proligands, such as sulfur, phosphorus and nitrogen, the scope of borane complexes has been significantly expanded, including Group 9 (Co[21], Rh[22], Ir[23]), 10 (Ni[24], Pd[24], Pt[25,26]) and 11 (Cu[24], Ag[24], Au[26]) metals, in which each boron atom is pyramidalized (to differing extents) with its three nonmetal substituents pointing away from the metal. Since a free borane has no free electrons and lacks appropriate orbitals for π-bonding with a fourth substituent, the electrons in the M-B 2-center-

bond can be thought to originate exclusively from the metal, thus recognizing the σ-character of the M-B bond.

1.2 Boryl complexes

Since the first structural authentication of metal boryl complexes **3** and **4** in 1990 (Fig. 3),[9,10] the ligand properties of boryls have been closely studies, thus revealing remarkably strong σ-donation abilities.[27-30]

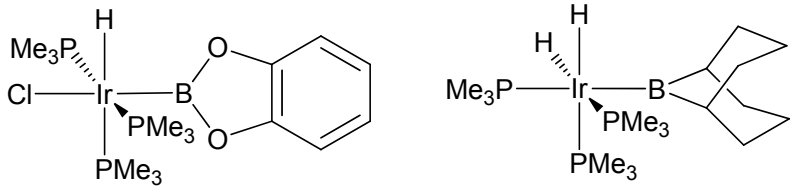

3 **4**

Fig. 3 First structurally characterized boryl complexes **3** and **4**.

The significant degree of π-backdonation was experimentally determined only recently by occupation of the vacant *p*-orbital of boron center in iron dihaloboryl complex [$CpFe(CO)_2BCl_2$] (**5**) by the Lewis base 4-methylpyridine and monitoring the change in the Fe-B linkage (Fig. 4).[31,32] Moreover, **6** exhibits carbonyl stretching bands in its IR spectrum at significantly lower frequencies (1976, 1916 cm^{-1}) than those of **5**, thus indicating the increased electron density at the iron center, as caused by a decrease in the strength of the Fe-B π-interaction.

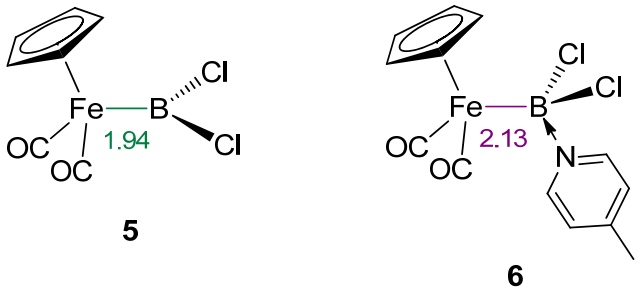

5 **6**

Fig. 4 Experimental evidence for Fe→B π backdonation by comparing the Fe-B bond lengths (Å) between **5** and its Lewis-base adduct **6**.

Furthermore, numerous studies have dealt with the synthesis and reactivity of those boryl ligands that are mainly coordinated to mid-transition metals. The oxidative addition of B-H, B-B, and B-E bonds (E=main-group element such as halogen and tin) to low-valent transition-metal complexes is the most common synthetic route to such compounds, and a variety of mono-, bis-, and tris(boryl) complexes were synthesized accordingly. In addition, salt-elimination reactions between anionic transition metal complexes and haloboranes or

halodiboranes(4) represent an important alternative synthetic pathway. More recently, the availability of both boryllithium[33,34] and borylmagnesium[33,35] species, which both exhibit the characterisitic reactivity of boryl anions, opened a new approach to boryl complexes by introducing the boryl moiety via nucleophilic attack and substitution of halides. In this manner, the first boryl complexes of group 11 (Cu, Ag, Au)[36,37] and group 4 (Ti, Hf)[38] metals were synthesized and characterized (Fig. 5).

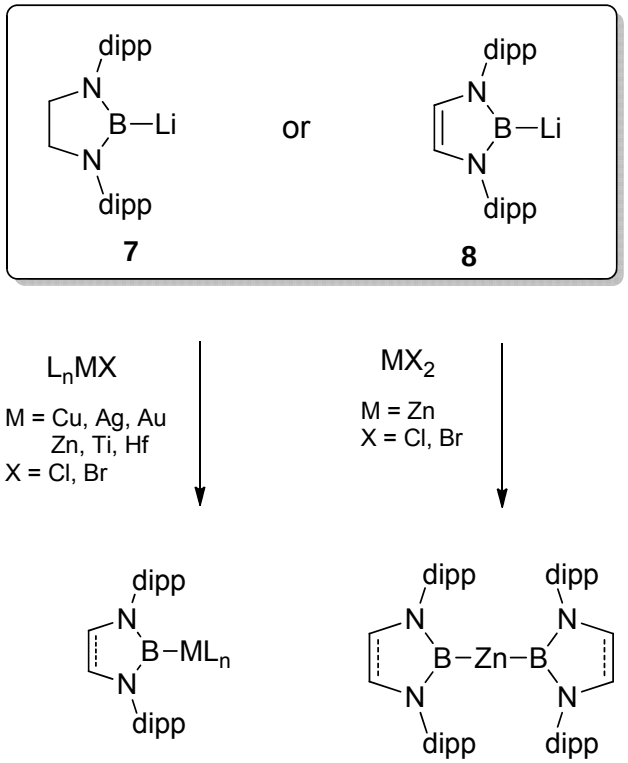

Fig. 5 Preparation of boryl complexes from boryl lithium reagents.

In addition, boryl complexes were involved as key reagents in the functionalization of unsaturated organic compounds by diboration[39-50], C-H[51,52] and C-F[53] bond activation, which underlines their importance.

In fact, the lability of the boryl ligand facilitates the aforementioned transition metal-mediated borylation process, but might also prevent its application in other functionalization reactions. Recently, stabilization of the boryl moiety was accomplished by its incorporation in tridentate ligand systems, yielding a range of boryl-based pincer complexes (Fig. 6).[54,55] The coordinatively unsaturated [PBP](hydrido)chloroiridium complex **9** was synthesized via a B-H oxidative addition reaction. Complex **9** can further react with carbon monoxide, affording **11** with the chloro ligand *trans* to the boryl moiety. The elongation of the Ir-C bond in comparison to that in the PCP analogue revealed a stronger σ-donor ability of the boryl-based

ligand PBP. Moreover, the reaction of **9** with LiTMP under an ethylene atmosphere yielded the [PBP](ethylene)iridium complex **10**.

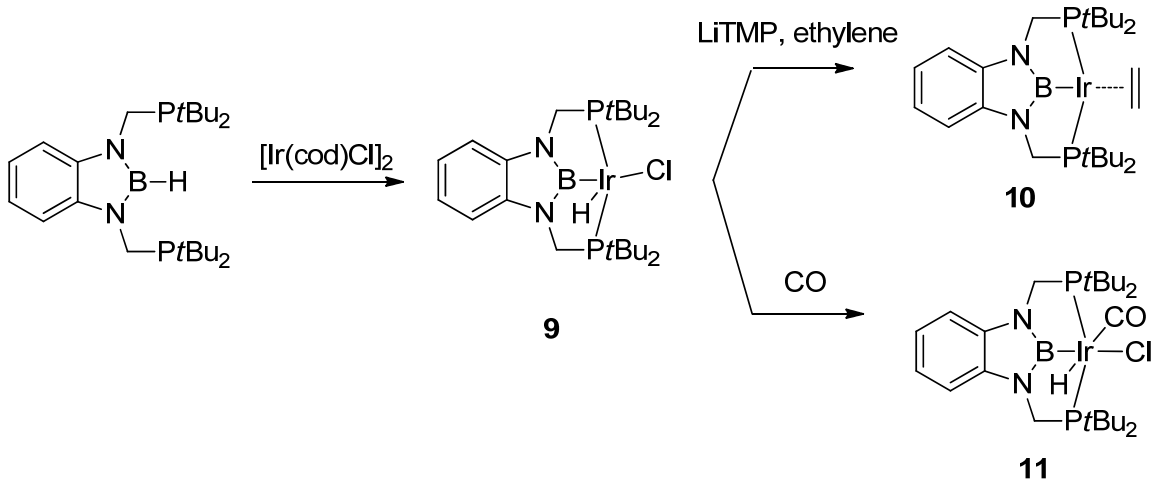

Fig. 6 First examples of boryl-based pincer complexes **9**, **10** and **11**.

1.3 Borylene complexes

Free borylenes of the general type ":B-R" constitute hypovalent, highly reactive species that can only be obtained by applying drastic conditions as shown by Timms et al. in the case of fluoroborylene ":B-F" in the 1960s.[56,57] Likewise, in 1984, West et al. published the photochemical generation of the silylborylene ":B-$SiPh_3$" in hydrocarbon matrices at -196°C and a number of well characterized trapping products derived thereof.[58] During the past decade borylene chemistry has once again become a focus, as it became possible to generate and stabilize borylenes as ligands in the coordination sphere of various transition metals.[59-70] The ligand properties of borylenes have been closely studied, in particular by computational methods,[71-79] thus revealing a close relationship to isolectronic carbonyl ligands in terms of bonding pattern and coordination modes. As shown in Fig. 7, the frontier orbitals of the free borylene species :BF and :BNR_2 had higher energy HOMO orbitals when compared to N_2 and CO, yet the LUMO orbitals of all four species remained relatively static energetically. Upon binding to a transition metal, the borylene is thus able to donate σ electron density to the metal center almost completely, providing marked thermodynamic stability. However, the imbalance between σ donation and π acidity was predicted to induce build up of positive charge on borylene moiety, thus leading to kinetic instability at the boron centre and its susceptibility to nucleophilic attack. Therefore, the presence of sterically protecting or electron-releasing substituents at boron was indicated as a necessary synthetic requisite for the stabilization of the borylene ligand.

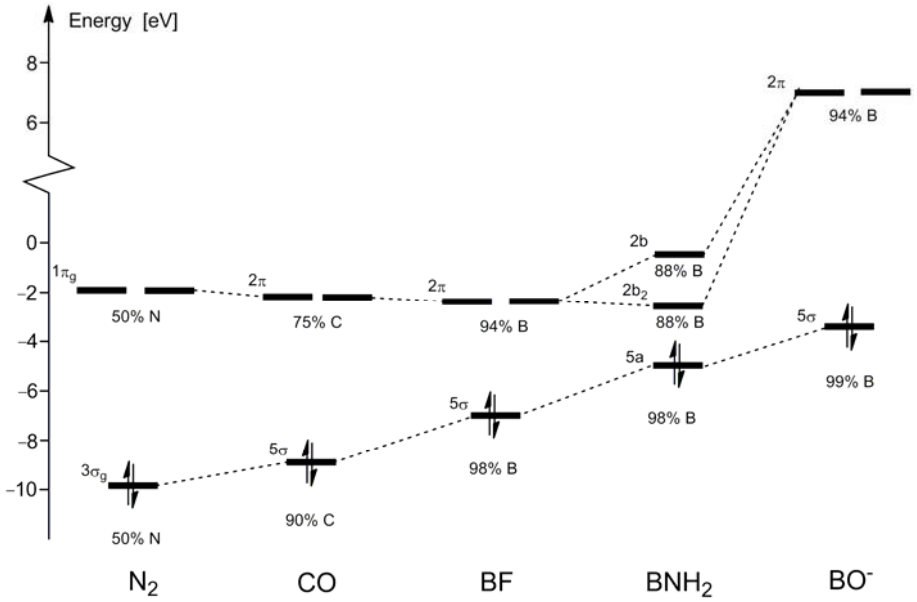

Fig. 7 Valence orbital energies (eV) of the AE system N_2, CO, BF, BNH_2 and BO^- and the percentage of atom A character of the orbitals.

1.3.1 Synthesis of first generation terminal borylene complexes

In 1998, A. H. Cowley reported the synthesis of the unusual terminal borylene complex $[(OC)_4Fe(BCp^*)]$ (**12**) by salt elimination from the dianionic complex $K_2[Fe(CO)_4]$ and the corresponding dichloroborane (Fig. 8 above). The boron atom in **12** is coordinated in a η^5-fashion to a Cp* ligand.[80] Later, synthesis of the related cationic borylene complex $[\{Cp^*Fe(CO)_2\}(BCp^*)]^+(AlCl_4)^-$(**13**) via halide abstraction of the corresponding haloboryl complex was reported from the same laboratory (Fig. 8 below).[81] The Fe-B distances of the two complexes are similar (**12**: 2.010(3); **13**: 1.977(3) Å) and are comparable to those of Fe-B single bonds in iron boryl complexes. This finding is in accord with the NBO analysis data for **13**, in which the Fe-B bond order was found to be unity. Furthermore, in stark contrast to other borylene complexes, the ^{11}B NMR resonances for **12** and **13** are both strongly highfield shifted (δ_B = -35.3(**12**) and -37.9(**13**)), indicating the presence of hypervalent boron nuclei.

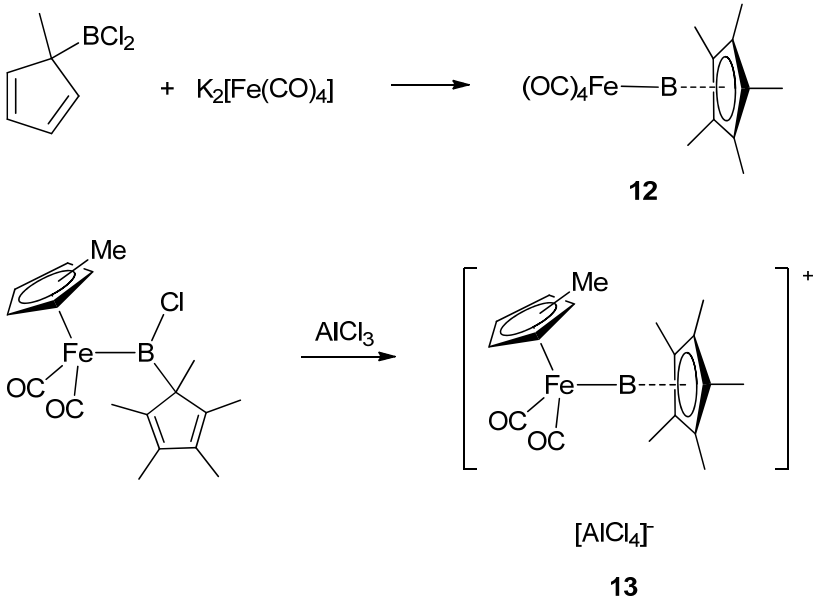

Fig. 8 Synthesis of Cp*-coordinated borylene complexes **12** and **13**.

Shortly after disclosing the atypical Cp*-coordinated borylene complexes of iron, the synthesis of group 6 pentacarbonyl terminal borylene complexes $[(OC)_5M{=}BN(SiMe_3)_2]$ (**14**: M = Cr; **15**: M = W) by double salt elimination from the corresponding reactive pentacarbonyl metalate species and a dihaloaminoborane was achieved in our laboratory (Fig. 9, above).[82] Later, the molybdenum analogue **16** was obtained in a similar manner. Comparison of W-B bond length (2.15 Å) with that (2.37 Å) of the amino-substituted boryl complex of tungsten $[Cp(OC)_3W\{B(NMe_2)\text{-}BCl(NMe_2)\}]$ confirmed the metal-boron double

bond character, which is in accord with "borylene" classification, thus constituting the first truly terminal borylene complexes.

Similarly, the "hypersilyl" derivative **17** could be prepared by applying a salt elimination protocol (Fig. 9, below).[83] In constrast to "amino" derivatives, the boron center in **17** lacks the stabilizing influence of a strongly π-donating substituent, which however allows stronger metal-to-boron π-retrodonation, thus decreasing the bond length (from 1.98 to 1.88 Å). Moreover, the strongly deshielded ^{11}B NMR signal at δ_B = 204.3 also indicated a reduced amount of electronic stabilization of the boron atom.

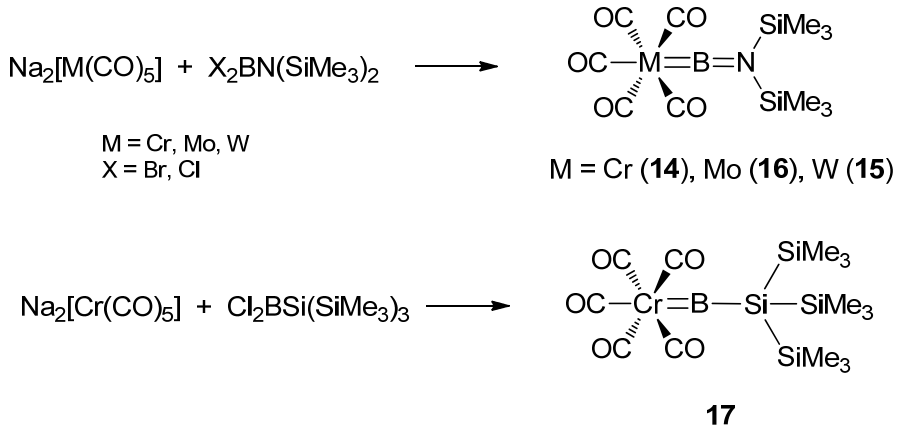

Fig. 9 Synthesis of terminal borylene complexes of group 6 metals.

In 2003, the group of Aldridge published the preparation of a cationic borylene complex [{Cp*Fe(CO)$_2$}(BMes)][BAr$^f_4$](**18**)[84] by halide abstraction from a neutral iron boryl complex (Fig. 10). Later, further examples of cationic group 8 borylene complexes [(η^5–C$_5$R$_5$)M(CO)$_2$(B=NR'$_2$)][BAr$^f_4$] (**19**: M = Fe, R = R' = Me[85]; **20**: M = Fe, R = H, R' = Cy[86]; **21**: M = Fe, R = H, R' = *i*Pr[87]; **22**: M = Ru, R = H, R' = Cy[86]) prepared by halide abstraction with Na[BAr$^f_4$] were reported from the same laboratory. The spectroscopic and structural properties of these complexes are mostly as expected: the mesityl complex **18** displays a short Fe-B distance (1.79 Å) and a deshielded ^{11}B NMR signal at δ_B = 145, while the amino complexes **19**-**21** contain relatively long Fe-B bonds (1.82-1.86 Å) and comparatively highfield-shifted ^{11}B NMR resonances between δ_B = 88 and 94. DFT calculations on **18** determined the relative contributions of B→Fe σ-donation and Fe→B π-retrodonation to the Fe-B bond and found them to be very similar to those found in Fischer carbene complexes, thus justifying their classification as true borylene complexes.[85]

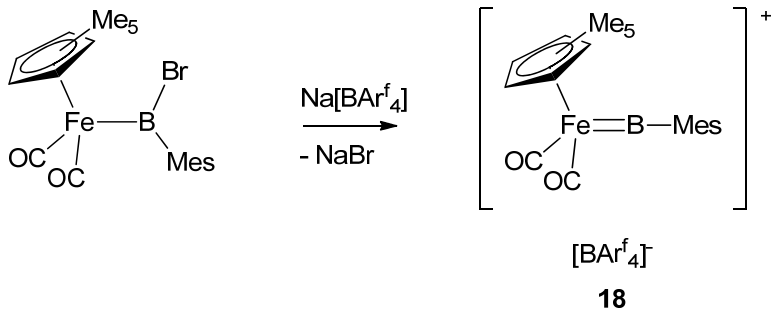

18

Fig. 10 Synthesis of cationic terminal borylene complex of iron **18**.

Shortly after the preparation of cationic group 8 borylene complexes via halide abstraction by the group of Aldridge, an analogous technique turned out to be also applicable for synthesizing cationic borylene complexes derived from group 10 metals, i.e. platinum. However, in this case, the halide removed in the first step was that attached to the platinum center, affording T-shaped cationic boryl complexes. At this point, the presence of strong donor ligand such as 4-pic or 4-*t*BuPy forced the migration of the boron-bound halide to the platinum center, thus yielding the corresponding base-stailized borylene complexes **23**-**26** (Fig. 11).[88,89] An exception was the case of a complex bearing the bulky mesityl boron substituent, which induced halide abstraction from the boron centre[Fig. 11]. The resulting complex **27** was the first example of a non-base-stabilized platinum borylene complex.[90]

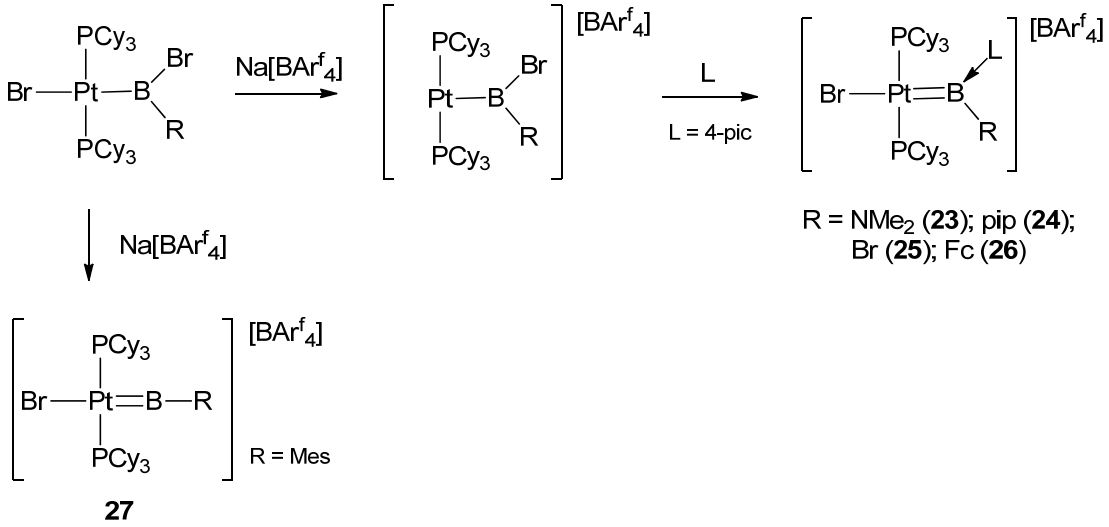

27

Fig. 11 Synthesis of base-stabilized and non-base-stabilized platinum borylene complexes.

Nevertheless, the scope of above mentioned synthetic strategies might still be limited by some hurdles, in particular the harsh conditions or reactive precursors required for the synthesis. More recently, Sabo-Etienne and co-workers reported the first example of neutral terminal arylborylene complex, which was synthesized via dehydrogenation of a mixture of $[RuHCl(H_2)(PCy_3)_2]$ and dihydroborane (Fig. 12).[91,92] In terms of structural parameters, the

Ru-B bond length of 1.78 Å is significantly reduced in comparison to that (1.96 Å) of amino-derivative **22** [86] as a result of the poorly π-donating mesityl substituent.

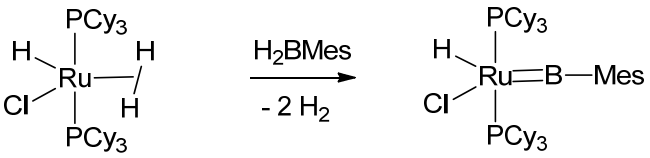

28

Fig. 12 Synthesis of a neutral arylborylene complex of ruthenium.

1.3.2 Synthesis of bridging first generation borylene complexes

The first complexes with definitive borylene character were prepared from the reaction of a manganese silane anion, i.e. a "dianion equivalent" complex, with a dihalodiborane(4), liberating 1 equivalent of a diborane(6) as a side-product (Fig. 13).[248] The M-B bond distances of the bridging borylene complexes are slightly longer than those of many terminal borylene complexes, and resemble closely the distances found in the base-stalilized borylene complexes. Computational studies on the manganese bridging borylene complexes were carried out by the groups of Stalke and Kaupp respectively.[93,94] Surprisingly, both excluded a direct bond path between the two manganese centers. Instead, the coupling of the electrons is accomplished via the boron atom in a delocalized fashion.

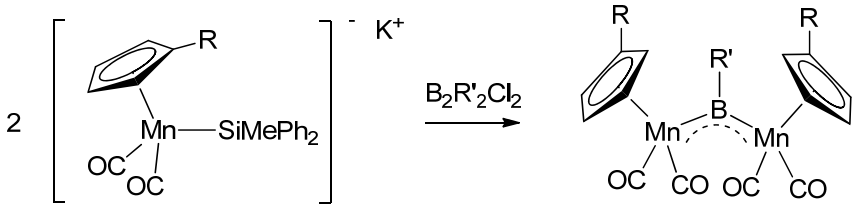

R = Me, R' = NMe_2 (**29**);
R = Me, R' = *t*Bu (**30**);
R = H, R' = NMe_2 (**31**).

Fig. 13 Synthesis of bridging borylene complexes based on manganese.

Another synthetic approach to bridging first generation borylene complexes is the (stepwise) salt elimination reaction between boranes of the general formula RBX_2 (X = Cl, Br; R = Cl, aryl, amino, pyrrolidinyl) and 2 equiv. monoanionic metalate species (Fig. 14), thus avoiding use of a diborane precursor. In this manner, dimanganese haloborylenes [{$(OC)_5Mn$}$_2$BX] (**32**: X = Cl; **33**: X = Br)[95] and a series of bridging dinuclear borylene complexes derived from group 8 metals (Fe, Ru)[95-101] were prepared.

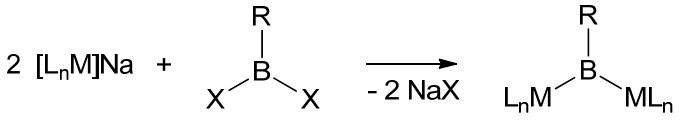

Fig. 14 Synthesis of bridging borylene complexes via salt elimination.

1.3.3 Application of borylene complexes

1. Synthesis of second generation borylene complexes

Since the first practical synthetic route to group 6 metal borylene complexes **14** and **15** was developed in 1998, the reactivity of these species has been in the focus of intense research. Most notably, these compounds have turned out to be convenient sources for the borylene fragment :$BN(SiMe_3)_2$, which can be transferred to suitable borylene acceptors. In the case of intermetal borylene transfer, the borylene moiety is transferred between two metal centers, affording a series of second generation borylene complexes that otherwise would be a great challenge to prepare.

Accordingly, the only known boron-centred ligand complex of vanadium **34** was prepared (Fig. 15). Under photolytic conditions, **14** undergoes borylene transfer to $[CpV(CO)_4]$ with replacement of one CO ligand.[102] The first rhenium borylene complex **35** was similarly prepared by irradiation of **15** in the presence of 2 equiv. $[CpRe(CO)_3]$ (Fig. 15).[103]

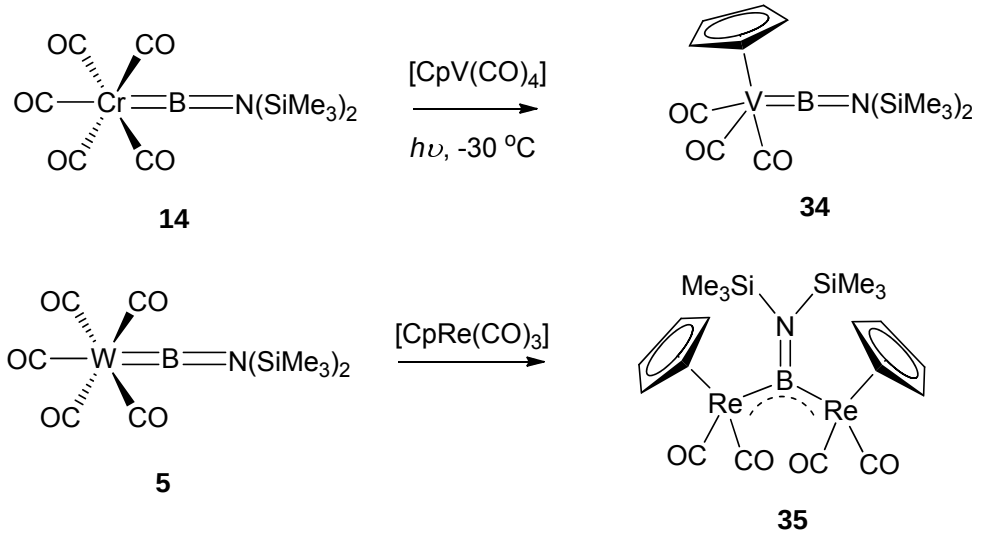

Fig. 15 Synthesis of group 5 and group 7 borylene complexes by intermetallic borylene transfer.

One of the most successful forays into the scope of the intermetallic borylene transfer has been their partial and complete transfer to group 9 metal complexes. Irradiation of group 6 aminoborylene complex **14** or **15** in the presence of $[Cp^{(*)}M(CO)_2]$ (M = Co, Rh, Ir) led first

to heterodinuclear borylenes **A**. The subsequent loss of the group 6 metal fragment afforded terminal borylene **B**, which were ready to undergo slow disproportionation reaction to form homodinuclear borylenes **C** (Fig. 16).[104-106] Only in the case of [CpCo(CO)$_2$] was each architecture accessible in series.

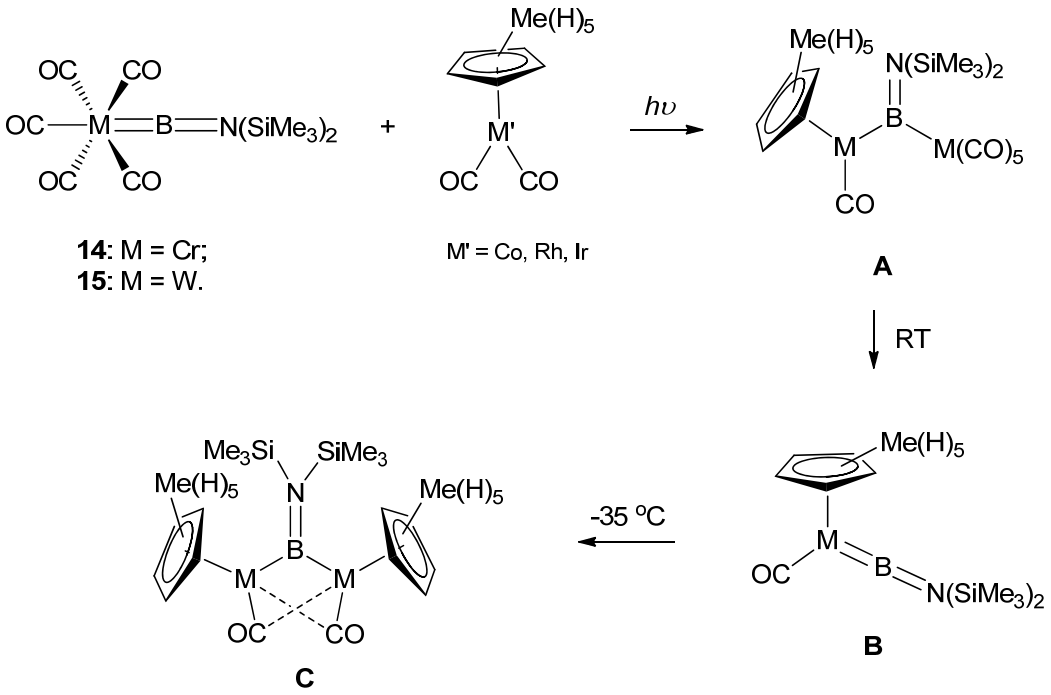

Fig. 16 Synthesis of group 9 metal borylene complexes by intermetal borylene transfer.

Furthermore, the intermetallic borylene transfer strategy allowed the preparation of the first examples of bis(borylene) complexes. Photolysis of **14** or **15** with [RhCl(CO)$_2$]$_2$ led unexpectedly to the unusual tetranuclear bis(borylene) complex **36**, which is the first example of a complex containing two borylene ligands (Fig. 17).[107] The two inner rhodium centers are bridged by the two borylene ligands and an additional CO, while the outer two rhodium centers connect to the inner centers through double chloride bridges. Later, (stepwise) transfer of two borylene ligands from **14** to [Cp*Ir(CO)$_2$] with replacement of both iridium-bound CO ligands afforded the first mononuclear bis(borylene) species [Cp*Ir{BN(SiMe$_3$)$_2$}$_2$] (**37**) (Fig. 17).[108]

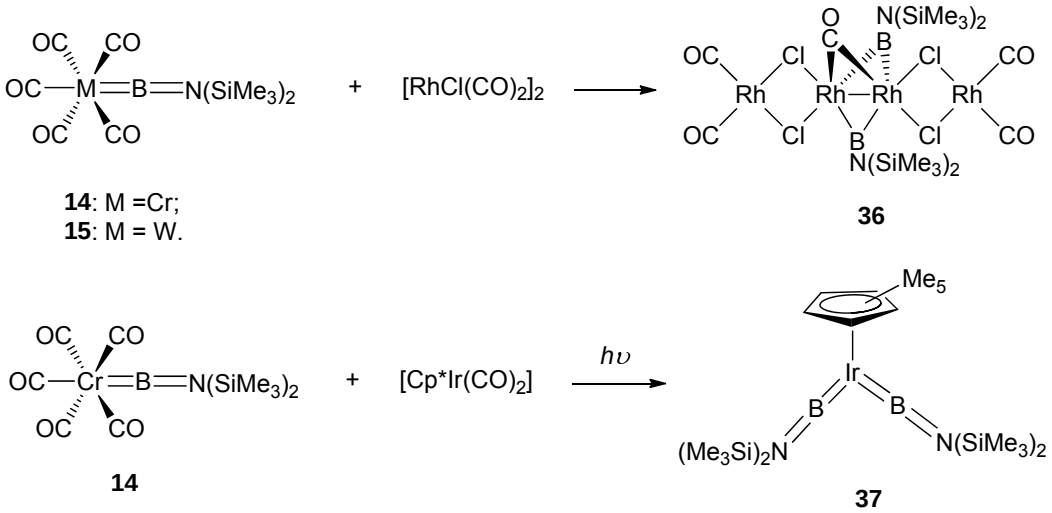

Fig. 17 Synthesis of group 9 metal bis(borylene) complexes.

2. Synthesis of borirenes

Borirenes are isoelectronic with cyclopropenium cations, and thus, constitute the smallest boron heterocycle that might exhibit 2π-aromatic stabilization.[109-112] Despite considerable fundamental interest in aromaticity and antiaromaticity, only a limited number of synthetic routes to borirenes have been published [58, 112, 113-115], and among these, most are laborious and low yielding. The reaction of trimethylstannylalkynes with 1,2-di-*tert*-butyl-1,2-dichlorodiborane(4) reported by Pues and Berndt afforded 1-*tert*-butylborirenes **38** and **39** in satisfactory yield (Fig. 18), although restricted in scope.[113]

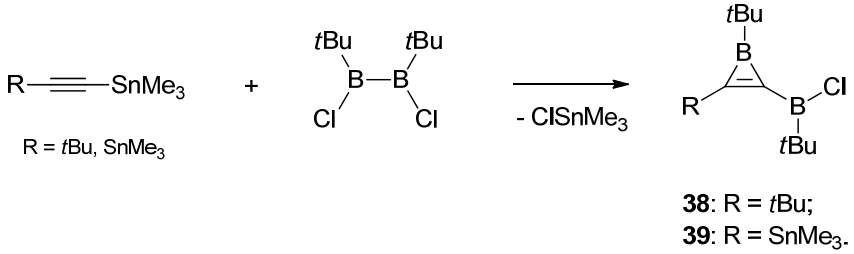

Fig. 18 Synthesis of 1-*tert*-butylborirenes **38** and **39**.

In 1987 Eisch et al. reported the first structurally characterized borirenes, i.e. 1-mesitylborirenes **40** and **41**, which were synthesized via photoisomerization of diaryl(arylethynyl)boranes (Fig. 19),[114,115], thus providing experimental evidence (shortened B-C and elongated C=C bond lengths) for the theoretically predicted Hückel aromaticity of this class of compounds. Nonetheless, the scope is severly limited with respect to the available substituents at the boron atom.

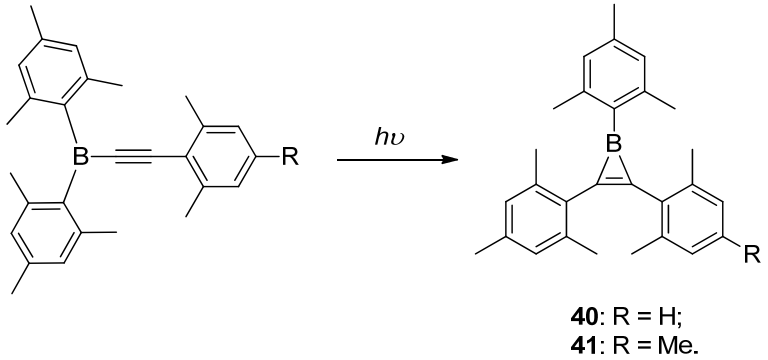

Fig. 19 Synthesis of 1-mesitylborirenes **40** and **41** by photoisomerization.

In 2005, the transition metal borylene functionalization of carbon-carbon triple bonds upon photolysis was reported from our laboratory, allowing facile and straightforward access to borirenes in good yields.[116] In further studies, borylene transfer protocols have turned out to be applicable to a wide range of organic substrates containing one or two alkynyl functions, and thus a variety of compounds consisting of one borirene unit (**A**), two borirene units (**B**) as well as two borirenes separated by a π-spacer (**C**) were synthesized and fully characterized (Fig. 20).[117] The proposed aromaticity of borirenes and extensive π-delocalization over the BCC ring has been confirmed by altered endocyclic bond lengths and a significantly decreased barrier to rotation about the exocyclic B–N double bond. This synthetic strategy gives access to a new class of boron-based π-conjugated systems that might possess particularly interesting photophysical properties[118-121].

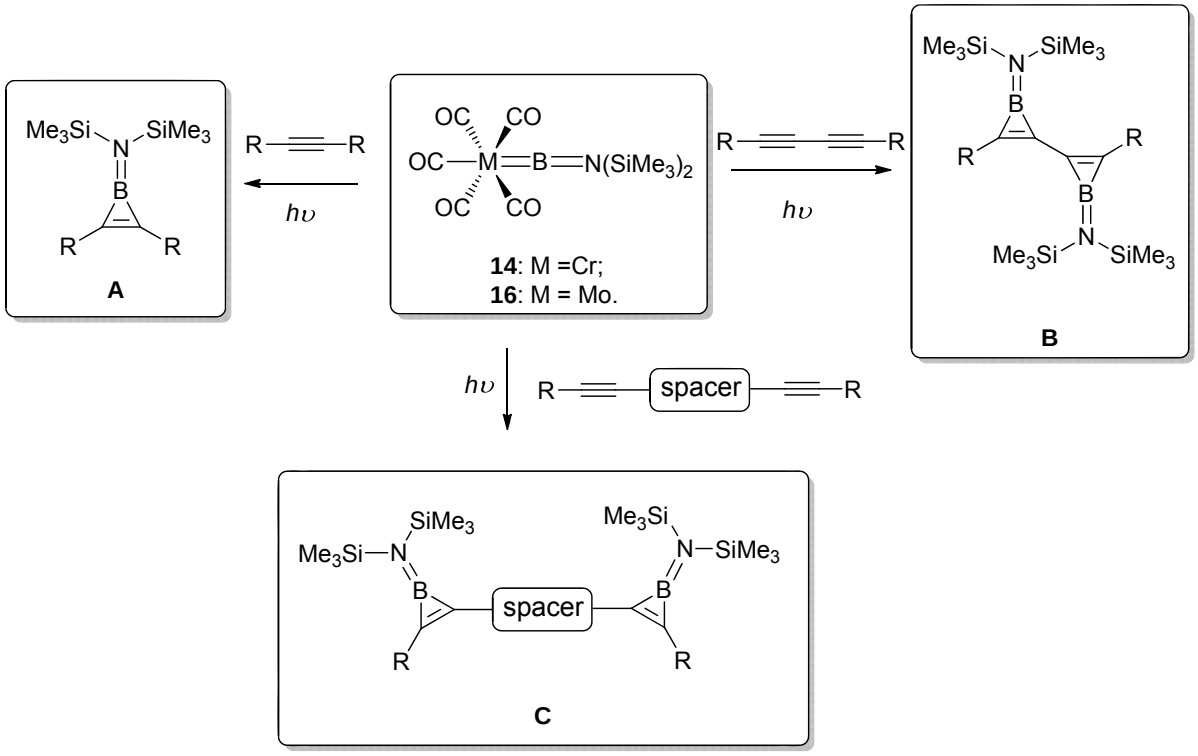

Fig. 20 Synthesis of borirenes and bis(borirenes) by borylene transfer.

3. Activation of olefinic C-H bonds

The somewhat different photochemical behaviour of borylene species in the presence of alkenes is intuitive in view of the lower reactivity of the C=C double bond and the absence of 2π-electron aromatic stabilization for the possible products, i.e. three-membered boriranes. Therefore, there would be less thermodynamic driving force for the reaction than in the analogous borirene syntheses. Accordingly, the reaction of **14** with 3,3-dimethylbut-1-ene led to two major products, the alkenyl(amino)borane **42** and its chromiumtetracarbonyl adduct **43** (Fig. 21).[122] Obviously, a geminal C-H bond of the alkene was functionalized by insertion of the borylene moiety, while **43** can be ascribed to additional loss of one CO ligand from **14** and coordination of **42** in a bidentate (σ, π) fashion. The $Cr(CO)_4$ fragment in **43** can be removed upon treatment with 2 equiv. tricyclohexylphosphine, with liberation of $[Cr(CO)_4(PCy_3)_2]$, thus allowing a selective preparation of **42**.

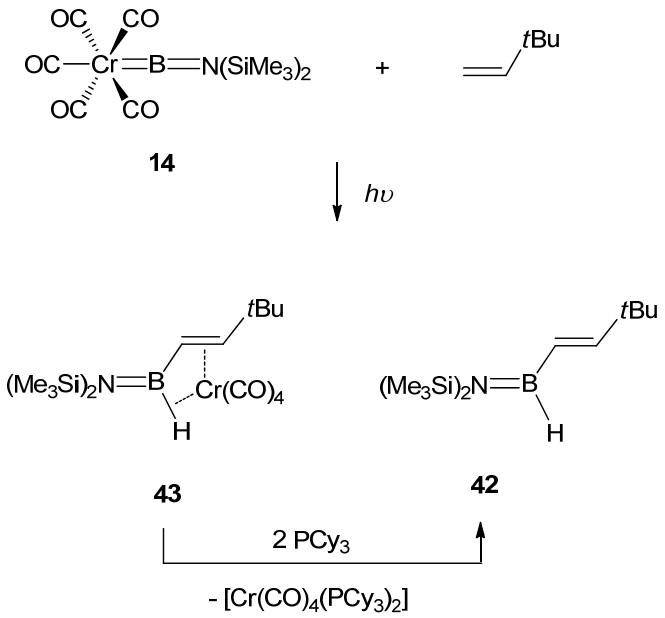

Fig. 21 Photochemical insertion of a borylene into a olefinic C-H bond.

The Suzuki–Miyaura coupling reaction, originally the palladium-mediated coupling of arylboranes and organic halides, has recently been extended with some success to include alkyl- and alkenylboranes, boronic acids and borates,[123-125] Consequently, the demand for new routes to alkenyl-boron compounds is intense, making the borylene instertion into an alkenyl C-H bond extremely significant.

4. Metathesis reactions

Another particularly intriguing area of terminal borylene chemistry is borylene metathesis through [2+2] cycloaddition. The first examples of reaction products of a formal borylene metathesis were reported by group of Aldridge. Addition of phosphine and arsine chalcogenides Ph_3PS and Ph_3AsO to **21** resulted in mild metathesis of the Fe-B with the P-S or As-O bonds, leading to $[CpFe(CO)_2(EPh_3)][BAr^f_4]$ (**44**: E = P; **45**: E = As) in both cases (Fig. 22), with the side products being the cyclic species $[iPr_2NBX]_n$ (X = S, n = 2; X = O, n =3). In contrast, the reaction of **21** with Ph_3PO led only to the oxygen-donor borylene adduct **46**, which is presumably due to the greater strength of the P-O bond over analogous P-S and As-O examples. Furthermore, the formation of the substrate-borylene adduct via a B-O bond (Fig. 22) instead of [2+2] cycloaddition strongly suggested a non-concerted mechanism for the methathesis reaction observed here.[87]

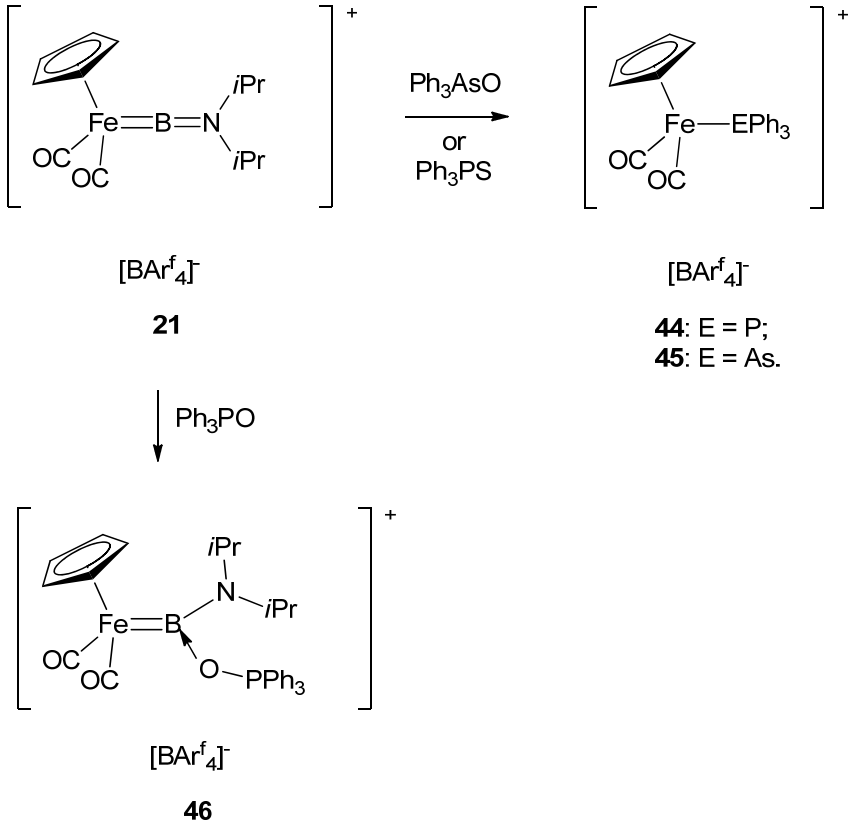

Fig. 22 Reactions of a cationic borylene complex 2**1** with phosphine and arsine chalcogenides.

The first examples of borylene metathesis reactions through a concerted mechanism were reported soon afterwards. Addition of benzophenone to manganese terminal borylene complex **47** provided cycloaddition product $[Cp(OC)_2Mn\{B(tBu)OC(Ph)_2\}]$ (**48**), which underwent spontaneous cycloreversion with clean formation of the metathesis products $[Cp(OC)_2Mn{=}CPh_2]$ (**49**) and $(tBuBO)_3$ (**50**) (Fig. 23).[126]

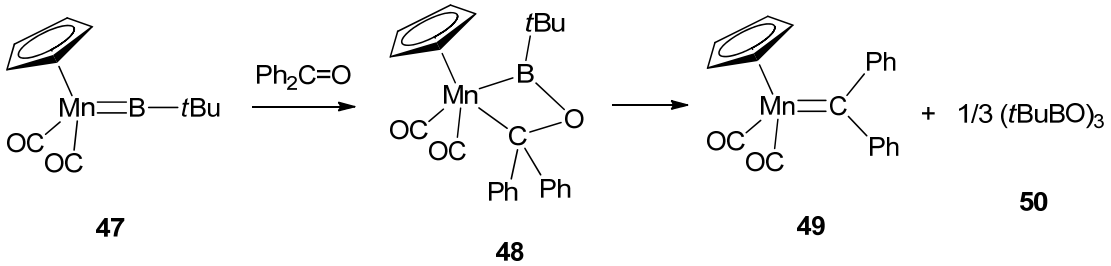

Fig. 23 Metathesis of a terminal borylene with ketones.

1.3.4 Further reactivity of borylene complexes

1. Borylene-base adducts

Cationic iron borylene complexes react with a variety of C-, N- and O- nucleophiles, affording a series of base-adducts. An example has been mentioned above, i.e. the reaction of **21** with oxygen-donor Ph_3PO (Fig. 22). Interestingly, in the case of the relatively weak Lewis base THF, adduct formation with $[\{CpFe(CO)_2\}(B{=}NCy_2)][BAr^f_4]$ (**21**) was found to be reversible (Fig. 24).[127]

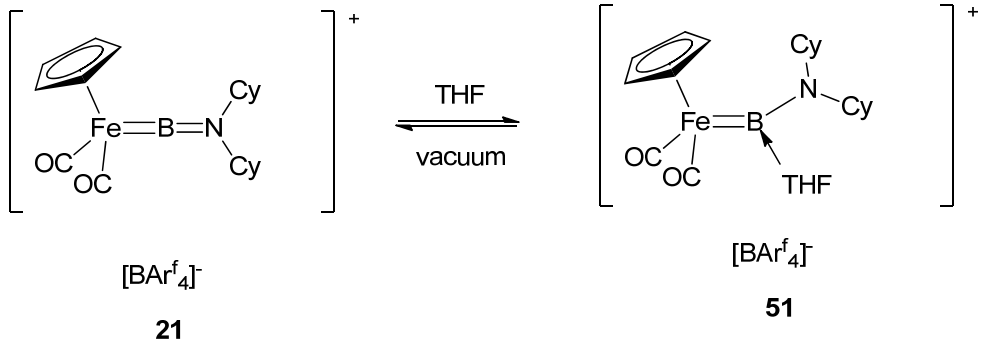

Fig. 24 Reversible borylene-THF adduct formation.

In addition, metal Lews bases such as $[M(PCy_3)_2]$ (**52**: M = Pt; **53**: M = Pd), which possess a electron-rich and highly unsaturated metal center, have turned out to be able to stabilize group 6 terminal aminoborylene complexes in an analogous fashion. In all cases, the group 6 and group 10 metal centers are connected through both a borylene and CO ligand (Fig. 25).[128-130]

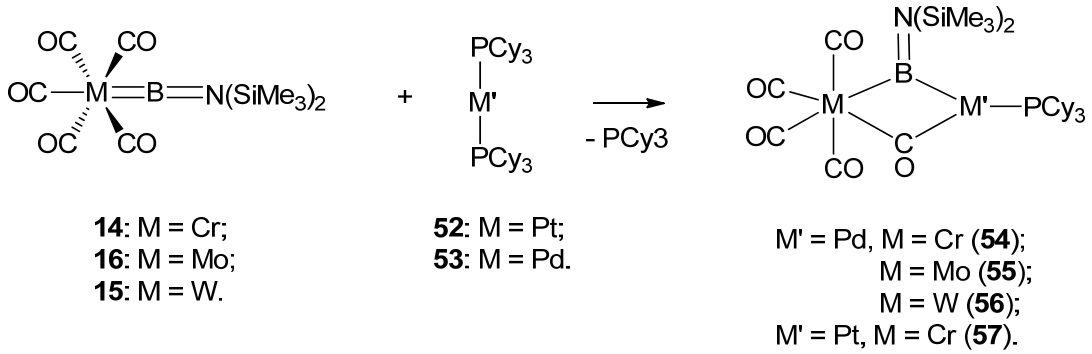

Fig. 25 Metal base stabilized borylene complexes.

2. Insertion of unsaturated molecules into the M=B double bonds

DCC is known to insert into Fe=B and B=N double bonds in cationic iron terminal borylene complexes. While double insertion of DCC occurred at ambient temperature, affording the spirocyclic boronium complexes **60** and **61**, products of monoinsertion into the Fe=B bond were detected at low temperature and were crystallographically confirmed (Fig. 26).[131,132]

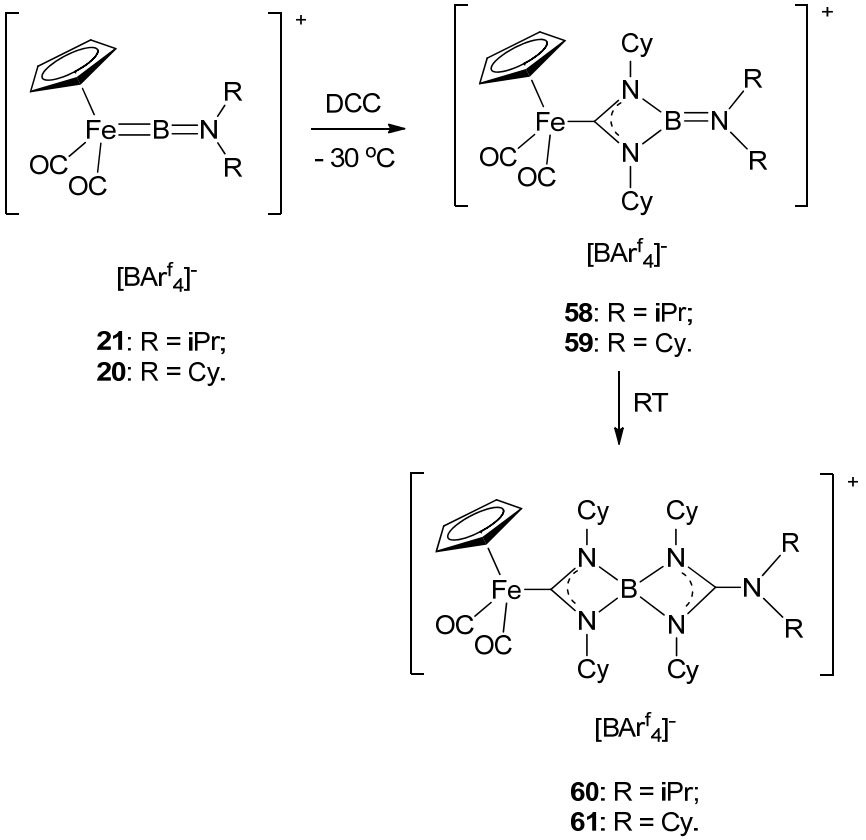

Fig. 26 Insertion reactions of DCC into Fe=B and N=B bonds.

3. Insertion of H_2 into Ru=B double bonds

While the synthesis of neutral ruthenium terminal arylborylene complex **28** from [RuHCl(H_2)(PCy_3)$_2$] was quantitative upon application of vacuum (see *1.3.1*), the reverse reaction upon pressurization with H_2 (3 atm) led to two products **62** and **63** as indicated by multinuclear NMR specstroscopy (Fig. 27). The reaction is the first example of hydrogenative cleavage of a metal-boron double bond.

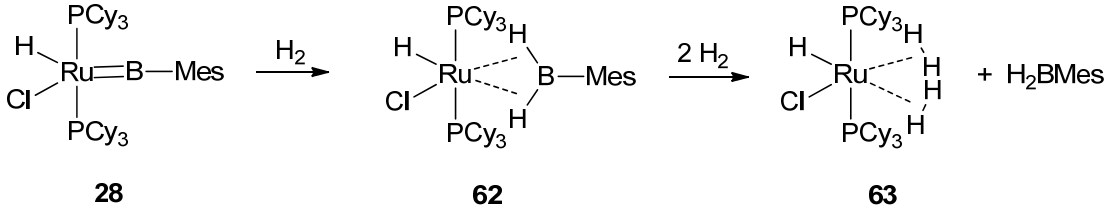

Fig. 27 Hydrogenation cleavage of a ruthenium-boron double bond.

2 Results and disscution

2.1 Functionalization of transition metal alkynyl σ-complexes by borylene transfer

Metal alkynyl σ complexes have attracted considerable interest since the mid-1980s. A variety of synthetic routes toward metal-alkynyl coupling was developed. To date, metal alkynyls have become a class of compounds that contain from one alkynyl group bound to the metal, up to as many as 10 000 M-C≡C- linkages in the polymeric chain. As a result of their linear structure and π-electron conjugation, σ-alkynyl complexes have turned out to possess particularly promising electronic and structural properties, which include nonlinear optical effects, luminescence and photoconductivity, electronic communication, and liquid crystallinity.[234] As the addition of d-block metal centers into the borirene-based π-conjugated system (Fig. 28) may introduce a range of novel properties including e.g. redox, magnetic, optical and electronic properties, we addressed the interest in functionalization of metal alkynyl σ complexes by borylene transfer.

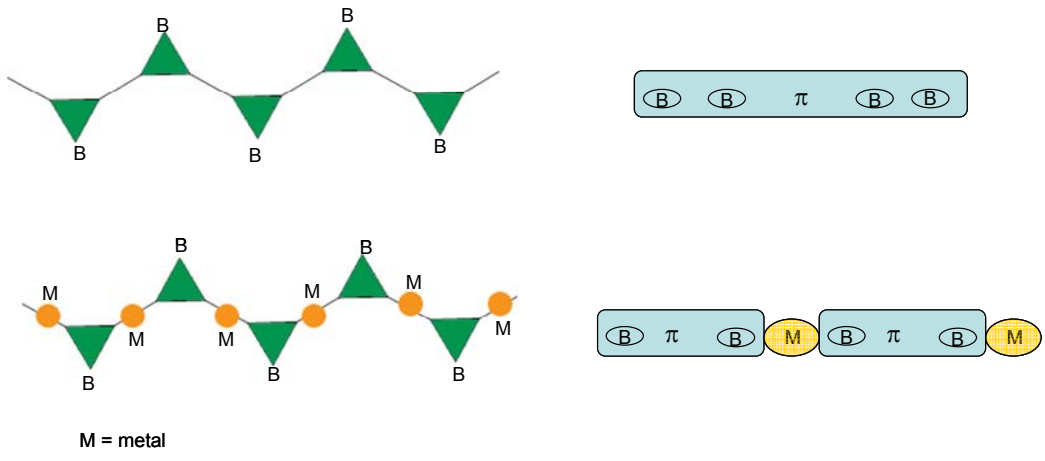

Fig. 28 Borirene-based π-conjugated system (above) and introduction of *d*-block metal centers (below).

2.1.1 Borylene transfer to iron-alkynyl σ-complexes

2.1.1.1 Thermal reaction of $[(OC)_5Mo{=}BN(SiMe_3)_2]$ (**16**) with $[Cp^*Fe(CO)_2(C{\equiv}CPh)]$ (**64**)

Substrates suitable for borylene transfer should possess considerable stability under corresponding reaction conditions. Hence, a solution (THF, benzene or toluene) of $[Cp^*Fe(CO)_2C{\equiv}CPh]$ (**64**) was irradiated or heated at 80°C. While **64** underwent slow dimerization of the $Cp^*Fe(CO)_2$ fragment under photolytic conditions, leading to $[Cp^*(OC)Fe(\mu\text{-}CO)]_2$ (**65**) as indicated by δ_H = 1.60 (Cp*) in ^{1}H NMR spectrum, no sign of decomposition under thermal conditions was observed. Therefore, reaction of a pale yellow solution (THF) of $[(OC)_5Mo{=}B{=}N(SiMe_3)_2]$ (**16**) in the presence of an equimolar amount of iron alkynyl **64** was carried out at 80°C (Scheme 1), and was monitored by ^{11}B NMR spectroscopy, which revealed, within 30 minutes, a nearly quantitative conversion of the borylene complex **16** (δ_B = 89.1) into a new boron-containing species with a resonance at δ_B = 36, which falls in the expected range for borirenes. Notably, in addition to the borirene-peak, a weak resonance at δ_B = 76 was observed, thus indicating the presence of an iron boryl species (see the discussion in *2.1.2.1*). After workup, the iron-substituted borirene **66** could be obtained as a yellow, moderately air- and moisture sensitive solid material in good yield (63%). Multinuclear NMR spectra of **66** displayed all relevant signals in the expected range, with the exception of those of the boron-bound carbon atoms that were not observed due to quadrupolar coupling, thus confirming its constitution in solution. The single resonance at δ_H = 0.32 in the ^{1}H NMR spectrum for the nitrogen-bound $SiMe_3$ groups indicates rapid rotation around the B-N bond at room temperature, which is consistent with related systems, indicating the reduced B-N π-contribution as a result of 2π-aromatic stabilization within the BCC-ring.[116,117]

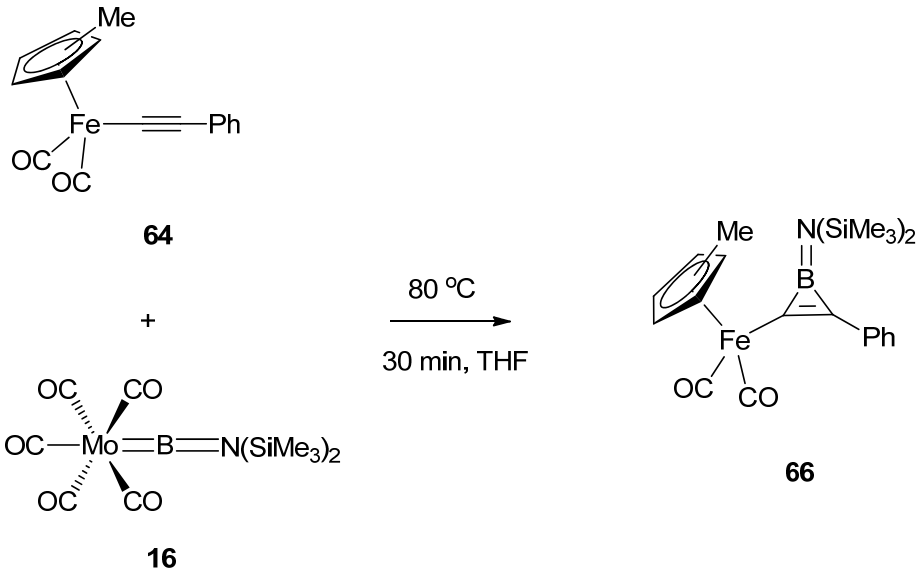

Scheme 1: Synthesis of iron-substituted borirene **66**.

Single crystals of **66** suitable for X-ray diffraction analysis were obtained from a hexane solution at –60°C. The molecule crystallizes in the monoclinic space group P2(1)/c (Fig. 29). The overall geometry, in particular the endocyclic distances i.e. C1-C2 1.3631(19) Å, C1-B1 1.501(2) Å, C2-B1 1.474(2) Å as well as the slightly elongated B-N separation of 1.4319(19) Å, resemble those of previously reported aminoborirenes. These data are in accord with extensive delocalization of the two π-electrons over a three-center bonding molecular orbital comprised of the *p* orbitals of boron and carbon. The phenyl ring and the borirene unit are not coplanar, but effect a dihedral angle of 67.03°, presumably due to steric congestion imposed by the bulky $N(SiMe_3)_2$ groups and the Cp* ligand. The distance of 1.9826(14) Å between Fe and the sp^2-hybridized C1 is somewhat greater than the corresponding bond in the alkynyl precursor **64** (1.924(7) Å) where the C1-atom is *sp*-hybdrized[133], which can be explained by increased coordination number and increased *p*-orbital character at C1.

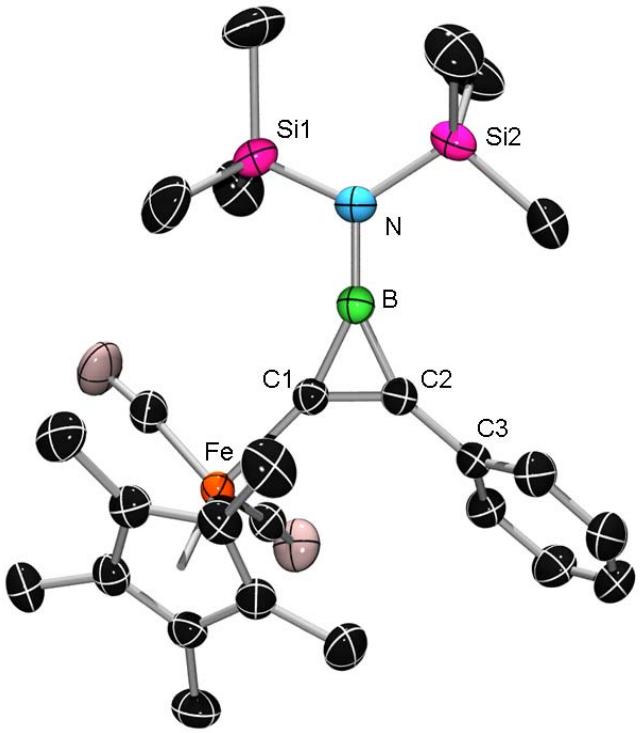

Fig. 29 Molecular structure of **66**. Ellipsoids drawn at the 50% probability level; hydrogen atoms have been omitted for clarity. Relevant bond lengths [Å] and angles [°]: Fe-C1 1.9826(14), C1-C2 1.3631(19), C1-B 1.501(2), C2-B 1.474(2), C2-C3 1.4699(19), B-N 1.4319(19), N-Si1 1.7517(13), N-Si2 1.7464(13), Fe-C1-C2 137.60(10), C1-C2-C3 140.19(13), B-C1-C2 61.73(10), B-C2-C1 63.76(10), C1-B-C2 54.52(9), C1-B-N 152.29(14), C2-B-N 153.03(15), B-N-Si1 112.67(10), B-N-Si2 121.10(10).

2.1.1.2 Thermal reaction of $[(OC)_5Mo{=}BN(SiMe_3)_2]$ (**16**) with $[Cp^*Fe(CO)_2(C{\equiv}CSiMe_3)]$ (**67**)

In order to probe the versatility of the synthetic method, and to introduce a trimethylsilyl group that could be used for further functionalization of the borirene ring, e.g. lithiation and borylation, $[Cp^*Fe(CO)_2(C{\equiv}CSiMe_3)]$ (**67**) was treated with an equimolar amount of $[(OC)_5Mo{=}BN(SiMe_3)_2]$ (**16**) under analogous conditions to those applied for the synthesis of **66** (Scheme 2). The reaction was monitored by multinuclear NMR spectroscopy, which indicated a complete conversion of **16** into a new boron-containing species within 1 h as indicated by δ_B = 78 in the ^{11}B NMR spectrum. This only slight upfield shifted resonance is in stark contrast to that of **66**, strongly suggesting the presence of a boryl species. However, the ^{1}H NMR spectrum clearly indicated the residue of **67** (δ = 0.38, $SiMe_3$), and four unassignable peaks between 0.16 and 0.36 ppm. The reaction mixture was heated at 80°C for a further 3 h. The ^{11}B NMR spectrum showed two new sharp singlets at δ_B = 25 and 44,

which, particularly the former, are in the expected region for borirenes. However, all attempts to isolate the unknown species by crystallisation, sublimation or chromatography failed.

As iron-substituted borirene **66** underwent borirene-boryl rearrangement under photolytic conditions (*vide infra*), an identical photoisomerization of the unknown boron-containing species displaying peaks at δ_B = 25 and 44 could be employed in order to gain further evidence for their chemical constitution. However no reaction was observed upon irradiation of the reaction mixture.

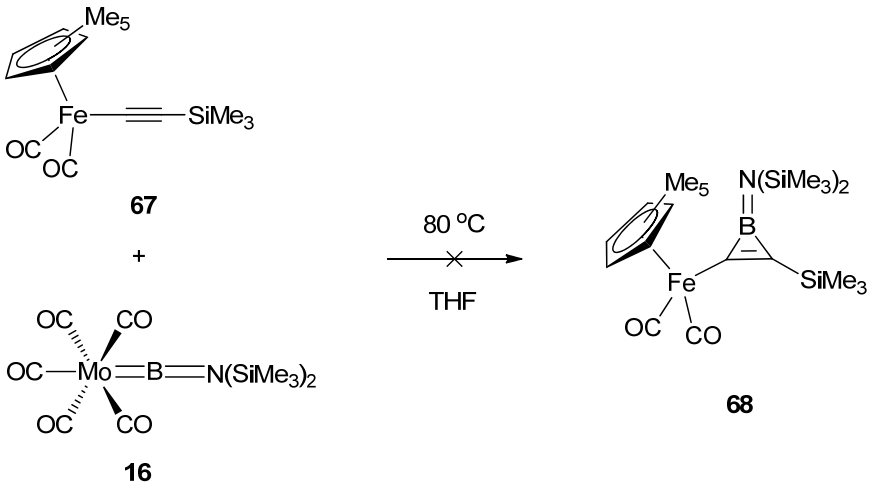

Scheme 2: Thermal reaction of $[(OC)_5Mo{=}BN(SiMe_3)_2]$ (**16**) with $[Cp^*Fe(CO)_2(C{\equiv}CSiMe_3)]$ (**67**).

2.1.1.3 Reaction of $[(OC)_5Mo{=}BN(SiMe_3)_2]$ (**16**) with $[1,4\text{-}\{Cp^*Fe(CO)_2C{\equiv}C\}_2\text{-}C_6H_4]$ (**69**)

The reaction of $[1,4\text{-}\{Cp^*Fe(CO)_2C{\equiv}C\}_2C_6H_4]$ (**69**) with 2 equiv. $[(OC)_5Mo{=}BN(SiMe_3)_2]$ (**16**) was carried out under identical conditions as those applied in *2.1.1.1*. After 1 h, while the ^{11}B NMR spectrum showed extremely weak peaks at δ_B = 54 and 17, which are not in the expected range for borirenes, the ^1H NMR spectrum showed many unassignable peaks between 0 and 1 ppm.

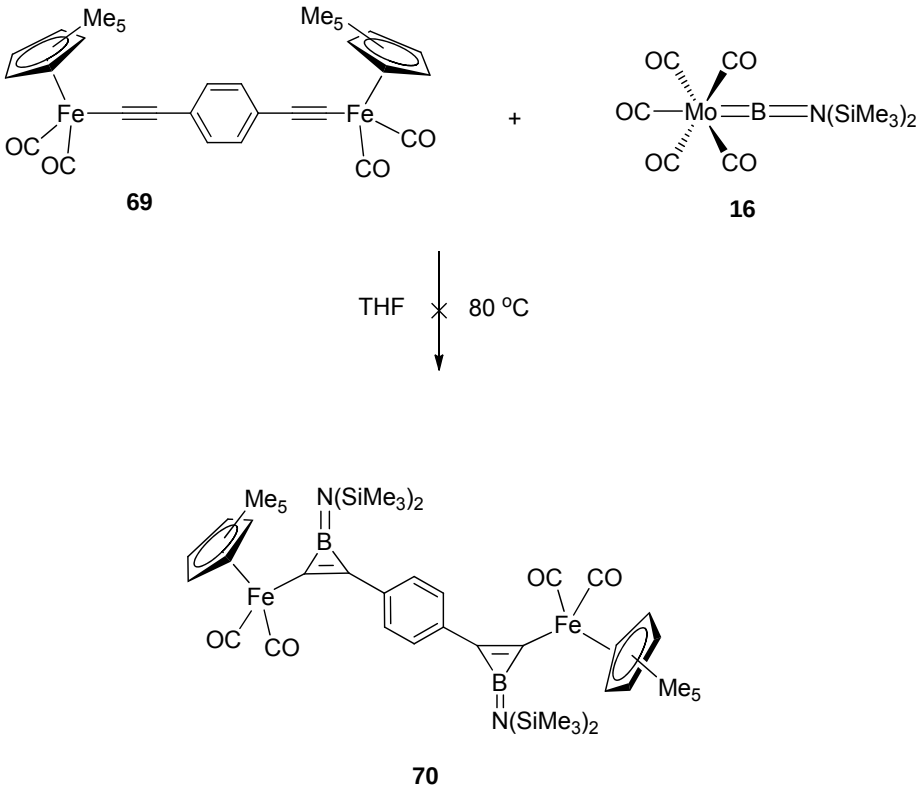

Scheme 3: Reaction of $[(OC)_5Mo{=}BN(SiMe_3)_2]$ (**16**) with $[1,4\text{-}\{Cp^*Fe(CO)_2C{\equiv}C\}_2C_6H_4]$ (**69**).

2.1.1.4 Reaction of $[(OC)_5M{=}BN(SiMe_3)_2]$ (**14**: M = Cr, **16**: M = Mo) with $[CpFe(dppm)(C{\equiv}CSiMe_3)]$ (**71**)

As borylene transfer to $[CpFe(CO)_2(C{\equiv}CSiMe_3)]$ (**67**) was not achieved in *2.1.1.2*, the chelate ligand dppm was utilized to increase the photochemical stability of the iron alkynyl complex, so that photolytic conditions could be probed for borylene transfer; and ii) the electron density on the C≡C triple bond is increased, which might facilitate the borylene transfer reaction.

Hence, iron alkynyl $[Cp(dppm)Fe(C{\equiv}CSiMe_3)]$ (**71**) was irradiated in the presence of an equimolar amount of **14** and **16** respectively. The reaction was monitored by multinuclear NMR spectroscopy, which revealed the considerable stability of **71** as indicated by remaining of the peak at δ_P = 43.3 in ^{31}P NMR spectrum. The concomitant slow decomposition of borylene complexes **14** and **16** was indicated by weakening of the peak at δ_B = 90 in the ^{11}B NMR spectrum. Similar reaction behavior was observed for the reaction between **71** and chromium borylene complex **14** under thermal conditoins.

Therefore, the reaction was again carried out under the same forcing conditions as those applied in *2.1.1.1*, and monitored by multinuclear NMR spectroscopy. The reaction was accomplished within 24 h. The ^{11}B NMR spectrum displayed an extremely weak and broad signal at $\delta_B = 25$. However, the ^{31}P NMR spectrum showed five main peaks between 0-100 ppm that were not assignable to the expected borirene **72**. All attempts to isolate the unknown species by crystallisation, sublimation or chromatography failed.

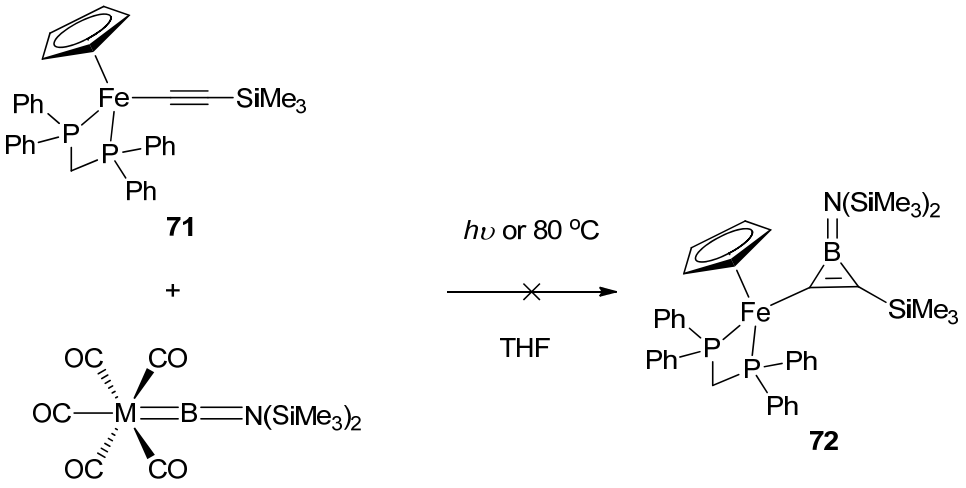

14: M = Cr, **16**: M = Mo

Scheme 4: Reaction of $[(OC)_5M{=}BN(SiMe_3)_2]$ (**14**: M = Cr, **16**: M = Mo) with $[CpFe(dppm)(C{\equiv}CSiMe_3)]$ (**71**).

2.1.1.5 Reaction of $[(OC)_5M{=}BN(SiMe_3)_2]$ (**14**: M = Cr, **16**: M = Mo) with $[Cp^*Fe(dppm)(C{\equiv}CPh)]$ (**73**)

To further study the influence of ligands on the iron center, the reaction of dppm-coordinated iron alkynyl **73** with an equimolar amount of **14** was carried out under same reaction conditions as those applied in *2.1.1.1*. Surprisingly, no reaction could be observed within 2 d, which is indeed in stark contrast to the reaction of **64** that differs from **73** only by the carbonyl ligand on iron center. As dppm is sterically more demanding in comparison to carbonyl, functionalization of the neighboring alkynyl was hindered. Furthermore, this finding implies the key role of the carbonyl ligand in the reaction mechanism, e.g. by CO dissociation (*vide infra*).

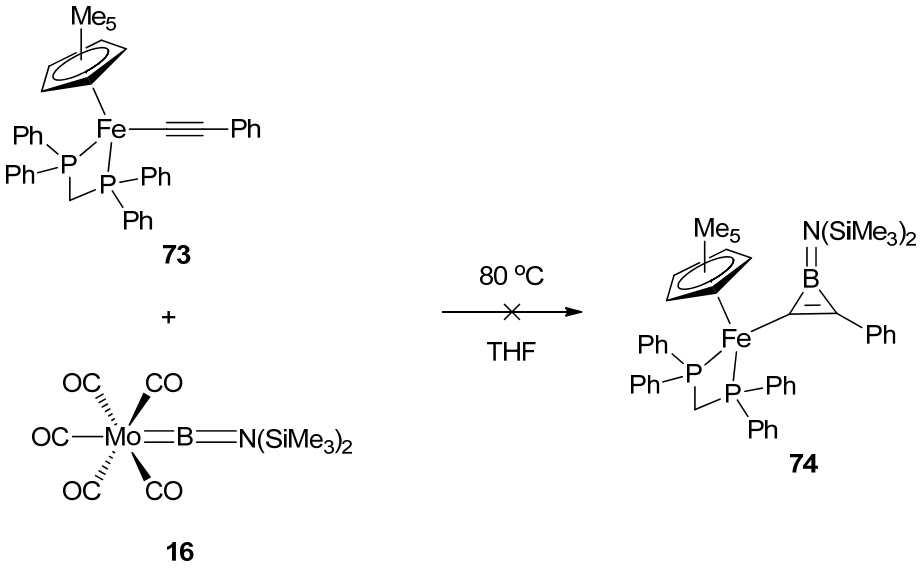

Scheme 5: Attempted reaction of $[(OC)_5M{=}BN(SiMe_3)_2]$ (**14**: M = Cr, **16**: M = Mo) with [Cp*Fe(dppm)C≡CPh] (**73**)

2.1.2 Reactivity investigation of iron-substituted borirenes

2.1.2.1 Reversible iron-borirene-boryl transformation

1. Photolysis of [{Cp*$(OC)_2$Fe}-(*cyclo*-$BN(SiMe_3)_2(C{=}CPh)$] (**66**)

Room temperature photolysis of a yellow C_6D_6 solution of **66** was carried out in a sealed Young NMR tube. The reaction was monitored by ^{11}B NMR spectroscopy, which revealed gradual consumption of the starting material **66** and formation of two new boron-containing compounds **75** and **76** in a ratio of approximately 3:1, as indicated by new resonances at δ_B = 76 and 87 respectively. After full characterization of these new compounds (*vide infra*) it became obvious that the formation of a mixture is due to the incomplete ejection of CO imposed by the closed reaction vessel. Thus, **66** was irradiated under similar conditions, but the atmosphere in the NMR tube was replaced every 30 min with dry argon, leading to complete conversion of **76** into **75** as evidenced by ^{11}B NMR spectroscopy (Scheme 6). After workup, complex **75** was isolated as a red, moderately air- and moisture-sensitive solid in 71% yield.

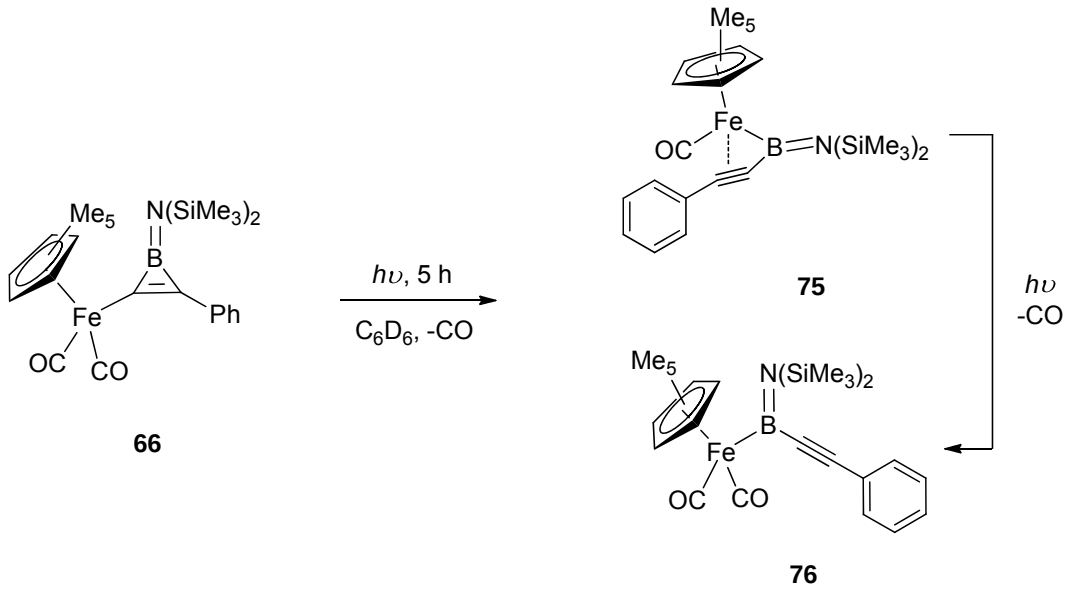

Scheme 6: Photolysis of the iron-substituted borirene **66**.

The significant downfield shift in the ^{11}B NMR spectrum of **75** in comparison to **66** of approximately 40 ppm indicates a rearrangement of the former borirene moiety, as such deshielded resonances are typically found for iron bound boryl groups.[96,134,135] Additionally, the observation of two broad signals for the nitrogen-bound trimethylsilyl groups at δ_H = 0.58 and 0.43 in a 1:1 ratio at ambient temperature in the ^{1}H NMR spectrum indicates a significantly increased rotational barrier of the nitrogen-boron bond. These spectroscopic data are in good agreement with the molecular structure of **75** as elucidated in the crystal, in which the B-N π-contribution is increased as a result of the BCC-ring opening.

Single crystals of **75** suitable for X-ray crystallography were obtained by cooling a hexane solution to –60 °C. The molecule crystallizes in the triclinic space group *P-1* with two almost identical molecules in the asymmetric unit. As the geometry of both subunits is identical within the experimental error, only one set of data will be discussed in the following. The overall appearance of **75** is that of an (alkynyl)boryl complex, in which the boron bound C-C triple bond coordinates in a η^2-fashion to the iron centre, thus constituting a highly unusual structural motif in boryl chemistry (Fig. 30). While the sum of angles around boron B (359.82°) and nitrogen N (359.28°) indicates a planar coordination for both atoms, the Fe-B-C1 angle of 71.09(9)° displays significant deviation from ideal trigonal planar geometry commonly observed for *sp*^{2}-hybdrized boron centers, thus indicating a highly strained molecular structure. Likewise, the Fe-B1 separation of 1.9950(17) Å is rather short for an iron-boryl bond and matches the one in [Cp(OC)Fe–BF{Si(SiMe$_3$)$_3$] (1.983(9) Å), despite the fact that the latter is sterically less congested due to the presence of the parent Cp ligand at

the iron center.[136] The side-on coordination of the alkynyl group has the expected effect on the C-C triple bond. Thus, the C1-C2 distance, which amounts to 1.268(2) Å is significantly elongated in comparison to the non-coordinated C-C triple bond in **76** (1.208(3) Å), but very similar to values typically found for alkynes that are η^2-coordinated to a metal of the iron triad [137]. The overall geometry of the C3-C2-C1-B moiety gives further evidence for the presence of molecular strain, as the boryl- and the phenyl group adopt a mutually *trans* disposition with respect to the C1-C2 multiple bond, with angles of 147.34(15)° (C1-C2-C3) and 133.98(14)° (B-C1-C2), respectively. Finally, the somewhat shortened B-N bond length of 1.403(2) Å in comparison to the value of 1.4319(19) Å found for the borirene complex **66** indicates a slightly stronger π-interaction between boron and the exocyclic nitrogen atom due to cleavage of the BCC-ring and cancelling of the endocyclic 2 π electron delocalization.

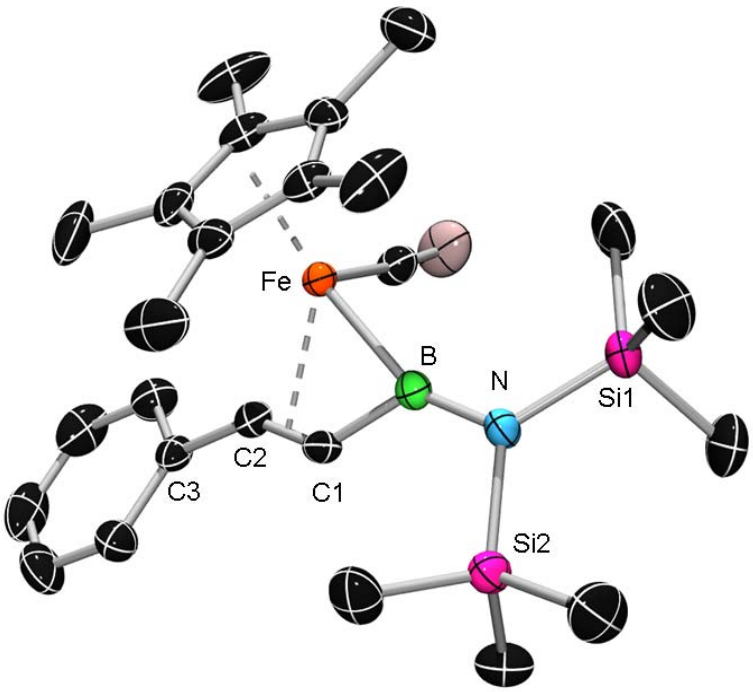

Fig. 30 Molecular structure of **75.** Ellipsoids drawn at the 50% probability level. Hydrogen atoms have been omitted for clarity. Relevant bond lengths [Å] and angles [°] for one of two independent molecules in the asymmetric unit, which feature very similar structures: Fe-B 1.9950(17), B-N 1.403(2), B-C1 1.521(2), C1-C2 1.268(2), C2-C3 1.453(2); Fe-B-N 153.59(12), C1-B-N 135.14(14), Fe-B-C1 71.09(9), B-C1-C2 133.98(14), C1-C2-C3 147.34(15), B-N-Si1 123.20(10), B-N-Si2 114.42(10), Si1-N-Si2 121.66(7).

2. Synthesis of [Cp*(OC)$_2$Fe{BN(SiMe$_3$)$_2$}(CCPh)] (**76**)

In order to provide selective access to the dicarbonyl complex **76**, the previously obtained monocarbonyl species **75** was treated with CO. To this end, a deep red solution of **75** in C_6D_6 was kept under an atmosphere of CO at ambient temperature for a couple of hours (Scheme 7). The progress of the reaction was monitored by multinuclear NMR spectroscopy, which revealed gradual consumption of the starting material **75**, and quantitative formation of a new boron-containing compound as indicated by the presence of a new resonance at $\delta_B = 87$ in the ^{11}B NMR spectrum. After workup, **76** was isolated by crystallization from hexanes at –60 °C as an analytically pure, light brown crystalline solid in 52 % yield.

The spectroscopic data confirmed the constitution of **76** in solution. In particular, the aforementioned deshielded ^{11}B NMR resonance of $\delta = 87$ indicates the presence of a metal-bound boryl ligand. Interestingly, the ^{1}H NMR spectrum at ambient temperature shows only one resonance at $\delta = 0.46$ for the nitrogen-bound SiMe$_3$ group, which suggests a reduced rotational barrier around the B-N bond in comparison to that in **75**. This finding is somewhat surprising as hindered rotation about B-N double bonds is well documented for both (amino)boryl complexes of the type [(η^5-C$_5$R$_5$)(OC)$_2$Fe–B(NR$_2$)R'][96] and alkynyl(amino)boranes R(R'$_2$N)B–C≡C–R'[138].

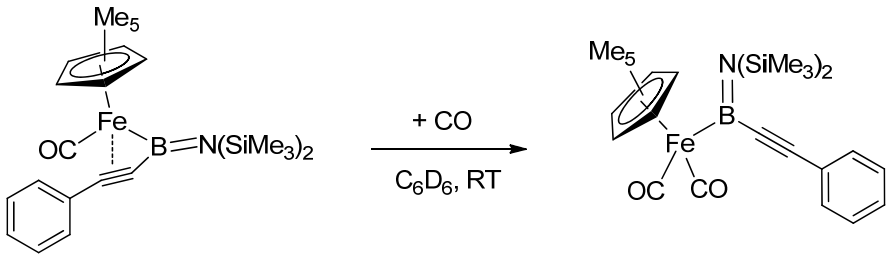

75 **76**

Scheme 7: Synthesis of **76** upon carbonylation of **75**.

The formation of **76** was further confirmed by X-ray diffraction analysis. Suitable single crystals were obtained from a hexane solution at –70°C and the molecule crystallizes in the orthorhombic space group *Pbca*. The major difference between **76** and **75** lies with the almost undistorted geometry of the boryl group in case of the former (Fig. 31). Again, the sum of the angles around boron (359.3°) and nitrogen (358.9°) prove planar coordination geometries for both atoms. However, due to the "free" alkynyl group, the angles Fe-B-C1 (111.64(13)°), Fe-B-N1 (131.84(15)°), and C1-B-N (115.83(16)°) indicate a non-strained, sp^2 hybridized boron atom. The Fe-B separation of 2.075(2) Å is significantly larger than that in **75** and marks the higher end of Fe-B distances commonly observed for neutral half-sandwich boryl complexes

of iron (1.96-2.09 Å)[61]. Furthermore, consistent with the results from ^{1}H NMR spectroscopy, the B-N bond length of 1.444(3) Å resembles that of the iron borirene complex **66** (1.4319(19) Å), and thus suggests a comparable B-N π-interaction.

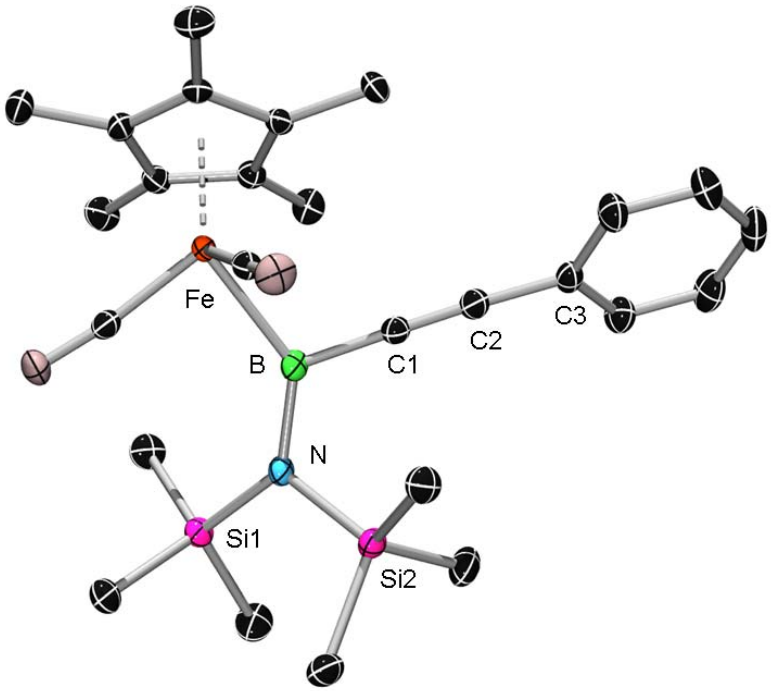

Fig. 31 Molecular structure of **76.** Ellipsoids drawn at the 50% probability level. Hydrogen atoms have been omitted for clarity. Relevant bond lengths [Å] and angles [°]: Fe-B 2.075(2), B1-C1 1.554(3), B-N 1.444(3), C1-C2 1.208(3), C2-C3 1.439(3); Fe-B-C1 111.64(13), Fe-B-N 131.84(15), C1-B-N 115.83(16), B-N-Si1 115.97(13), B-N-Si2 125.21(13), Si1-N-Si2 117.69(9), B-C1-C2 178.4(2), C1-C2-C3 177.0(2).

3. Stepwise iron-boryl-borirene transformation

A light brown C_6D_6 solution of **76** was heated at 80°C under argon in a sealed Young NMR tube, and the reaction was monitored by multinuclear NMR spectroscopy. ^{11}B NMR spectra revealed a gradual consumption of **76** (δ_B = 87) with concomitant formation of **75** (δ_B = 76), and interestingly a small amount of **66** (δ_B = 36). Based on the assumption that part of the thermally dissociated CO was not lost into the gas phase, thus enabling the formation of the borirene(dicarbonyl) complex **66**, the reaction mixture was heated under a dry atmosphere of CO. Multinuclear NMR spectroscopy indicated complete conversion of **75** into **66** within a couple of minutes.

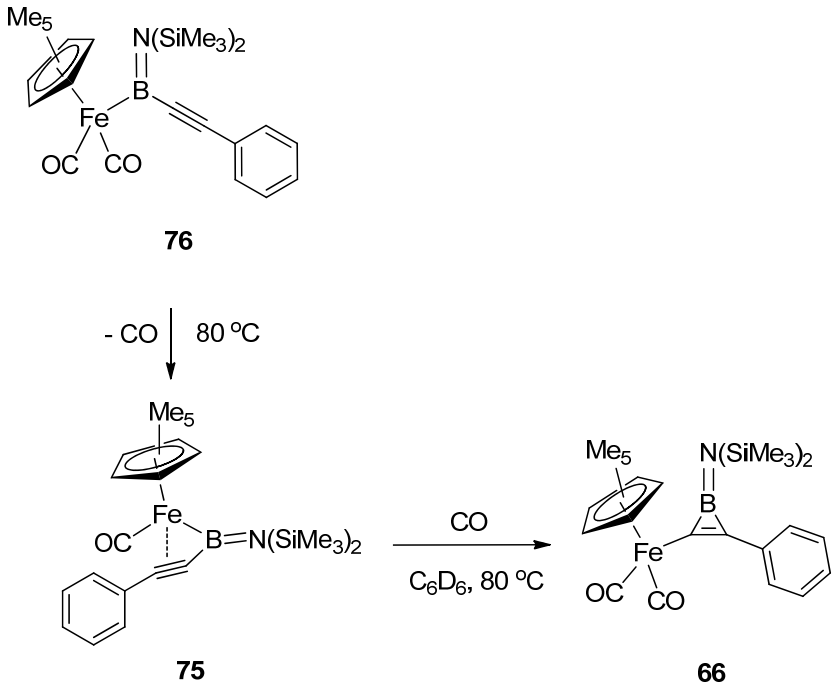

Scheme 8: Stepwise transformation from **76** to **66** under thermal conditions

The thermal conversion of the iron (alkynyl)boryl **76** into the iron borirene **66** is unprecedented in metal boryl/borirene chemistry and suggests that **66** is thermodynamically favoured over **76**, which is confirmed by computational studies of these compounds, i.e. **76** is 12.4 kcal/mol higher in energy than **66**. Similarly interesting is the fact that the isomerization of an alkynylborane into a borirene has been reported by Eisch et al.[114,115] (Fig. 19), although under photolytic conditions. Thus, the thermal reaction depicted in Scheme 8 constitutes a complementary synthetic approach to borirenes.

4. Synthesis of [Cp*(OC)(Me_3P)Fe{*cyclo*-BN($SiMe_3$)$_2$C=CPh}] (**77**)

Being able to generate the key "intermediate" **75** for the synthesis of iron-borirene **66**, we addressed whether this thermally induced isomerization in the presence of CO can be extended to different ligands such as phosphines. Hence, the reaction of a deep red solution of **75** with an equimolar amount of PMe_3 was carried out under analogous conditions (scheme 9). The reaction was monitored by multinuclear NMR spectroscopy, which revealed the complete conversion of **75** into **77** within 1 h as indicated by the presence of a new resonance at δ_B = 38 in the ^{11}B NMR spectrum, and at δ_P = 35.4 in the ^{31}P NMR spectrum. The iron borirene derivative **77** was isolated in the form of yellow crystals by filtration of the reaction mixture and subsequent crystallization from hexanes at –70°C.

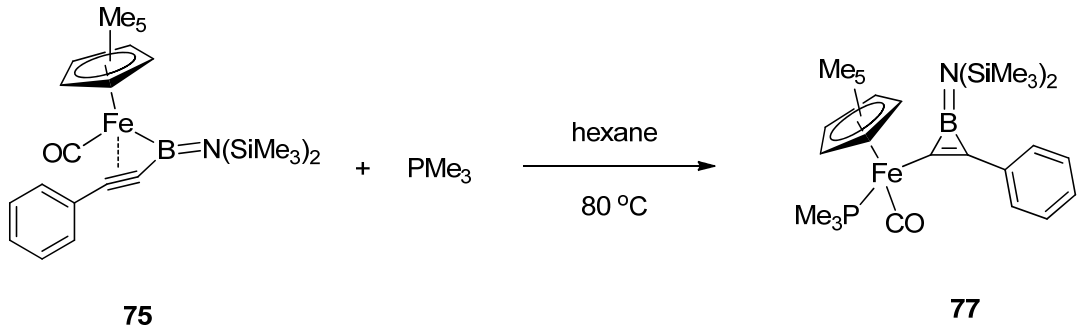

75 **77**

Scheme 9: Synthesis of phosphine complex **77**.

Single crystals of **77** suitable for X-ray diffraction analysis were obtained from a hexane solution at –70°C. The molecule crystallizes in the triclinic space group *P-1* and the overall geometry resembles that of **66**, and is consistent with extensive delocalization of the two π-electrons within the BCC-ring (Fig. 32). Due to the stronger σ-donor ability of the phosphine ligand, the B-C1, C1-C2 and B-N bonds are slightly elongated in comparison to those in **66**. The dihedral angle of 86.69° between the phenyl ring and the boracyclopropene unit is larger than that in **66**, which may be due to the presence of the phosphine ligand and its higher steric demand in comparison to CO.

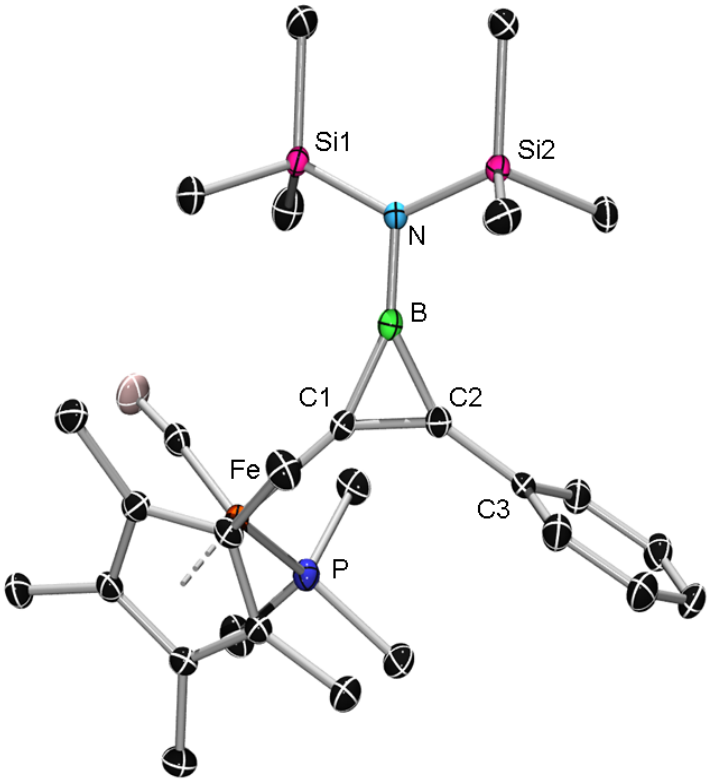

Fig. 32 Molecular structure of **77.** Ellipsoids drawn at the 50% probability level. Hydrogen atoms have been omitted for clarity. Relevant bond lengths [Å] and angles [°]: Fe-C1 1.9727(16), Fe-P 2.1753(5), C1-C2 1.380(2), C1-B 1.506(2), C2-B 1.473(2), C2-C3 1.473(2); B-N 1.443(2), Fe-C1-C2 142.59(12), N-Si1 1.7491(13), N-Si2 1.7475(14); Fe-C1-B 155.98(12), C2-C1-B 61.21(11), C1-C2-B 63.62(12), C1-C2-C3 143.45(15), C3-C2-B 152.57(15), C1-B-N 156.17(15), C2-B-N 148.63(16), B-N-Si1 113.78(11), B-N-Si2 111.46(10), Si1-N-Si2 134.23(8)

5. Postulated reaction mechanism of thermic borylene transfer

In view of the above results, the following reaction mechanism (Fig. 33) is assumed. Presumably, the borylene moiety was inserted into the iron-carbon σ-bond in the first step, leading to an iron-boryl complex **76**. Subsequently, accompanied with CO dissociation, the alkynyl was activated by side-on coordination to the iron center. Finally the thermodynamically favored borirene was generated via a boryl-borirene rearrangement. Iron-carbon bond activation, CO-dissociation and carbonylation appear to be involved in this process, which might explain the inertness of [Cp*(dppm)Fe(C≡CPh)] (**73**) that lacks carbonyl ligands. Furthermore, as mentioned in *2.1.1.1*, a weak signal at δ_B = 76 in the ^{11}B NMR spectrum was observed in addition to the borirene-signal at δ_B = 36, which could be another proof for this postulated mechanism. In this case, the ^{11}B resonance at 76 ppm is presumably the corresponding iron boryl complex with a side-on coordinated alkynyl **75**, which requires an equimolar amount of CO to be converted into iron-borirene **66**. Because the released CO in reaction vessel could not all be recycled, small amount of residue **75** were observed.

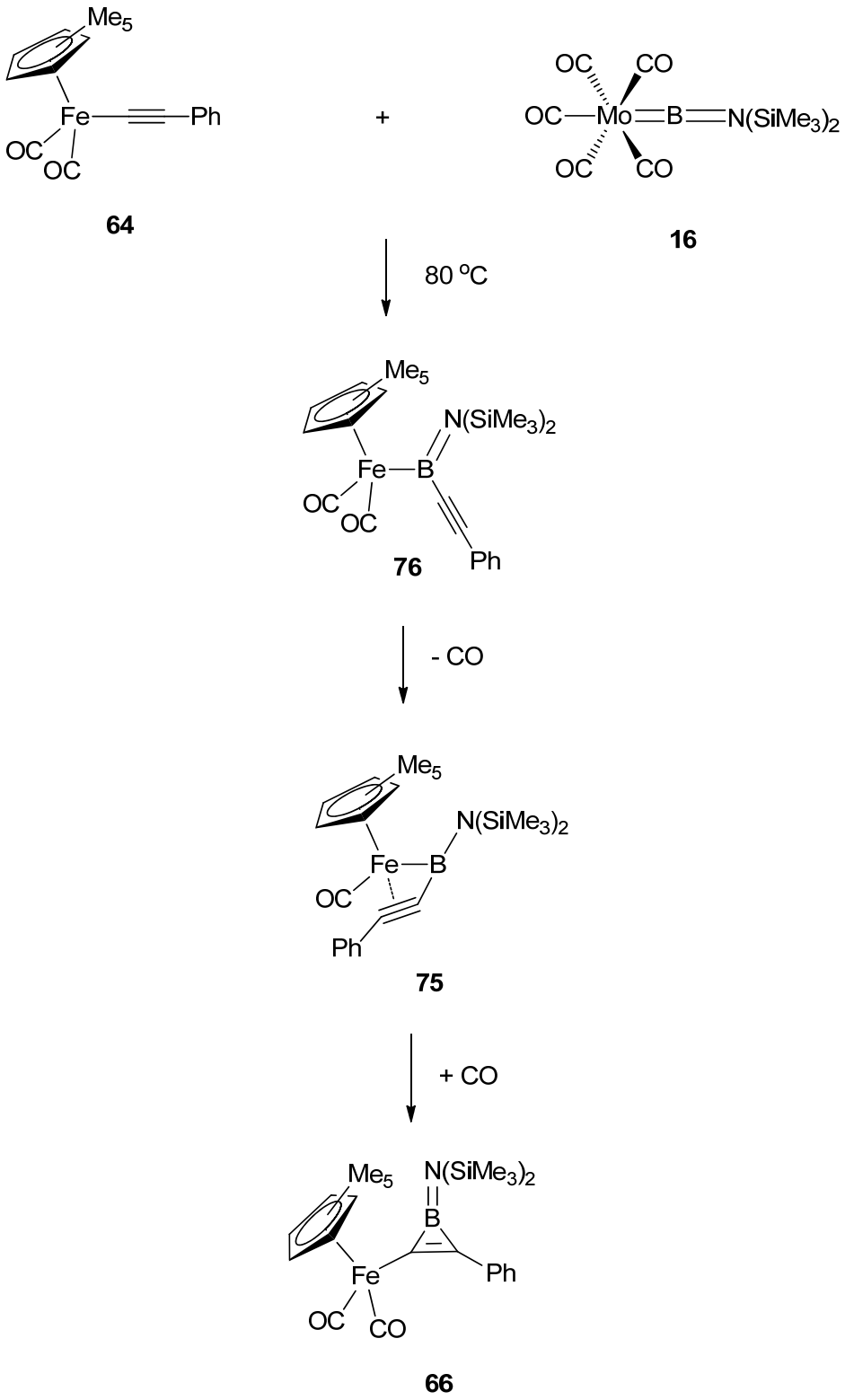

Fig. 33 Postulated reaction mechanism.

2.1.2.2 Reaction of [Cp*(OC)$_2$Fe{*cyclo*-BN(SiMe$_3$)$_2$C=C}Ph] (**66**) with HCl

The *exo*-amino group of the borirenes obtained by borylene transfer provides steric shielding as well as a certain amount of B-N π-contribution. Substitution of the amine function with halogens (e.g. Cl and Br), would not only introduce altered properties of the borirene ring, e.g. enhanced 2π-electron delocalization, but also provide access to a wide variety of new boracyclopropene derivatives.

To this end, iron-substituted borirene **66** was treated with equimolar amount of HCl at –60°C. After slowly warming the reaction mixture to ambient temperature, ^{11}B NMR spectroscopy revealed a fairly weak new signal at δ_B = 45 that is somewhat downfield-shifted compared to **66**. In addition, the presence of several signals in the range for Cp* in the ^{1}H NMR spectrum indicated that **66** had mainly decomposed. However, the conspicuous singlet at 8.99 ppm implied the presence of an olefinic proton, thus suggesting that a ring-opening reaction had taken place (Scheme 10). Unfortunately all attempts to isolate the ring-opening product **78** failed. In fact, borirenes that are substituted exclusively by organic functionalities are known to undergo ring-opening reactions by cleavage of one endocyclic B-C bond, initiated by weak Brønsted acids such as water, methanol, ethanol,[115] or by hydroboration with 9-BBN.[139]

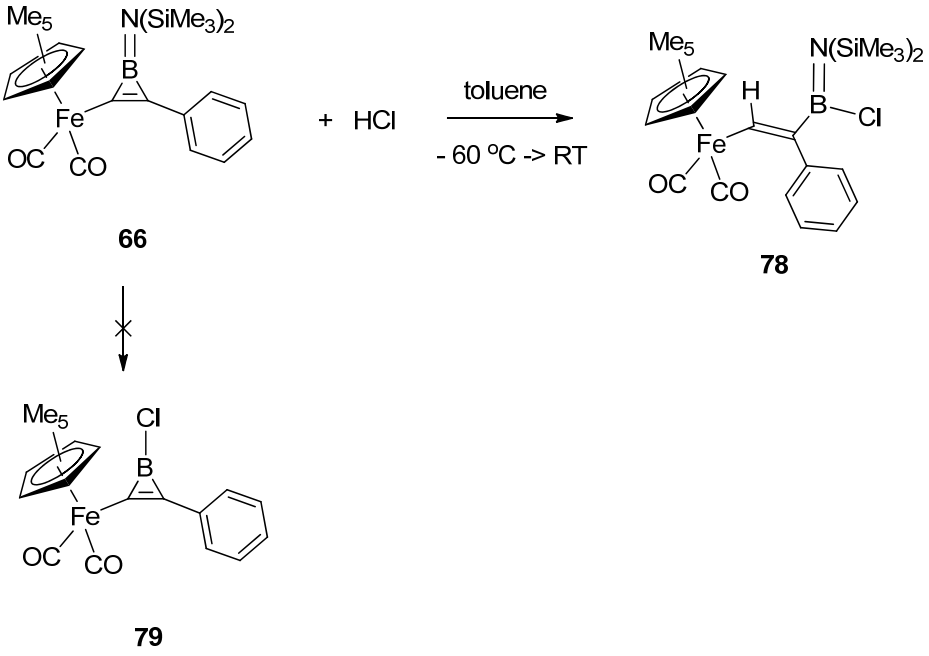

Scheme 10: Reaction of [Cp*(OC)$_2$Fe{*cyclo*-BN(SiMe$_3$)$_2$C=C}Ph] (**66**) with HCl.

2.1.3 Attempt to synthesize chloroborirene by iron-boryl-borirene transformation

As the Cp*Fe(CO)$_2$-substituted (alkynyl)boryl complex **76** undergoes boryl-borirene transformation under thermal conditions, we addressed whether this unprecedented reaction could be utilized as a synthetic approach to otherwise synthetically challenging cholorborirenes (Fig. 34).

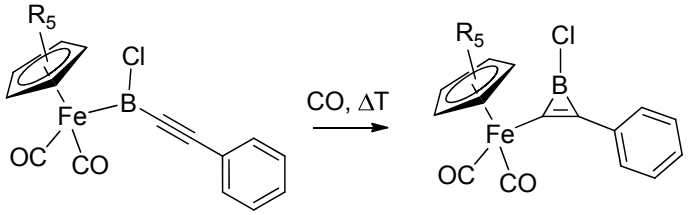

Fig. 34 Proposed synthesis of chloroborirenes.

In order to synthesize the (alkynyl)boryl precursor **80**, the anionic complex **81** was treated with approximately 1 equiv. amount of in-situ generated **82** at –60°C (Scheme 11, above). After slowly warming the reaction mixture to ambient temperature, no signal could be observed in the ^{11}B NMR spectrum. ^{1}H NMR spectroscopy revealed mainly the dimerization of the CpFe(CO)$_2$ fragment. Similar spectroscopic data were obtained upon the reaction of iron-boryl **5** with an equimolar amount of **83**.

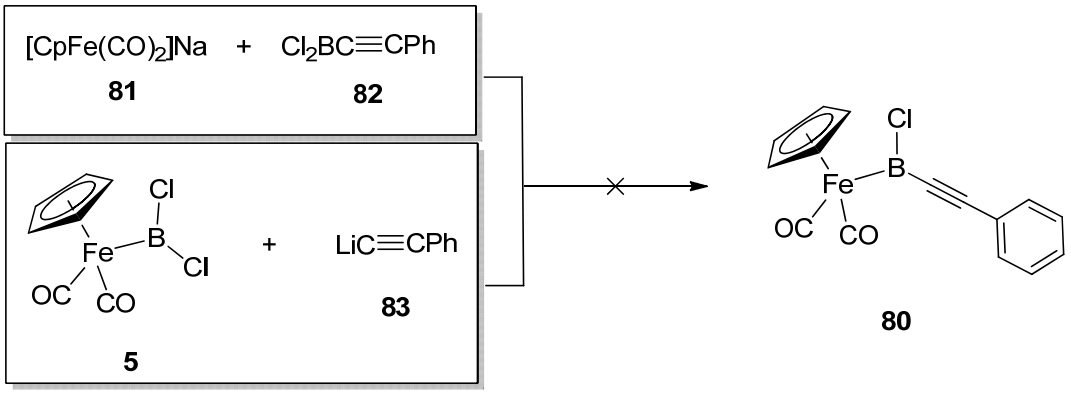

Scheme 11: Attempt to synthesize the iron-boryl complex **80**.

2.1.4 Borylene transfer to platinum alkynyl σ-complexes

2.1.4.1 Reaction of $[(OC)_5Cr{=}BN(SiMe_3)_2]$ (**14**) with $[ClPt(PR_3)_2C{\equiv}CPh]$ (**84**: R = Me, **85**: R = *n*Bu)

Platinum-substituted borirene **86** was obtained upon irradiation of a pale yellow THF solution of **14** in the presence of an equimolar amount of platinum alkynyl complex **84** for 7 h at room temperature (Scheme 12). The reaction was monitored by multinuclear NMR spectroscopy, which revealed gradual consumption of the starting materials and quantitative formation of a new boron- and phosphorus-containing compound, as indicated by the presence of a new resonance at δ_B = 32.0 in the ^{11}B NMR spectrum and at δ_P = -16.2 ($^1J_{Pt,P}$ = 3377) in the ^{31}P NMR spectrum. The former signal falls in the expected range for a borirene product. After workup, **86** was isolated as an analytically pure, colorless solid in 53% yield. The constitution of **86** was confirmed by multinuclear NMR spectroscopy and X-ray structure analysis. At ambient temperature, the ^{1}H NMR signal of the nitrogen bound $SiMe_3$-groups appears as a singlet, implying rapid rotation around the B-N bond. However, at –75°C the ^{1}H NMR spectrum clearly shows two signals for the nitrogen-bound trimethylsilyl groups, which are separated by 40 Hz. From 500 MHz VT ^{1}H NMR spectroscopy, the barrier to rotation about the boron-nitrogen bond was obtained with a value of $\Delta G^{\neq}$ = 45.2 kJ/mol at the coalescence temperature of –55°C, which is in good agreement with previously reported data for borirenes with a conjugated spacer [1,4-bis-{*cyclo*-$BN(SiMe_3)_2(SiMe_3C{=}C)\}_2C_6H_4$] (38.7 kJ/mol) and the bis(borirene) [{*cyclo*-$BN(SiMe_3)_2(SiMe_3C{=}C)\}_2$] (43.1 kJ/mol).[117] These values are signifcantly smaller than those commonly observed for aminoboranes of the general formula $R_2N{=}BR_2$ (71 - 100 kJ/mol),[140] thus supporting the presence of 2π aromatic stabilization within the ring system, which reduces the B-N π-contribution.

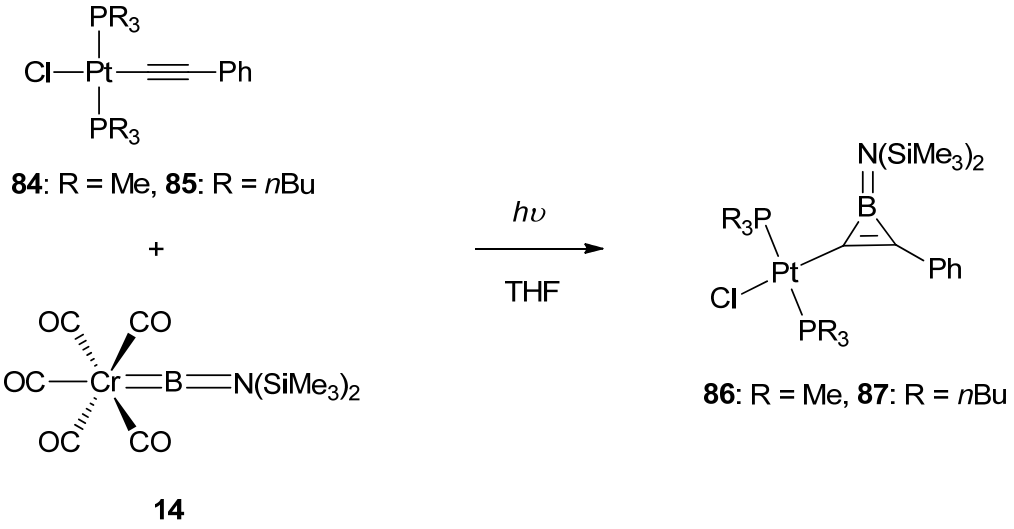

Scheme 12: Synthesis of borirene **86** and **87**.

Single crystals of **86** were grown from hexane via evaporation at room temperature. The molecule crystallizes in the monoclinic space group $P2_1/c$ with two independent molecules in the asymmetric unit, which feature very similar structures (Fig. 35). The bond lengths within the ring system (C2-B = 1.482(8) Å, C1-B = 1.511(8) Å, C1-C2 = 1.374(7) Å) and the exo-B-N separation (1.428(7) Å) are comparable to those of previously reported structurally characterized aminoborirenes, which indicates the extensive delocalization of the two electrons over a three-center, bonding molecular orbital comprised of the p_z-atomic orbitals of boron and carbon,[105,116,117] and thus a reduced π interaction between the boron and nitrogen centers, which is consistent with the observation in VT ^{1}H NMR experiments as well. The distance between Pt and the sp^2-hybridized C1 (1.974(5) Å) is slightly elongated in comparison to that between Pt and the *sp*-hybridized carbon in *trans*,*trans*-[$(Ph_3P)_2$(Cl)Pt-C≡C-Pt$(PPh_3)_2$(Cl)] (1.958(4) Å)[141], which can be explained by increased *p*-character on C1.

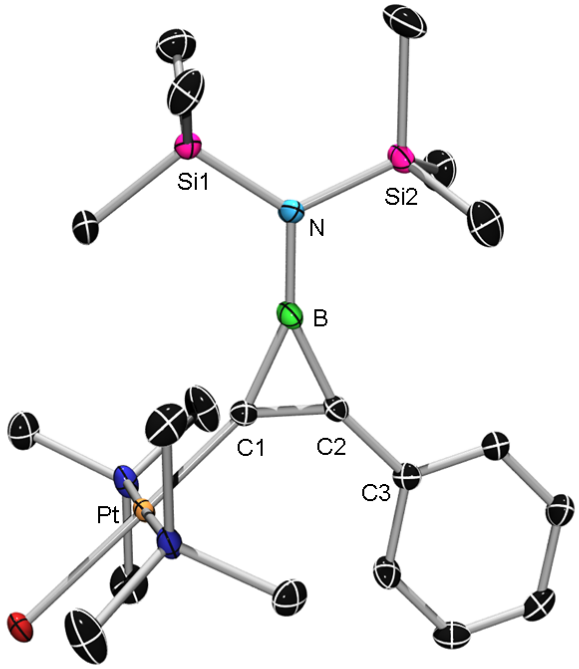

Fig. 35 Molecular structure of **86** in the solid state. Ellipsoids drawn at the 50% probability level. Hydrogen atoms have been omitted for clarity. Relevant bond lengths [Å] and angles [°] for one of two independent molecules in the asymmetric unit, which feature very similar structures: C1-C2 1.374(7), C1-B 1.511(8), C2-B 1.482(8), B-N 1.428(7), Pt-C1 1.974(5), C2-C3 1.466(7); C1-C2-B 63.7(4), B-C1-C2 61.6(4), C1-B-C2 54.6(3), C1-B-N 153.9(5), C2-B-N 151.4(5), B1-C1-Pt 157.3(4), C2-C1-Pt 140.9(4), B-N-Si1 119.3(4), Si1-N-Si2 125.2(3).

UV-vis spectra of the Pt alkynyl precursor **84** and the borirene **86** were recorded in hexane solution (Fig. 36). While UV-vis spectra of **84** exhibit similar absorption bands between 250 and 300 nm with vibronic contributions particularly of the C≡CPh ligand to those of analogous platinum-alkynyl compounds reported in the literature,[142-145] spectra of the platinum-borirene **86** display broad, featureless absorptions with maxima occouring at higher energies. Furthermore, most likely due to the organometallic substituent, the absorption maximum (λ_{max} = 247 nm) of **86** is somewhat blue-shifted with respect to those of previously reported main-group borirene compounds (257 - 276 nm).[117]

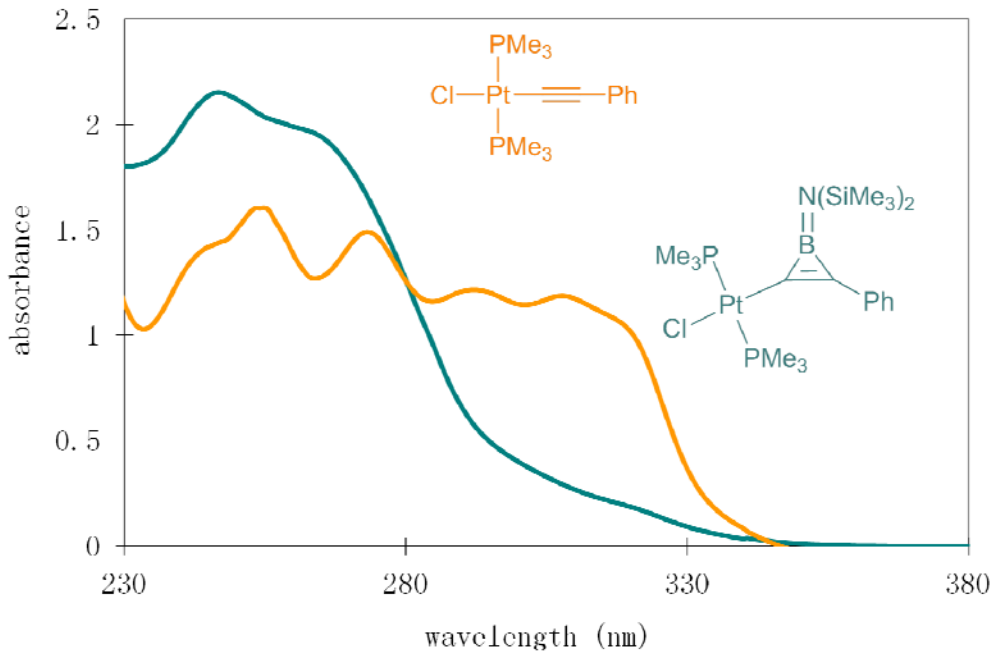

Fig. 36 UV-visible spectra of compounds **84** and **86** in hexane.

The fragment *trans*-$PtL_2(C{\equiv}C)$ is an important building block for oligomeric or polymeric chains, which are of particular interest as substrates for borylene transfer reactions. One possibility to tune the properties such as the solubility of alkynyl precursors as well as those of metal-borirenes is the variation of L. To this end, the sterically more demanding phosphine ligand P(*n*Bu)$_3$ was employed, which might increase the solubility of the corresponding compounds.

The reaction of **85** with **14** was carried out under identical conditions as those applied for synthesis of **86**. The conversion of **14** into **87** was indicated by the presence of a new resonance at $\delta_B = 33$ in the ^{11}B NMR spectrum and at $\delta_P = 6.4$ ($^1J_{Pt,\,P} = 2763$) in the ^{31}P NMR spectrum. The former signal is in good accord with **87**. In addition, presumably due to steric reasons, the reaction is much slower: complete conversion required 30 h. Unfortunately, as a result of the oily consistency, **87** could not be isolated by crystallization.

2.1.4.2 Reaction of [(OC)$_5$Cr=BN(SiMe$_3$)$_2$] (**14**) with [1,4-{ClPt(PEt$_3$)$_2$C≡C}$_2$(C$_6$H$_4$)] (**88**)

The reaction of [1,4-{ClPt(PEt$_3$)$_2$C≡C}$_2$(C$_6$H$_4$)] (**88**) in the presence of 2 equiv. of [(OC)$_5$Cr=BN(SiMe$_3$)$_2$] (**14**) was carried out under identical reaction conditions to those applied in 2.1.2.1. Multinuclear NMR spectroscopy revealed gradual consumption of the

starting materials and nearly quantitative formation of a new boron- (δ_B = 34) and phosphorus-containing (δ_P = 13.0, $^1J_{Pt,\,P}$ = 2768) compound. The ^{11}B resonance falls in the expected range for borirene compounds. Moreover, in respect that only one new signal was observed in the ^{31}P NMR spectrum, the formation of monofunctionalized product can be excluded, thus indicating the formation of the expected bis(borirene) **89**. After workup, **89** was isolated as an analytically pure, light yellow solid in 34% yield. The constitution of **89** was confirmed by multinuclear NMR spectroscopy and X-ray structure analysis. Notably, its ^1H NMR spectrum displayed only one singlet at δ_H = 8.65 for the central aromatic spacer, which is in agreement with the expected symmetric structure of **89**. In addition, the extensive 2π electron delocalization within the borirene-unit was again indicated by the singlet (δ_H = 0.53) for the nitrogen bound $SiMe_3$ groups and the similar endocyclic and exocyclic bond distances in comparison to those of **86**. Most remarkably, while the previously reported bis(borirene) with a conjugated π-spacer [1,4-bis-{(*cyclo*-(BN(SiMe$_3$)$_2$)(SiMe$_3$C=C)}$_2$C$_6$H$_4$] (**90**) that differs from **89** only by the terminal substituent, i.e. trimethylsilyl instead of ClPt(PEt$_3$)$_2$, posesses a dihedral angle of 56.2° between the phenyl ring and the borirene ring,[117] the platinum-capped bis(borirene) **89** features coplanarity of the π-system (Fig. 37, below). Hence an extended π-electron delocalization throughout the conjugated rings is probable.

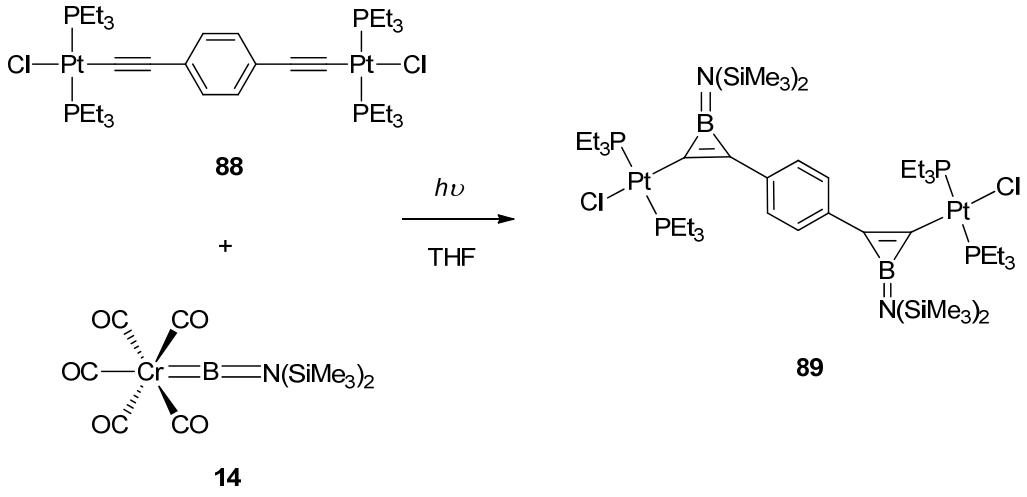

Scheme 13: Synthesis of bisborirene **89**.

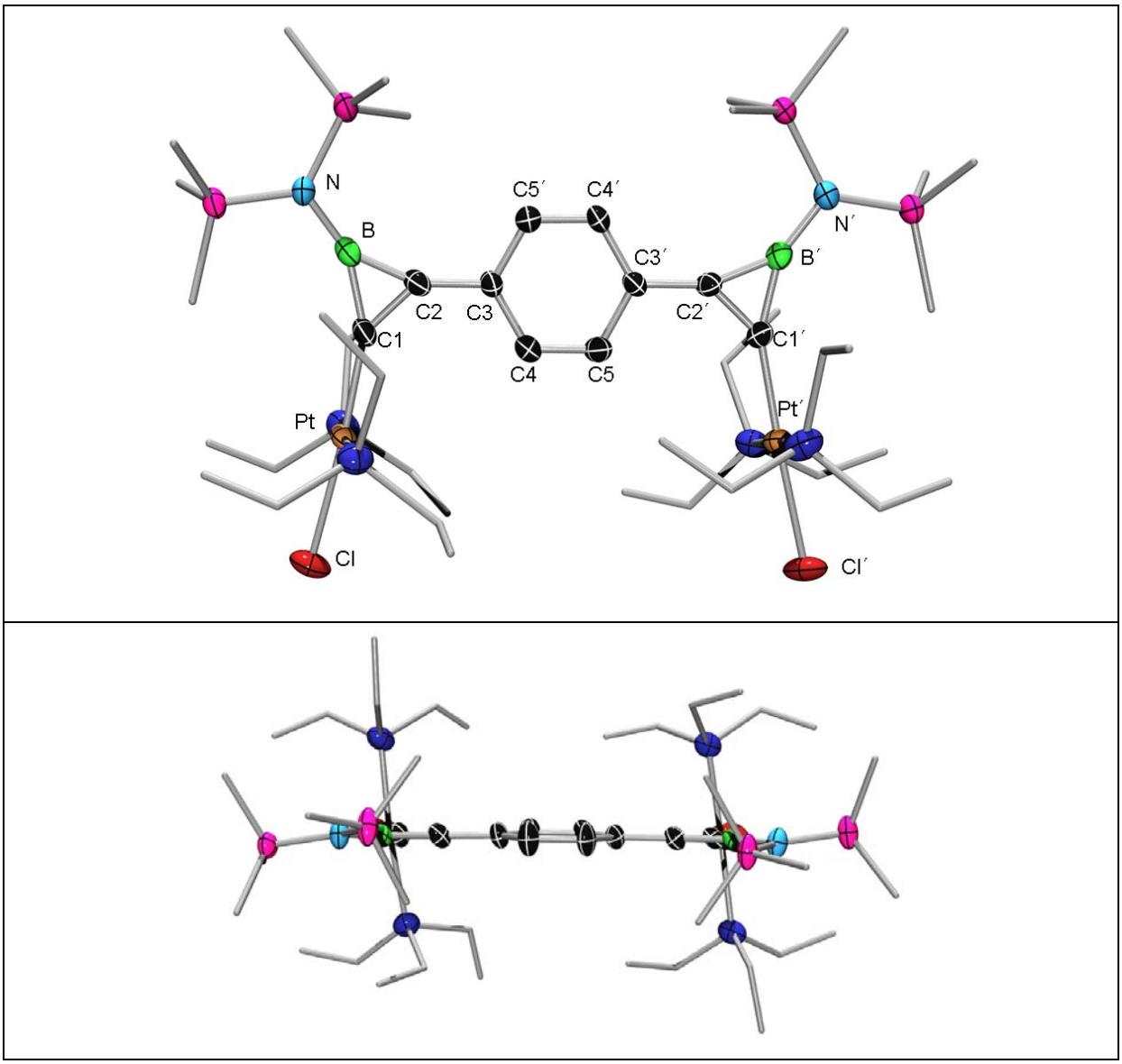

Fig. 37 Molecular structure of **89**. Ellipsoids drawn at the 50% probability level. Hydrogen atoms have been omitted for clarity. Relevant bond lengths [Å] and angles [°]: Pt-C1 1.972(6), C1-C2 1.370(8), C2-C3 1.463(9), C3-C4 1.388(9), C4-C5 1.381(9), C5-C3' 1.401(8), C3'-C2' 1.466(9), C2'-C1' 1.361(9), C1'-Pt' 1.966(6), C1-B 1.502(10), C2-B 1.476(11), C2'-B 1.467(10), C1'-B' 1.478(9), B-N 1.409(10), B'-N' 1.438(9); C1-C2-C3-C5' -176.5(8), C4'-C3'-C2'-C1' 177.5(8).

UV-vis spectra of the Pt-capped bis(borirene) **89** were recorded in toluene solution (Fig. 38). Analogous to those of reported aminoborirenes, spectra of **89** display broad, featureless absorptions. However, the absorption maxima occurring at 314 nm is remarkably red-shifted with respect to those of the previously reported main-group borirene compounds (257 - 276 nm),[117] as well as the platinum-subsituted monoborirene **86** (λ_{max} = 247 nm). This finding is in good agreement with our assumption that the π electrons of the conjugated and coplanar rings are extensively delocalized over the molecular orbital comprised of the p_z-atomic

orbitals of boron and carbon. In addition, potential participation of platinum *d* orbitals in the delocalized π system prompted us to investigate the electronic structure of **89** computationally.

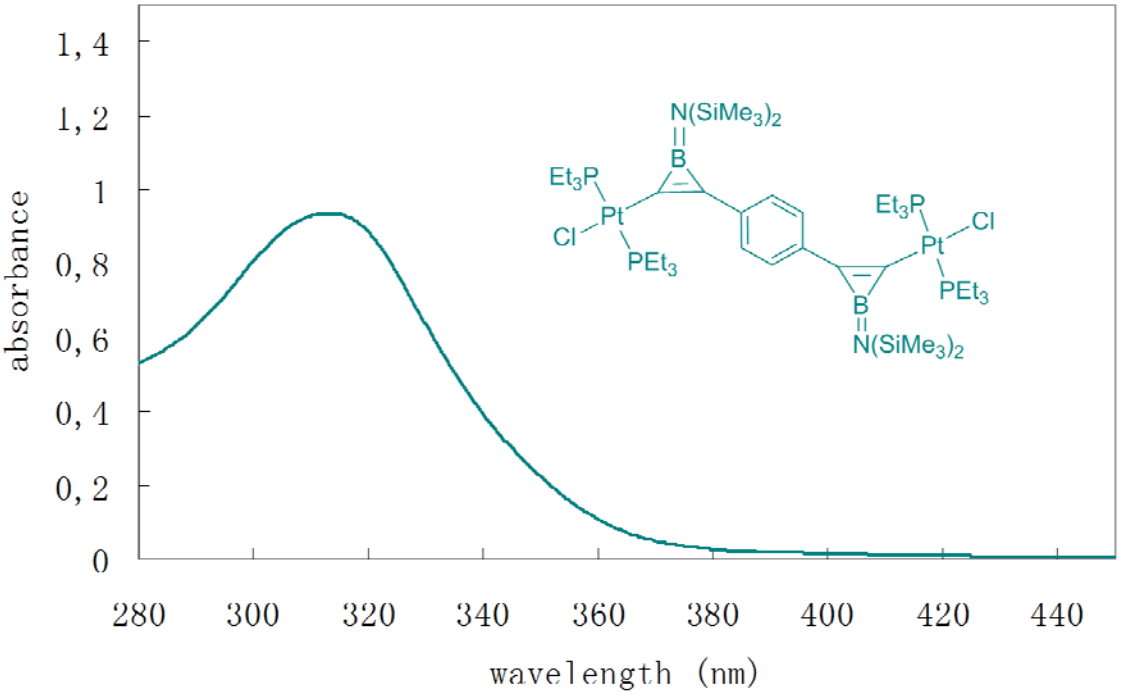

Fig. 38 UV-visible spectra of **89** in toluene.

2.1.4.3 Reaction of $[(OC)_5Cr{=}BN(SiMe_3)_2]$ (**14**) with *trans*-$[Pt(PEt_3)_2(C{\equiv}CPh)_2]$ (**91**)

We then sought to functionalize the oligomeric or polymeric chain $[1\text{-}\{(Et_3P)_2PtC{\equiv}C\}\text{-}4\text{-}(C{\equiv}C)\text{-}(C_6H_4)]_n$ by borylene transfer, in order to address the following questions: i) can the borylene unit be transferred onto an alkynediyl ligand bridging two metals (see *2.1.4.2*); ii) can the borylene unit be transferred onto two alkynyl functions bound to a single metal. To this end, a C_6D_6 solution of **91** was irradiated in the presence of 2 equiv. of $[(OC)_5Cr{=}BN(SiMe_3)_2]$ (**14**). ^{11}B NMR spectroscopy revealed a gradual conversion of the starting material **14** into new boron-containing compounds displaying a broad peak at 37 ppm, which falls in the expected range for borirenes. However, three new sets of signals (δ_P = 9.89, $^1J_{Pt,\,P}$ = 2596, **92**; 5.93 and 5.88, $^1J_{Pt,\,P}$ = 2761, **93** and **94**) in the ^{31}P NMR spectrum and three corresponding signals for trimethylsilyl groups (δ = 0.51, s, **92**; 0.57 and 0.59, s, **93** and **94**) in the ^1H NMR spectrum were observed. Upon further irradiation (16 h), a conversion of the

former set of signals into the latter two sets of signals was observed, thus suggesting monoborirene **92** as an intermediate for the reaction. Moreover, the ratio of the latter two sets of signals remained 1:1. Following these informations, it became obvious that the intermediate is most likely the mono-functionalized product **92**. Furthermore, the boron atoms of the borirene rings can adopt mutual *trans* or *cis* disposition with respect to the C-Pt-C linear skeleton, whose rotation is hindered by congestion between bulky trimethylsilyl groups and PEt_3 ligands. As a result, concomitant formation of both conformations occurred. After workup, crystals containing **93** and **94** in a ratio of 1:1 were obtained. Whereupon, X-ray structure analysis for **94** confirmed its chemical constitution. However, due to the poor data quality, detailed discussion with regard to structural parameters was impossible. Unfortunately, all attempts to isolate both isomers **93** and **94**, as well as to measure the crystal structure of **93** failed.

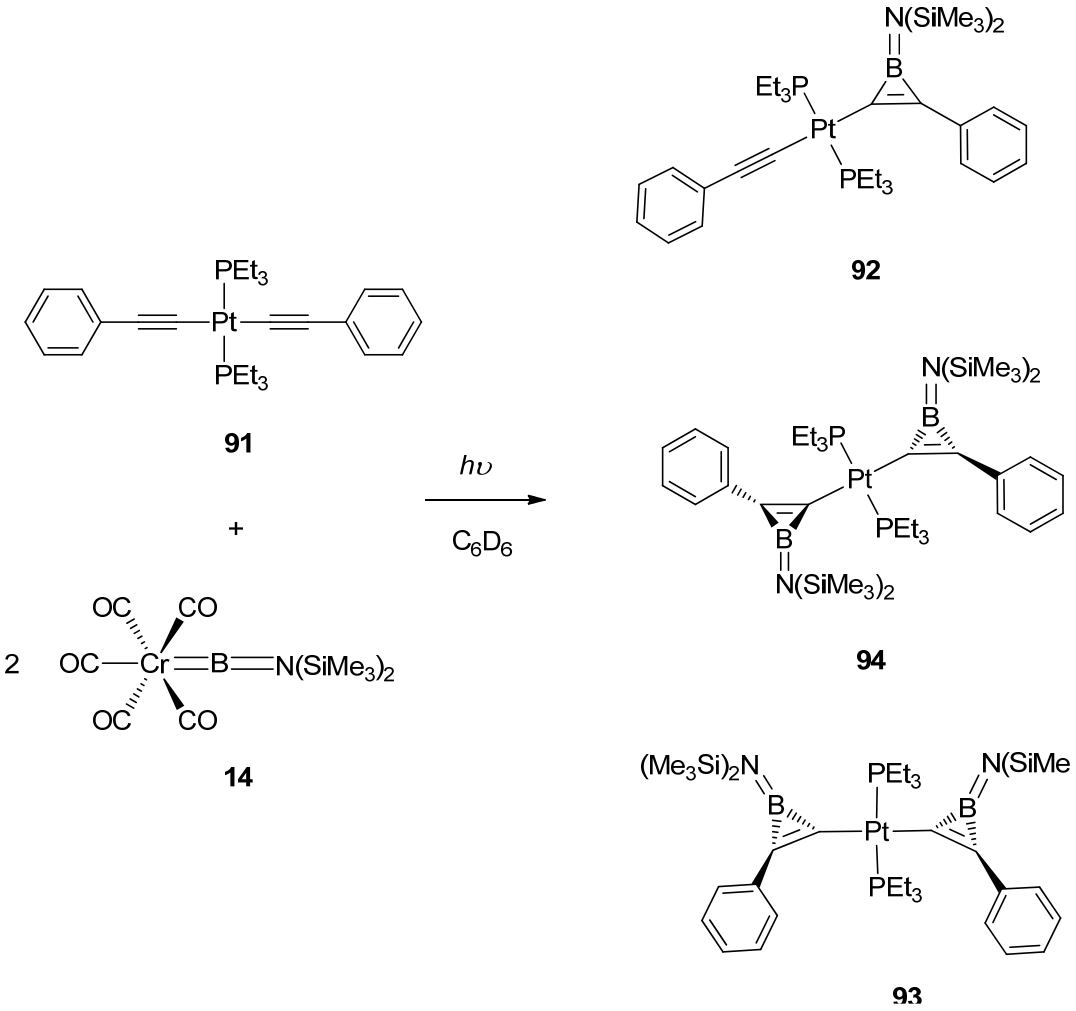

Scheme 14: Reaction of $[(OC)_5Cr{=}BN(SiMe_3)_2]$ (**14**) with *trans*-$[Pt(PEt_3)_2(C{\equiv}CPh)_2]$ (**91**).

2.1.5 Reactivity investigation of platinum-substituted borirenes

2.1.5.1 Platinum-borirene-boryl transformation

A yellow C_6D_6 solution of the platinum borirene *trans*-[$(Me_3P)_2PtCl${*cyclo*-$BN(SiMe_3)_2C{=}CPh$}] (**86**) was irradiated at room temperature (Scheme 15). The reaction was monitored by multinuclear NMR spectroscopy, which revealed gradual consumption of the starting materials and the quantitative formation of a new boron- and phosphorus-containing species with ^{11}B and ^{31}P NMR resonances at δ_B = 49 and δ_P = 15.8 ($^1J_{Pt,P}$ = 3085), respectively. However, in contrast to the photoisomerization of the related iron borirene, which was accompished within 5 hours, full conversion of platinum borirene **95** required 4 days.

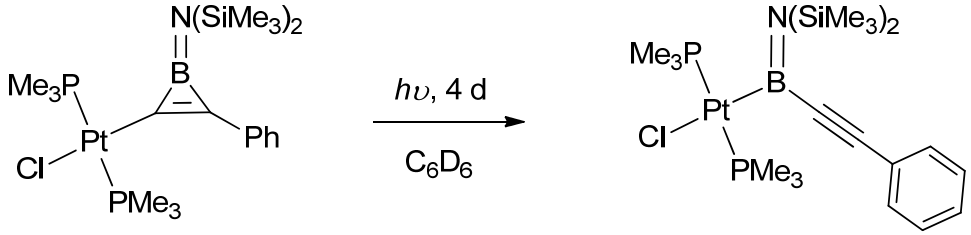

86 **95**

Scheme 15: Photolysis of *trans*-[$Cl(PMe_3)_2Pt${*cyclo*-$BN(SiMe_3)_2C{=}CPh$}] (**86**).

The product of the photochemical rearrangement, the platinum (alkynyl)boryl complex *trans*-[$Cl(PMe_3)_2PtBN(SiMe_3)_2(C{\equiv}CPh)$] (**95**), was isolated by crystallization from a toluene/hexane mixture at –30°C as an analytically pure, colorless crystalline solid in 65% yield. The spectroscopic data of **95** in solution are in good agreement with the proposed structure. In particular, two sharp signals for the nitrogen-bound trimethylsilyl groups at δ_H = 0.64 and 0.70 with a relative intensity of 1:1 in the ^1H NMR spectrum at room temperature indicate a significantly enlarged rotational barrier about the boron-nitrogen bond, which is a consequence of the BCC ring-opening and a more pronounced B=N π-contribution. Furthermore, the resonance at δ_B = 49 in the ^{11}B NMR spectrum falls in the expected range for a platinum boryl complex.[146-148] Single crystals of **95** suitable for X-ray diffraction analysis were obtained by cooling a solution of **95** in toluene/hexane to –35°C. Complex **95** crystallizes in the monoclinic space group $P2_1/c$, and a graphical representation of the molecular structure in the solid state is depicted in Fig. 39. Even though the quality of the crystals was satisfactory, extensive disorder of the whole boryl substituent precludes any

detailed discussion of the structural parameters within this moiety. However, the data unambiguously confirm the presence of a square-planar platinum boryl species with the anticipated connectivity derived from spectroscopy in solution.

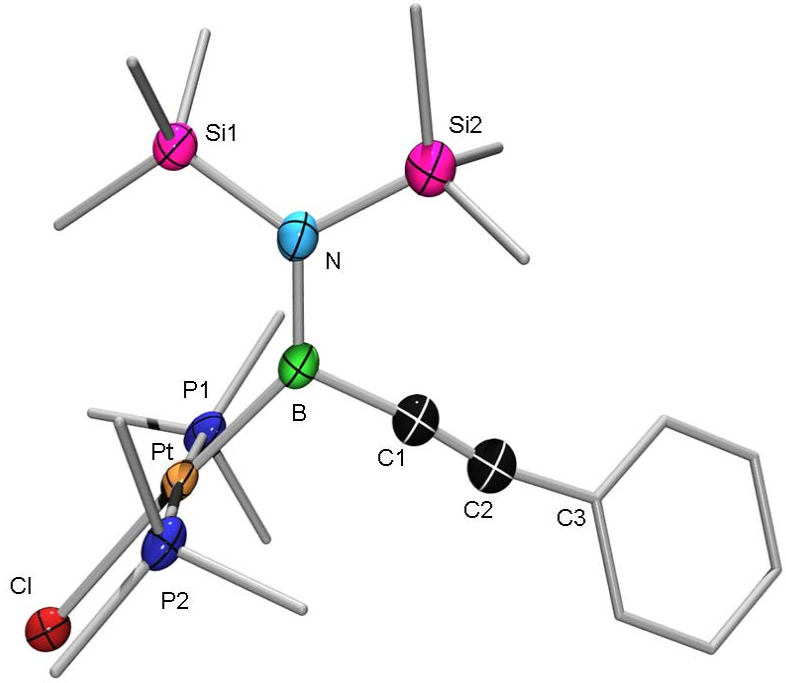

Fig. 39 Molecular structure of **95** in the solid state. Hydrogen atoms, disorder of the boryl substituent, and co-crystallized solvent molecules are omitted for clarity. Due to the extensive disorder of the whole boryl substituent, a discussion of the structural parameters is not possible.

2.1.5.2 Reaction of platinum-borirene (**86**) with HCl

The reaction of **86** with an equimolar amount of HCl was carried out under analogous conditions to those applied in 2.2.2. The ^{1}H NMR spectrum features one triplet at δ = 9.77 ($^{3}J_{P,H}$ = 4.6) for an olefinic proton, thus confirming the boron-carbon bond cleavage. Interestingly, despite the BCC ring-opening, the rotational barrier of the B=N bond is not significantly increased, as indicated by the presence of only one resonance at δ_H = 0.28 for the nitrogen-bound $SiMe_3$ group. Furthermore the ^{11}B NMR resonance at δ_B = 45 is shifted to lower field by 12 ppm in comparison to **86**, which is comparable with that observed in *2.1.2.2*. After workup, **96** was isolated by crystallization from hexane at –30°C as an analytically pure, colorless crystalline solid in 38 % yield (Scheme 16).

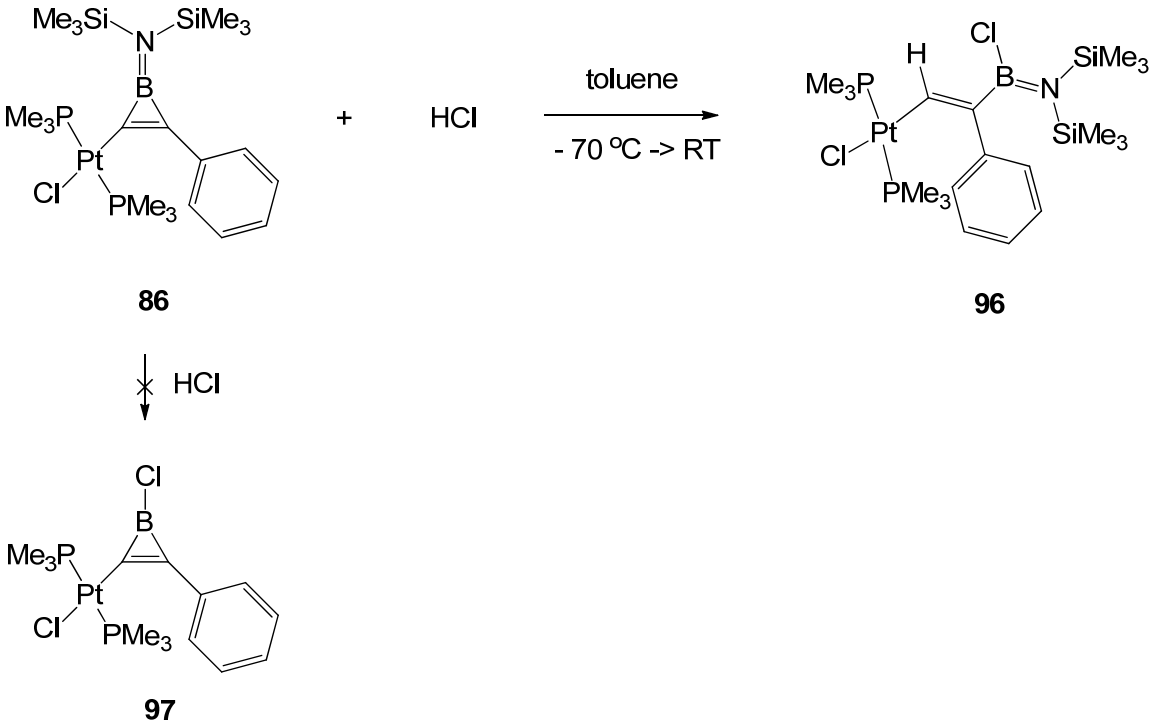

Scheme 16: Ring-opening of platinum-substituted borirene **86** with HCl.

Single crystals suitable for X-ray diffraction analysis were obtained by cooling a saturated hexane solution of **96** to –35°C. The molecule crystallizes in the monoclinic space group $P2_1/c$ with two independent molecules in the asymmetric unit, both featuring very similar structural parameters (Fig. 40). The results of the X-ray diffraction analysis confirm the C1-B bond cleavage with addition of a proton to C1 and attack of the nucleophile Cl at the boron centre. The C1-C2 distance (1.357(10) Å) and the C2-B distance (1.557(11) Å) are in the expected ranges for C=C double and C-B single bonds, respectively, and are comparable to those determined for the ring-opening product of a metal-free borirene with 9-BBN (C1-C2 1.369(2) Å; C2-B 1.575(2) Å).[139] The sums of angles around B (Σ = 359.9°) and N (Σ = 360.0°) document a planar coordination geometry for both atoms. The B-N separation of 1.424(10) Å is similar to that in **86** (1.428(7) Å). Furthermore, the Si1-N-B-C2 torsion angle of 38.91° suggests a reduced B=N π-contribution, which is presumably a result of an additional Cl-B π-interaction in combination with the pronounced steric congestion imposed by the bulky $N(SiMe_3)_2$ and Ph moieties. Moreover, the cleavage of the B-C1 bond is accompanied by a slight increase of the Pt-C1 separation (**96**: 1.993(7) Å; **86**: 1.974(5) Å).

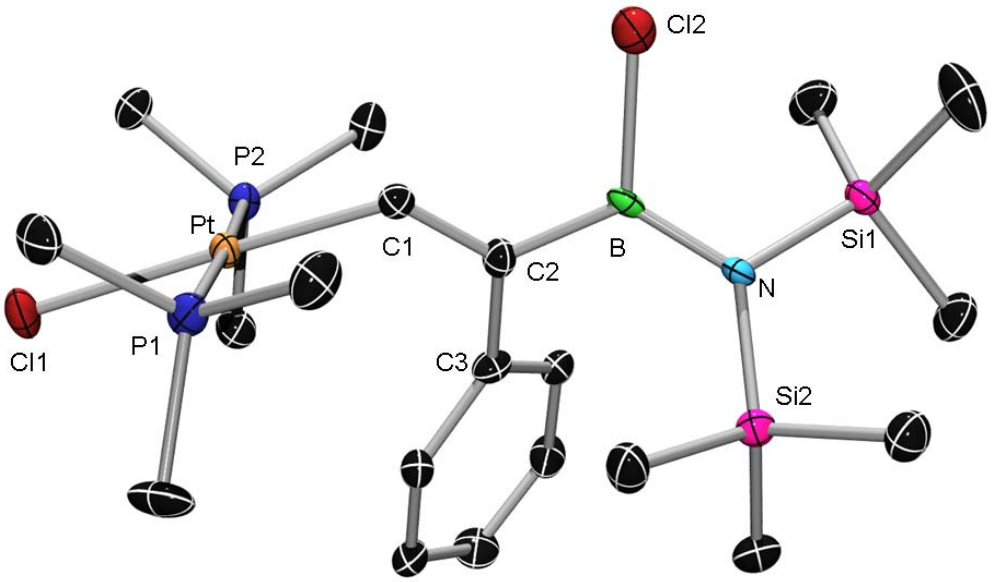

Fig. 40 Molecular structure of **96** in the solid state. Ellipsoids drawn at the 50% probability level. Hydrogen atoms and the second independent molecule in the asymmetric unit are omitted for clarity. Relevant bond lengths [Å] and angles [°]: Pt-C1 1.993(7), C1-C2 1.357(10), C2-B 1.557(11), B-N 1.424(10), C2-C3 1.505(10), B-Cl2 1.810(9); C2-B-Cl2 114.7(6), C2-B-N 128.0(7), N-B-Cl2 117.2(6), B-N-Si1 121.1(5), B-N-Si2 118.3(5), Si1-N-Si2 120.6(3), C1-C2-C3 120.6(7), B-C2-C3 117.8(6), B-C2-C1 121.5(7).

2.1.5.3 Reaction of platinum-borirene (**86**) with BBr_3

In addition to HCl, other typical reagents employed to cleave B-N bonds are the trihaloboranes. Hence, a toluene solution of **86** was treated with 1 equiv. of BBr_3 at –70°C. The reaction was monitored by multinuclear NMR spectroscopy, which indicated the formation of a new boron- and phosphorus-containing species featuring resonances at $\delta_B = 33$ and $\delta_P = -19.1$ ppm in the ^{11}B and ^{31}P NMR spectrum, respectively. After workup, an analytically pure, colorless crystalline solid was isolated by crystallization from hexane at –30°C. Unexpectedly, ^{1}H NMR spectroscopy provided clear evidence for the presence of nitrogen-bound trimethylsilyl groups ($\delta_H = 0.47$), which is obviously inconsistent with the anticipated platinum-substituted bromoborirene **99**. Since the chemical shift of the ^{11}B NMR spectrum remains almost unaffected by this chemical transformation, we reasoned that a Cl-Br ligand exchange reaction had occurred with retention of the overall structure of the BCC ring (Scheme 17).

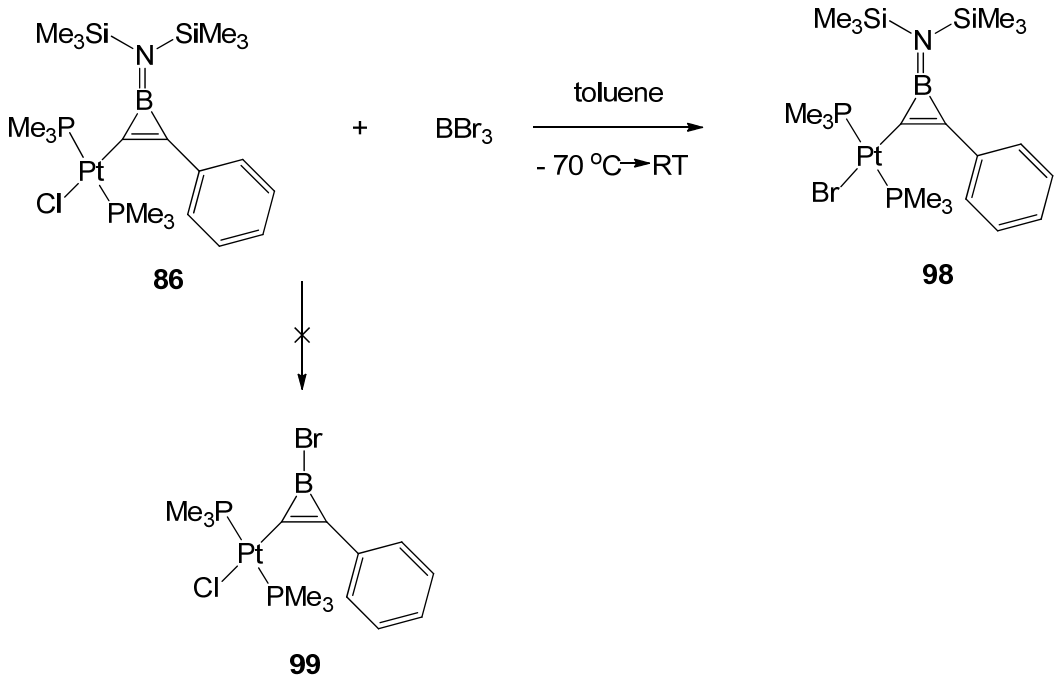

Scheme 17: Reaction of platinum-borirene (**86**) with BBr_3.

The formation of **98** was confirmed by X-ray diffraction analysis (Fig. 41). Complex **98** crystallizes in the monoclinic space group $P2_1/n$. As shown in Table 1, the overall geometry of **98** resembles that of the precursor **86** and the iron-substituted borirenes **66** and **77**, particularly with respect to the lengths of the endocyclic (C1-C2 1.367(4) Å; C1-B 1.485(4) Å; C2-B 1.488(4) Å) and exocyclic bonds (B=N 1.431(4) Å), which suggests extensive 2π-electron delocalization within the BCC ring. In addition, the phenyl ring and the boracyclopropene unit adopt a slightly staggered arrangement, as indicated by a dihedral angle of 9.64°.

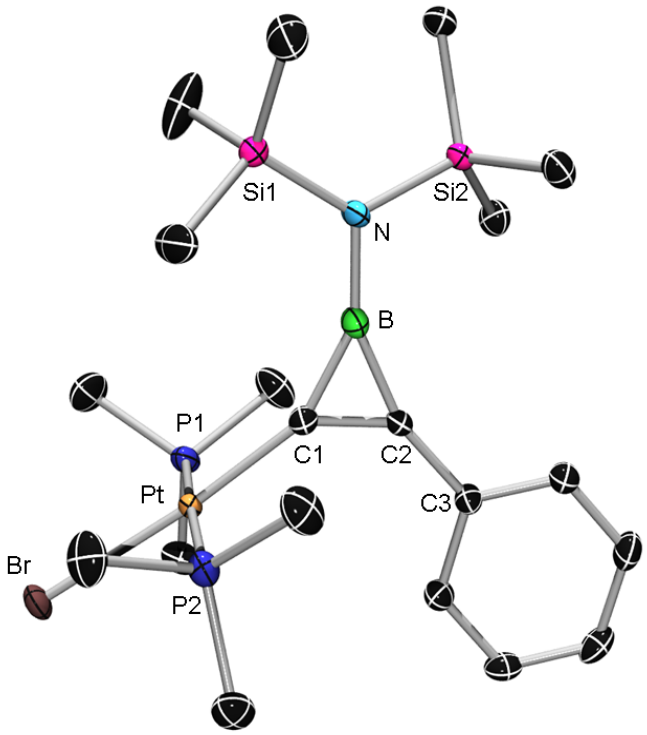

Fig. 41 Molecular structure of **98** in the solid state. Ellipsoids drawn at the 50% probability level. Hydrogen atoms are omitted for clarity. Relevant bond lengths [Å] and angles [°]: Pt-C1 1.970(3), C1-C2 1.367(4), C2-C3 1.462(4), C1-B 1.485(4), C2-B 1.488(4), B-N 1.431(4); Pt-C1-C2 142.2(2), Pt-C1-B 154.8(2), B-C1-C2 62.72(19), C3-C2-C1 135.8(2), C3-C2-B 161.7(2), B-C2-C1 62.53(19), C1-B-C2 54.76(18), N-B-C1 151.0(3), N-B-C2 154.0(3), Si1-N-B 118.21(19), Si2-N-B 114.86(19), Si1-N-Si2 126.90(13).

Table 1 Selected bond lengths [Å] of metal-substituted borirenes:

	86	**98**	**66**	**77**
M-C1	1.974(5)	1.970(3)	1.9826(14)	1.9727(16)
C1-C2	1.374(7)	1.367(4)	1.3631(19)	1.380(2)
B-C1	1.511(8)	1.485(4)	1.501(2)	1.506(2)
B-C2	1.482(8)	1.488(4)	1.474(2)	1.473(2)
B-N	1.428(7)	1.431(4)	1.4319(19)	1.443(2)

2.2 Attempt to synthesize a diazaboracyclopropane by borylene transfer

As an important permutation of small ring heterocycles, diazaboracyclopropanes attracted considerable attention in the 1980s. The synthetic approach to the strained NNB-ring includes salt elimination between lithiated hydrazines and corresponding dihaloboranes, and the ring-closing reaction of hydrazino(halo)borane upon treatment with *t*BuLi (Fig. 42).[149-151] However, the scope of application of the salt elimination protocol is severly limited by the exocyclic substituents, as they must be bulky enough to hinder the formation of thermodynamically favoured 6-membered ring. Alternatively, functionalization of N=N double bond by borylene transfer might provide straightforward access to this class of compounds.

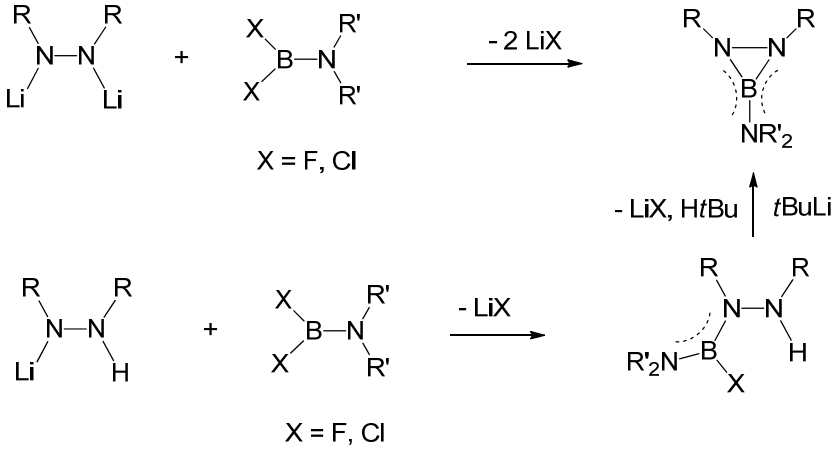

Fig. 42 Reported synthetic approaches to diazaboracyclopropanes.

2.2.1 Reaction of $[(OC)_5Mo{=}BN(SiMe_3)_2]$ (**16**) with azobenzene (**100**)

To avoid unwanted photoisomerization of azobenzene (**100**), the reaction with an equimolar amount of $[(OC)_5Mo{=}BN(SiMe_3)_2]$ (**16**) was carried out under thermal conditions (Scheme 18). The ^{11}B NMR spectrum revealed a complete conversion of **16** into new boron-containing species displaying a broad peak at δ_B = 26 within 3 d. However, ^1H NMR spectroscopy revealed eight signals in the range for nitrogen-bound trimethylsilyl groups, which indicated poor selectivity of the reaction. Moreover, a conspicuous broad singlet peak at δ_H = 4.71 implied the presence of a nitrogen-bound proton (NH). After workup (combination of chromatography and crystallization), the boron- and NH-containing species was isolated from

the product mixture as colorless crystalline solid. According to the results of X-ray structure analysis (Fig. 43), it became obvious that the N-N bond of the expected product **101** was additionally hydrogenatively cleaved (Scheme 18), affording the ring-opening product **102**. Considering that the utilized solvent could be the source of protons, the reaction was carried out as a melt without solvent. However, the characteristic peak at δ_H = 4.71 in the ^{1}H NMR spectrum was still observed.

Triaminoborane **102** crystallizes in in the monoclinic space group *P2$_1$/n*. The boron and nitrogen atoms all adopt a trigonal-planar geometry. The very similar values (1.43-1.46 Å) of all three B-N separations are comparable with those of exocyclic B-N bonds of aminoborirenes, thus suggesting a similarly reduced B-N π-interaction as a result of the competition among the π-donating nitrogen atoms surrounding the central boron atom.

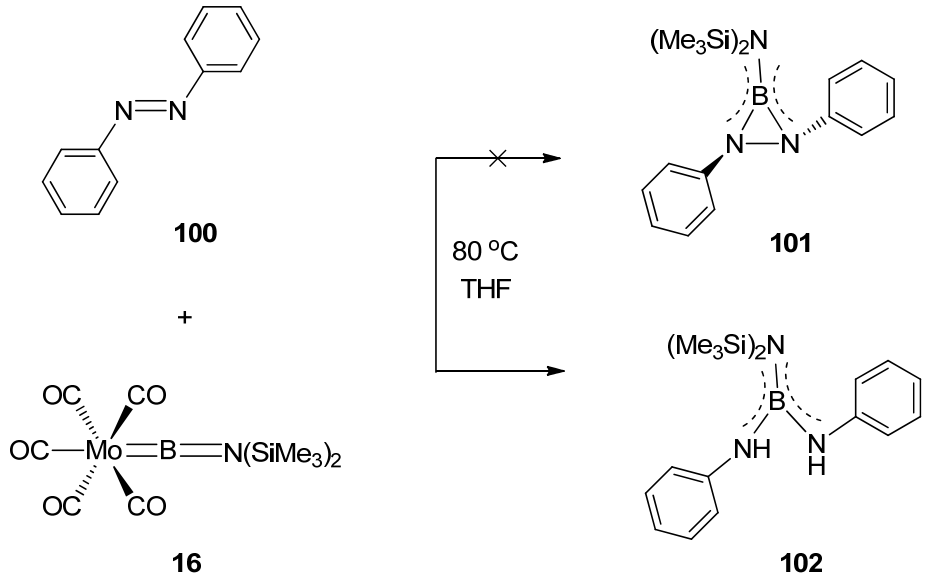

Scheme 18: Reaction of [(OC)$_5$Mo=BN(SiMe$_3$)$_2$] (**16**) with azobenzene (**100**).

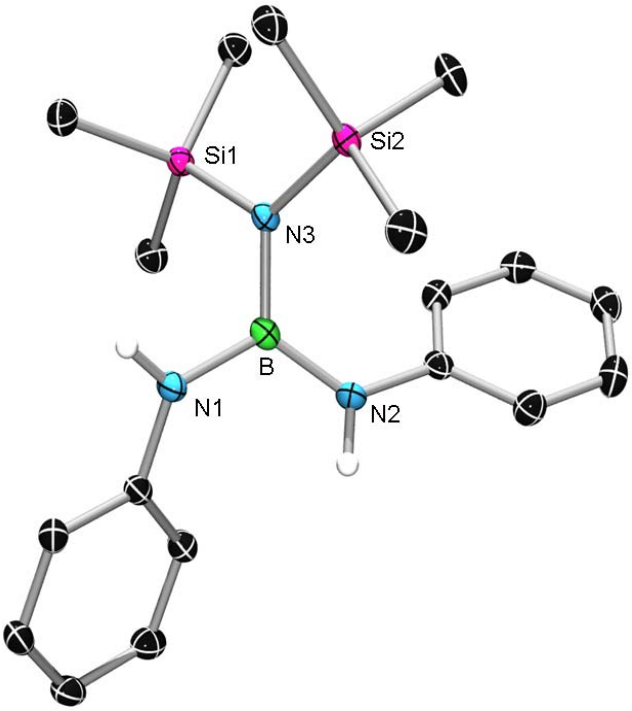

Fig. 43 Molecular structure of **102** in the solid state. Ellipsoids drawn at the 50% probability level. Except for the nitrogen-bound H, hydrogen atoms are omitted for clarity. Selected bond lengths [Å] and angles [°]: B-N1 1.4412(19), B-N2 1.428(2), B-N3 1.4568(18); N3-B-N1 117.74(13), N2-B-N3 123.35(12), N1-B-N2 118.89(12).

2.2.2 Reaction of $[(OC)_5Mo{=}BN(SiMe_3)_2]$ (**16**) with 4-[(*E*)-(4-methylphenyl)diazenyl]phenylamine (**103**)

The reaction was carried out under identical conditions to those applied in *2.2.1*. The complete conversion of **16** required 36 h. However, the selectivity of the reaction was not improved. Moreover, the characteristic NH signal was observed in ^{1}H NMR spectrum, thus indicating the formation of ring-opening product. Unfortunately all attempts to separate and characterize all components of the product mixture failed.

2.3 Synthesis of boracumulene complexes by borylene transfer

Compounds with cumulated double bonds have attracted interest due to their highly unsaturated structure since the first reports of allenes more than a century ago.[152,153] [3]-Cumulene, or butatriene (**II**), consists of three cumulated carbon-carbon double bonds and can potentially coordinate with transition metal (**III**-**V**), however mostly in a η^2-fashion via the central C=C bond (**III**).[154] In 2002 Suzuki reported the coordination of a butatriene to low-valent zirconocene in a novel κ^2-σ,σ bonding mode, the first example of a five-membered metallacycloalkyne (**V**).[155] Interestingly, in some cases, highly reactive butatrienes (e.g. tetrafluorobutatriene, which decomposes slowly even at –80°C) can be trapped and stabilized via transition metal coordination.[156,157]

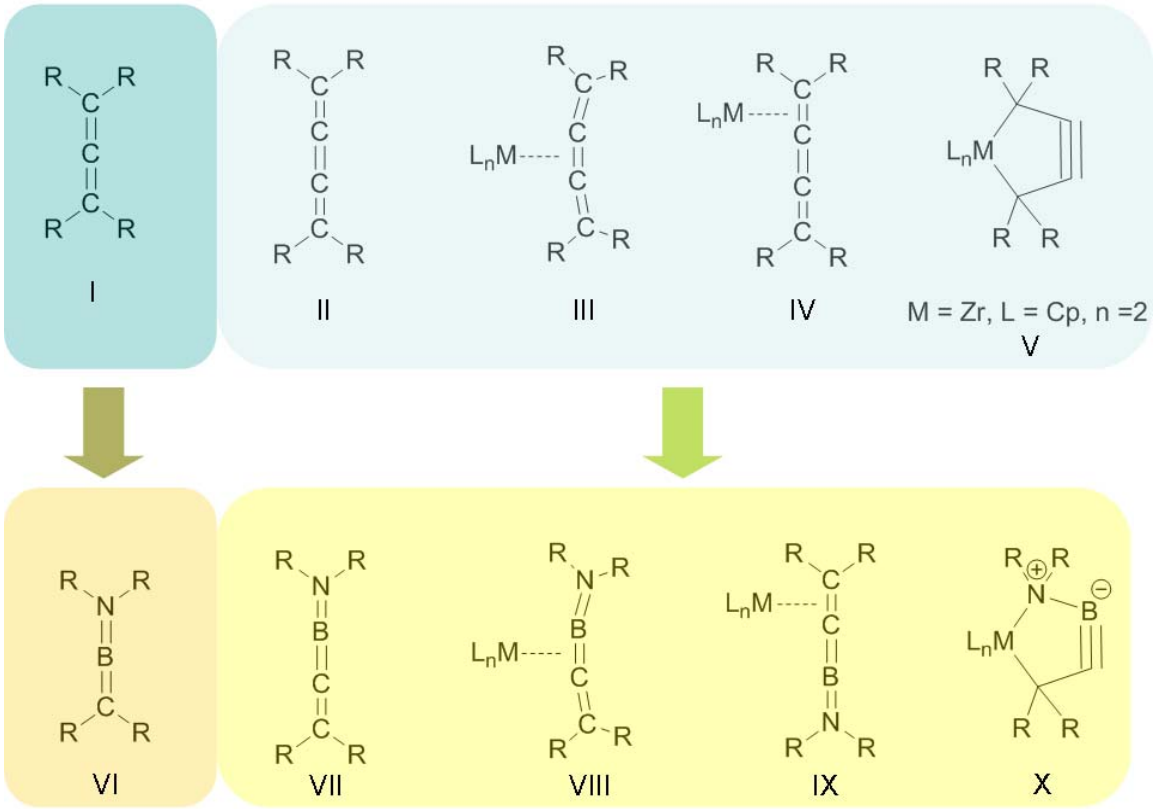

Fig. 44 From traditional cumulenes to novel boracumulenes.

As boron-based π systems have attracted much attention due to their interesting photophysical properties,[158,159] we turned our attention to boron-containing cumulene systems. Amino(methylene)boranes (**I**), isoelectronic to allenes (**VI**), can be isolated when the kinetically unstable B=C double bond is sterically protected by bulky substituents.

Structural characterization revealed such amino(methylene)boranes to adopt an allene-like structure with a linear N=B=C skeleton.[160-162]

B-amino-1-boraallenes (**VII**) are isoelectronic to butatriene (**II**) and might represent boron-containing [3]-cumulene systems when the boron-nitrogen π interaction is considered. Currently, very little is known about this class of compounds, and no successful synthetic approach has been reported. Ab initio calculations on the parent compound **VII** and its constitutional isomer aminoborirene have been carried out,[163] suggesting that the former is 12.9 kcal/mol higher in energy than the latter, unsurprising given the borirene's 2π-electron aromatic stabilization.[164-167] However, the possibly unstable boracumulenes could be stabilized by complexation with transition metals (**VII-X**). In addition, functionalization of vinylidene complexes might provide a synthetic approach to **VIII**.

2.3.1 Reaction of $[(OC)_5Mo{=}BN(SiMe_3)_2]$ (**16**) with $[Cp(iPr_3P)Rh{=}C{=}CH_2]$ (**104**)

When the vinylidenerhodium complex **104** was added to an equimolar amount of $[(OC)_5Mo{=}B{=}N(SiMe_3)_2]$ (**16**) in benzene and slightly warmed to 40°C, multinuclear NMR spectroscopy revealed a gradual consumption of the starting materials and formation of a mixture of expected product **105** and the rhodium monocarbonyl complex $[CpRh(CO)(PiPr_3)]$ (**106**)[168] in a ratio of approximately 2:1 as indicated by ^{1}H NMR spectrum. The ^{11}B and ^{31}P NMR spectra of **105** feature signals at $\delta_B = 68$ and at $\delta_P = 66.4$ ($^1J_{Rh\text{-}P} = 202.5$) respectively, which are both shifted upfield relative to the signals for the starting materials **16** ($\delta_B = 89$) and **104** ($\delta_P = 73.5$, $^1J_{Rh\text{-}P} = 209.0$). In the ^{1}H NMR spectrum of **105**, a new set of signals is present in the expected ratio for one Cp ligand and two trimethylsilyl groups thus confirming its constitution in solution. Most notably, the observation of two broad signals for trimethylsilyl groups at $\delta_H = 0.30$ and 0.62 in a 1:1 ratio and two signals for olefinic protons at $\delta_H = 7.31$ (dd, $^3J_{Rh\text{-}H} = 4.1$, $^4J_{P\text{-}H} = 1.1$) and 6.48 (dd, $^3J_{Rh\text{-}H} = 2.9$, $^4J_{P\text{-}H} = 2.2$) suggests both a considerable rotational barrier of the nitrogen boron double bond, and the asymmetry of the product, which is in good accordance with the proposed structure. This coupling pattern of olefinic protons is confirmed by comparison with a $^1H\{^{31}P\}$ NMR spectrum, which features doublet instead of doublet-of-doublet signals and thus geminal H-H coupling is excluded. The assignment of the resonances for *endo*- and *exo*-H or *endo*- and *exo*-$SiMe_3$ is based on the NOESY correlation with protons of P*i*Pr$_3$. Furthermore, **105** possess considerable stability. No sign of decomposition in solution at ambient temperature was observed. The complexes were also stable towards chromatography at room temperature without significant loss of

material. Unfortunately, as a result of its oily consistency, single crystals of **105** suitable for X-ray diffraction could not be obtained.

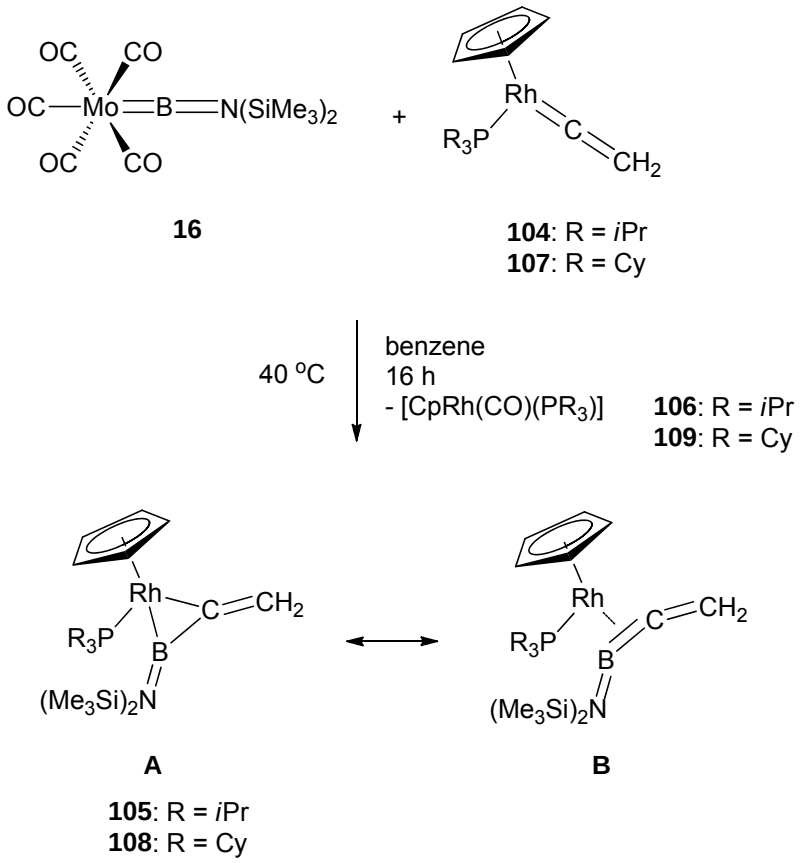

Scheme 19: Synthesis of 1-aza-2-bora-butatriene rhodiumcomplexes **105** and **108**.

2.3.2 Reaction of $[(OC)_5Mo{=}BN(SiMe_3)_2]$ (**16**) with $[Cp(Cy_3P)Rh{=}C{=}CH_2]$ (**107**)

In order to probe the versatility of the synthetic method and structurally characterize the target compound, we synthesized the sterically more demanding PCy_3-substituted rhodium vinylidene **107** (Fig 45, see details of preparation in the experimental section). The reaction of $[(OC)_5Mo{=}B{=}N(SiMe_3)_2]$ (**16**) with **107** was carried out under analogous conditions to those applied for the synthesis of compound **105** and monitored by multinuclear NMR spectroscopy. The formation of **108** was indicated by a new resonance at $\delta_B = 69$ in the ^{11}B NMR spectrum, and at $\delta_P = 56.6$ ($^1J_{Rh\text{-}P} = 201.9$) in the ^{31}P NMR spectrum. Resembling that of **105**, the ^1H NMR spectrum is characterized by two signals for trimethylsilyl groups at $\delta_H = 0.33$ and 0.64 and two signals for olefinic protons at $\delta_H = 7.37$ (d, $^3J_{Rh\text{-}H} = 3.5$) and 6.55 (d, $^3J_{Rh\text{-}H} = 2.9$). Notably, and in contrast to the common behaviour of aminoboranes,[169] the amino groups in

105 and **108** show no roation around the B=N bond up to 80 °C as indicated by variable-temperature NMR experiments in C_6D_6, thus suggesting significant double bond character. The byproduct **109**, analogous to [CpRh(CO)(P*i*Pr$_3$)] (**106**), was detected in a ratio of 1:2 relative to **108**, as indicated by the resonance at δ_P = 68.7 ($^1J_{Rh-P}$ = 189.6) and δ_H = 5.32 (s, Cp) in ^{31}P NMR and ^{1}H NMR spectroscopy respectively. Moreover, the reaction is accompanied by the concomitant formation of [Mo(CO)$_6$] as indicated by a resonance at δ_C = 201.49 in the ^{13}C NMR spectrum, which is in accordance with the previously reported results on borylene transfer reactions of group 6 carbonyl species.[106] Resembling **105**, considerable stability of **108** in solution as well as towards chromatography was observed. After workup, **108** was isolated in the form of pale yellow crystals by crystallization from hexanes at –30°C. Complex **108** crystallizes in the monoclinic space group *P2$_1$/c*.(Fig. 46) The coordinated B-C bond (1.489(12) Å) is ca. 6% longer than the B=C double bonds in non-coordinated amino(methylene)boranes **VI** (e.g. 1.391(4)[161] and 1.424(3) Å[162]), and is ca. 3% shorter than the B-C single bond found between two coordinated boron and four coordinated carbon (1.531(11) Å)[170]. This finding indicates considerable back-bonding from rhodium to an antibonding π* orbital of the ligand, a bonding situation which was also found for the butatriene complexes **III**. In particular, a corresponding increase by ca. 10 % for the coordinated C-C double bond in comparison to the free tetrafluorobutatriene was observed here.[156,157] In the case of **108**, coordination of the 1-aza-2-bora-butatriene is accompanied by significant bending. The N-B-C1 angle of 142.1(7)° is comparable to the values of corresponding C-C-C angles (137.5°-145.5°) in tetrafluorobutatriene complexes of rhodium or iridium[156,157], while the B-C1-C2 angle of 152.9(7)° is much wider and increased by more than 5% as compared to those values, thus suggesting some boron-carbon double bond character. The B-N (1.400(10) Å) and C1-C2 (1.331(10) Å) distances are both slightly elongated in comparison to those of amino(methylene)borane (e.g. 1.363(4) Å)[161] and free triene (1.3162(3) Å)[156,157] respectively, which can be explained by decrease of the *s*-character in the B-C σ-bond orbitals on bending the [3]-boracumulene. Comparison of the structural characteristics of the **108** with those of free amino(methylene)boranes **VI**, butatrienes **II** and butatriene complexes **III** suggest an overall bonding situation with the contribution from both mesomeric forms **A** and **B** in Scheme 19.

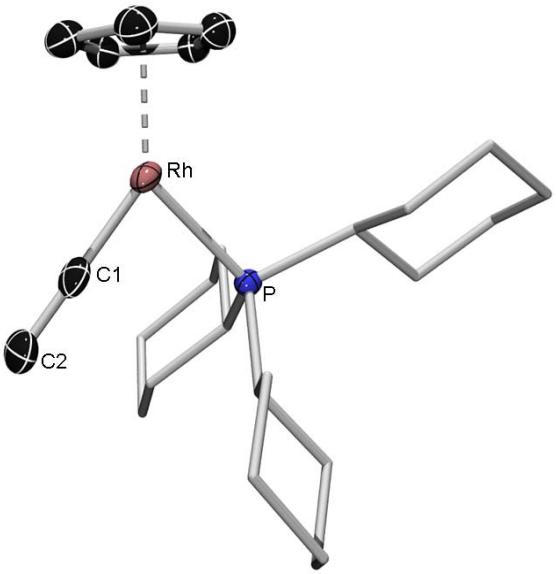

Fig. 45 Molecular structure of **107**. Hydrogen atoms, ellipsoids of Cy and disorder of Cp have been omitted for clarity. Ellipsoids drawn at the 50% probability level. Selected bond lengths [Å] and angles [°]: Rh-C1 1.816(3), C1-C2 1.312(4); Rh-C1-C2 179.3(3).

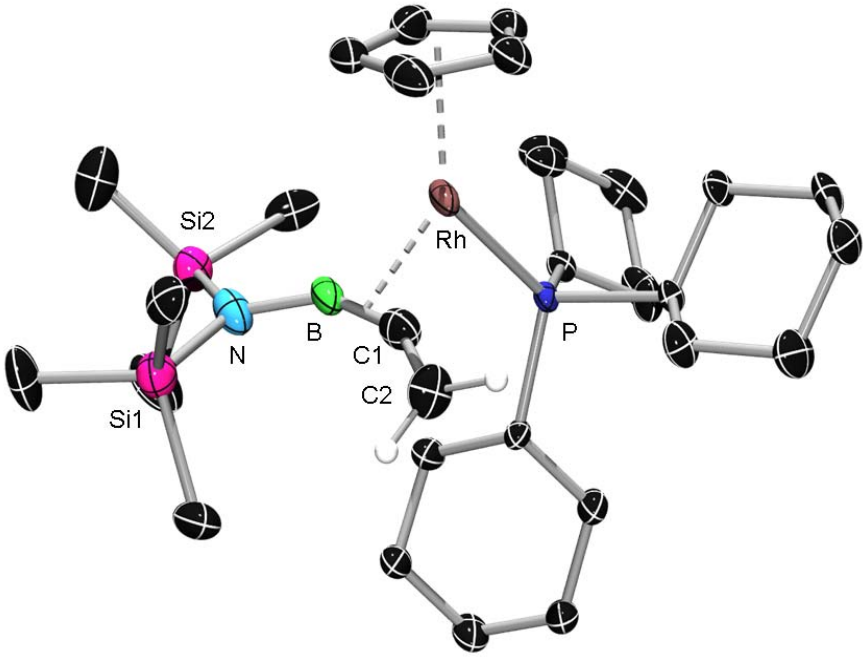

Fig. 46 Molecular structure of **108**. Except for the two olefinic protons, hydrogen atoms have been omitted for clarity. Ellipsoids drawn at the 50% probability level. Selected bond lengths [Å] and angles [°]: N-B 1.400(10), B-C1 1.489(12), C1-C2 1.331(10), Rh-B 2.027(8), Rh-C1 2.056(7), N-Si1 1.769(6), N-Si2 1.765(6), Rh-P 2.2799(17); N-B-C1 142.1(7), B-C1-C2 152.9(7).

2.3.3 Reaction of *trans*-[(OC)$_4$(Cy$_3$P)Mo{BN(SiMe$_3$)$_2$}] (**110**) with [Cp(R$_3$P)Rh=C=CH$_2$] (**104**: R = *i*Pr, **107**: R = Cy)

In order to improve the reaction selectivity by reducing the the generation of unwanted rhodium carbonyl complexes **106** and **109**, the analogous terminal borylene complex **110**, in which the *trans*-position is substituted by a phosphine ligand, was employed as borylene source. The reaction was carried out under identical conditions as those applied in *2.3.2*. However, in stark contrast to the reaction with **16** that differs from **110** merely by the presence of a *trans*-carbonyl, no borylene transfer was observed. This finding could be explained by strengthened molybdenum-boron bond as a result of enhanced Mo→borylene back-bonding in the presence of a *trans*-phosphine ligand.

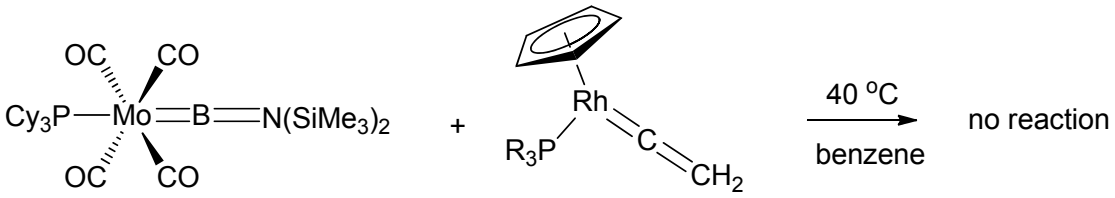

110

104: R = *i*Pr
107: R = Cy

Scheme 20: Reaction of **110** with rhodium vinylidene complexes **104** and **107**.

2.3.4 Reaction of [(OC)$_5$Mo=BN(SiMe$_3$)$_2$] (**16**) with [Cp(Cy$_3$P)Rh=C=CH(Me)] (**111**)

The borylene transfer reaction from [(OC)$_5$Mo=BN(SiMe$_3$)$_2$] (**16**) to the Rh=C double bond in [Cp(Cy$_3$P)Rh=C=CH(Me)] (**111**, Fig. 47, see details of preparation in the experimental section) was monitored by multinuclear NMR spectroscopy. While ^{11}B NMR spectrum revealed complete conversion of borylene into boracumulene complexes (δ_B = 68) within 16 h, ^{31}P NMR spectrum indicated the formation of two new phosphorus-containing species featuring similar ^{31}P resonances (δ_P = 56.6, $^1J_{Rh\text{-}P}$ = 205.8; δ_P = 58.3, $^1J_{Rh\text{-}P}$ = 205.4) in a ratio of ca. 3:1. Correspondingly, two peaks with integrals in a ratio of ca. 3:1 (δ_H = 6.69, m; δ_H = 7.52, m) were observed for olefinic protons in ^{1}H the NMR spectrum. These spectroscopic data are in good accordance with the formation of the stereomers **112** and **113** as shown in Scheme 21. After workup (chromatography and fractional crystallization), single crystals of **112** that possess an *exo*-methyl group was obtained. X-ray diffraction analysis confirmed its chemical constitution (Fig 48). Complex **112** crystallizes in the monoclinic space group *C*2/*c*. The overall geometry resembles that of n(published one), confirming the *B*,*C*-η^2 coordination

of the 1-aza-2-borabutatriene species to the rhodium center. Unfortunately, all attempts to isolate **113** with an *endo*-methyl group failed.

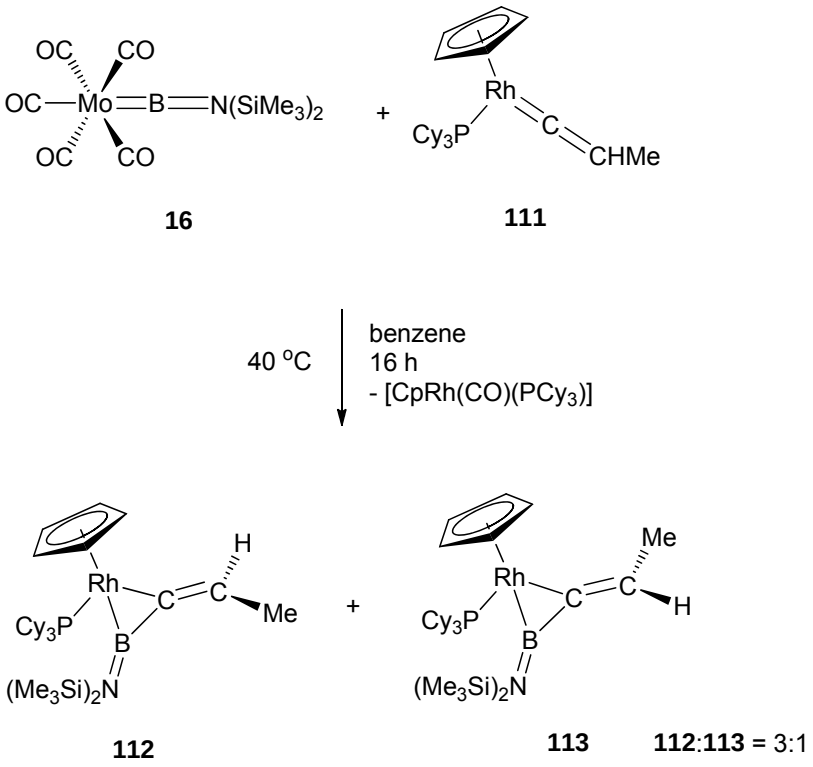

Scheme 21: Reaction of $[(OC)_5Mo{=}BN(SiMe_3)_2]$ (**16**) with $[Cp(Cy_3P)Rh{=}C{=}CH(Me)]$ (**111**).

Interestingly, pure **112**, with an *exo*-methyl group, readily underwent isomerization in solution at ambient temperature, affording its stereomer **113** as indicated by multinuclear NMR spectroscopy (Scheme 22). This finding implied the significantly lowered energy of the transition state for rotation around the B=C bond that side-on coordinates to a metal. The chemical equilibrium with **112** and **113** in an approximate ratio of 2:1 was reached within 16 h, thus suggesting **112**, in which less steric congestion exists, is thermodynamically favoured over **113**.

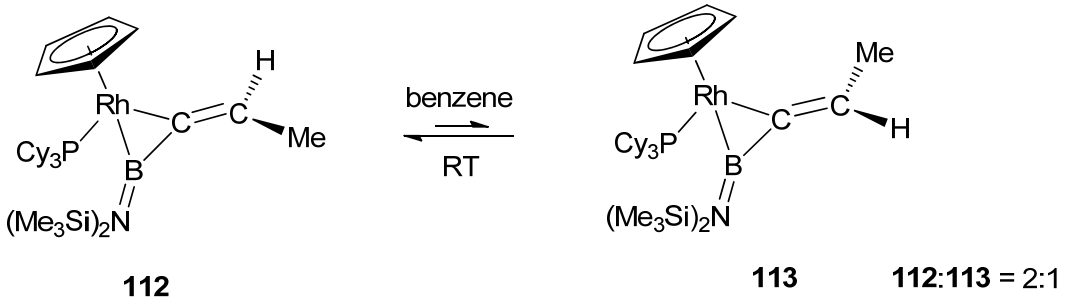

Scheme 22: Isomerization of **112** in solution.

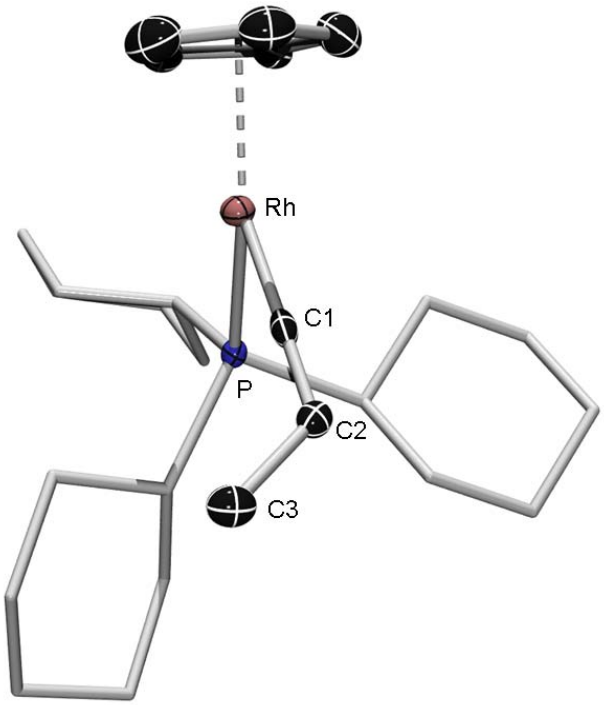

Fig. 47 Molecular structure of **111** in the solid state. Hydrogen atoms, ellipsoids of PCy_3 ligand and disorder of the CpRh=C=CH(Me) fragment are omitted for clarity. Ellipsoids drawn at the 50% probability level. Due to the extensive disorder of the whole CpRh=C=CH(Me) fragment, a discussion of the structural parameters is not possible.

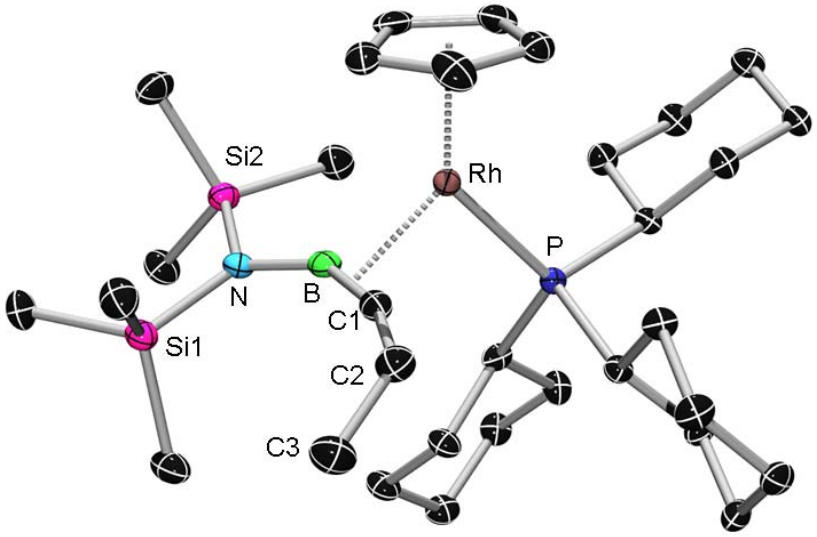

Fig. 48 Molecular structure of **112**. Hydrogen atoms have been omitted for clarity. Ellipsoids drawn at the 50% probability level. Selected bond lengths [Å] and angles [°]: N-B 1.410(6), B-C1 1.498(6), C1-C2 1.319(6), Rh-B 2.034(5), Rh-C1 2.068(4), C2-C3 1.495(6), Rh-P 2.2662(10); N-B-C1 144.6(4), B-C1-C2 160.8(4).

2.3.5 Attempt to eliminate the 1-aza-2-bora-butatriene species from rhodium

In the case of butatriene rhodium complexes, ligand exchange process takes place in the presence of CO to afford the free butatriene species.[154] Hence we are prompted to investigate whether an analogous ligand exchange reaction could be utilized to generate free *B*-amino-1-boraallene species, which is expected to be labile as a result of deficient steric protection and might undergo secondary reactions.

In stark contrast to butatriene rhodium complexes, 1-aza-2-bora-butatriene-complexes **108** proved to be stable in the presence of CO at ambient temperature, even under photolytic conditions (Scheme 23). However, upon warming to 85°C, multinuclear NMR spectroscopy revealed a gradual and almost quantitative transformation of the starting material as indicated by ^{11}B (δ_B = 43) and ^{31}P NMR (δ_P = 74.3, $^1J_{Rh-P}$ = 187.8) spectra. Unexpectedly, neither ^{31}P nor $^{13}C\{^1H\}$ NMR spectra suggested the formation of the corresponding carbonyl complex. Moreover, the significant upfield shift of the ^{11}B NMR resonance by 26 ppm implies a B-C to C-C coordination mode shift (**VII→VIII** in Fig. 44), which could conceivably take place equally as well without CO. Thus, an analogous experiment in the absence of CO was carried out, which confirmed our assumption. In fact, the analogous central C-C to outer C-C coordination mode shift of butatriene complexes (**III→IV** in Fig. 44) under thermal conditions was reported previously.[154]

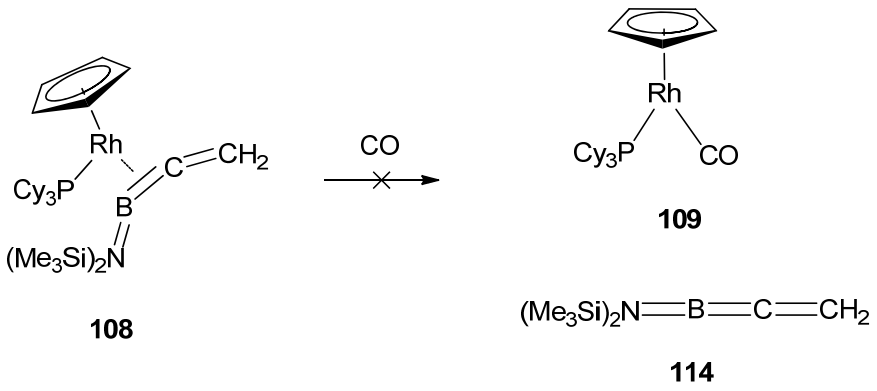

108 **109** **114**

Scheme 23: Attempt to eliminate the free 1-aza-2-bora-butatriene species **114**.

Complete conversion of **108** required two weeks at 85°C. After workup, single crystals were obtained from a hexane solution at ambient temperature. The product **115** crystallizes in the triclinic space group *P-1* with two independent molecules in the asymmetric unit, both featuring very similar structural parameters. The results of X-ray diffraction analysis partially confirm our proposed structure (Scheme 24). As shown in Fig. 49, the C=C double bond coordinates in an η^2 fashion to the rhodium center. Despite the presence of the $N(SiMe_3)_2$

group, which provides both steric shielding and π-electron donation, the released B=C double bond is highly reactive and undergoes an addition reaction with the C4-H bond (Fig. 49) of one cyclohexyl group of the coligand PCy_3, affording the RhC1BC4C3P six-membered ring. The C1-C2 bond (1.417(6) Å) is elongated by ca. 6% as a result of the side-on coordination, which is comparable to that observed for the B=C bond in **108**. The B-C1 (1.533(7) Å) and B-C4 (1.615(8) Å) separations fall within the expected range for the corresponding single bonds.[170] The elongation of the B-C4 in comparison to the B-C1 bond can be attributed to a lower amount of *s* character in C4. Both boron and nitrogen atoms adopt a trigonal planar geometry as indicated by the sum of angles of 359.1° and 359.9° respectively. The Si2-N-B-C4 torsion angle of 51.8° suggests a reduced B=N π-contribution, which corresponds to the significant elongation of the B-N bond (1.492(6) Å) in comparison to that of **108** (1.400(10) Å), and is presumably a result of the pronounced steric congestion imposed by the bulky $N(SiMe_3)_2$, Cp and Cy-substituent bound to boron.

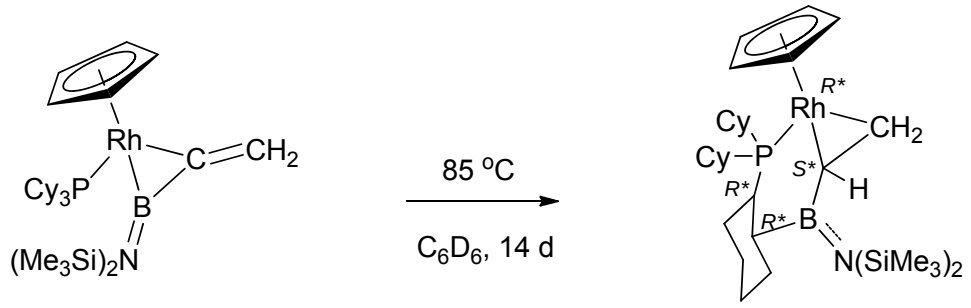

108 **115**

Scheme 24: Quantitative formation of **115** (*RSRR/SRSS*) by thermally-induced B-C to C-C coordination mode shift and subsequent C-H activation by the B=C double bond.

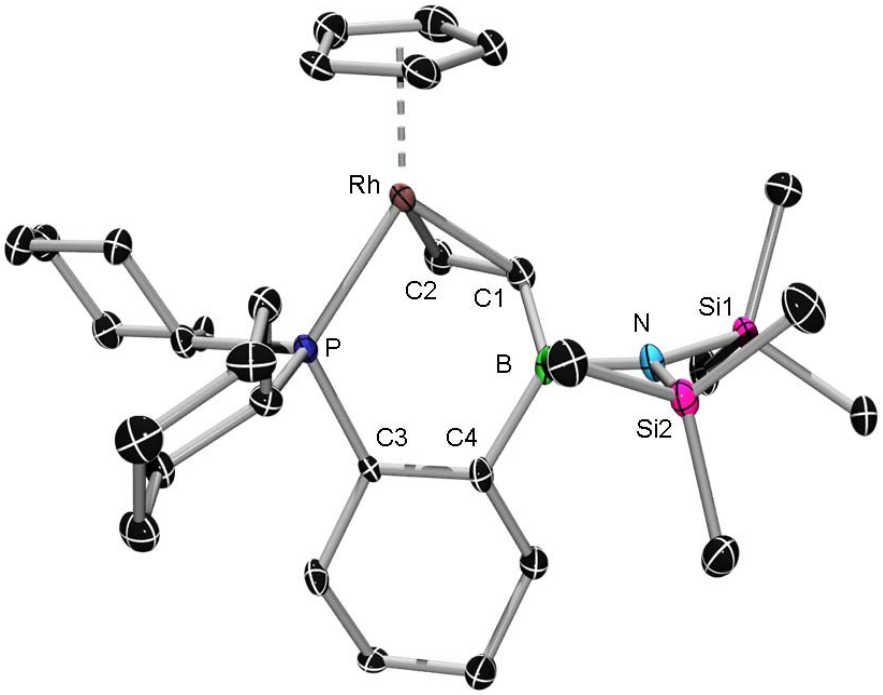

Fig. 49 Molecular structure of **115** (R_{Rh},S_{C1},R_{C3},R_{C4}). Hydrogen atoms, the co-crystallized solvent molecules and the second independent molecule (S_{Rh},R_{C1},S_{C3},S_{C4}) in the asymmetric unit have been omitted for clarity. Ellipsoids drawn at the 50% probability level. Selected bond lengths [Å] and angles [°]: C1-C2 1.417(6), C1-B 1.533(7), B-C4 1.615(8), C3-C4 1.546(6), P-Rh 2.2631(13), B-N 1.492(6); C2-C1-B 131.6(5), C1-B-C4 125.1(4), C1-B-N 116.6(4), N-B-C4 117.4(4), B-N-Si1 115.9(3), B-N-Si2 123.2(3), Si1-N-Si2 120.8(2).

While complex **115** exists as a racemate (as the R_{Rh},S_{C1},R_{C3},R_{C4}-**115** and S_{Rh},R_{C1},S_{C3},S_{C4}-**115** enantiomers), remarkably, no other diastereomers were detected in the material. Since the two carbon atoms on the P-CH-CH-B system are both chiral centres, as are the Rh centre and the Rh-bound CH atom, there exist eight possible sets of enantiomers for the complex **115**. If we assume the olefin ligand is coordinatively labile, the Rh and adjacent CH atoms would then be configurationally unstable, reducing the possible products to two sets of enantiomers. However, careful examination of the ^{1}H and ^{13}C NMR spectra of the reaction mixture and isolated material showed no indication of diastereomers other than the R_{Rh}^{*},S_{C1}^{*},R_{C3}^{*},R_{C4}^{*}-**115** racemate. Therefore, the C-H insertion reaction must proceed with a high degree of diastereoselectivity.

Furthermore, we studied the reactivity of the bound 1-aza-2-bora-butatriene ligand towards unsaturated substrates. Diphenylacetylene and benzophenone were chosen as representative non-polar and polar reagents, respectively, to investigate the propensity of the *B*-amino-1-boraallene species to undergo [2+2]cycloaddition reactions. However, no reaction was

observed at ambient temperature, even upon irradiation. Under more forcing thermal conditions, the aforementioned intramolecular C-H addition with formation of **115** was again observed.

2.3.6 Reaction of [CpRh(PCy$_3$){(η^2-*B,C*)-(SiMe$_3$)$_2$N=B=C=CH$_2$}] (**108**) with *I*Me (**116**) and *I*Mes (**117**)

When the N-heterocyclic carbene *I*Me (**116**) was added to an equimolar amount of [CpRh(PCy$_3$){(η^2-B,C)-(SiMe$_3$)$_2$N=B=C=CH$_2$)}] (**108**) in toluene at room temperature, the color of the reaction mixture turned immediately from light yellow to deep red. The formation of a new boron- and phosphorus-containing species was indicated by the presence of a new resonance at δ_B = 18 in the ^{11}B NMR spectrum and a new signal at δ_P = 55.1 ($^1J_{Rh\text{-}P}$ = 208.7) in the ^{31}P NMR spectrum. The remarkable upfield shift of the ^{11}B resonance by ca. 50 ppm is most likely due to the increased coordination number on the boron center, which strongly suggests the formation of a carbene-boron adduct. After workup, single crystals were obtained upon storage of a saturated toluene/hexane solution at –30°C for 2 weeks. The product **118** crystallizes in the triclinic space group *P*-1. The results of X-ray diffraction analysis partially confirm our speculation (Fig. 50). However, carbene-boron bond formation is accompanied by B-C to C-C coordination mode shift. Interestingly, while the ^{1}H NMR signals of the nitrogen-bound trimethylsilyl groups (δ_H = 0.12) and of the nitrogen-bound methyl groups (δ_H = 3.63) appear as broad singlets at ambient temperature, the ^{1}H NMR spectrum shows clearly two signals for N(SiMe$_3$)$_2$ (δ_H = 0.38 and 0.00) and for NMe (δ_H = 3.98 and 3.02) at –50°C respectively. This finding implies a certain degree of rotational barrier about the B-N1 and B-C3. The bond length of B-N1 (1.532(3) Å) is remarkably elongated by 7% in comparison to those of aminoborirenes (around 1.43 Å, see Table 1), in which the B-N π-interaction is reduced as a result of the endocyclic 2π-electron delocalization. The B-C3 bond distance of 1.583(3) Å falls in the expected range for the corresponding single bonds.[170] Based on these observations, it becomes obvious that the rotational barrier around the B-N1 and B-C3 bonds is due to the steric congestion between the bulky trimethylsilyl groups and the methyl groups of carbene unit. The B-C1 bond length of 1.438(4) Å is comparable with those of non-coordinated amino(methylene)boranes (e.g. 1.424(3) Å[162]), thus indicating the presence of a B=C double bond. In contrast to the B-C to C-C coordination mode shift reaction in *2.3.5*, the released B=C double bond in this case displayed no reactivity towards the C-H bond of the coligand PCy$_3$. In fact, this finding is unsurprising, as NHCs have been proven to have great stabilizing effect on highly reactive

species, e.g. borylenes, thus enabling selective trapping of carbene-borylene adducts[171] and even generation of a stable bis(carbene)-borylene adduct[172].

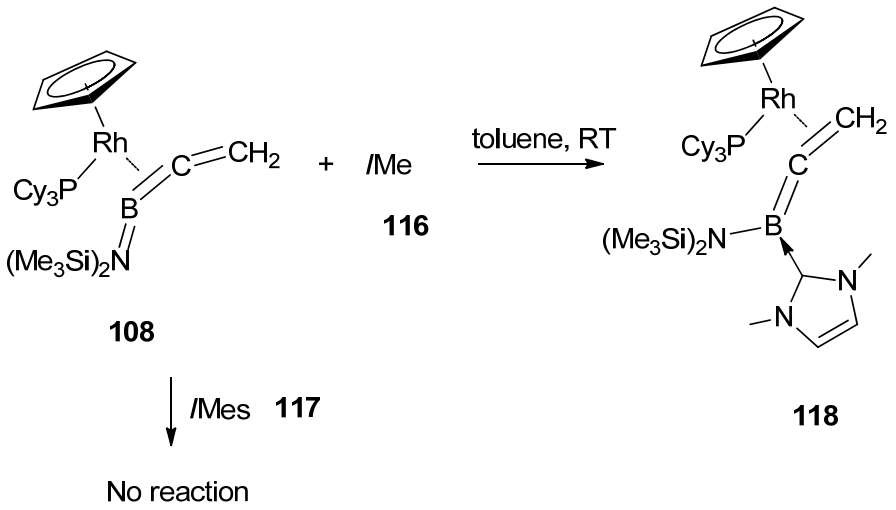

Scheme 25: Reaction of [CpRh(PCy$_3$){(B,C-η^2)-(SiMe$_3$)$_2$N=B=C=CH$_2$)}] (**108**) with *I*Me (**116**).

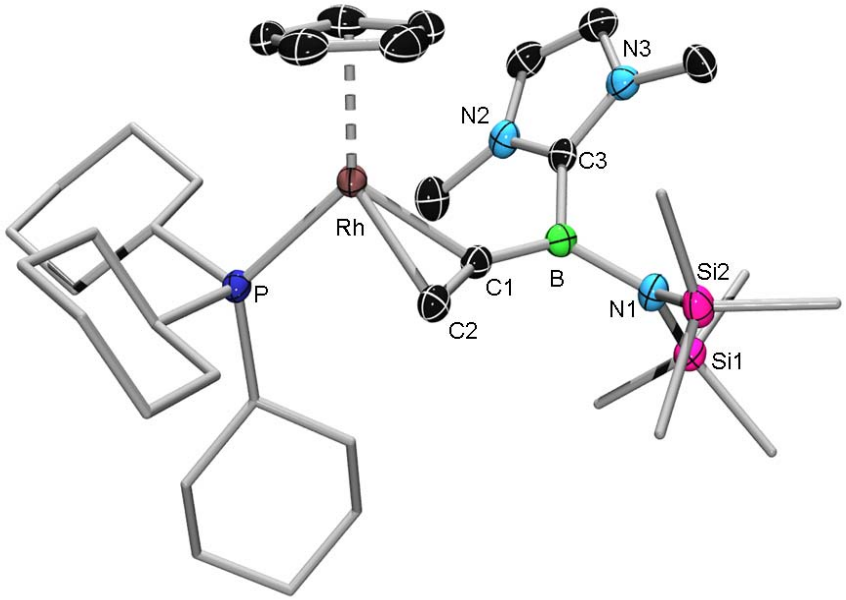

Fig. 50 Molecular structure of **118**. Hydrogen atoms, ellipsoids of ligands have been omitted for clarity. Ellipsoids drawn at the 50% probability level. Selected bond lengths [Å] and angles [°]: C1-C2 1.398(3), C1-B 1.438(4), B-C3 1.583(3), B-N1 1.532(3); C2-C1-B 145.9(2), Rh-C1-C2 71.04(13), Rh-C1-B 135.18(17).

In contrast, no reaction was observed upon addition of sterically more demanding N-heterocyclic carbene *I*Mes (**117**). This can be explained by steric congestion imposed by

mesityl, trimethylsilyl and cyclohexyl groups, which hindered the approach of the *I*Mes (**117**) to the boron center.

Finally we investigated whether the NHC-stabilized 1-boraallene **119** can be separated from the coordination sphere of rhodium upon ligand exchange with CO (Scheme 26). However, the 1-boraallene rhodium complex **118** displayed considerable stability under CO atmosphere (ca. 1.5 atm).

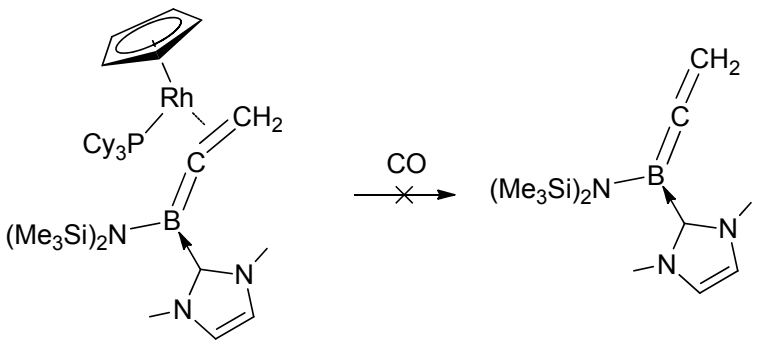

118 **119**

Scheme 26: Attempt to eliminate the NHC-stabilized 1-boraallene **119**.

2.4 Elimination of borylene ligands under reducing conditoins

Reduction of the amine complexes $[M(CO)_5(NMe_3)]$ (**120**: M = Cr, **121**: M = Mo, **122**: M = W) with sodium naphthalenide in THF provides a convenient route to the pentacarbonylmetalates of the group 6 metals.[173] The reaction is accompanied by elimination of a labile ligand; in this case amine (Fig. 51). In view of this, we turned our attention to the terminal borylene complexes of group 6 transition metals $[(OC)_5M{=}BN(SiMe_3)_2]$ (**14**: M = Cr, **16**: M = Mo), in which the borylene ligands are well known to be stronger ligand-to-metal σ donors and comparable metal-to-ligand π-acceptors.[71-74,80,82] Hence, we became interested in whether elimination of borylene or elimination of CO would take place upon treatment with reduction agents.

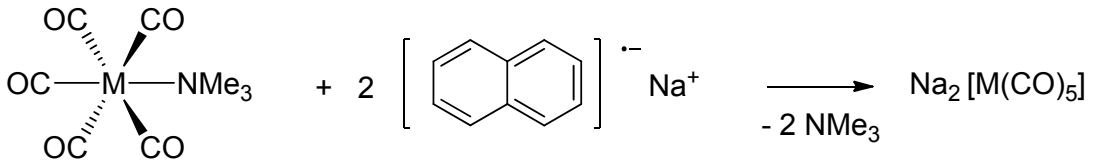

120: M = Cr
121: M = Mo
122: M = W

123: M = Cr
124: M = Mo
125: M = W

Fig. 51 Elimination of a labile ligand under reductive condtitions.

2.4.1 Reaction of $[(OC)_5M{=}BN(SiMe_3)_2]$ (**14**: M = Cr, **16**: M = Mo) with KC_8

Borylene complexes **14** and **16** were treated with KC_8 in THF-D_8 respectively. The reactions were monitored by multinuclear NMR spectroscopy. A nearly quantitative formation of a new boron-containing species was immediately indicated by the new resonance at δ_B = 48 in the ^{11}B NMR spectrum. The significant upfield shift by ca. 40 ppm strongly implied the separation of borylene ligand $:BN(SiMe_3)_2$ from the metal center. Interestingly, two singlet peaks at δ_H = 0.06 and –0.03 in a ratio of approximately 1:1 were observed in the ^1H NMR spectrum. According to these findings, the following speculation was made. The highly reactive free borylene species $:BN(SiMe_3)_2$ was presumably generated in the first step. Subsequently, one of the nitrogen-bound trimethylsilyl groups may migrate to boron, affording the corresponding iminoborane **126**. Iminoboranes, which are isoelectronic to alkynes, have great tendency towards oligomerization as a result of the kinetic lability of B≡N

triple bonds.[174,175] The iminoborane **127,** which is analogously substituted by sterically demanding group, i.e. *t*Bu, readily underwent dimerization (Fig. 52 below), affording the diazadiboretidine **128** displaying signal at δ_B = 41 in the ^{11}B NMR spectrum.[176] Moreover, the slight downfield shif of the ^{11}B NMR resonance from δ_B = 41(**128**) to 48(**129**) is expected for alkyl- and silylboranes, e.g. δ_B = 65 for $Cl_2B(CMe_2iPr)$[177] and δ_B = 79 for $Cl_2B(SiMe_3)$[136]. Following these informations, the formation of a four-membered ring most likely occurred (Scheme 27).

After adding 18-crown-6 to the reaction mixture and storing the mixture at –30°C for 2 d, colorless crystals were obtained. The results of X-ray diffraction analysis are depicted in Fig. 53, which confirmed the elimination of the aminoborylene ligand and the formation of the dianionic dinuclear complex **130**. However, due to poor quality of the diffraction analysis data, discussion of the structural parameters is not possible. Moreover, it should be mentioned, that dianionic dinuclear group 6 metal complexes are previously reported and were prepared under more drastic conditions, i.e. irradition of a mixture of metal haxacarbonyl and sodium amalgam (Fig. 52 above).[178]

Unfortunately, due to the oily consistency and poor stability (slow decomposition during the workup), all attempts to isolate the elusive boron-containing species from the mother liquor failed.

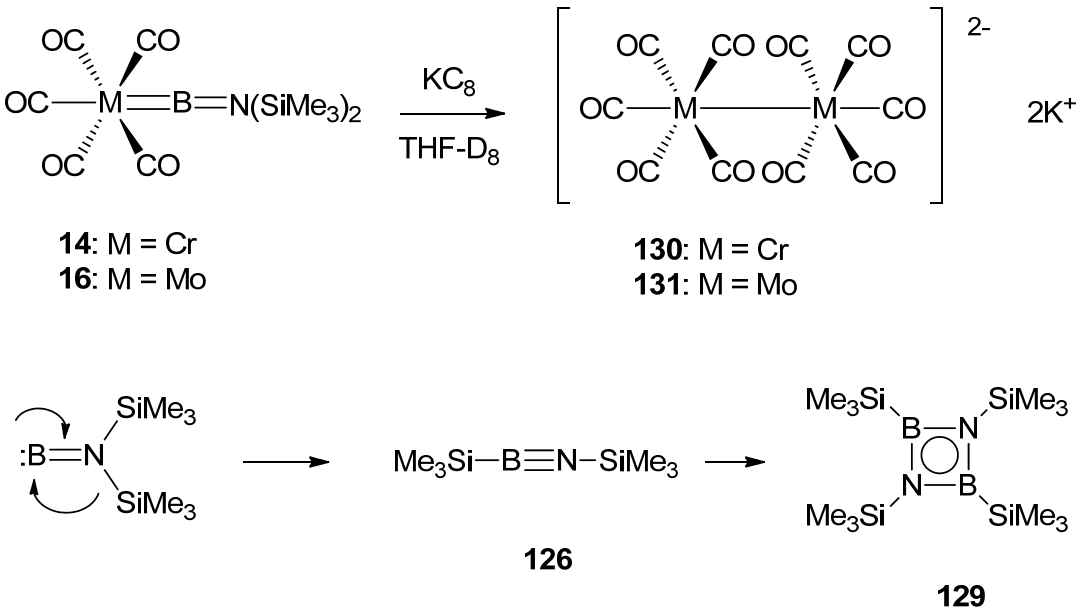

Scheme 27: Elimination of aminoborylene ligands under reducing conditoins and postulated subsequent reactions.

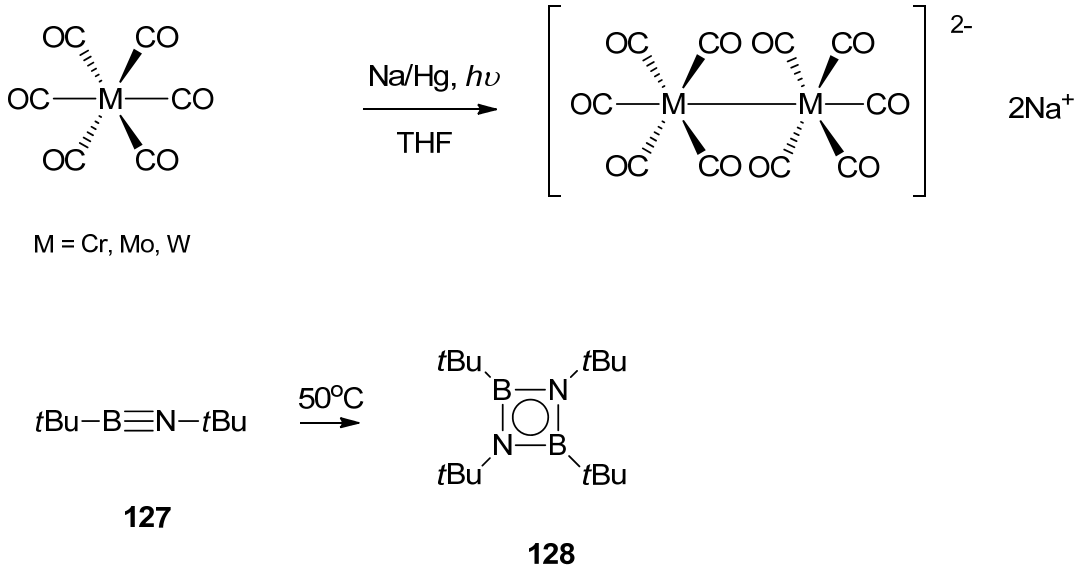

Fig. 52 Reduction of hexacarbonyl complexes derived from group 6 metals and dimerization of the iminoborane **127**.

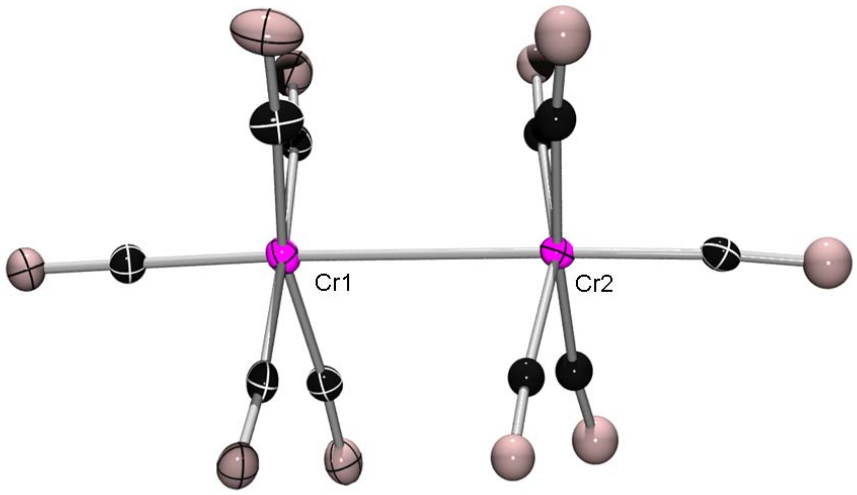

Fig. 53 Molecular structure of **130**. The counterion potassium, as well as the co-crystallized 18-crown-6 and THF are omitted for clarity. Due to poor quality of the diffraction analysis data, discussion of the structural parameters is not possible.

2.4.2 Reaction of $[(OC)_4(Cy_3P)Cr\{BN(SiMe_3)_2\}]$ (**132**) with KC_8

Due to the presence of a strong σ-donor and weak π-acceptor phosphine ligand at the position *trans* to the borylene, the metal→borylene back-bonding is considerably enhanced, thus leading to a stronger metal-boron bond. This has is indicated by the shortened metal-boron bond distance,[179] as well as the observations in *2.3.3*.

Demonstrating the significant influence of the *trans*-ligand on reactivities of group 6 terminal borylene complexes, we became interested in the behaviour of **132** upon treatment with

reducing agent, e.g. KC_8. Hence, the reaction was carried out under identical conditions to those applied in 2.4.1, and monitored by multinuclear NMR spectroscopy, which merely revealed slow decomposition of the starting materials ($\delta_B = 93$, $\delta_P = 64.8$) over three days.

2.5 Synthesis of novel iron-arylborylene complexes

In comparison to the family of aminoborylene complexes, which benefit from a boron-bound substituent that provides both steric and π-electron stabilization, the number of neutral arylborylene complexes is severely limited. To date, the dehydrogenation protocol reported by Sabo-Etienne and coworkers constitutes the only synthetic approach to such species (Fig. 12).[91] Furthermore, borirenes synthesized by applying standard borylene transfer protocols are limited by the boron-bound exocyclic substituent. This fact prompted us to develop other facile synthetic routes to carbonyl-rich (analogous to the intensively investigated borylene transfer agent **14** and **16**) terminal borylene complexes with different substituents at boron center, e.g. aryl and alkyl, which could be potentially utilized for borylene transfer.

2.5.1 Reaction of $K[(OC)_3(Me_3P)Fe(SiMe_3)]$ (**133**) with Cl_2BDur (**134**)

Iron boryl complex **135** was obtained via salt elimination between $K[(OC)_3(Me_3P)Fe(SiMe_3)]$ (**133**) and Cl_2BDur (**134**) according to Scheme 28. After workup, **135** was isolated as grey crystalline solid, whose constitution was confirmed by multinuclear NMR spectroscopy, elemental analysis and X-ray structure analysis. The ^{11}B NMR resonance of **135** was observed as a broad signal at δ_B = 114, which resembles that (δ_B = 112) of the iron mesitylboryl complex $[CpFe(CO)_2(BBrMes)]$ (**136**) reported by Aldridge.[98,99] In addition, ^1H, ^{31}P NMR data confirm the presence of PMe_3 and duryl fragments.

Compound **135** crystallizes in monoclinic space group $P2_1/n$, and exhibits an octahedral geometry at iron with *cis*-positioned silyl and boryl groups (Si-Fe-B 92.55(5)°), which might facilitate elimination of the halosilane (Fig. 54). The Fe-B bond distance of 2.0360(19) Å falls in the range of those commonly observed for neutral iron half-sandwich boryl complexes (1.96-2.09 Å).[60] However, all attempts (applying forcing thermal conditions at 80°C and/or vacuum) to eliminate the halosilane $ClSiMe_3$ led to decomposition of **135**.

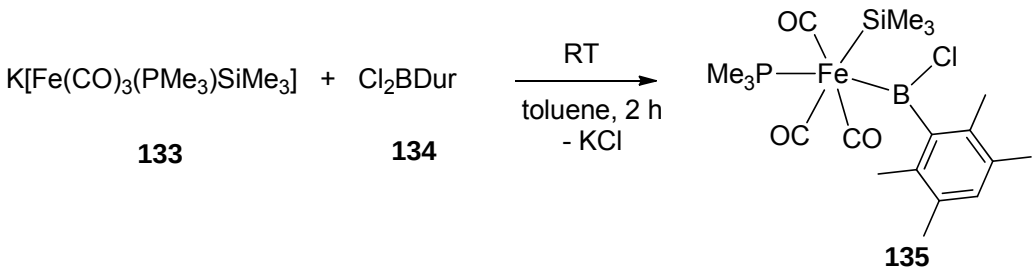

133 **134** **135**

Scheme 28: Reaction of $K[(OC)_3(Me_3P)Fe(SiMe_3)]$ (**133**) with Cl_2BDur (**134**)

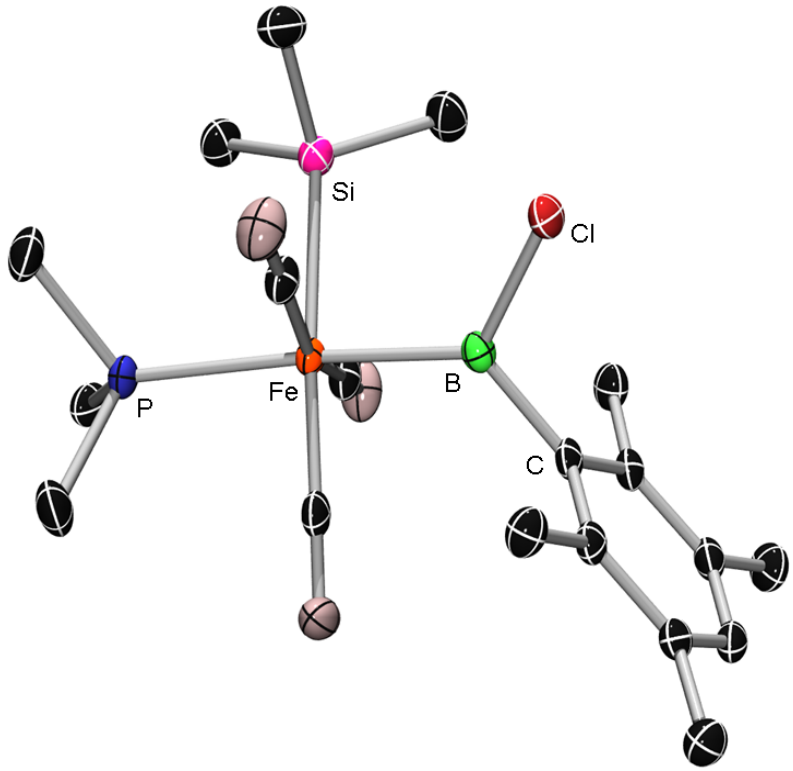

Fig. 54 Molecular structure of **135**. Hydrogen atoms have been omitted for clarity. Ellipsoids drawn at the 50% probability level. Selected bond lengths [Å] and angles [°]: Fe-P 2.2706(5), Fe-Si 2.4527(5), Fe-B 2.0360(19), B-Cl 1.8159(18), B-C 1.584(2); Si-Fe-B 92.55(5).

2.5.2 Reaction of $K[(OC)_3(Me_3P)FeSiMe_3]$ (**133**) with Br_2BDur (**137**)

The high yield (60%) synthesis of $[(Me_3P)(OC)_3Fe{=}BDur]$ (**138**) was achieved by salt elimination and subsequent liberation of trimethylsilylbromide from $K[Fe(CO)_3(PMe_3)SiMe_3]$ (**133**) and Br_2BDur (**137**) (Scheme 29). The advantages of this procedure are the facile work-up, mild reaction conditions (RT) and scale-up capability. The product **138** was isolated by simple filtration and crystallization at low temperature. The constitution of **138** was confirmed by multinuclear NMR spectroscopy, elemental analysis, IR spectroscopy and X-ray structure analysis. The ^{11}B NMR resonance of **138** was observed as a broad signal at δ_B = 146, which resembles that (δ_B = 145) of the cationic iron mesitylborylene complex $[Cp^*Fe(CO)_2(BMes)]^+[BAr^f_4]^-$ (**18**) reported by Aldridge.[84] ^1H, ^{13}C and ^{31}P NMR data for **138** confirm the presence of PMe_3, duryl and carbonyl fragments. IR spectra show one band (1878 cm^{-1}) for the carbonyl groups, which is considerably shifted to lower frequency in comparison to those of $[Fe(CO)_4(PMe_3)]$ (2051, 1977, 1935 cm^{-1}), but resembles those of *trans*-$[Fe(CO)_3LL']$ (L, L' = phosphine, ca. 1880 cm^{-1})[180], thus suggesting a mutual *trans* disposition of phosphine and borylene ligands for **138**. Moreover, these data are in line with the well known characteristics of borylene ligands, i.e. a stronger ligand-to-metal donation

and a similar degree of metal-to-ligand backbonding in comparison to carbonyl groups, which corresponds to previous observations[80,82,179] and again confirms theoretical predictions.

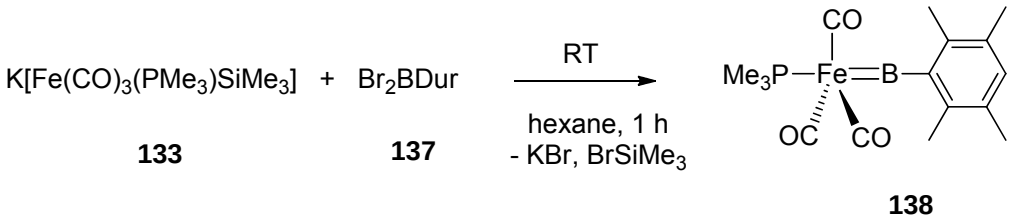

133 **137** **138**

Scheme 29: Synthesis of [(Me$_3$P)(OC)$_3$Fe=BDur] (**138**).

Single crystals suitable for X-ray crystallography were obtained by cooling a saturated hexane solution of **138** to –30°C (Fig. 55).

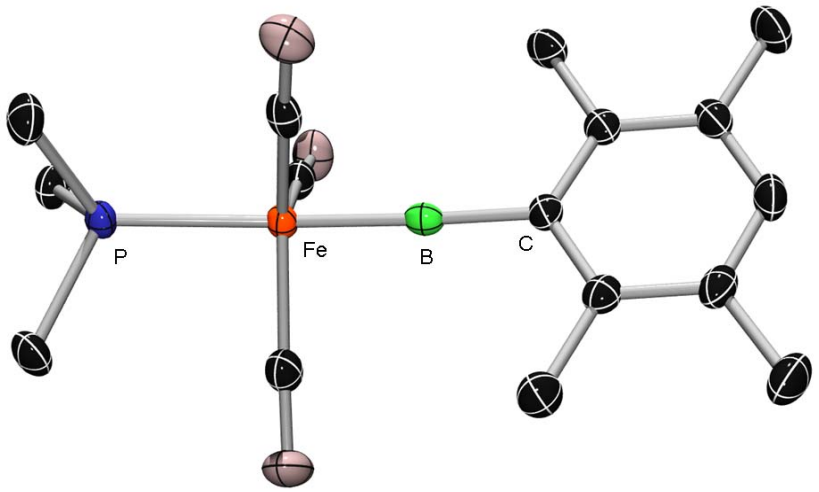

Fig. 55 Molecular structure of *trans*-[(Me$_3$P)(OC)$_3$Fe=BDur] (**138**). Ellipsoids drawn at the 50% probability level. Hydrogen atoms have been omitted for clarity. Relevant bond lengths [Å] and angles [°]: Fe-B 1.7929(13), Fe-P 2.2719(3), B-C 1.5255(16); Fe-B-C 176.12(10), P-Fe-B 172.20(4).

Compound **138** crystallizes in the monoclinic space group $P2_1/c$, and exhibits a trigonal bipyramidal geometry at iron with coordination of trimethylphosphine and durylborylene ":BDur" at axial sites (P-Fe-B = 172.20(4)°). The latter is coordinated to iron terminally via the *sp*-hybridized boron atom (Fe-B-C = 176.12(10)°). The Fe-B distance of 1.7929(13) Å resembles that of the cationic iron mesitylborylene complex [Cp*Fe(CO)$_2$(BMes)]$^+$[BAr$^f_4$]$^-$ (**18**) (1.792(8) Å)[84,85], and thus indicates the presence of significant Fe-B multiple bond character. In addition, the Fe-B bond is 3.7% shorter than that of the corresponding cationic iron aminoborylene complex [CpFe(CO)$_2$(BNCy$_2$)]$^+$ (**20**) (1.859(6) Å)[127] and even 10.8% shorter than in the neutral iron complex [Cp*BFe(CO)$_4$] (**12**) (2.101(3) Å)[80], in which the boron atom resides at the apex of a *nido*-tetracarbapentaborane unit and binds *via* an

exohedral lone pair to the iron center. This distinctively shortened Fe-B bond can be explained by an enhanced π acidity of the boron center in **138** due to the absence of a π donating amino substituent or its incorporation into a cluster cage and the presence of the weakly π-acidic phosphine ligand *trans* to the borylene ligand, and thus an increased degree of Fe→B π backbonding.[179]

2.5.3 Reaction of $K[(OC)_3(Me_3P)FeSiMe_3]$ (**133**) with other dihalo(di)boranes

In order to probe the versatility of the synthetic method, reactions of $K[(OC)_3(Me_3P)FeSiMe_3]$ (**133**) with a variety of dihaloboranes, i.e. $X_2BN(SiMe_3)_2$ (**139**: X = Cl, **140**: X = Br), *t*$BuBBr_2$ (**141**), 1,3,5-$(Br_2B)_3(C_6H_3)$ (**142**), Cl_2BMes (**143**) or dihalodiborane $(ClMesB)_2$ (**144**) were carried out. However, multinuclear NMR spectroscopy revealed either decomposition of boranes or formation of several boron-containing species between δ_B = 0 - 60, which are obviously inconsistent with expected ^{11}B resonance for borylene complexes.

2.6 Reactivity investigation of iron-arylborylene complexes

2.6.1 Reaction of $[(OC)_3(Me_3P)Fe{=}BDur]$ (**138**) with $[Pt(PCy_3)_2]$ (**52**)

During the last few years, $[Pt(PCy_3)_2]$ (**52**), which possesses a electron-rich and highly unsaturated platinum center, was intensively investigated in our laboratory as a transition metal Lewis base toward metal-coordinated boron-based ligands,[128,181-184] thereby establishing the concept of transition metal stabilized terminal borylene complexes. As corresponding examples are restricted to alkylborylene and aminoborylene species, we sought to contribute a hitherto unknown arylborylene metal-adduct.

To this end, **138** was treated with **52** (Scheme 30) affording the heterodinuclear species $[(OC)_2(Me_3P)Fe(\mu\text{-}CO)(\mu\text{-}BDur)Pt(PCy_3)]$ (**145**), as indicated by a slightly upfield-shifted broad resonance at $\delta_B = 126$ in the ^{11}B NMR spectrum and two signals at $\delta_P = 66.8$ (Pt-PCy_3, $^1J_{Pt\text{-}P} = 4967$, $^4J_{P\text{-}P} = 14.6$) and 36.1 (Fe-PMe_3, $^4J_{P\text{-}P} = 14.6$) in the $^{31}P\{^1H\}$ NMR spectrum. The concomitant formation of free PCy_3 was indicated by a ^{31}P NMR resonance at $\delta_P = 9.8$.

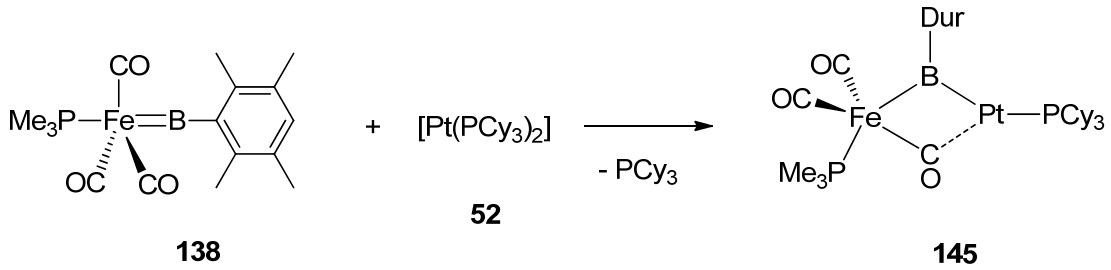

138 **52** **145**

Scheme 30: Reaction of $[(OC)_3(Me_3P)Fe{=}BDur]$ (**138**) with $[Pt(PCy_3)_2]$ (**52**).

Complex **145** was isolated as deep red crystals by crystallization from toluene/hexane solutions at –35 °C and subjected to X-ray diffraction analysis (Fig. 56).

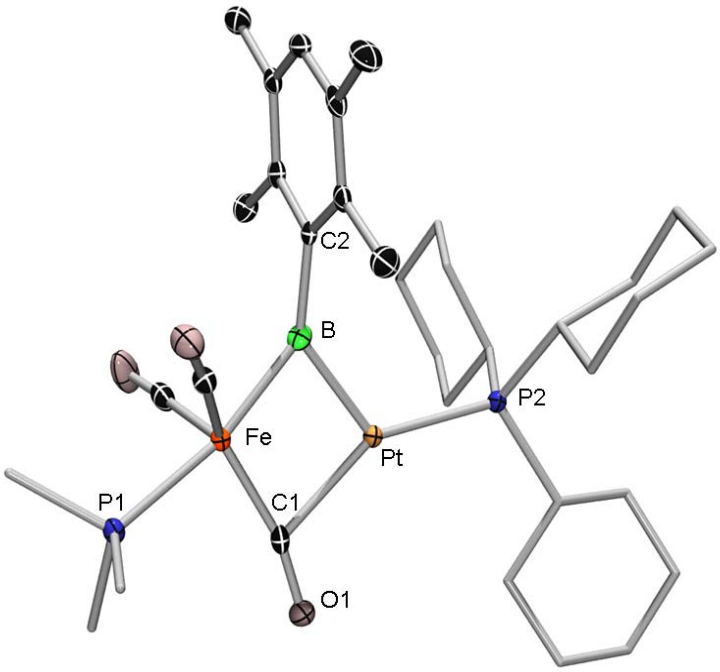

Fig. 56 Molecular structure of $[(OC)_2(Me_3P)Fe(\mu\text{-}CO)(\mu\text{-}BDur)Pt(PCy_3)]$ (**145**). Ellipsoids drawn at the 50% probability level. Ellipsoids of the ligands, hydrogen atoms and co-crystallized solvent molecules have been omitted for clarity. Relevant bond lengths [Å] and angles [°]: Fe-Pt 2.5710(5), Fe-B 1.970(4), Pt-B 1.976(4), Fe-P1 2.2037(10), Pt-P2 2.2621(9), Fe-C1 1.789(4), Pt-C1 2.185(4); Fe-B-Pt 81.32(14), Fe-C1-O1 165.2(3), Fe-C1-Pt 79.93(13), Pt-C1-O1 114.8(3), Fe-B-C2 142.0(3), Pt-B-C2 136.2(3).

Complex **145** crystallizes in the triclinic space group *P*-1, and the overall geometry of the central Fe-B-Pt-C1 fragment, which is approximately planar as indicated by the sum (359.8°) of angles within the four-membered ring, revealed the semi-bridging coordination mode for both arylborylene (:BDur) and carbonyl ligands[128-130]. The Fe-B separation (1.970(4) Å) is lengthened by more than 10% in comparison to the precursor **138** as a result of the increased coordination number at boron. The Pt-B bond length of 1.976(4) Å falls in the expected range for the previously reported heterodinuclear borylene species.[128,185] Moreover, the almost orthogonal orientation of the duryl substituent at boron with respect to the Fe-B-Pt-C1 four membered ring is presumably due to steric congestion imposed by the duryl group and the PCy_3 ligand.

2.6.2 Reaction of [(OC)$_3$(Me$_3$P)Fe=BDur] (**138**) with benzophenone (**146**)

Iron borylene **138** was treated with benzophenone (**146**) as a representative carbonyl substrate, yielding a new cyclic species **147** as indicated by a significantly upfield shifted ^{11}B NMR resonance at δ_B = 75, which resembles that of **48** at δ_B = 72. Accordingly, a new singlet at δ_P = 12.4 was observed in the ^{31}P NMR spectrum.

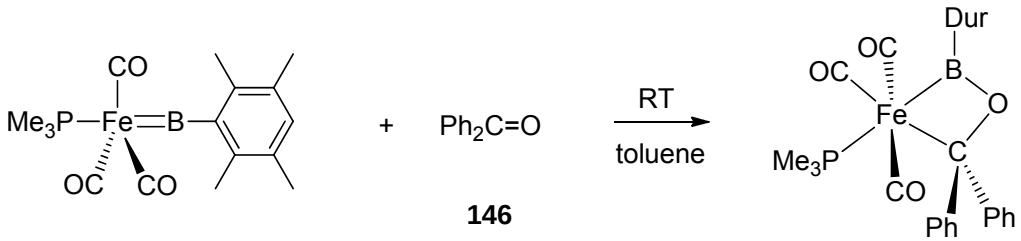

Scheme 31: Reaction of [(OC)$_3$(Me$_3$P)Fe=BDur] (**138**) with benzophenone (**146**).

Complex **147** was isolated in high yield (80%) as colorless crystals upon cooling a hexane/toluene solution to –35 °C. X-ray diffraction analysis confirmed the constitution of **147**, which crystallizes in the triclinic space group *P*-1 with two independent molecules in the asymmetric unit, both featuring very similar structural parameters. The overall geometry, in particular the Fe-B-O-C four-membered ring, resembles that of the previously reported manganese analogue **48** (Fig. 57). That is, (i) the planarity of the ring as indicated by sum of the internal angles (360.0°), (ii) significant elongation of the Fe-B separation (2.0882(16) Å, falling in the expected range for iron boryl complexes[105] as a result of the increased coordination number at boron atom and loss of Fe=B double bond character, and (iii) very similar B-O and C-O bond lengths.

However, in stark contrast to the maganese analogue **48**, which spontaneously undergoes a cycloreversion in solution within a couple of hours, leading to a corresponding manganese carbene complex and boroxine as a trimerisation product of R-B=O, **147** undergoes merely slow decomposition ($t_{1/2}$ = 4 d in benzene). As indicated by ^{1}H, ^{11}B and ^{31}P NMR spectra, no clean formation of the expected boroxine and iron carbene complexes was observed.

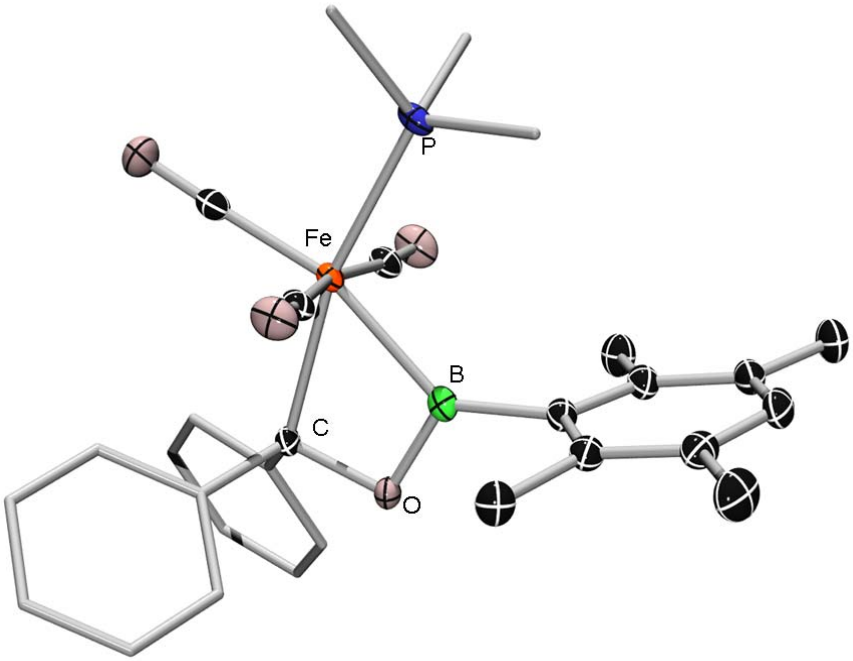

Fig. 57 Molecular structure of $[(OC)_3(Me_3P)Fe\{B(Dur)OC(Ph)_2\}]$ (**147**). Ellipsoids drawn at the 50% probability level. Ellipsoids of the ligands, hydrogen atoms and the second independent molecule in asymmetric unit have been omitted for clarity. Relevant bond lengths [Å] and angles [°]: Fe-B 2.0882(16), B-O 1.3503(18), O-C 1.4690(15), C-Fe 2.1116(13); B-Fe-C 62.56(5), Fe-C-O 95.59(7), C-O-B 101.25(10), O-B-Fe 100.60(9).

2.6.3 Reaction of $[(OC)_3(Me_3P)Fe{=}BDur]$ (**138**) with alkynes and metal alkynyl σ-complexes

An essential reactivity pattern of pentacarbonyl borylene complexes derived from group 6 metals is borylene transfer to C≡C triple bonds of alkynes, which provides a facile and straightforward approach to a variety of borirenes with different exocyclic substituents, e.g. alkyl, aryl and organometallic fragment. However, the boron-bound substituent is limited to the amino group $N(SiMe_3)_2$. Hence, we addressed whether the borylene moiety ":BDur" of $[(OC)_3(Me_3P)Fe{=}BDur]$ (**138**) can be likewise transferred to alkynes or metal alkynyl σ-complexes, which might afford duryl borirenes.

To this end, reactions of $[(OC)_3(Me_3P)Fe{=}BDur]$ (**138**) with 3-hexyne (**148**), 2-butyne (**149**), bis(trimethylsilyl)acetylene (**150**), diphenylacetylene (**151**) as well as metal alkynyl σ-complexes $[Cp^*Fe(CO)_2C{\equiv}CPh]$ (**67**) and $[Cl(Me_3P)_2PtC{\equiv}CPh]$ (**84**) were carried out under either thermal or photolytic conditions (except for **67**, due to its photochemical lability). However, in all cases, merely slow decomposition of iron borylene complex **138** was observed according to the multinuclear NMR spectroscopic data.

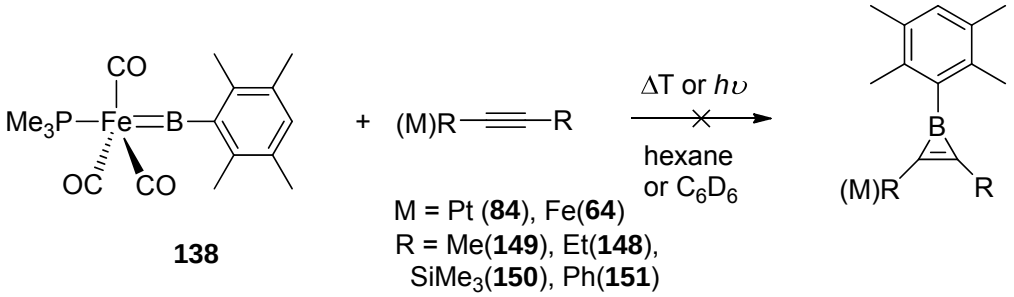

Scheme 32: Reaction of $[(OC)_3(Me_3P)Fe{=}BDur]$ (**138**) with alkynes.

2.6.4 Reaction of $[(OC)_3(Me_3P)Fe{=}BDur]$ (**138**) with naphthalene

$[(OC)_3(Me_3P)Fe{=}BDur]$ (**138**) was irradiated in the presence of an equimolar amount of naphthalene in C_6D_6. The reaction was monitored by multinuclear NMR spectroscopy, which revealed complete conversion of starting materials into a new boron- and phosphorus-containing species (δ_B = 30, which is significantly upfield shifted with respect to that of **138**; δ_P = 21.3, bs) within 16 h. After workup, the product was isolated as a pale yellow fibrous solid. In the ^1H NMR spectrum, the singlet at δ_H = 2.64 (6H), 2.30 (6H), 7.04 (1H) and the doublet at δ_H = 0.77 ($^2J_{H\text{-}P}$ = 7.4, 9H) confirmed the presence of PMe_3 ligand and duryl group. Interestingly, the signals for eight protons derived from naphthalene are shifted upfield to varying degrees, i.e. δ_H = 6.62-6.70 (m, 4H), 5.87 (d, $^1J_{H\text{-}H}$ = 9.7 Hz, 1H), 5.18 (bs, 1H), 3.89 (bs, 1H), 3.06 (bs, 1H). Furthermore, COSY NMR experiments revealed correlations between the peaks at 5.87, 5.18 ppm and between the peaks at 5.18, 3.89 ppm (Fig. 58). Notably, no sign of COSY correlation between the proton at δ_H = 3.06 and other protons was observed, thus suggesting the borylene insertion into an aromatic C-H bond. The ^1H-^1H long range correlations, in particular those depicted in Fig. 58 reinforced the proposed connectivity. In addition, the resonance at δ_C = 227.6 in the ^{13}C NMR spectrum as well as two bands at 1990 and 1942 cm^{-1} in IR spectra confirmed the presence of carbonyl ligands. Furthermore, m/z values of 460, 432, 404 in EI-MS spectra are consistent with the molecular formula $[DurBH(C_{10}H_7)Fe(PMe_3)(CO)_2]$ and those of the corresponding decarbonylation products, thus implying the presence of $Fe(PMe_3)(CO)_2$ fragment, which is presumably coordinated to the borylated naphthalene in an η^4 fashion (Scheme 33) in view of the upfield shifted peaks at δ_H = 5.87, 5.18 and 3.89 (Fig. 58). Unfortunately, all attempts to obtain single crystals suitable for X-ray diffraction analysis failed.

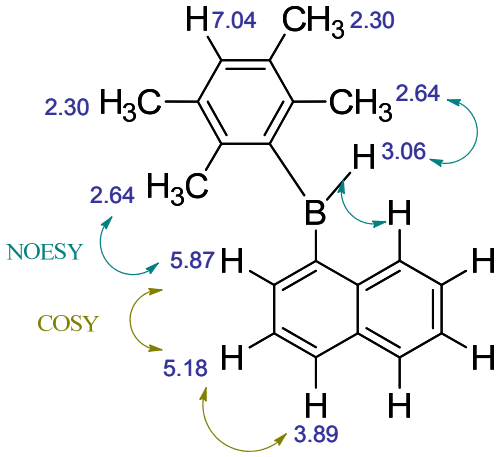

Fig. 58 Assignment of ^{1}H NMR spectrum peaks and selected COSY and NOESY correlations in **152**.

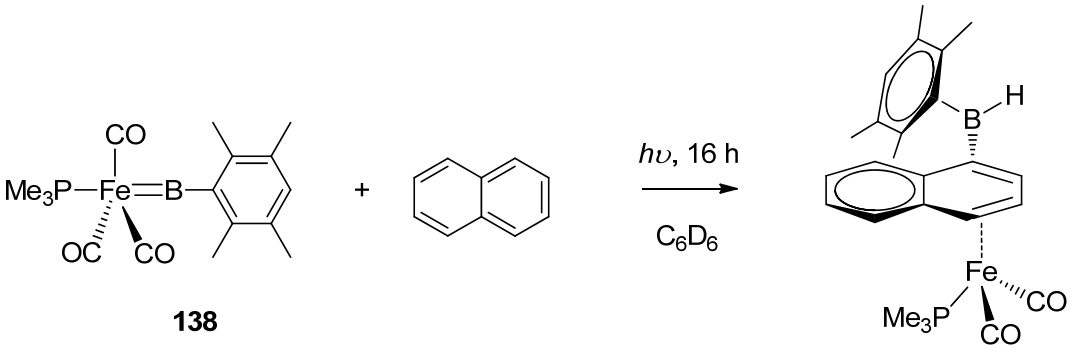

138 **152**

Scheme 33: Reaction of [(OC)$_3$(Me$_3$P)Fe=BDur] (**138**) with naphthalene and the proposed product **152**.

2.7 Catenation of borylene units in the coordination sphere of iron

The homonuclear σ-bond enthalpy (D_0 = 293 kJ mol^{-1}) of boron is significantly higher than most of the elements that are willing to form oligomeric or polymeric chains, e.g. D_0 = 345 (C), 222 (Si), 201 (P), 146 (As), 121 (Sb), 226 (S), 172 (*Se*), 126 (Te) kJ mol^{-1}.[186-188] Whereas examples of boron catenation are extremely rare. In fact, the rarity of catenated boron compounds stems not from an instability of the σ-bonds involved, but instead from boron's tendency to go beyond catenation. As shown in Fig. 59, while the chloro and *tert*-butyl derivatives of tetraborane **153**[189,190] and **154**[191] have a tetrahedral structure, **156**, **157** and **158** that benefit from π-electron donating boron-bound substituents were shown to possess a bent ring structure[192-194]. However, presence of the rigid and more bulky amino substituent TMP in **155** favors again the tetrahedral structure, which can be explained by the fact that boron prefers to form three-dimensional hypercoordinate compounds with non-classical bonding as a way to offset its inherent electron deficiency. Hence, non-polyhedral oligo- or polyboranes of the forms $X(BR)_nY$ or *cyclo*-$(BR)_n$ may be accessible if the π-basicity of the R group is strong enough to circumvent the need for polyborane cluster formation.

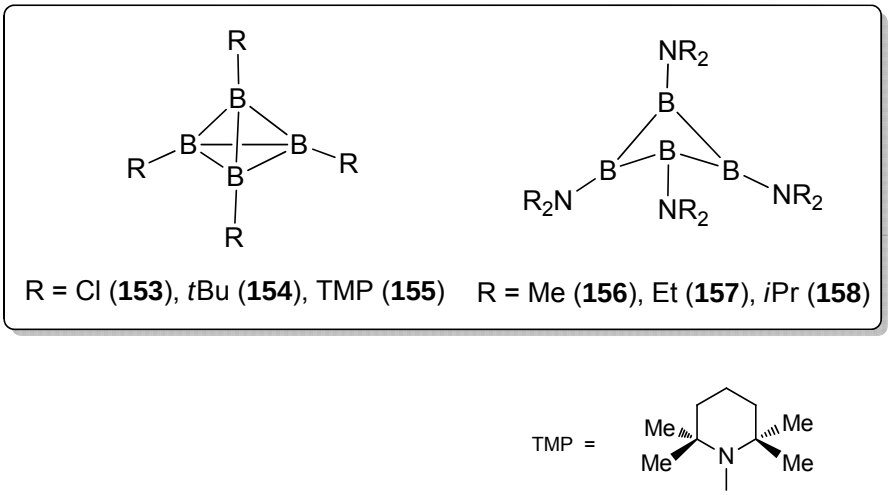

Fig. 59 Tetrahedral and bent ring structure of cyclotetraboranes.

The handful of known catenated boron compounds, the longest being linear $B_6(NMe_2)_8$ and *cyclo*-$B_6(NR_2)_6$ (R = Me, Et), are exclusively prepared by uncontrolled reductions of haloboranes in poor yields and with poor control of geometry[192-197]. Nöth and Pommerening reported in 1980 the first structurally characterized catenated polyborane species, i.e. *cyclo*-$B_6(NMe_2)_6$ (**159**), which was synthesized by dehalogenation of $ClB(NMe_2)_2$ (**160**) with Na/K

alloy (1:3) in yield of ca. 0.1% (Fig. 60).[194] In 1994, Nöth *et al.* reported an optimized codehalogenation of $ClB(NMe_2)_2$ (**160**) and $(Me_2N)_3B_2Cl$ (**161**) with Na/K alloy (1:2.8), uncontrollably yielding the $B_n(NMe_2)_{n+2}$ (n = 1-6) series, in which **162**, **163** and **164** were isolated in poor yields (Fig. 61).[198]

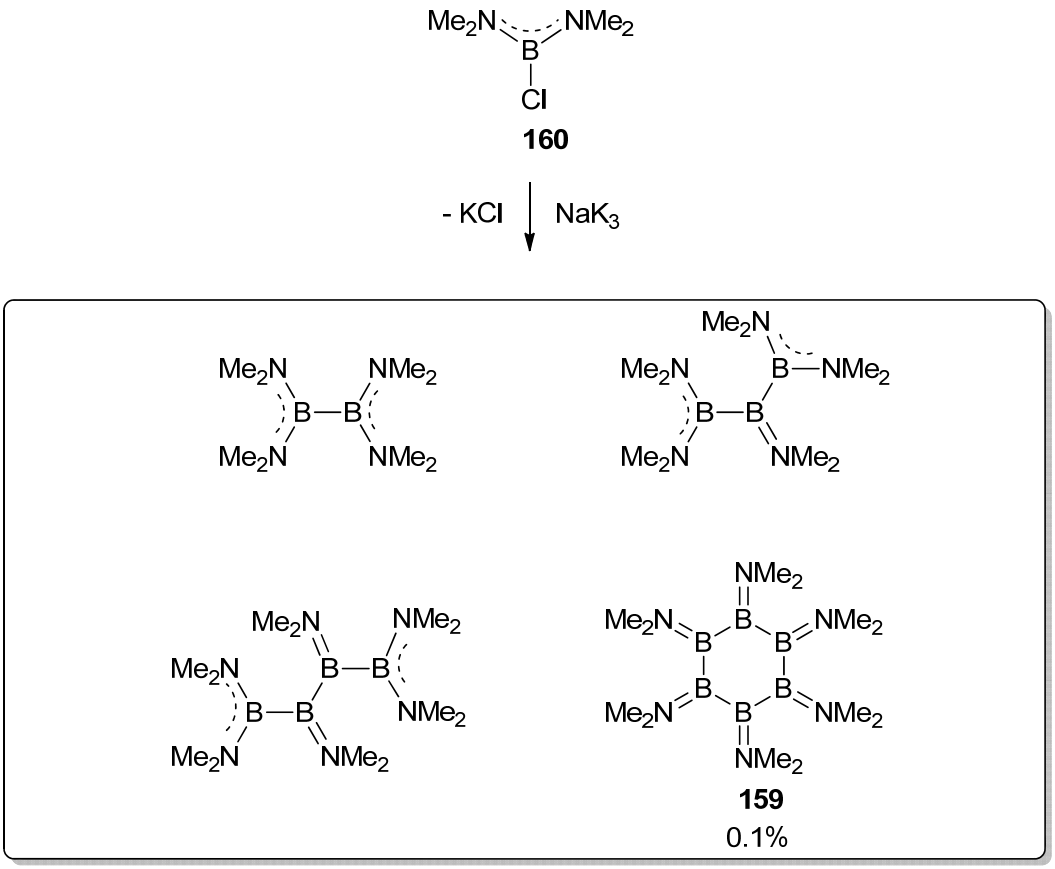

Fig. 60 Dehalogenation of $ClB(NMe_2)_2$ (**160**) with NaK_3.

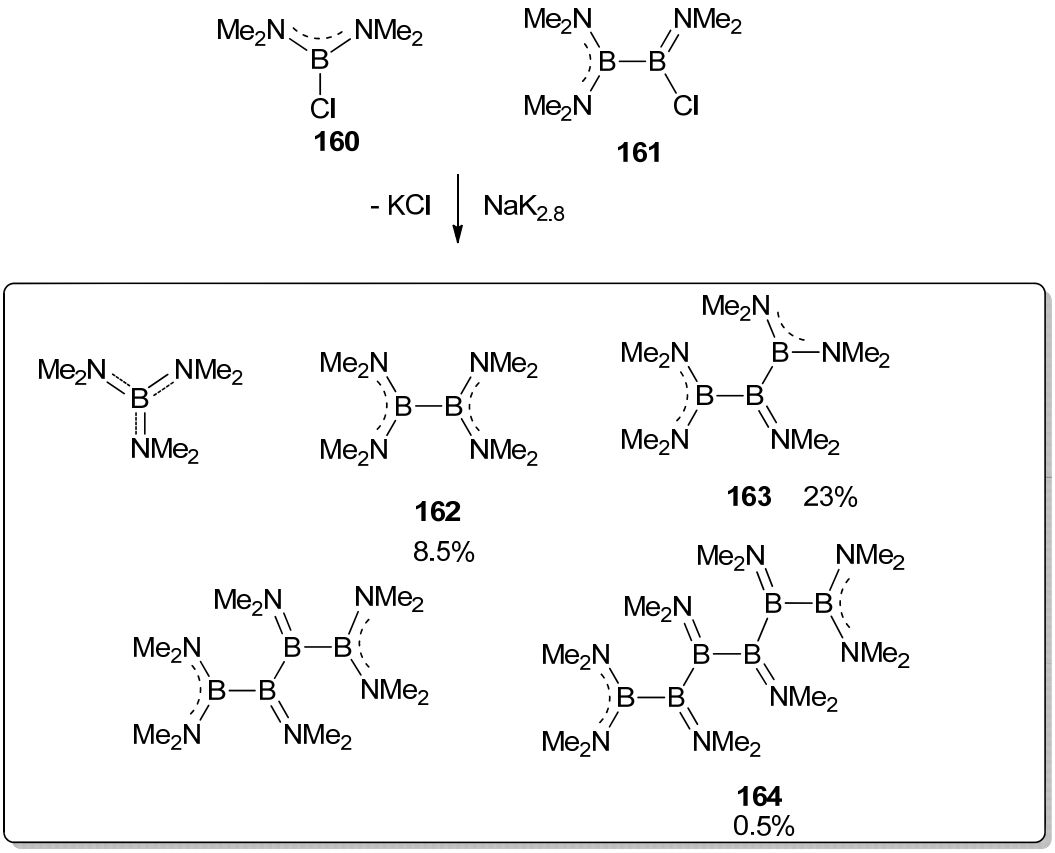

Fig. 61 Codehalogenation of $ClB(NMe_2)_2$ (**160**) and $(Me_2N)_3B_2Cl$ (**161**) with $NaK_{2.8}$.

Experimentally, the borylene repeat unit of a boron chain, ":BR", features as a stable motif only in the coordination sphere of transition metals[66,199], although limited borylene reactivity can be harnessed using base-stabilized examples[171,172,200]. Borylene ligands on transition metals have shown the potential to couple and form dimetallic clusters both experimentally[201] and computationally[202] (Fig. 62). Upon irradiation of bridged chloroborylene complex of manganese **165** under CO atmosphere, the labile terminal chloroborylene borylene complexes **166** were presumably generated as a transient intermediate, which dimerized with concomitant B-B coupling with a bond distance of 1.70 Å, affording a *nido*-Mn_2B_2 cluster.[201] In addition, Schaefer *et al.* predicted the coupling of two bridged fluoroborylene ligands in the coordination sphere of a diiron system with the B-B separation of 1.91 Å, thus constituting a difluorodiborene system.[202]

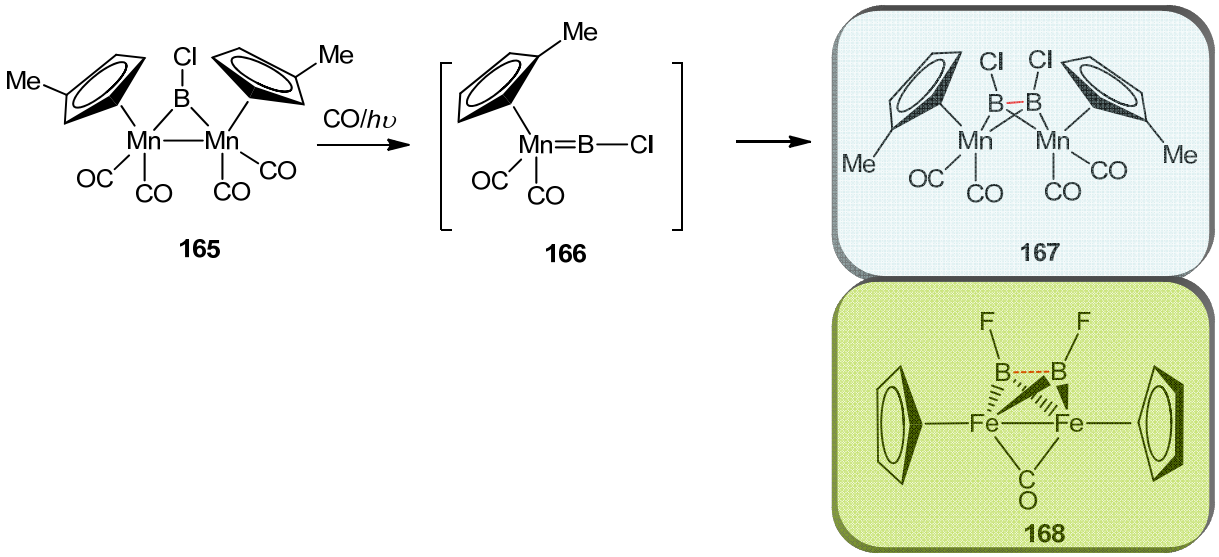

165 166 167 168

Fig. 62 Experimentally observed (above) and computationally predicted (below) borylene coupling in the coordination sphere of transition metals.

Hence, we addressed whether borylene ligands :BR could be catenated in a controlled fashion in the coordination sphere of metals, and upon a subsequent reductive elimination to form either chain-like polyborylenes "$X(BR)_nY$" or *cyclo*-polyborylenes "$(BR)_n$" (Fig. 63).

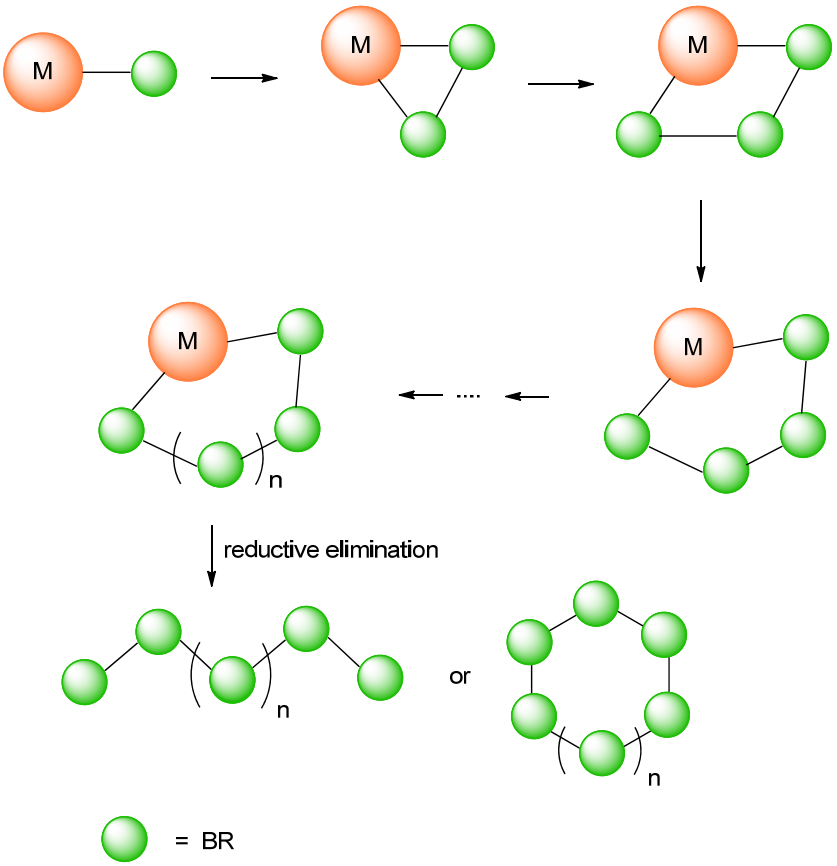

Fig. 63 Proposed borylene catenation in the coordination sphere of metals and subsequent reductive elimination to form polyborylene chains or cycles.

2.7.1 Synthesis of $[(OC)_3Fe(BDur)\{BN(SiMe_3)_2\}]$ (**169**)

Iron bis(borylene) complex $[(OC)_3Fe(BDur)\{BN(SiMe_3)_2\}]$ (**169**) was obtained upon warming (40°C) a pale yellow hexane solution of **138** in the presence of an equimolar amount of $[(OC)_5Mo{=}BN(SiMe_3)_2]$ (**16**) (Scheme 34). Analysis by means of ^{11}B NMR spectroscopy revealed gradual consumption of starting materials (δ_B = 146 and 90) and quantitative formation of new boron-containing species showing new resonances at δ_B = 129 and 78 that are both up-field shifted by more than 10 ppm. This shift was however not observed in the synthesis of iridium bis(borylene) complex $[Cp^*Ir\{BN(SiMe_3)_2\}_2]$ (**37**)[108]. The boron-containing product was isolated in good yield (67%) as deep red crystals upon cooling the reaction mixture to –75°C and recrystallization from a saturated hexane solution at –30°C. The identity of **169** was further confirmed by multinuclear NMR spectroscopy, elemental analysis, IR spectroscopy and X-ray structure analysis (Fig. 64). Complex **169** crystallizes in triclinic space group *P*-1. In stark contrast to disubstituted iron carbonyls $[(OC)_3FeLL']$ (L = phosphine, L' = phosphine or borylene), which exhibit trigonal bipyramidal geometry with L and L' at axial sites [141], bis(borylene) iron carbonyl **169** features a remarkably acute B-Fe-B angle (65.91(9)°) when compared to that of iridium bis(borylene) $[Cp^*Ir\{BN(SiMe_3)_2\}_2]$ (**37**) (78.4°). The B-B separation of 1.982(3) Å, which is significantly shorter than that of the iridium analogue (2.36 Å), is comparable with the theoretically predicted bond length of difluorodiborene (1.91 Å) in the coordination sphere of a diiron system[202]. This finding is indeed consistent with the unusual up-field shift of ^{11}B NMR resonances, suggesting coupling of "$BN(SiMe_3)_2$" and "BDur" on the iron center to form the side-on-bound diborene ligand $(Me_3Si)_2NB{=}BDur$.

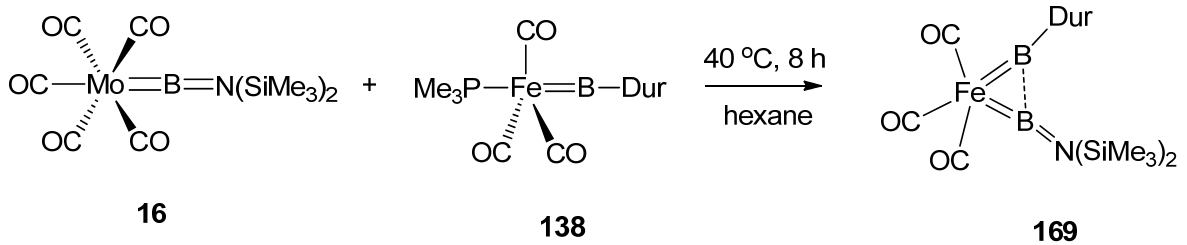

16 **138** **169**

Scheme 34: Synthesis of $[(OC)_3Fe(BDur)\{BN(SiMe_3)_2\}]$ (**169**).

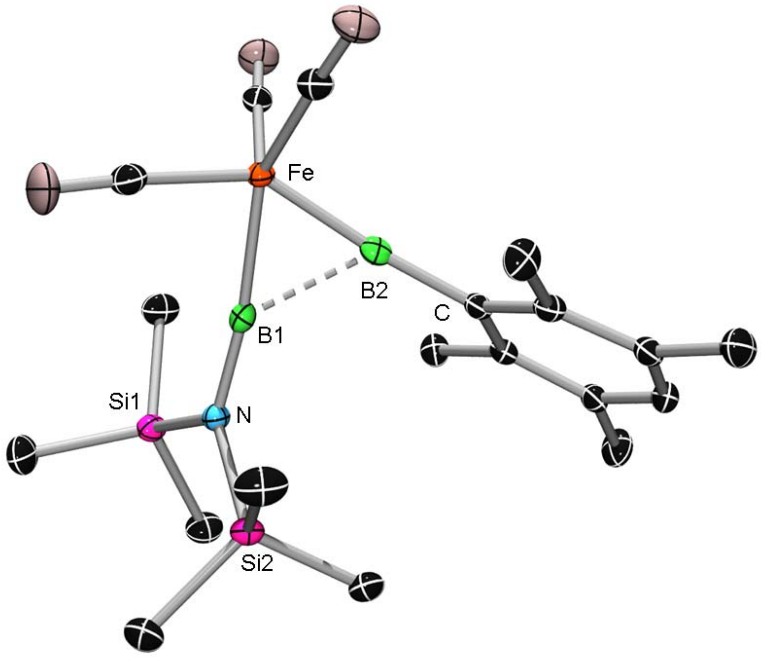

Fig. 64 Molecular structure of $[(OC)_3Fe(BDur)\{BN(SiMe_3)_2\}]$ (**169**). Thermal ellipsoids depicted at the 50% probability level. For clarity, hydrogen atoms have been removed. Selected bond lengths (Å) and angles (°): Fe-B1 1.844(2), Fe-B2 1.799(2), B1-N 1.362(2), B2-C 1.531(3), B1-B2 1.982(3); Fe-B1-N 172.02(16), Fe-B2-C 174.91(15), B1-Fe-B2 65.91(9).

To provide further insight into the bonding situation in the molecules **169**, DFT calculations at the OLYP/TZVP level of theory were carried out. The results for complex **169** show that while the B-B distance (experimental: 1.982(3) Å; theory: 1.994 Å) is longer than that of normal B-B single bonds, there is a significant bonding interaction (WBI: 0.78) corresponding to almost complete coupling of the boron atoms (Fig. 65, left). Natural Bond Orbital (NBO) second-order perturbation energy analysis shows donor-acceptor interaction between a filled B-B σ-bond and an empty orbital on the Fe (Fig. 65, right). Only a very weak metal-to-ligand back-bonding interaction was observed, which may explain the high positive charge on the two boron atoms.

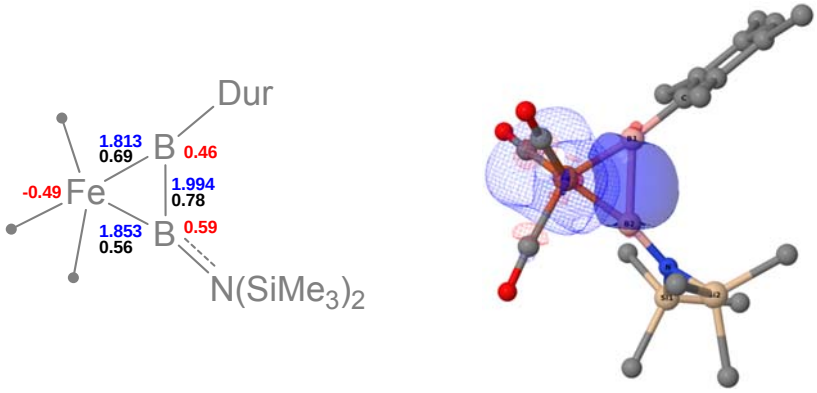

Fig. 65 Results of DFT calculations on complexes **169**. Calculated bond lengths are shown in blue (Å), Wiberg bond indices in black, and natural charges in red.

2.7.2 Photolysis of $[(OC)_3Fe(BDur)\{BN(SiMe_3)_2\}]$ (**169**)

Subsequently a hexane solution of **169** was irradiated at ambient temperature for 48 h (Scheme 35). Iron dinuclear tetra(borylene) complex **170** was obtained in the form of deep red crystals in yield of 60 %. The constitution of **170** was confirmed by multinuclear NMR spectroscopy, elemental analysis, IR spectroscopy and X-ray structure analysis (Fig. 66). The ^{11}B NMR spectrum revealed new resonances at δ_B = 140 and 86 that are both slightly down-field shifted in comparison to those of **169** (δ_B = 146 and 90). The singlet signals at δ_H = 7.02, 2.23, 1.94 and -0.01 with integral in a ratio of 1:6:6:18 in the ^{1}H NMR spectrum confirm the presence of duryl and bistrimethylslilylamino groups in a ratio of 1:1. Moreover, the resonance at δ_C = 214.9 in ^{13}C NMR spectrum as well as two bands at 1959, 1921 cm^{-1} in IR spectra confirmed the presence of carbonyl ligand. Single crystals suitable for X-ray diffraction analysis were obtained upon irradiation of a hexane solution of **169** in an NMR tube at ambient temperature overnight. Complex **170** crystallizes in monoclinic space group *C*2/*c*. Again, considerable interaction between two adjacent boron atoms in the coordination sphere of the two iron centers was observed (Fig. 66), which could be supported by the following findings: i) an acute B1-Fe-B2 angle (67.02(8)°) that is comparable with that of **169**; ii) significant bending of Fe-B1-N (165.56(16)°); iii) significantly shorter Fe-B2 distance (1.963(2) Å) in comparison to Fe' -B2 (2.0328(19) Å), which allows the bridging boron to approach the adjacent terminal borylene ligand. Furthermore, while **170** possesses considerable stability in solid state, its parent compound $[Fe_2(CO)_8]$ is highly reactive and has only been prepared as a transient species[203-205]. The Fe-Fe separation of 2.3554(5) Å is significantly shorter than the single Fe-Fe bond of classical $[Fe_2(CO)_9]$ (2.52 Å)[206] and thus

can be interpreted as a formal double bond as required for an 18-electron configuration at each iron center.

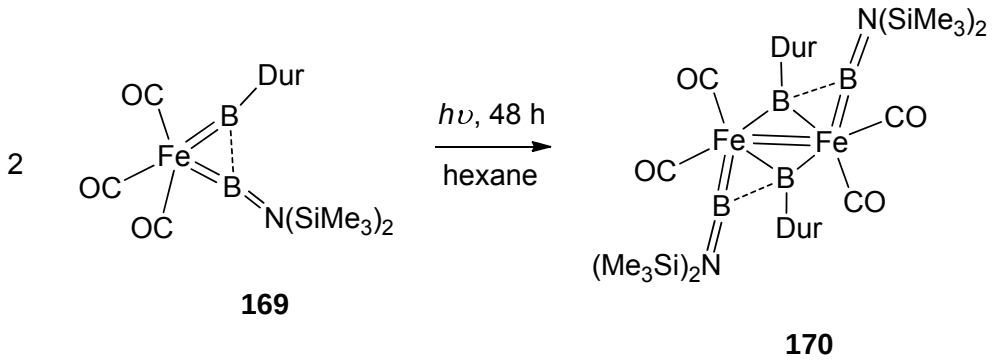

169 **170**

Scheme 35: Photolysis of $[(OC)_3Fe(BDur)\{BN(SiMe_3)_2\}]$ (**169**).

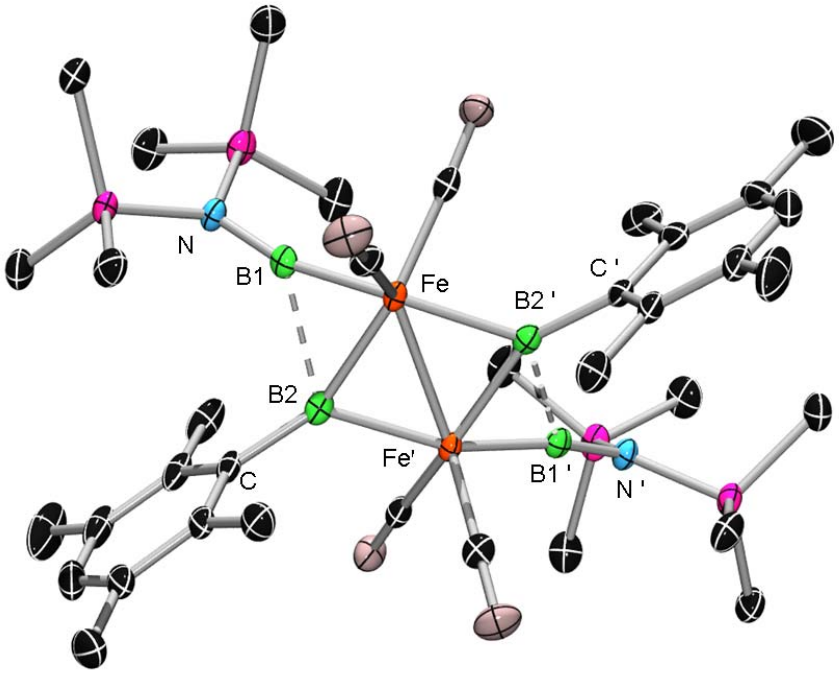

Fig. 66 Molecular structure of **170**. Thermal ellipsoids depicted at the 50% probability level. For clarity, hydrogen atoms have been removed. Selected bond lengths (Å) and angles (°): Fe-B1 1.839(2), Fe-B2 1.963(2), Fe-B2' 2.0328(19), Fe-Fe' 2.3554(5), B1-B2 2.102(3); Fe-B1-N 165.56(16), B1-Fe-B2 67.02(8).

2.7.3 Snythesis of $[(OC)_2Fe(\{BN(SiMe_3)_2\}_2\{BDur\}_2)]$ (**171**)

A suspension of **170** in hexane was heated at 80°C under CO atmosphere (Scheme 36). Over 2 h, the reaction mixture became homogeneous. Upon cooling the reaction solution to –30°C, **171** was obtained as orange crystals in 80% yield and could be fully characterized by multinuclear NMR spectroscopy, elemental analysis, IR spectroscopy and X-ray structure analysis (Fig. 67). Notably, the ^{11}B NMR spectrum revealed new resonances at δ_B = 83 and 76. Comparing with ^{11}B NMR peaks of the starting material **170**, both signals were up-field shifted, however to varying degrees. The singlet signals at δ_H = 6.74, 2.08, 2.02 and 0.23 with integral in a ratio of 1:6:6:18 in ^{1}H NMR spectrum clearly indicated the presence of duryl and bis(trimethylsilyl)amino groups in a ratio of 1:1. Moreover, the resonance at δ_C = 214.9 ppm in the ^{13}C NMR spectrum as well as two bands at 1981 and 1934 cm^{-1} in IR spectra confirmed the presence of carbonyl ligands. Complex **171** crystallizes in triclinic space group *P*-1. Remarkably, the central Fe-B1-B2-B3-B4 ring is approximately planar as indicated by the sum (538.0°) of angles within the five-membered ring. Furthermore, the acute angles Fe-B1-B2 (64.2(2)°) and Fe-B4-B3 (63.8(2)°) display significant deviation both from that expected for an *sp*^{2}-boron centre (120°) and from the internal angles of a pentagon (108°). Accordingly, the B2-B3 bond is held close to the iron center, thus suggesting a significant interaction between the three atoms. The Fe-B1 and Fe-B4 separations (1.90 Å) are lengthened by more than 3% in comparison to the borylene precursor **169** as a result of the increased coordination number at boron. The B-B bond distances of 1.792(6), 1.686(6) and 1.814(6) Å are comparable to those found in the *cyclo*-$B_6(NMe_2)_6$ (1.70, 1.78 and 1.68 Å)[196], suggesting a strong similarity between the two structures.

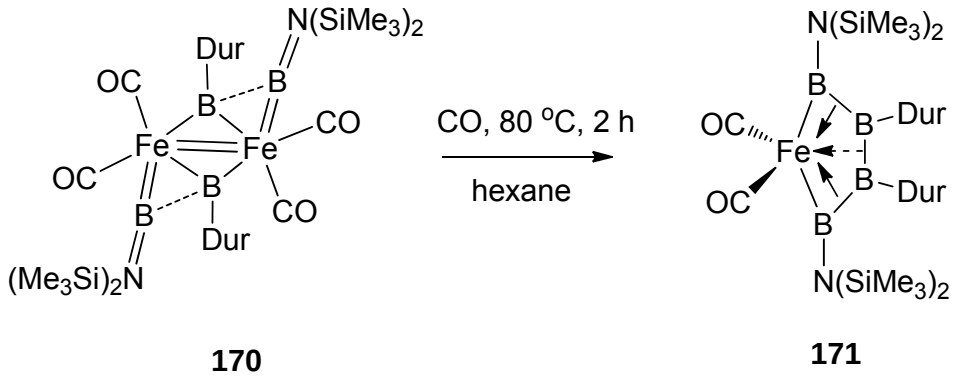

170 **171**

Scheme 36: Snythesis of $[(OC)_2Fe(\{BN(SiMe_3)_2\}_2\{BDur\}_2)]$ (**171**).

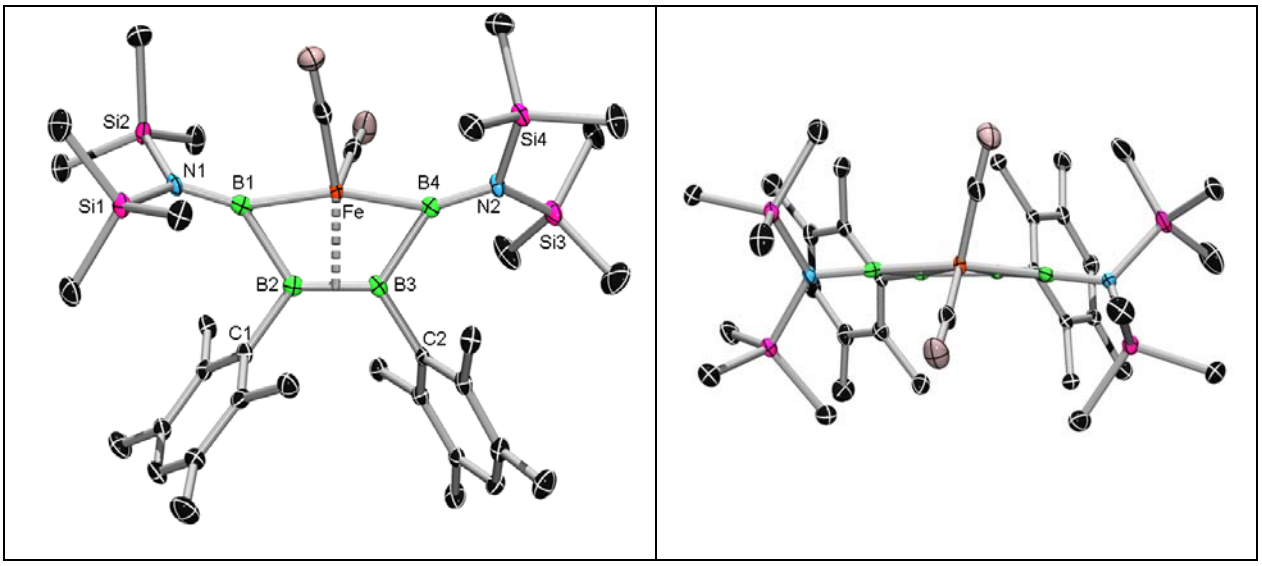

Fig. 67 Molecular structure of $[(OC)_2Fe(\{BN(SiMe_3)_2\}_2(BDur)_2)]$ (**171**). Thermal ellipsoids depicted at the 50% probability level. For clarity, hydrogen atoms have been removed. Selected bond lengths (Å) and angles (°): Fe-B1 1.896(4), Fe-B4 1.898(5), Fe-B2 1.961(4), Fe-B3 1.962(4), B1-B2 1.792(6), B2-B3 1.686(6), B3-B4 1.814(6); Fe-B1-B2 64.2(2), Fe-B4-B3 63.8(2), B1-Fe-B4 160.63(19), B1-B2-B3 124.7(3), B2-B3-B4 124.7(3).

DFT calculations (OLYP/TZVP level of theory) were carried out to provide further insight into the bonding situation in **171**. The calculated structure of **171** shows the B_4 chain to be a network of three fully-formed single B-B bonds (WBI: 0.86, 1.00 and 0.87; see **a**, Fig. 68), convincing evidence for the catenation of the boron atoms on the metal center. In addition, the HOMO of **171** consists of three conventional σ-bonds between the boron atoms, with single ("boryl-like") Fe-B bonds (**c** and **d**, Fig. 68). Crucially, there appears to be no classical σ-bonds between the central boron atoms and the Fe. Instead, NBO second-order perturbation energy analysis reveals interactions corresponding to side-on σ-coordination of all three B-B bonds to the metal (**b**, Fig. 68). These three donations are reminiscent of those found in σ-complexes and, importantly, the interaction energies for the two outer σ-bond donations (5.28 and 5.21 kcal mol^{-1}) are significantly stronger than those from the central B-B bond (2.34 kcal mol^{-1}). NBO analysis also showed a moderately strong interaction corresponding to back-bonding from a metal d_{z2} orbital to antibonding B-B orbitals (3.98 kcal mol^{-1}; **e** and **f**, Fig. 68). These two interactions, i.e. the strong donation to the metal from the outer B-B σ-bonds compared to that from the inner B-B σ-bond, and the significant back-bonding into the outer B-B σ* orbitals, might conspire to make the outer B-B bonds significantly longer than the inner B-B bond (outer: 1.792(6), 1.814(6) Å *vs.* inner: 1.686(6) Å).

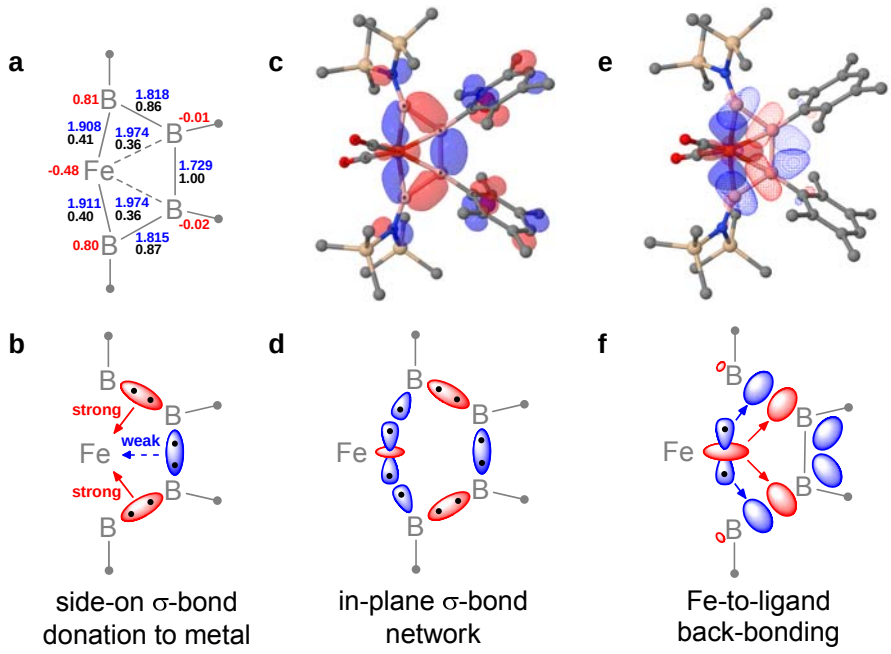

Fig. 68 Results of DFT calculations on complexes **171**. Calculated bond lengths are shown in blue (Å), Wiberg bond indices in black, and natural charges in red.

In conclusion, according to the results of DFT calculations, the overall picture of **171** is that of a tetraborane bound to the Fe predominantly as a *cis*-bis(boryl) ligand through the outer boron atoms, which might serve as a crucial step towards polyborylenes (see proposal in Fig. 63).

2.7.4 Reaction of $[(OC)_3Fe(BDur)\{BN(SiMe_3)_2\}]$ (**169**) with PMe_3

As the considerable interaction between boron atoms in **169** has been proven both experimentally and computationally (see *2.7.1*), and in view of the donor-acceptor interaction between the filled B-B σ-bond and an empty orbital on the Fe that might increase the B-B separation, we attempted to increase the B-B bond order by employing a strong σ-donor ligand such as phosphines, in the hope that the B-B σ-bond→Fe interaction could be reduced, and thus affording the iron-diborene complex **173**.

To this end, a red hexane solution of iron-bis(borylene) **169** was treated with an equimolar amount of PMe_3 at ambient temperature. The color turned immediately from red to purple. A nearly quantitative conversion of starting materials into new boron- and phosphorus-containing species was indicated by the presence of up-field shifted ^{11}B resonances at $\delta_B = 77$ and 50 and $\delta_P = 20.0$ in the ^{11}B and ^{31}P NMR spectrum respectively. Single crystals suitable for X-ray diffraction analysis were obtained upon concentration and subsequent storage of the purple reaction solution at –30°C overnight. Complex **172** crystallizes in the triclinic space

group *P*-1 with two independent molecules in the asymmetric unit, both featuring very similar structural parameters. The results of X-ray diffraction analysis partially confirmed our proposed structure. As shown in Fig. 69, the B1-B2 bond distance (1.671(4) Å) is significantly shortened in comparison to that (1.982(3) Å) in the precursor **169**, and is comparable with the central B-B bond length (1.686(6) Å) in **171**, and thus together with the acute Fe-B2-B1 angle (66.29(15)°) indicating an analogous side-on σ-coordination of B-B bond with the iron center. However, the B1-C1 separation of 1.617(4) Å as well as the significant bending of Fe-C1-O (152.1(2)°) clearly indicated the presence of a B1-C1 σ-bond, which might likewise interact with the electron-deficient iron center (formally 16e) *via* a side-on σ-coordination. The interaction between the iron and B-C σ-bond could be supported by the acute Fe-C1-B1 (70.63(15)°) angle as well. Moreover, the central Fe-B1-B2-C1 ring is approximately planar as indicated by the sum (359.7°) of angles within the four-membered ring (Fig. 69, right). Accordingly, the Fe-B2 separations (1.976(3) Å) are lengthened by ca. 7% in comparison to the corresponding bond in borylene precursor **169** as a result of the increased coordination number at boron.

In conclusion, a phosphine-induced migratory insertion of a carbonyl ligand and coupling of the two boron atoms is achieved in the coordination sphere of an iron center.

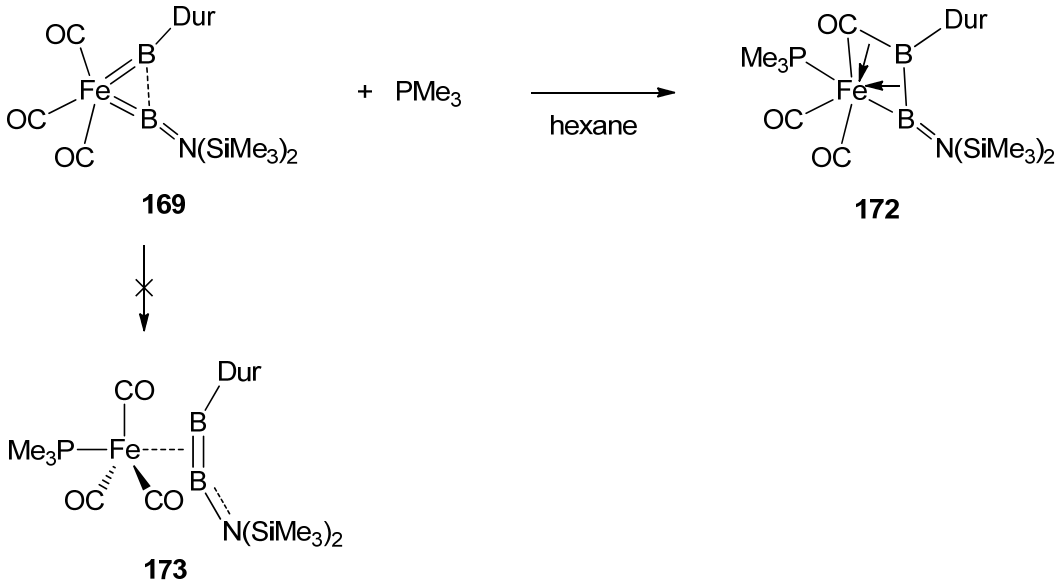

Scheme 37: Reaction of $[(OC)_3Fe(BDur)\{BN(SiMe_3)_2\}]$ (**169**) with PMe_3.

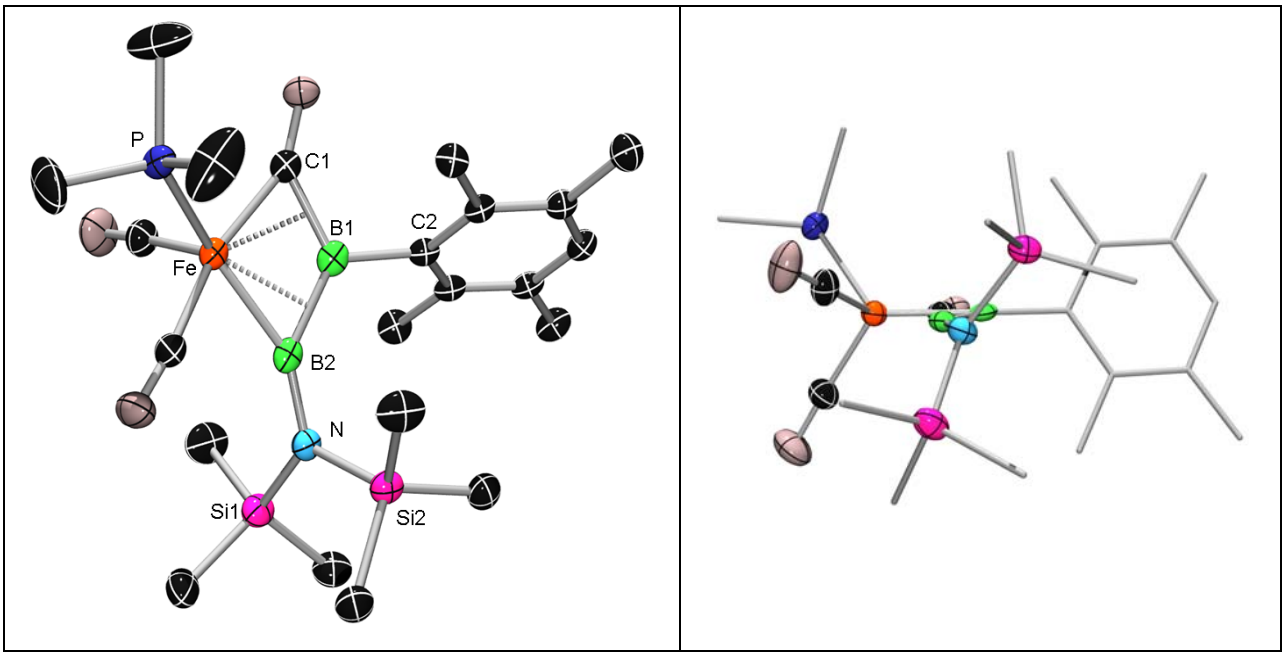

Fig. 69 Molecular structure of $[(OC)_2(Me_3P)Fe\{(CO)(BN(SiMe_3)_2)_2(BDur)_2\}]$ (**172**). Thermal ellipsoids depicted at the 50% probability level. For clarity, hydrogen atoms have been removed. Selected bond lengths (Å) and angles (°): B1-B2 1.671(4), B1-C1 1.617(4), Fe-B2 1.976(3), Fe-B1 2.011(3), Fe-C1 1.846(3), B2-N 1.397(4); Fe-C1-B1 70.63(15), Fe-B2-B1 66.29(15), C1-B1-B2 124.0(2), C1-Fe-B2 98.78(12), Fe-C1-O 152.1(2).

2.8 Reactivity of iron-bis(borylene) complexes

2.8.1 Reaction of [(OC)$_3$Fe(BDur){BN(SiMe$_3$)$_2$}] (**169**) with [Pt(PCy$_3$)$_2$] (**52**)

In 2.7.1, we were able to show the first example of an arylborylene metal complex. Having demonstrated the high yield synthesis of **169**, we became interested in the behaviour of bis(borylene) complexes upon treatment with transition metal Lewis bases.

Hence, the reaction of **169** in the presence of an equimolar amount of **52** was carried out. A nearly quantitative formation of the heterodinuclear species [(OC)$_3$Fe{μ-BN(SiMe$_3$)$_2$}(μ-BDur)Pt(PCy$_3$)] (**174**) was indicated by two broad resonances at δ_B = 122 and 98 in the ^{11}B NMR spectrum and the signal at δ_P = 74.4 (Pt-PCy$_3$, $^1J_{Pt-P}$ = 4123.4) in the ^{31}P{^{1}H} NMR spectrum. The concomitant formation of free PCy$_3$ was indicated by a ^{31}P NMR resonance at δ_P = 9.8.

Complex **174** was isolated as red crystals upon storage of the the concentrated reaction solution at –35^{o}C overnight and subjected to X-ray diffraction analysis (Fig. 70).

Compound **174** crystallizes in the monoclinic space group $P2_1/c$, and the overall geometry of the central Fe-B1-Pt-B2 fragment, which is in contrast to the approximately planar Fe-B-Pt-C1 ring of [(OC)$_2$(Me$_3$P)Fe(μ-CO)(μ-BDur)Pt(PCy$_3$)] (**145**), adopts a slightly bent ring structure (Fig. 70, right). However, both structures reveal a semi-bridging coordination mode for both arylborylene and aminoborylene ligands[107]. Accordingly, the Fe-B separation (Fe-B1 1.934(4), Fe-B2 1.945(3) Å) is lengthened by ca. 6% in comparison to the precursor **169** as a result of the increased coordination number at boron. Notably, comparing the overall geometry between **174** and **145** and in particular the central four-membered ring, while the Fe-B bond lengths in **174** are slightly shorter than that (1.970(4) Å) in **145**, the Pt-B separations (Pt-B1 2.004(3), Pt-B2 2.063(4) Å) in **174** are somewhat longer than that (1.976(4) Å) in **145**. This could be explained by the presence of two electron deficient boron atoms in **174**, which leads to a weakening of electron donation from platinum to each boron center and correspondingly an enhanced iron to boron π-donation. Moreover, the almost orthogonal orientation of the boron-bound duryl and bismethylsilylamino substituents with respect to the the BR$_3$ plane is presumably due to steric congestion imposed by the duryl group and the PCy$_3$ ligand.

After isolating **174** in good yield, we became interested in whether **174** could further react with a second equivalent of metal Lewis base **52** to afford a four-coordinate boron center, e.g.

175. However, most likely due to the steric congestion imposed by the bulky groups in **174**, i.e. $N(SiMe_3)_2$, PCy_3 and Dur, no reaction was observed.

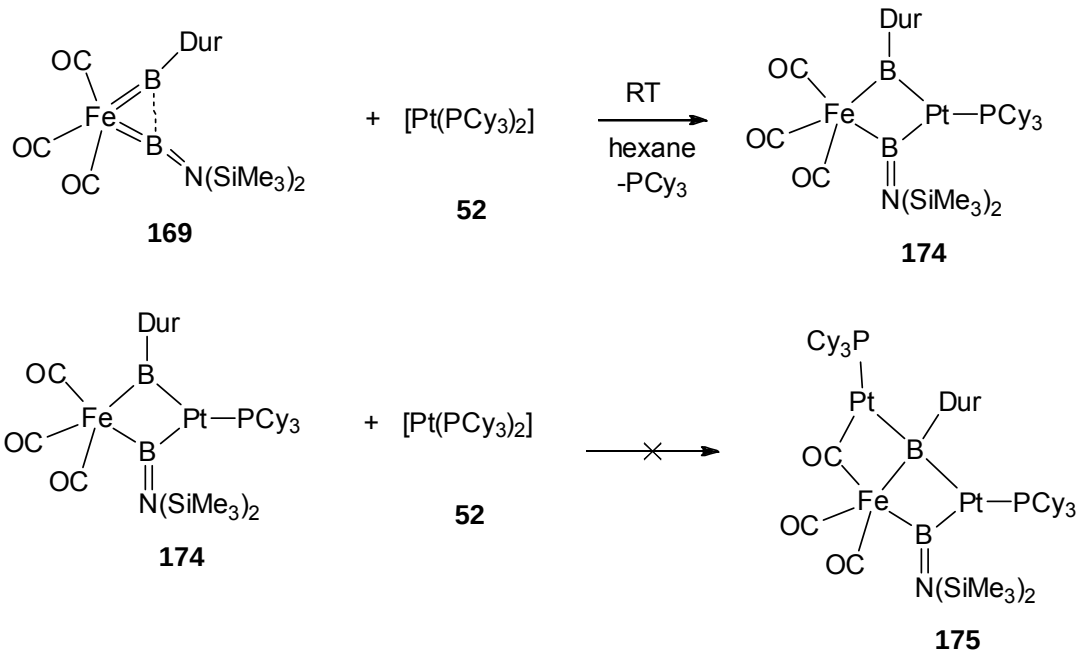

Scheme 38: Reaction of $[(OC)_3Fe(BDur)\{BN(SiMe_3)_2\}]$ (**169**) with $[Pt(PCy_3)_2]$ (**52**).

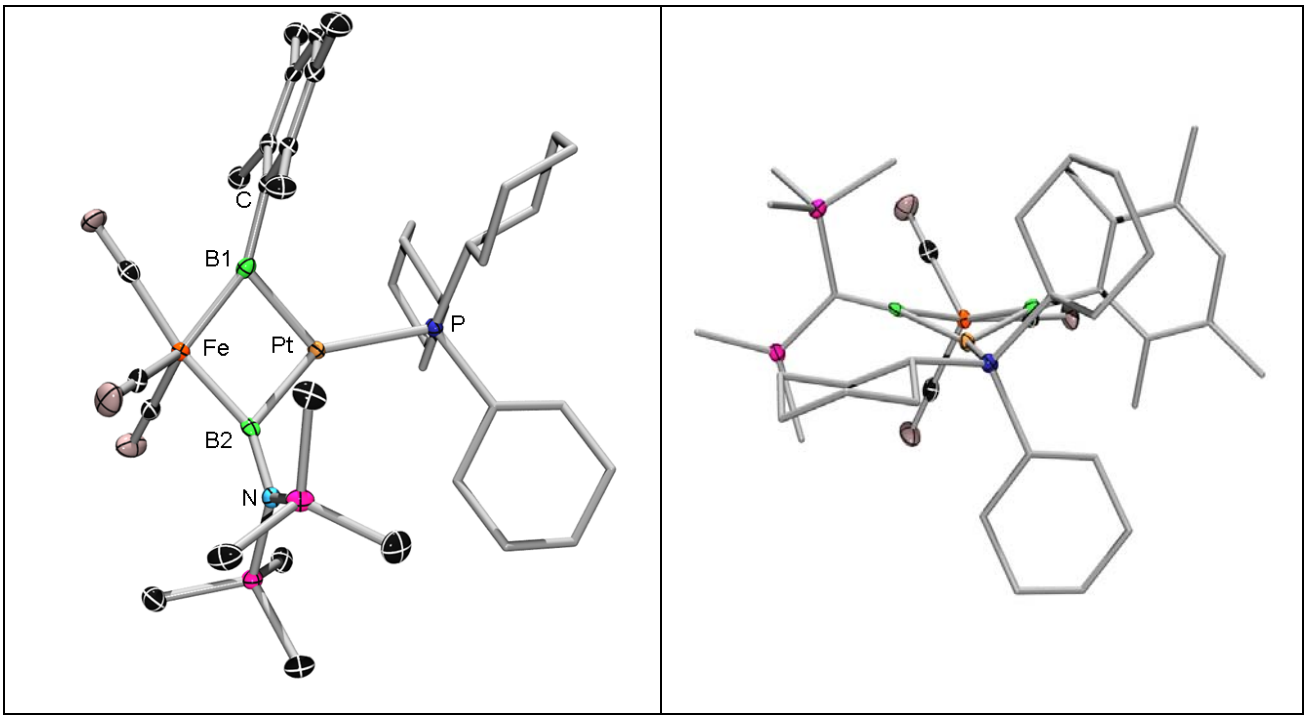

Fig. 70 Molecular structure of $[(OC)_3Fe\{\mu\text{-}BN(SiMe_3)_2\}(\mu\text{-}BDur)Pt(PCy_3)]$ (**174**). Thermal ellipsoids depicted at the 50% probability level. For clarity, ellipsoids of phosphine ligand, hydrogen atoms have been removed. Selected bond lengths (Å) and angles (°): Fe-B1 1.934(4), Fe-B2 1.945(3), Pt-B1 2.004(3), Pt-B2 2.063(4), B2-N 1.393(4); B1-Fe-B2

96.88(15), Fe-B2-N 153.7(3), Fe-B2-Pt 80.06(13), N-B2-Pt 126.2(2), Fe-B1-C 155.0(2), Pt-B1-C 123.2(2), Fe-B1-Pt 81.80(14).

2.8.2 Reaction of $[(OC)_3Fe(BDur)\{BN(SiMe_3)_2\}]$ (**169**) with BCl_3

Here we attempted to substitute the boron-bound amine function with a halogen, e.g. Cl, in the hope that the chloroborylene moiety in the generated molecule **176** could be stabilized by an enhanced B-B interaction.

To this end, a red hexane solution of iron bis(borylene) complex **169** was treated with an approximately equimolar amount of BCl_3 at ambient temperature. However, according to the ^{11}B NMR spectrum, only slow decomposition of **169** was observed ($t_{1/2}$ = ca. 24 h).

Alternatively, an equimolar amount of BCl_3 was added to a suspension of iron bis(borylene) **169** in hexane at –70°C with stirring. Surprisingly, homogenization of the reaction mixture with concomitant color change from red to yellow was observed within 30 min. Unfortunately, upon concentration and storage of the pale yellow reaction solution at –70°C for several weeks, the solution remained homogeneous. Therefore, it was slowly warmed up to ambient temperature. During this period, a slow color change from yellow to green was observed. The ^{11}B NMR spectrum revealed six new peaks, i.e. δ_B = 149, 113, 108, 72, 42, 41. Upon concentration and storage of this deep green solution at –30°C for several days, green single crystals suitable for X-ray diffraction analysis were obtained.

Complex **177** crystallizes in the monoclinic space group $P2_1/n$, and resembling that of **145**, the overall geometry of the approximately planar central Fe-B1-Fe-B2 fragment is consistent with the bridging coordination mode for both arylborylene and aminoborylene ligands (Fig. 71). The significant lengthening of Fe-B separations (Fe1-B2 2.0243(15), Fe2-B1 1.9887(15) Å) with respect to those of the precursor **169** can be explained by the increased coordination number at boron. Furthermore, the Fe-Fe separation of 2.4379(3) Å is significantly shorter than the single Fe-Fe bond of classical $[Fe_2(CO)_9]$ (2.52 Å)[206] and thus can be interpreted as a formal double bond as required for an 18-electron configuration at each iron center. Analogous to **170**, and as a borylene derivative of highly reactive $[Fe_2(CO)_8]$, **177** possesses considerable stability in the solid state. Green crystals of **177** could be stored at −30 °C for several months without any sign of decomposition. Unfortunately, all attempts to isolate other boron-containing species by crystallization failed.

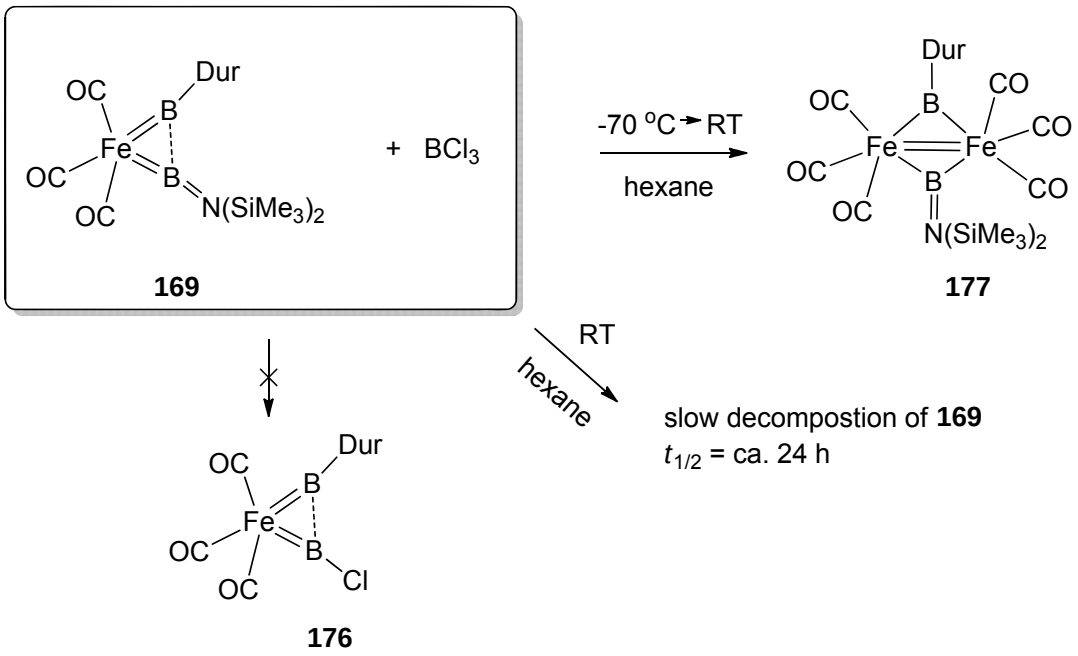

Scheme 39: Reaction of $[(OC)_3Fe(BDur)\{BN(SiMe_3)_2\}]$ (**169**) with BCl_3.

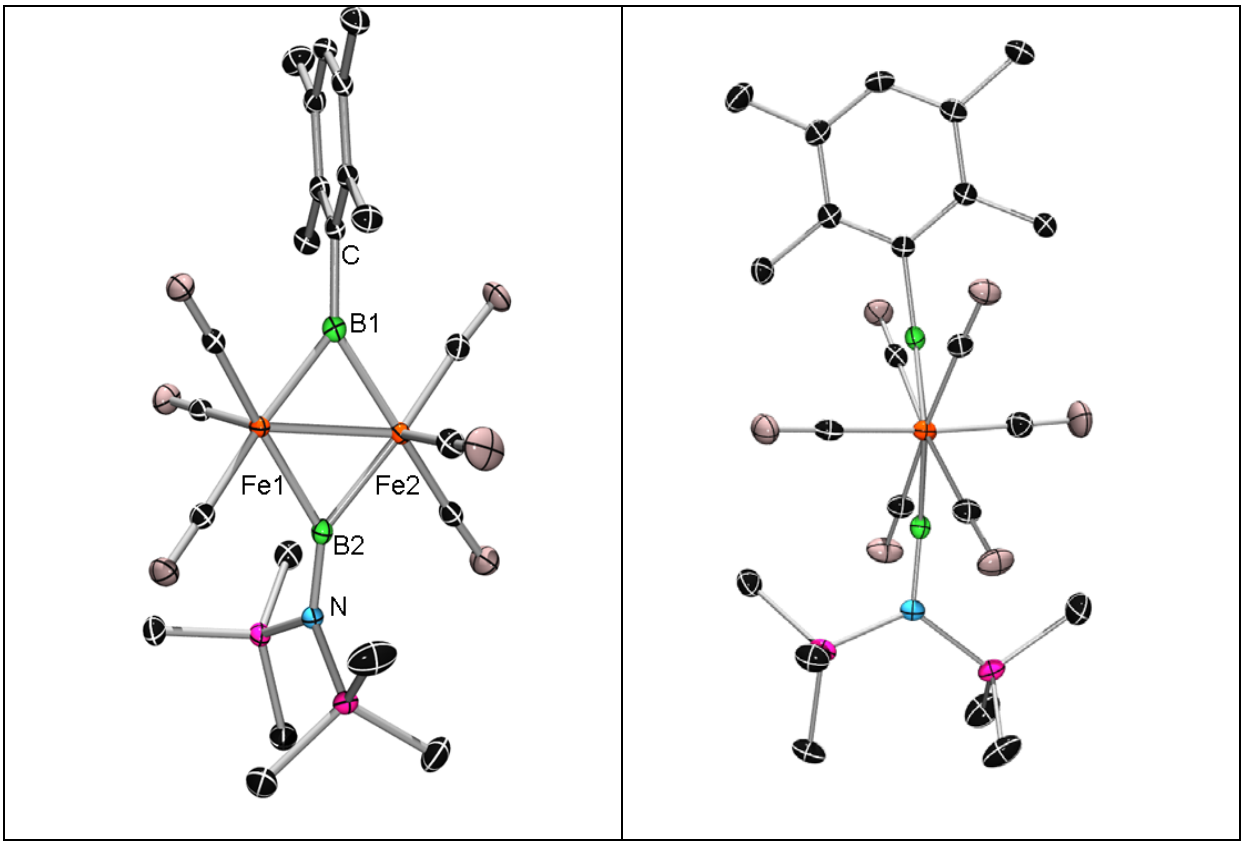

Fig. 71 Molecular structure of $[(OC)_3Fe\{\mu\text{-}BN(SiMe_3)_2\}(\mu\text{-}BDur)Pt(PCy_3)]$ (**169**). Right side is the picture along the Fe1-Fe2 bond. Thermal ellipsoids depicted at the 50% probability level. For clarity, co-crystallized solvent molecules, hydrogen atoms have been removed. Selected bond lengths (Å) and angles (°): Fe1-Fe2 2.4379(3), Fe1-B1 1.9807(15), Fe1-B2 2.0243(15), Fe2-B1 1.9887(15), Fe2-B2 2.0249(15), B2-N 1.3981(18); Fe1-B1-Fe2 75.78(5), Fe1-B1-C 140.12(10), Fe2-B1-C 144.06(11), Fe1-B2-Fe2 74.04(5), Fe1-B2-N 141.58(11), Fe2-B-N 144.24(11).

2.8.3 Double borylene transfer

We have noted in *2.3.3* and *2.6.3*, that borylene complexes which undergo borylene transfer exclusively have CO ligands in *trans* position. Hence, we reasoned that the iron bis(borylene) complex **169**, containing three CO ligands, should be a superior candidate for borylene transfer and may even facilitate double borylene transfer. In contrast to aforementioned borylene transfer reactions that yield borirenes, transfer of two borylene units onto alkynes might afford diboraheterocycles, i.e. 1,4-diboracyclohexadienes, the heretofore unknown 1,4-diborabutenes, and even their constitutional isomers 1,4-dibora-1,3-butadienes.

Similar to other boraheterocycles, only a limited number of synthetic routes to 1,4-diboracyclohexadienes have been published, and most of them are laborious. The procedure reported by Timms in 1968[207] and by Van Der Kerk[208] *et al.* in 1980 involved generation of the highly reactive borylene species :BF by the reaction of BF_3 with boron at 1800-2000 ^oC and generation of :BMe upon reduction of Br_2BMe with KC_8 respectively. The subsequent borylene capturing reaction with alkynes afforded unselectively 1,4-diboracyclohexadienes. In 1978, Herberich *et al.* reported the tin-boron exchange reaction between 1,1,4,4-tetramethyl-l,4-distanna-2,5-cyclohexadiene and organoboron dihalides, which led to the expected product in satisfactory yield.[209] Nevertheless, the scope of this synthetic approach is severly limited by the boron-bound substituent, i.e. the ferrocenyl. Moreover, 1,4-diboracyclohexadienes with small boron-bound substituents such as methyl or hydrogen are susceptible to rearrangement, forming thermodynamically favored carboranes.[210,211] The labile diboraheterocycles of this type can nevertheless be stabilized by complexation with transition metals in an η^4-fashion.[212-214]

2.8.3.1 Reaction of $[(OC)_3Fe(BDur)\{BN(SiMe_3)_2\}]$ (**169**) with 2-butyne (**149**)

A red hexane solution of iron bis(borylene) complex **169** was irradiated in the presence of 2 equiv. of 2-butyne (**149**) at ambient temperature. The reaction was monitored by ^{11}B NMR spectroscopy, which revealed gradual consumption of **169** and formation of new boron-containing species with significantly upfield shifted resonances at δ_B = 28 and 26. The reaction was accomplished within 24 h. A certain amount of dinuclear byproduct $[(OC)_2Fe(\mu\text{-}BDur)\{BN(SiMe_3)_2\}]_2$ (**170**) was concomitantly generated as a black solid. After workup, the boron-containing product was obtained as yellow crystals. Notably, the ^1H NMR spectrum showed four singlet peaks (δ_H = 2.70, 2.28, 2.23 and 2.10) for the duryl group and two singlet (δ_H = 0.55 and 0.19) signals for the amino group, suggesting a considerable rotational barrier

around the exocyclic B2-N and B1-C5 bonds. This is most likely due to the steric congestion imposed by exocyclic substituents (Fig. 72). Furthermore, the presence of methyl groups derived from 2 equiv. of 2-butyne (**149**) was confirmed by two singlet peaks (δ_H = 1.63 and 1.45) in the ^{1}H NMR spectrum. The ^{13}C NMR resonance at δ_C = 212.04 indicated the presence of carbonyl ligands, and thus strongly suggested the complexation of generated 1,4-diboracyclohexadiene with iron tricarbonyl fragment. Complex **178** crystallizes in triclinic space group *P*-1 with two independent molecules in the asymmetric unit, both featuring very similar structural parameters. The results of X-ray structure analysis are depicted in Fig 72. The overall geometry of the diboracyclohexadiene ring resembles previously determined structure of this type[212-214]: i) similar endocyclic B-C and C-C bond distances; ii) the ring bends slightly away from iron center with respect to C1-C2 and C3-C4; iii) remarkable elongation of the exocyclic B2-N (1.491(5) Å) and B1-C5 (1.600(6) Å) bond distances in comparison to that (1.39 Å) between three coordinated boron and nitrogen and that (1.55 Å) between three coordinated boron and sp^2-hybridized carbon in **147** respectively. The almost orthogonal orientation of the duryl substituent at boron and boron-bound trimethylsilylamino group with respect to the central six membered ring confirmed the above mentioned steric congestion around the B2-N and B1-C5 bonds. In view of the overall structural parameters, the diboracyclohexadiene ring can be regarded as a four-electron donor with pronounced olefinic η^2-coordination and comparatively weak interaction between vacant p-orbital of boron and filled d-orbital of iron. The latter might explain the elongation of the exocyclic B2-N and B1-C5 bonds.

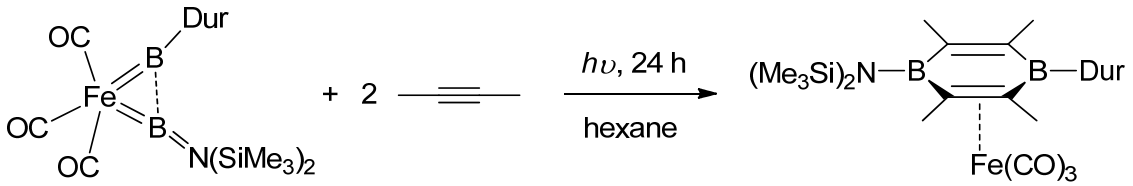

169 **149** **178**

Scheme 40: Reaction of [(OC)$_3$Fe(BDur){BN(SiMe$_3$)$_2$}] (**169**) with 2-butine (**149**).

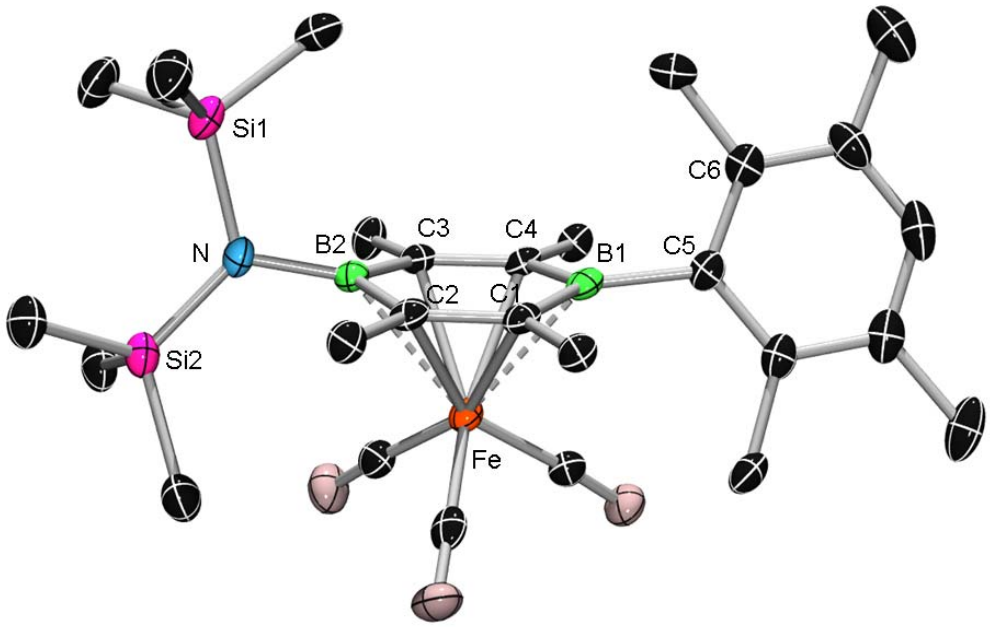

Fig. 72 Molecular structure of **178** in the solid state. Ellipsoids drawn at the 50% probability level. Hydrogen atoms and the second independent molecule in the asymmetric unit are omitted for clarity. Relevant bond lengths [Å] and angles [°]: C1-C2 1.424(5), C2-B2 1.537(6), B2-C3 1.550(6), C3-C4 1.420(5), C4-B1 1.550(6), B1-C1 1.537(6), B2-N 1.491(5), B1-C5 1.600(6), Fe-B1 2.311(5), Fe-B2 2.334(4); Si1-N-B2-C2 97.1(4), C6-C5-B1-C4 62.1(5).

2.8.3.2 Reaction of $[(OC)_3Fe(BDur)\{BN(SiMe_3)_2\}]$ (**169**) with diphenylacetylene (**151**)

In order to probe the versatility of the synthetic method, the reaction of iron bis(borylene) **169** with 2 equiv. diphenylacetylene (**151**) was carried out under identical reaction conditions. A complete conversion of the starting material **169** into the expected product **179** required 3 d as indicated by two new resonances at δ_B = 35 and 26 in the ^{11}B NMR spectrum. After removing the byproduct **170** by filtration and subsequent concentration and storage of the reaction solution at –30°C for one week, **179** was isolated as orange crystals. Multinuclear NMR spectra of **179** displayed all relevant signals in the expected range. Analogous to **178**, the presence of boron-bound substituents, i.e. duryl and bistrimethylsilylamino, was indicated by four singlet peaks (δ_H = 2.42, 2.29, 1.98 and 1.97) and two singlet signals (δ_H = 0.30 and 0.03) respectively, suggesting a significant rotational barrier about B2-N and B1-C5 as a result of steric congestion imposed by the bulky exocyclic substituents. Complex **179** crystallizes in the monoclinic space group $P2_1/n$. The overall geometry of **179** in the solid state, in particular the central six membered ring with a propeller-like arrangement of the

exocyclic substituents strongly resembles that of **178**, thus suggesting an identical coordination mode of the 1,4-diboracyclohexadiene ligand (Fig. 73).

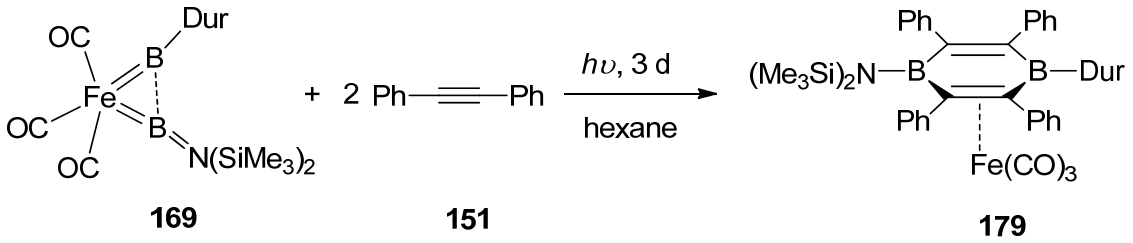

169 **151** **179**

Scheme 41: Reaction of $[(OC)_3Fe(BDur)\{BN(SiMe_3)_2\}]$ (**169**) with diphenylacetylene (**151**).

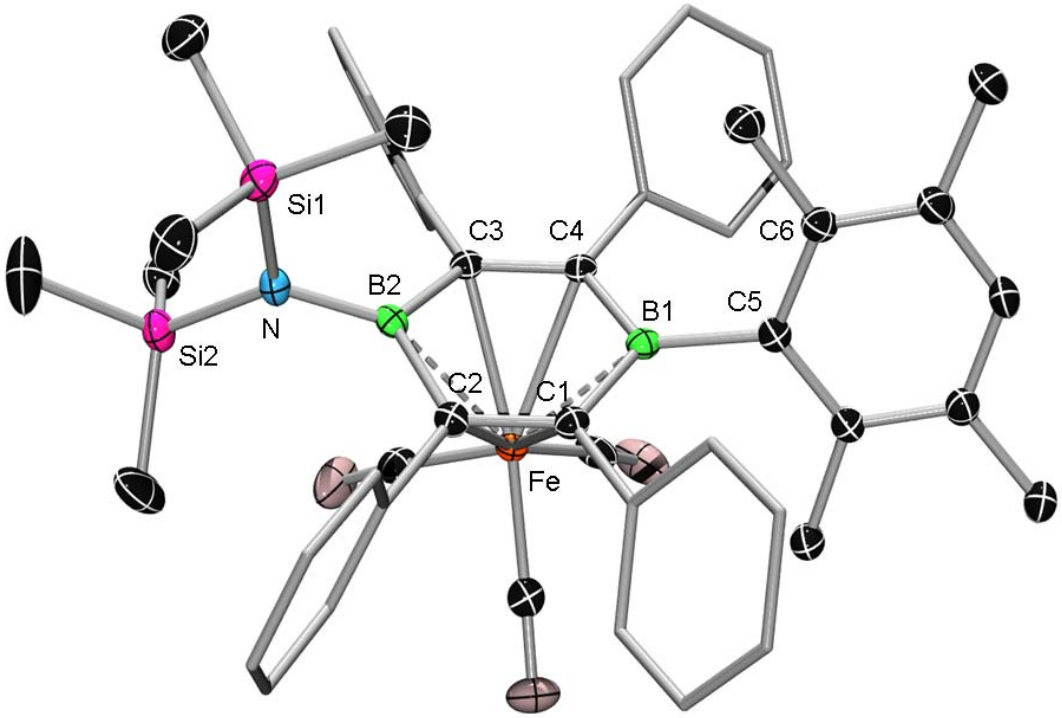

Fig. 73 Molecular structure of **179**. Thermal ellipsoids depicted at the 50% probability level. For clarity, ellipsoids of phenyl groups, hydrogen atoms have been removed. Selected bond lengths (Å) and angles (°): C1-C2 1.429(2), C2-B2 1.561(2), B2-C3 1.569(3), C3-C4 1.425(2), C4-B1 1.552(2), B1-C1 1.537(3), B2-N 1.481(2), Fe-B1 2.3629(19), Fe-B2 2.4113(19); Si2-N-B2-C2 98.23(18), C1-B1-C5-C6 65.7(2).

2.8.3.3 Reaction of $[(OC)_3Fe(BDur)\{BN(SiMe_3)_2\}]$ (**169**) with bis(trimethylsilyl)acetylene (**150**)

After demonstrating the generation of 1,4-diboracyclohexadienes by borylene transfer from a bis(borylene) complex, we became interested in the steric influence of acetylenic substituents.

In view of the steric congestion imposed by exocyclic substituents as shown in Fig. 73, substitution of the phenyl ring by a sterically more demanding group such as trimethylsilyl might impede the reaction with a second equiv. of alkyne.

Hence, the reaction of iron bis(borylene) **169** with an equimolar amount of bistrimethylsilylacetylene (**150**) was carried out under identical reaction conditions, in the hope that the borylene moieties in **169** are selectively transfered to only one C≡C triple bond. The reaction was monitored by ^{11}B NMR spectra, which revealed gradual formation of new boron-containing species showing ^{11}B resonances at δ_B = 93 and 60. These values, which differ significantly from those of 1,4-diboracyclohexadiene complexes **178** and **179**, are in good agreement with the proposed structure (Scheme 42). The photochemical reaction was accomplished within 2 d. Upon filtration and storing the reaction solution at –30°C, **180** was isolated as yellow crystals. The constitution of **180** in solution and in solid state was confirmed by multinuclear NMR spectroscopy and X-ray diffraction analysis (Fig. 74) respectively. Again, impeded rotation about B2-N and B1-C3 was indicated by the presence of six singlet peaks in the expected range for the methyl groups of duryl and bistrimethylsilylamino substituents. The Fe1-B2-N-Si1 torsion angle of –2.9(5)° as well as the significantly shortened B2-N separation (1.385(4) Å) in comparison to that (1.481(2) Å) in **179** indicated a pronounced B-N π-interaction in **180**. Furthermore, the bond distances of Fe-B1 (2.043(4) Å) and Fe-B2 (2.135(4) Å) are comparable to the Fe-B distances commonly observed for neutral iron half-sandwich boryl complexes of iron (1.96-2.09 Å)[61]. The inner C1-C2 (1.452(4) Å) can be regarded as a double bond that is side-on coordinated to the iron center in an η^2-fashion, thus explaining the bond lengthening relate to non-coordinated C-C double bond (1.357(10) Å) in **96**. On the other hand, the C1-C2 bond (1.452(4) Å) is slightly longer compared with those (e.g. 1.417(6) Å in **115**, 1.398(3) Å in **118**, 1.42 Å (mean) in **178** and **179**) of other η^2-coordinated C-C double bonds, but still somewhat shorter than the C-C single bond (e.g. 1.4699(19) Å in **66**, 1.466(7) Å in **86**, 1.505(10) Å in **96**) between two sp^2-hybridized carbon atoms, which was also observed for complexation of 1,3-dienes with a ruthenium tricarbonyl fragment[215]. In addition, the central B-C bond in **180**, in particular, the decrease of B1-C1 (1.512(5) Å) in comparison to the adjacent B1-C3 single bond (1.557(5) Å), as well as in comparison to the endocyclic B-C bonds (mean value of 1.56 Å) in **179**) strongly suggests the presence of B-C double bond character. Hence, the central BCCB skeleton can be regarded as a four electron donor ligand with double B=C η^2-coordination. In view of these findings, the overall bonding situation in **180** can be described with both

mesomeric forms **A**, i.e. iron-*cis*-bis(boryl) complex with side-on coordinated alkenyl function, and **B**, i.e. iron 1,4-dibora-1,3-butadiene complex (Scheme 42).

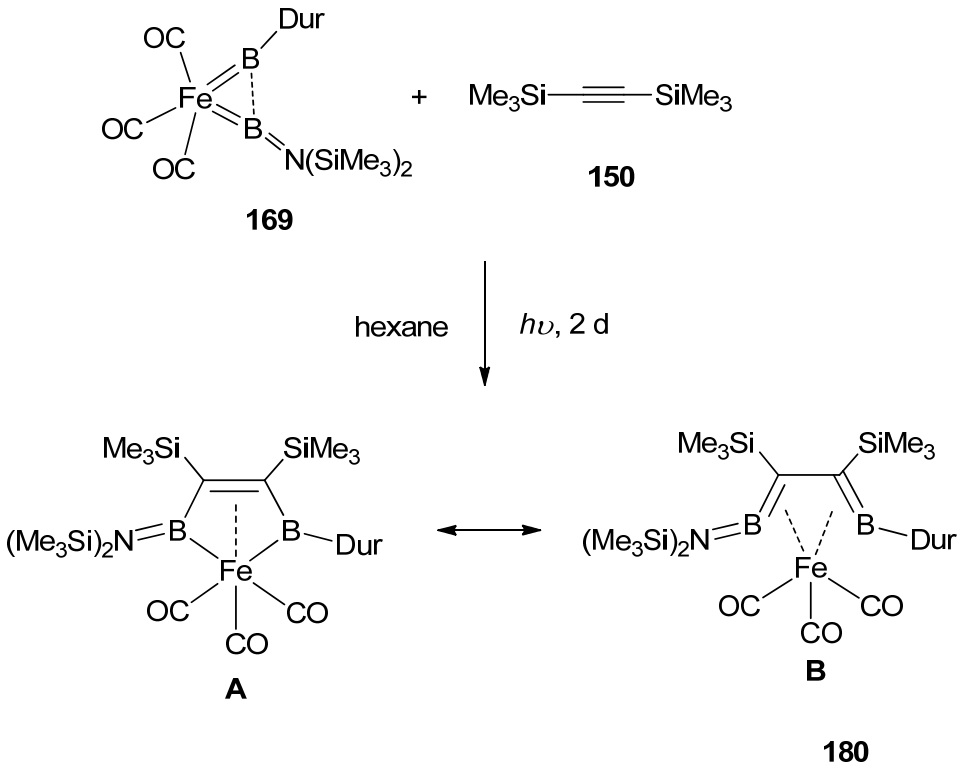

Scheme 42: Reaction of $[(OC)_3Fe(BDur)\{BN(SiMe_3)_2\}]$ (**169**) with bis(trimethylsilyl)-acetylene (**150**).

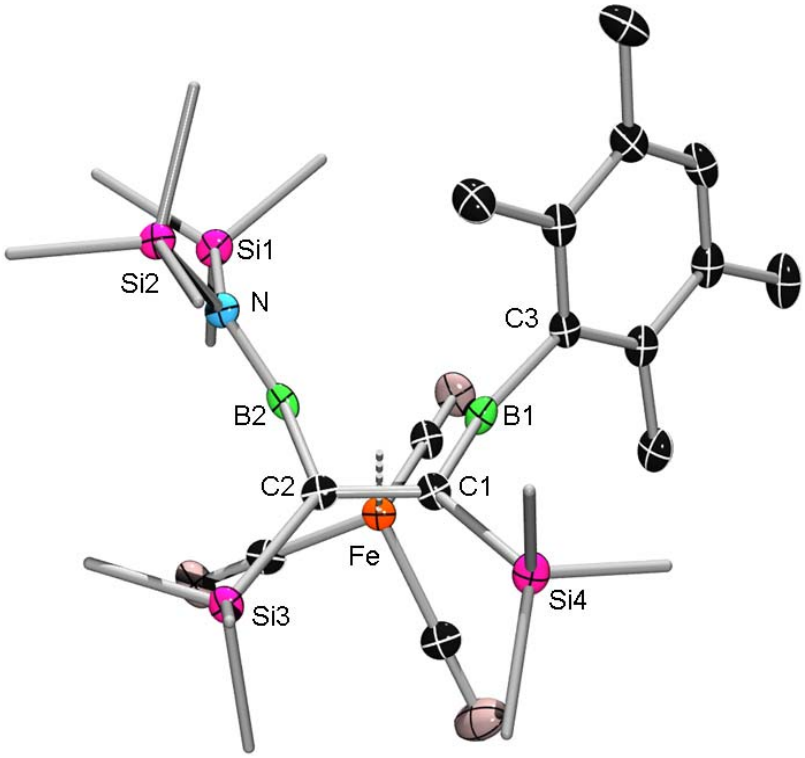

Fig. 74 Molecular structure of **180**. Thermal ellipsoids depicted at the 50% probability level. For clarity, ellipsoids of trimethylsilyl groups, hydrogen atoms have been removed. Selected bond lengths (Å) and angles (°): B1-C1 1.512(5), C1-C2 1.452(4), C2-B2 1.528(5), B2-N 1.385(4), B1-C31.557(5), Fe-B1 2.043(4), Fe-B2 2.135(4), Fe-C1 2.118(3), Fe-C2 2.140(3); N-B2-C2 145.7(3), C1-B1-C3 143.6(3), Fe1-B2-N-Si1 -2.9(5).

3 Summary

Within the scope of this thesis, the area of borylene transfer has been broadened by including transition-metal σ-alkynyl complexes and metal-carbon double bonds as borylene acceptors. In addition to double salt elimination, halide abstraction and dehydrogenation processes, a novel high-yield synthetic procedure for terminal borylene complexes was established, i.e. salt elimination and subsequent silylhalogenide liberation. Accordingly, it was possible to prepare [$(OC)_3(Me_3P)Fe$=BDur] (**138**) as a rare example of a neutral arylborylene species. Moreover, **138** has been demonstrated to possess great potential for metathesis reactions and the functionalization of polycyclic aromatic hydrocarbons such as naphthalene. Moreover, **138** could undergo a phosphine-borylene exchange reaction, yielding the iron bis(borylene) complex [$(OC)_3Fe$(BDur){$BN(SiMe_3)_2$}] (**169**), which has turned out to be applicable for preparation of 1,4-diboracyclohexadiene and unprecedented 1,4-dibora-1,3-butadiene complexes, thus establishing a new type of borylene transfer. Most interestingly, upon transfer of further borylene moieties into the coordination sphere of iron, borylene-catenation was accomplished in a highly controlled manner.

In terms of borylene-based functionalization of transition-metal σ-alkynyl complexes, one of the most successful forays has been borylene transfer to group 10 metal complexes. The platinum-borirene complexes **86**, **87**, **89**, **93** and **94** were prepared by photochemical borylene transfer from [$(OC)_5Cr$=$BN(SiMe_3)_2$] (**14**) to the corresponding platinum-alkynyls (Fig. 75), thus demonstrating the feasibility of the proposed framework (Fig. 28) by borylene transfer. Notably, in terms of geometry of bis(borirene) complexes **89** and **94**, X-ray diffraction analysis revealed a coplanar arrangement of the aromatic rings in both cases, which is in stark contrast to previously reported bis(borirene) compounds. Furthermore, preliminary studies on their photophysical properties have revealed a significant red-shift of the absorption maxima in UV-vis spectra (from 247 nm found for **86** to 314 nm found for **89**) by extending the π-system.

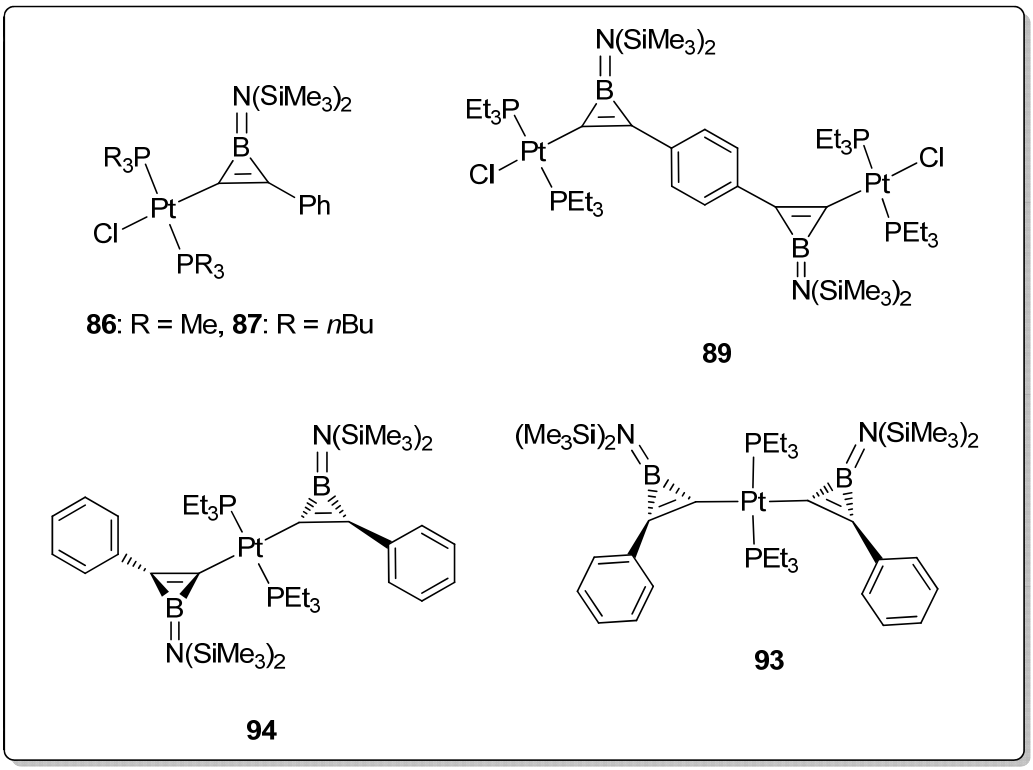

Fig. 75 Borirene- and platinum-based π-system.

This work has also included the results of reactivity studies on **86** upon UV irradiation, involving the migration of the borylene unit from the C≡C triple bond to the metal carbon σ-bond with concomitant formation of an alkynylboryl complex **95** (Fig. 76). Moreover, **86** undergoes a ring-opening reaction upon treatment with HCl, thus affording the new amino(vinyl)borane complex **96**, which was formed by selective cleavage of the B-C bond. It should be mentioned that this is the first example of a ring-opening reaction of an asymmetric borirene. When treated with BBr_3, no cleavage of the boron-nitrogen bond in **86** was observed, but instead a Br-Cl ligand exchange on the platinum atom occurred, thus enabling the isolation of the Br-derivate **98**.

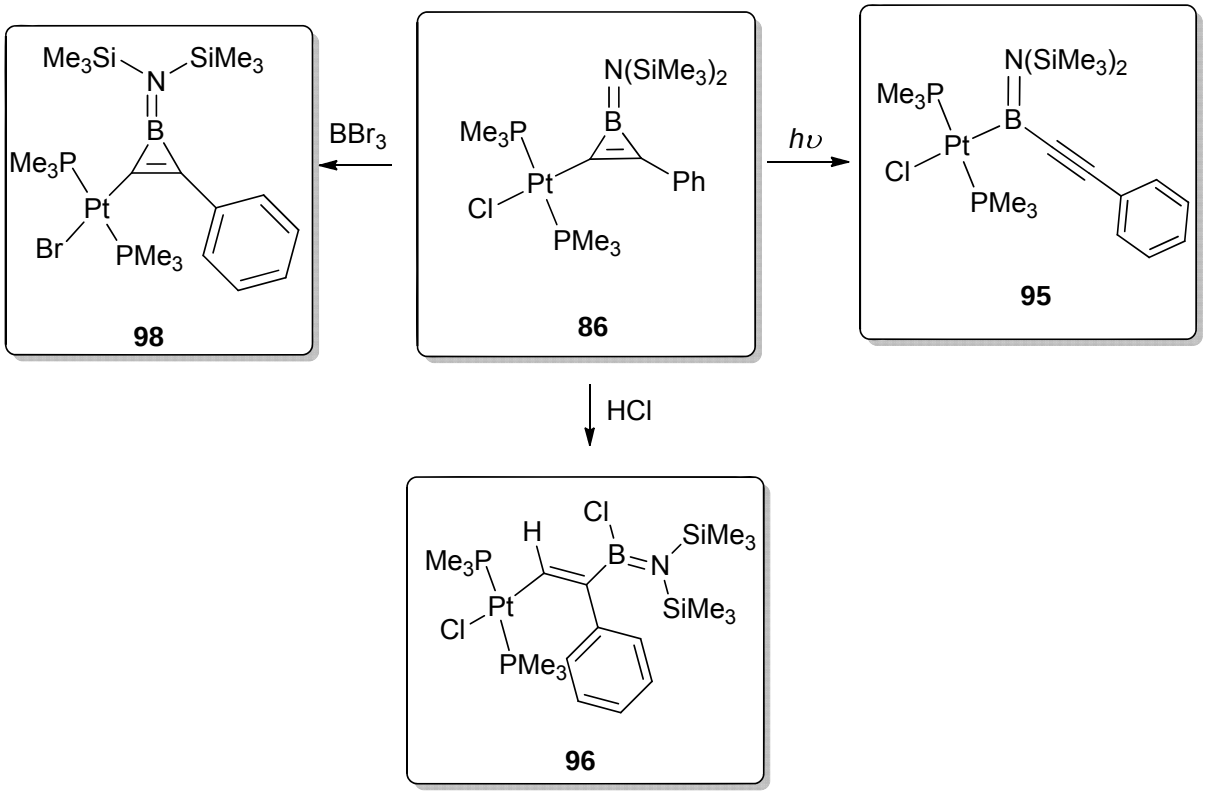

Fig. 76 Reactivity investigation of **86**.

Thermally induced chemoselective borylene transfer from $[(OC)_5Mo{=}BN(SiMe_3)_2]$ (**16**) to the C≡C triple bond of an iron dicarbonyl alkynyl complex $[Cp^*Fe(CO)_2C{\equiv}CPh]$ (**64**) led to the isolation of an iron-substituted aminoborirene complex $[Cp^*(OC)_2Fe\{\textit{cyclo}\text{-}BN(SiMe_3)_2C{=}C\}Ph]$ (**66**) in satisfactory yield. Room temperature photolysis of **66** resulted in an unprecedented rearrangement and a concurrent decarbonylation, affording a novel C_2 side-on coordinated iron-boryl complex $[Cp^*(OC)FeBN(SiMe_3)_2(\eta^2\text{-}CC)Ph]$ (**75**) (Fig. 77). Carbonylation of **75** under a CO atmosphere at ambient temperature yielded **76**, which is the isomer of **66**. Decarbonylation of **76** at 80°C led to **75**, which could be, upon introduction of CO gas, subsequently converted into **66** under the same conditions. Reaction of **75** with PMe_3 at 80°C yielded the phosphine complex $[Cp^*(OC)(PMe_3)Fe\{\textit{cyclo}\text{-}BN(SiMe_3)_2C{=}C\}Ph]$ (**77**), which might provide an alternative synthetic approach to metal-borirene complexes.

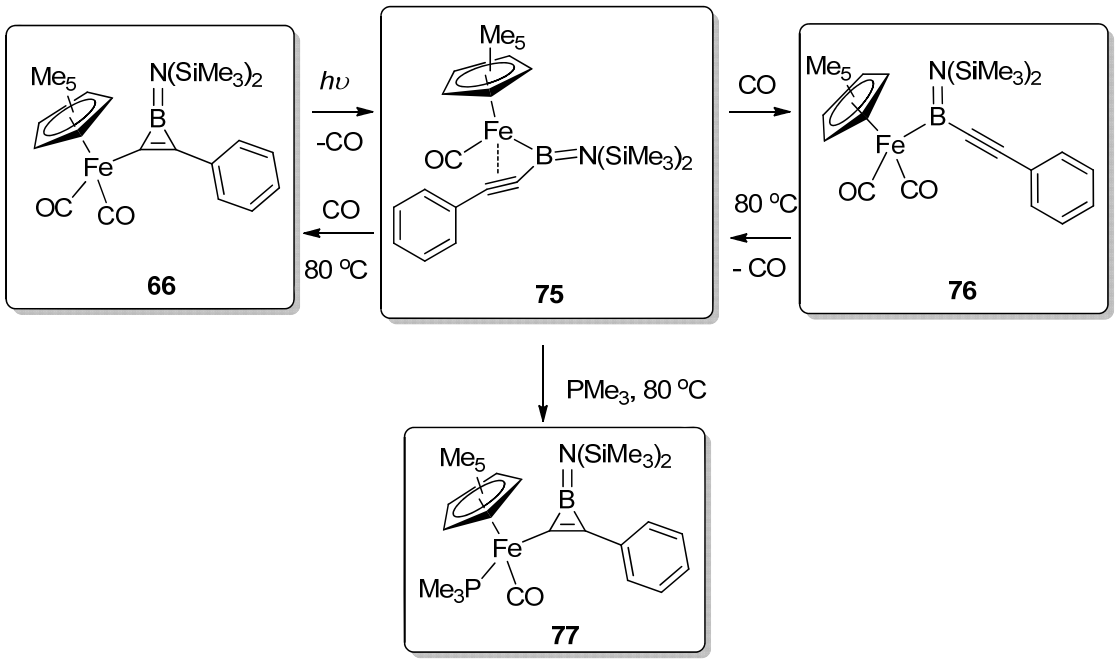

Fig. 77 Reactivity investigation of **66**.

In addition to known borylene acceptors, that is, C≡C triple bond and olefinic C-H bond containing substrates as well as transition-metal carbonyl fragments, this work has extended the borylene transfer process to include N=N and Rh=C double bonds (Fig. 78). In case of the former, the aminoborylene unit :$BN(SiMe_3)_2$ is surprisingly inserted into the N=N bond with a complete cleavage of the double bond, leading to the triaminoborane **102**, whose formation could be proven by multinuclear NMR spectroscopy and crystal structure analysis. However, it must be mentioned that the yield for the isolated compound was extremely low, thus implying a non-selective transformation.

More success was accomplished in the functionalization of Rh=C double bonds by borylene transfer. Accordingly, a variety of 1-aza-2-borabutatriene rhodium complexes could be synthesized in a straightforward fashion by borylene transfer from [$(OC)_5Mo$=$BN(SiMe_3)_2$] (**16**) to the corresponding rhodium vinylidene complexes (Fig. 78). In case of **111**, two stereomers **113** and **112**, which feature *endo*- and *exo*-methyl groups respectively, were obtained in a ratio of ca. 1:3. Interestingly, the *exo*-methyl isomer undergoes isomerization in solution at ambient temperature to give a chemical equilibrium of **112** and **113** in a ratio of ca. 2:1, suggesting that the former is thermodynamically favoured over the latter.

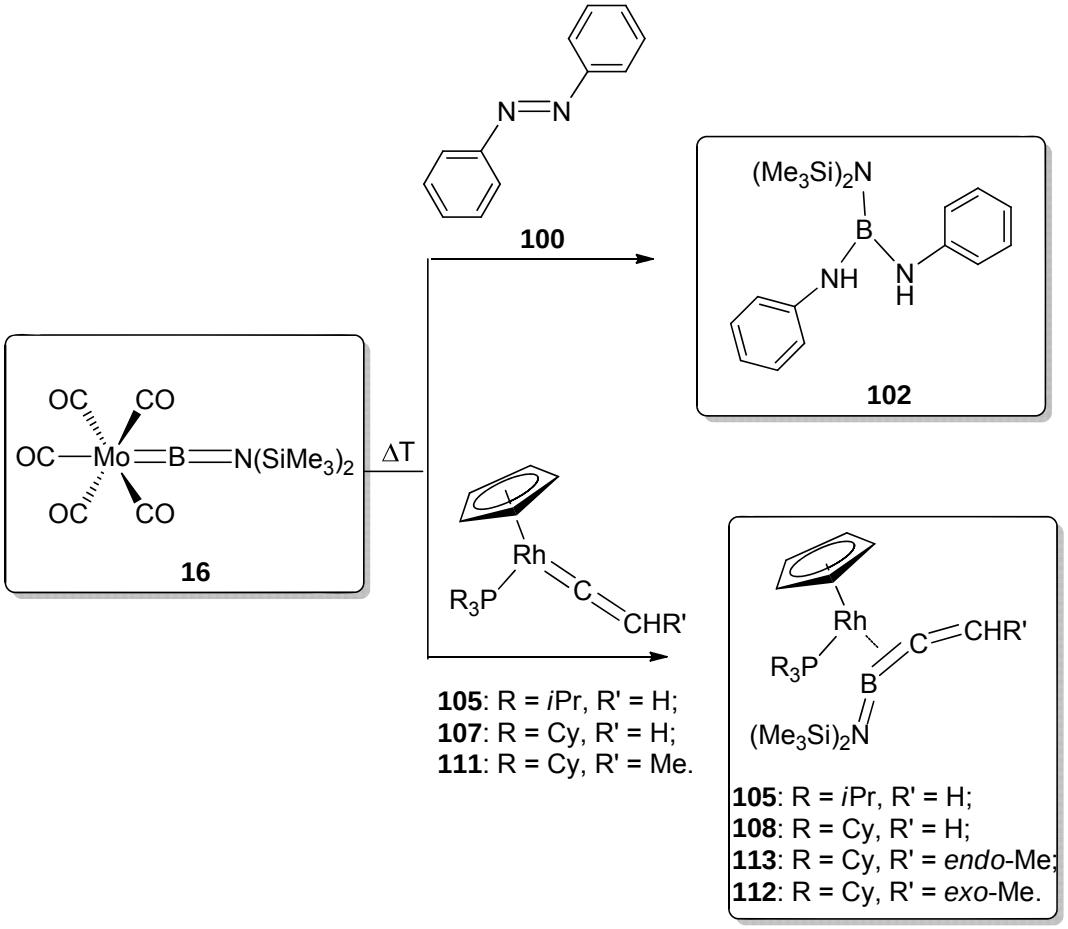

Fig. 78 Borylene transfer to Rh=C and N=N double bonds.

Subsequently, reactivity studies on rhodium boracumulene complexes revealed a thermally induced B-C to C-C coordination mode shift with concomitant highly stereoselective intramolecular C-H activation involving the released B=C double bond (Fig. 79). An analogous coordination mode shift could be observed upon addition of a strong σ-donor, i.e. *I*Me (**116**). In contrast to **115**, the B=C double bond in **118** is efficiently stabilized by the N-heterocyclic carbene, and thus has allowed the isolation of the 1-bora-[2]-cumulene complex **118**.

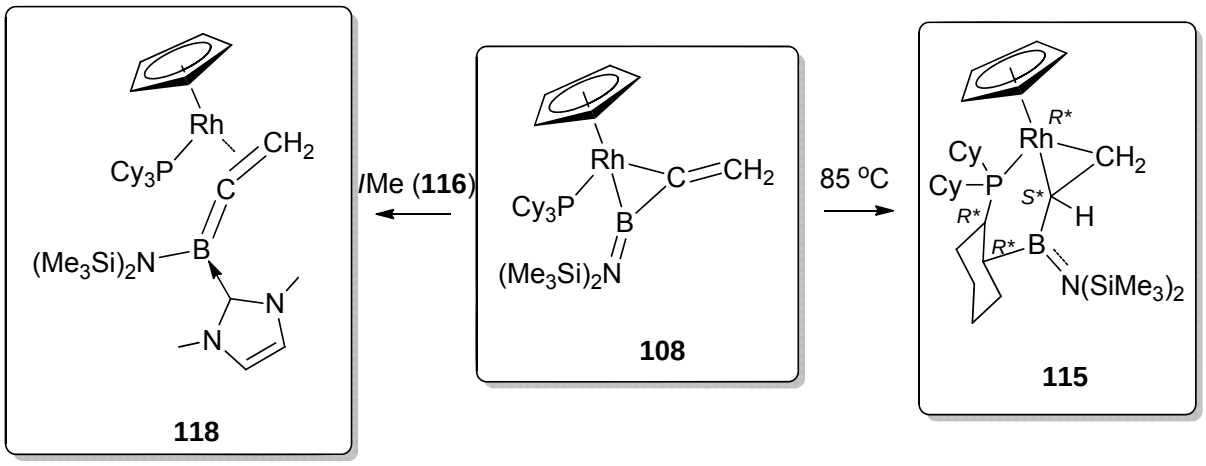

Fig. 79 Reactivity investigation of 1-aza-2-borabutatriene rhodium complexes.

In addition, this work has presented the high-yield synthesis of the carbonyl-rich durylborylene complex [$(PMe_3)(OC)_3Fe$=BDur] (**138**) as a rare example for an arylborylene species (Fig. 80). Reactivity studies have furnished the first example of a metal base stabilized arylborylene complex and the product of a selective [2+2] cycloaddition with benzophenone as a representative unsaturated, polar substrate. In particular, the latter result conveys a tentative impression of the reactivity of arylborylenes, suggesting a behaviour between that of amino- and alkylborylene complexes. The C-H bond activation upon photolysis of a mixture of **138** and naphthalene was confirmed by multinuclear NMR, IR and EI-MS spectra.

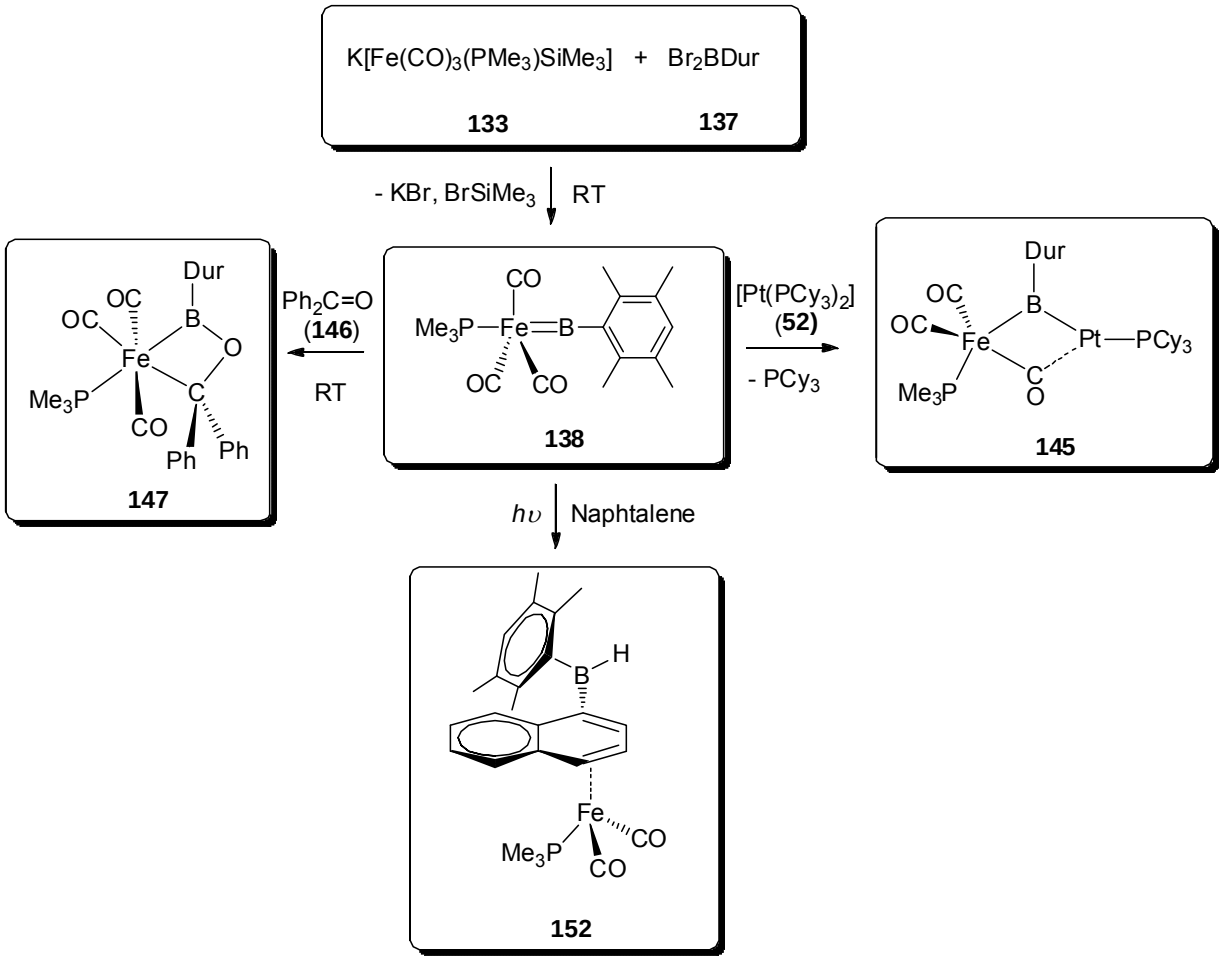

Fig. 80 Synthesis and reactivity investigation of [(PMe$_3$)(OC)$_3$Fe=BDur] (**138**).

The carbonyl-rich durylborylene complex [(PMe$_3$)(OC)$_3$Fe=BDur] (**138**) undergoes a phosphine-borylene exchange reaction in the presence of [(OC)$_5$Mo=BN(SiMe$_3$)$_2$] (**16**), yielding the iron bis(borylene) complex [(OC)$_3$Fe{BN(SiMe$_3$)$_2$}{BDur}] (**169**) (Fig. 81), which displays a remarkable inclination for borylene coupling as indicated by the short B-B separation observed. The reaction with the metal-base complex [Pt(PCy$_3$)$_2$] (**52**) constitutes the first example of a (bis)borylene-base adduct. Furthermore, upon tuning the size of acetylenic substituents, 1,4-diboracyclohexadiene and unprecedented 1,4-dibora-1,3-butadiene complexes were generated in a controlled manner by borylene transfer from a bis(borylene) complex. Hence, the established bis(borylene)-transfer process displays great potential for the synthesis of a variety of heretofore inaccessible dibora-heterocycles.

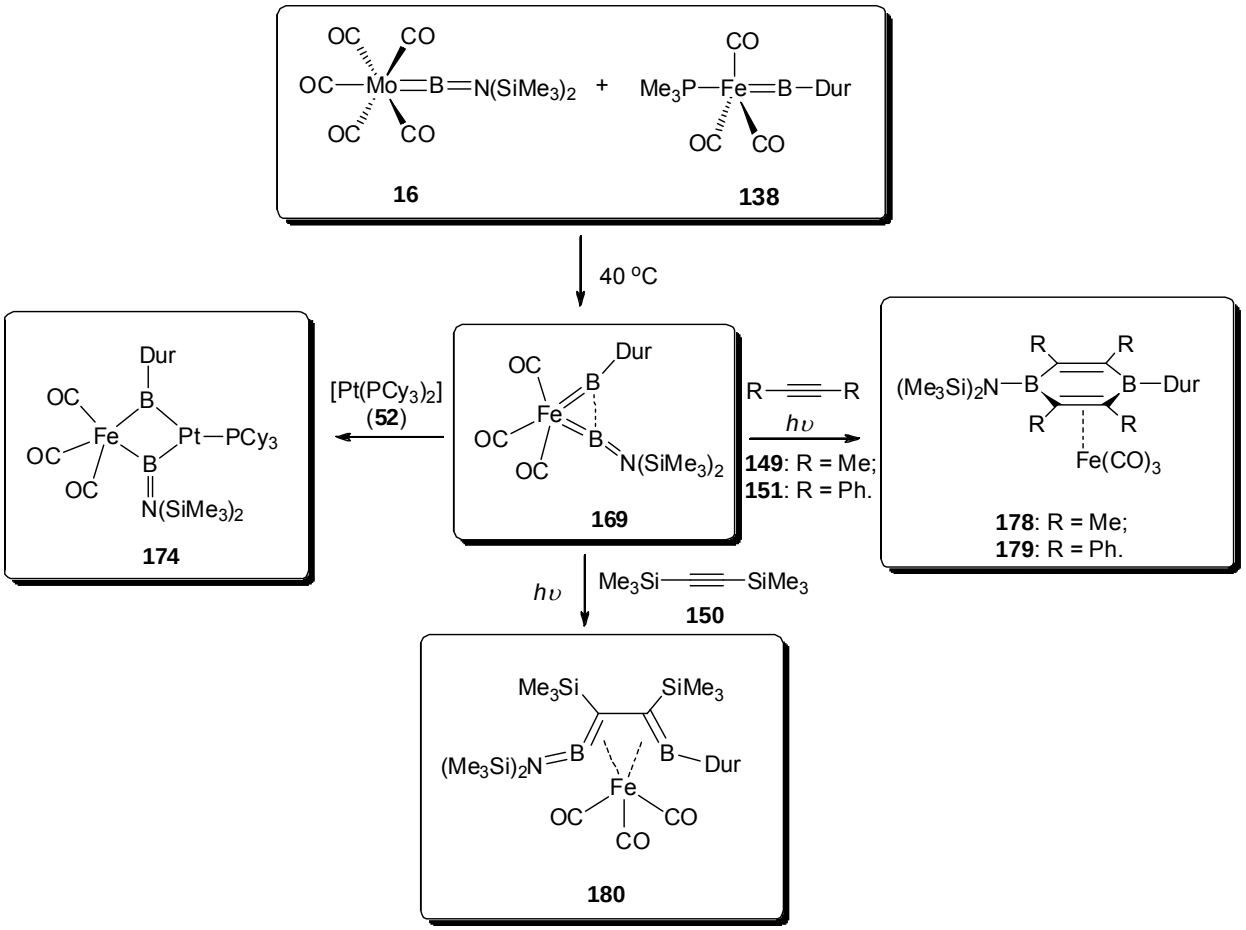

Fig. 81 Synthesis and reactivity investigation of **169**.

Finally, a Fe-mediated borylene catenation has been demonstrated both experimentally and computationally (Fig. 82). Irradiation of the mononuclear bis(borylene) complex **169** afforded the dinuclear tetra(borylene) complex **170**, both with partially-formed B-B bonds. Selectively removing an iron center from the latter upon applying CO atmosphere and thermal conditions resulted in the one-step creation of three boron-boron bonds and the synthesis of a highly unusual mononuclear tetraboron complex with a catenated B_4 chain. DFT calculations revealed three conventional σ-bonds between the boron atoms, and the interactions corresponding to side-on σ-coordination of all three B-B bonds to the metal as well as the back-bonding from a metal d_{z2} orbital to antibonding B-B orbitals. Interestingly, addition of a good σ-donor phosphine ligand to the iron bis(borylene) **169** induced migratory insertion of a carbonyl ligand and coupling of the two boron atoms.

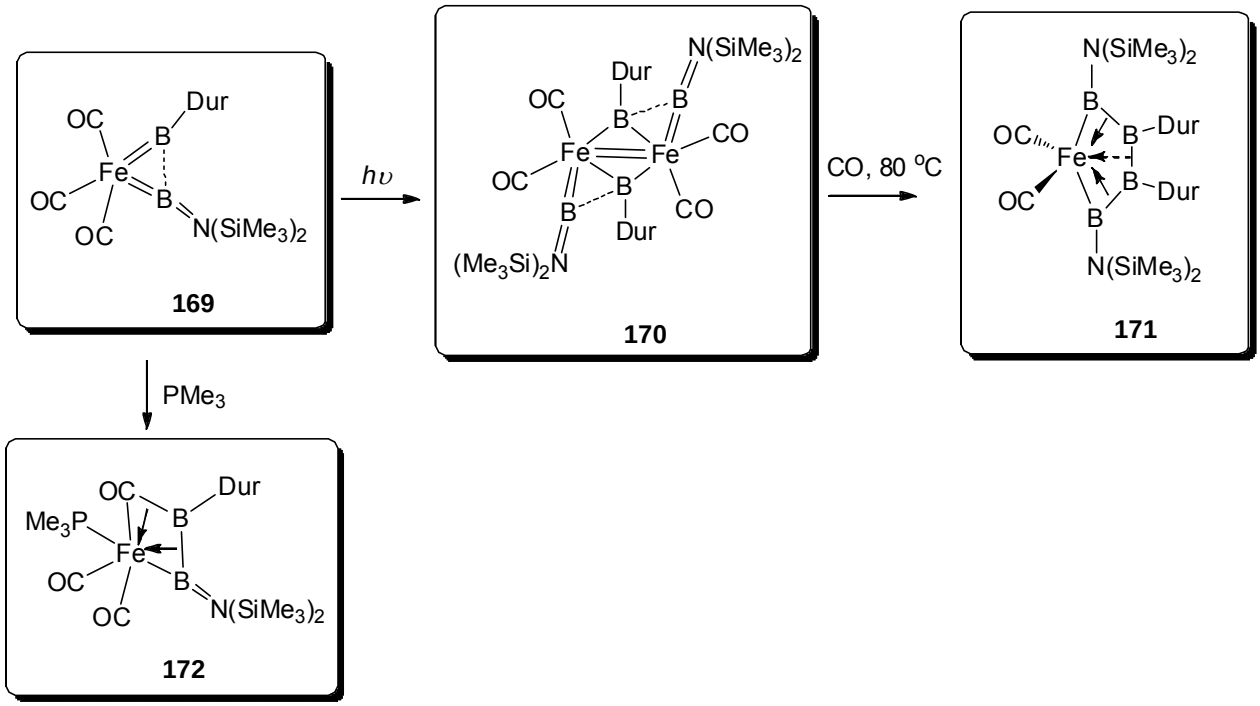

Fig. 82 Fe-mediated borylene catenation.

4 Zusammenfassung

Im Rahmen dieser Arbeit wurde das Spektrum des Borylentransfers ausgeweitet, indem Übergangsmetall-σ-Alkinylkomplexe und Metall-Kohlenstoff- Doppelbindungen als Borylen-Akzeptoren eingeschlossen wurden. Neben der Salzeliminierung, Halogenidabstraktion und Dehydrierung, wurde eine neuartige Syntheseroute zu terminalen Borylenkomplexen durch Salz- und Silylhalogenideliminierung etabliert. Mithilfe dieser Strategie gelang die Darstellung von $[(OC)_3(Me_3P)Fe{=}BDur]$ (**138**), ein seltenes Beispiel für einen neutralen Arylborylenkomplex. Im Speziellen hat die Verbindung **138** ein großes Anwendungspotenzial für Metathesereaktionen und die Funktionalisierung von polycyclischen aromatischen Kohlenwasserstoffen, wie z. B. Naphthalin, gezeigt. Außerdem konnte ein Eisen-Bis(borylen)-Komplex $[(OC)_3Fe(BDur)\{BN(SiMe_3)_2\}]$ (**169**) durch einen Phosphan-Borylen-Austausch dargestellt werden. Ausgehend von Komplex **169** gelang die Darstellung von 1,4-Diboracyclohexadien bzw. des ersten 1,4-Dibora-1,3-Butadien-Komplexes, wodurch eine neue Art von Borylentransfer etabliert werden konnte. Höchst interessant ist es, dass der Transfer von weiteren Borylen-Einheiten in die Koordinationssphäre des Eisenatoms zu einer kontrollierten Borylen-Verkettung geführt hat.

In Bezug auf die Borylen-basierte Funktionalisierung von Übergangsmetall-σ-Alkinylkomplexen war der Borylentransfer auf Gruppe-10-Metallkomplexe einer der erfolgreichsten Fortschritte. Die Platin-Boriren-Komplexe, die durch photochemischen Borylentransfer von $[(OC)_5Cr{=}BN(SiMe_3)_2]$ (**14**) auf die entsprechenden Platin-Alkinyle dargestellt wurden (Abb. 83), haben die grundsätzliche Machbarkeit des vorgeschlagenen Synthesewegs (Abb. 28) aufgezeigt. Die dargestellten Verbindungen **89** und **94** zeigen im Gegensatz zu bekannten Bis(boriren)-Komplexen eine koplanare Anordnung der aromatischen Ringe. Darüber hinaus zeigten Studien in Bezug auf deren photophysikalische Eigenschaften eine signifikante Rotverschiebung der Absorptionsmaxima in den UV-Vis Spektren (von 247 nm für **86** zu 314 nm für **89**), die auf eine Erweiterung des π-Systems zurückzuführen sein könnte.

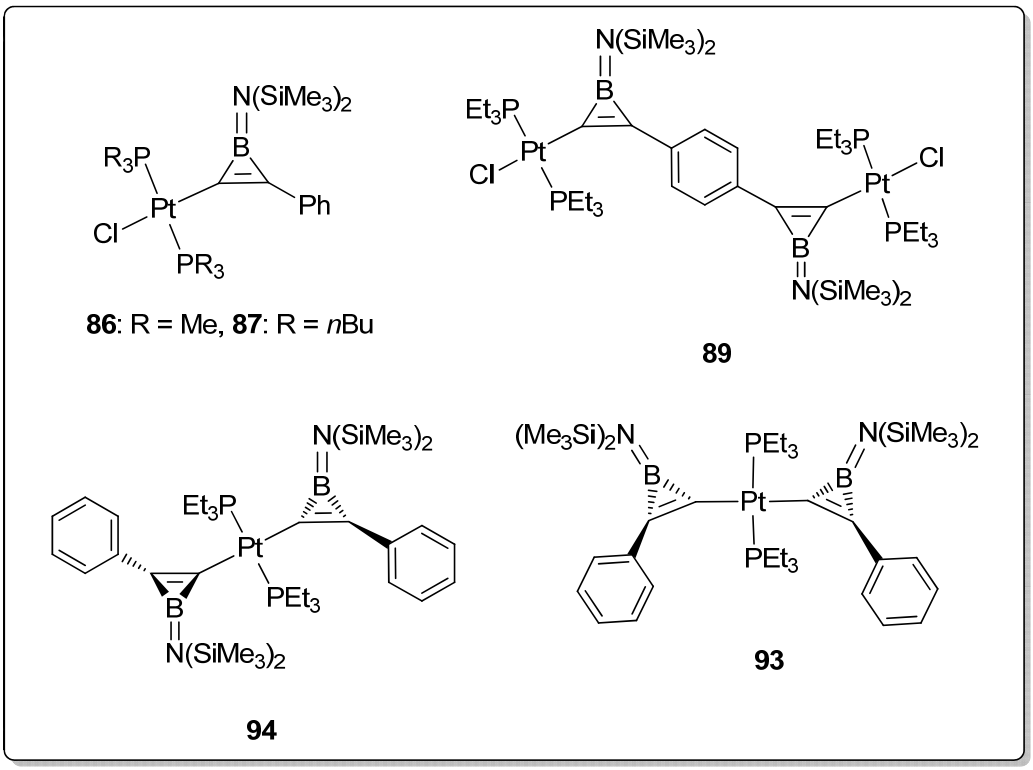

Abb. 83 Boriren- und Platin-basierte π-Systeme.

Reaktivitätsuntersuchungen zum Platin-Boriren-Komplex **86** zeigten, dass die Borylen-Einheit durch UV-Bestrahlung von der C≡C Dreifachbindung auf die Metall-Kohlenstoff-σ-Bindung unter gleichzeitiger Bildung eines Alkinylboryl-Komplexes wandert (Abb. 84). Darüber hinaus führte die Umsetzung von **86** mit HCl zu einer Ringöffnungsreaktion, wodurch der neue Amino(vinyl)boran-Komplex **96** durch die selektive Spaltung der B-C-Bindung gebildet wurde. Dies stellt das erste Beispiel für eine Ringöffnungsreaktion eines asymmetrischen Borirens dar. Die Umsetzung von **86** mit BBr_3 ergab keine Spaltung der Bor-Stickstoff-Bindung, sondern führte zu einem Br-Cl Ligandenaustausch am Platin, was die Isolierung eines Br-Derivats ermöglichte.

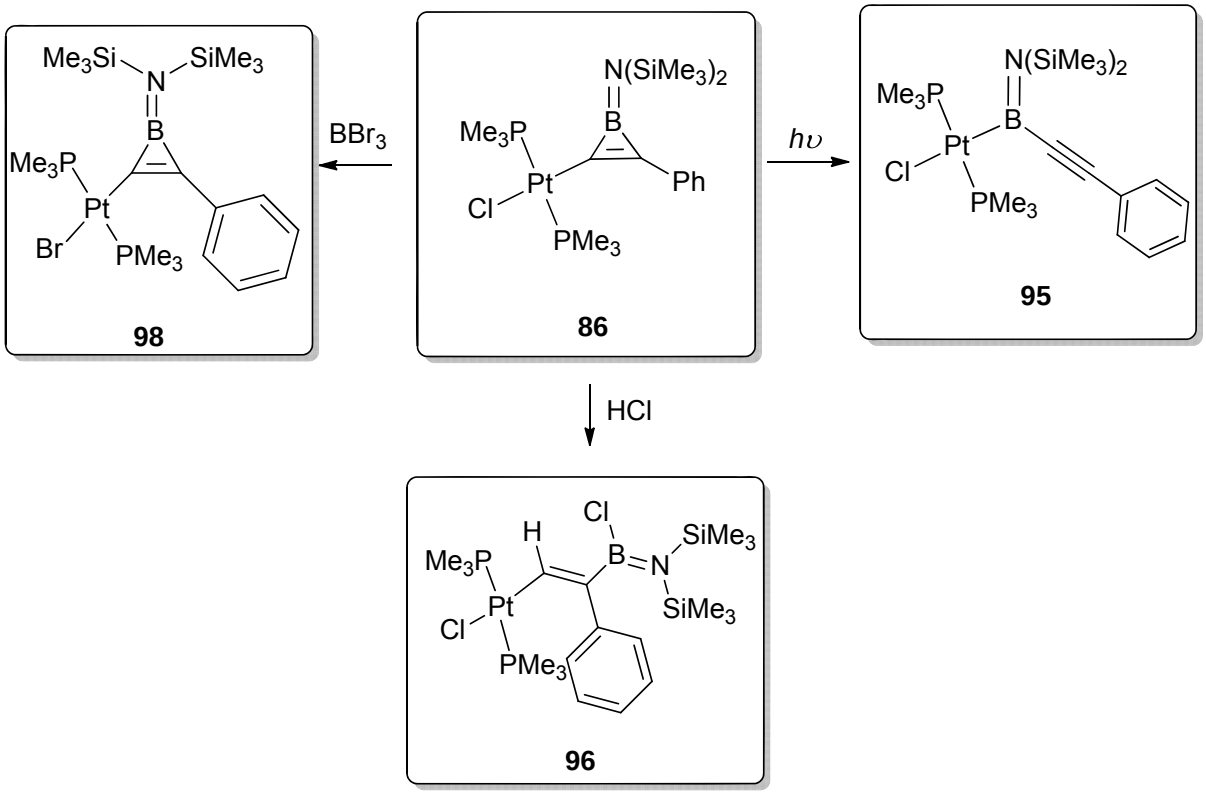

Abb. 84 Untersuchung der Reaktivität von **86**.

Das Eisen-substituierte Boriren [Cp*(OC)$_2$Fe{*cyclo*-BN(SiMe$_3$)$_2$C=C}Ph] (**66**) wurde durch einen thermisch induzierten, chemoselektiven Borylentransfer von [(OC)$_5$Mo=BN(SiMe$_3$)$_2$] (**16**) auf die C≡C-Dreifachbindung des Eisen-Alkynyl-Komplexes [Cp*Fe(CO)$_2$C≡CPh] (**64**) in befriedigenden Ausbeuten synthetisiert. Die Photolyse von **66** bei Raumtemperatur führte zu einer beispiellosen Umlagerung und einer gleichzeitigen Decarbonylierung, wodurch der neuartige C2 "side-on" koordinierte Eisen-Boryl-Komplex [Cp*(OC)FeBN(SiMe$_3$)$_2$(η^2-CC)Ph] (**75**) erhalten werden konnte (Abb. 85). Carbonylierung von **75** unter CO Atmosphäre bei Raumtemperatur ergab den Eisen-Borylkomplex **76**, der ein Isomer vom Eisen-Boriren **66** ist. Decarbonylierung von **76** bei 80°C führte zu Verbindung **75**, welche anschließend durch Einleitung von CO-Gas in ein Eisen-Boriren umgewandelt werden konnte. Die Umsetzung von **75** mit PMe$_3$ bei 80°C ergab den Phosphan-Komplex [Cp*(OC)(PMe$_3$)Fe{*cyclo*-BN(SiMe$_3$)$_2$C=C}Ph] (**77**), der einen alternativen Zugang zu Metall-Boriren-Komplexen eröffnete.

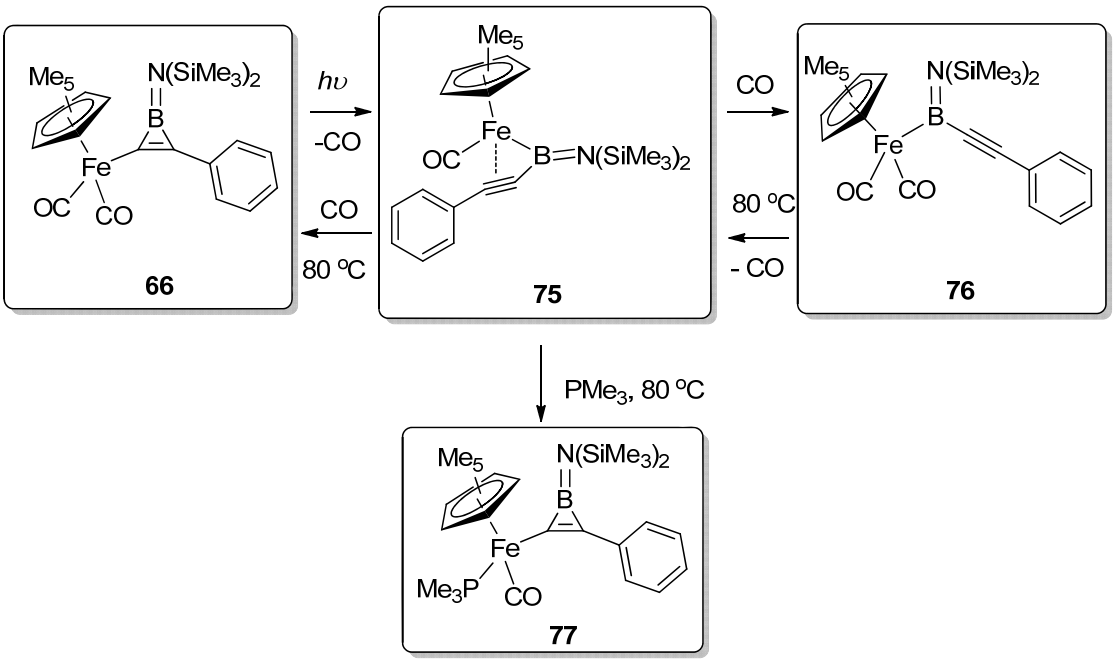

Abb. 85 Untersuchung zur Reaktivität von **66**.

Neben bekannten Borylen-Akzeptoren, wie der C≡C-Dreifachbindung, olefinischen C-H-Bindung oder dem Übergangsmetall-Carbonyl-Fragment, hat diese Arbeit das Anwendungsspektrum von $[(OC)_5Mo{=}BN(SiMe_3)_2]$ (**16**) erweitert, indem N=N- und Rh=C-Doppelbindungen einbezogen wurden (Abb. 86). Im Falle der ersteren wurde die Aminoborylen-Einheit "$:BN(SiMe_3)_2$" überraschend in die N=N-Bindung unter der kompletten Spaltung der Doppelbindung insertiert, wobei das Triaminoboran **102** entstand, das durch NMR-Spektroskopie und Kristallstrukturanalyse nachgewiesen wurde. Jedoch muss erwähnt werden, dass die Ausbeute für die isolierte Verbindung extrem niedrig ist, was auf eine wenig selektive Umwandlung hindeutet.

Ein weiterer Erfolg konnte bei der Funktionalisierung von Rh=C-Doppelbindungen durch Borylentransfer erzielt werden. Dementsprechend konnte eine Vielzahl von 1-Aza-2-Borabutatrien-Rhodium-Komplexe durch Borylentransfer von $[(OC)_5Mo{=}BN(SiMe_3)_2]$ (**16**) auf entsprechende Rhodium-Vinylidenkomplexe dargestellt werden (Abb. 86). Im Falle von **111** wurden zwei Diastereomere **113** und **112** im Verhältnis von ca. 1:3 erhalten, die jeweils über eine *endo*- und *exo*-Methylgruppe verfügen. Interessanterweise reagiert das isolierte *exo*-Methyl-Isomer **112** in Lösung bei Raumtemperatur unter Isomerisierung zum *endo*-Methyl-Isomer **113**, wobei sich ein chemisches Gleichgewicht von **112** und **113** im Verhältnis von ca. 2:1 einstellt, das darauf hindeutet, dass das *exo*-Methyl-Isomer **112** gegenüber dem *endo*-Methyl Isomer **113** thermodynamisch bevorzugt ist.

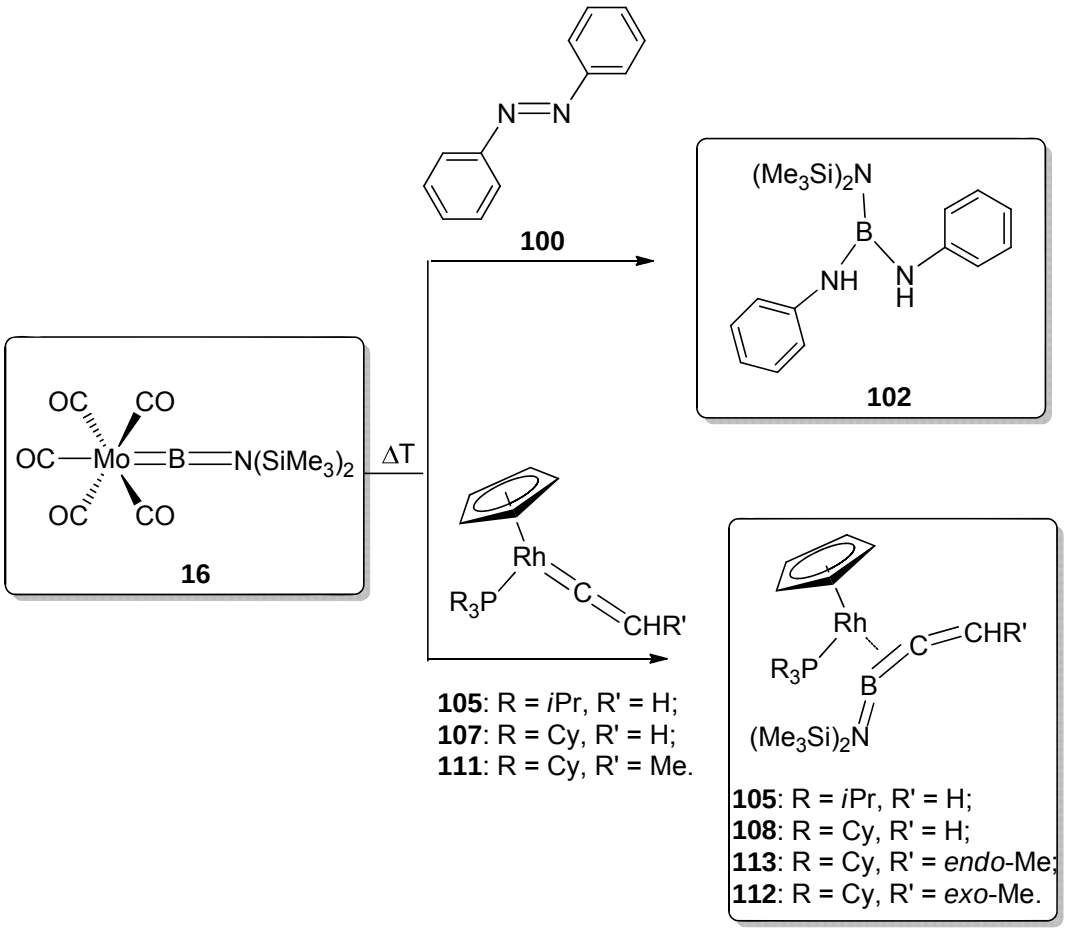

Abb. 86 Borylentransfer auf Rh=C und N=N Doppelbindungen.

Reaktivitätsstudien zu den Rhodium-Boracumulen-Komplexen zeigten einen thermisch induzierten Wechsel des Koordinationsmodus von B-C nach C-C mit nachfolgender hoch stereoselektiver C-H-Aktivierung durch die B=C-Doppelbindung (Abb. 87). Ein analoger Wechsel des Koordinationsmodus konnte bei der Zugabe von einem starken σ-Donor *I*Me (**116**) beobachtet werden. Im Gegensatz zu **115** wird die B=C-Doppelbindung in **118** effizient durch NHC stabilisiert, was die Isolierung des 1-Bora-[2]-Cumulen-Komplexes **118** ermöglichte.

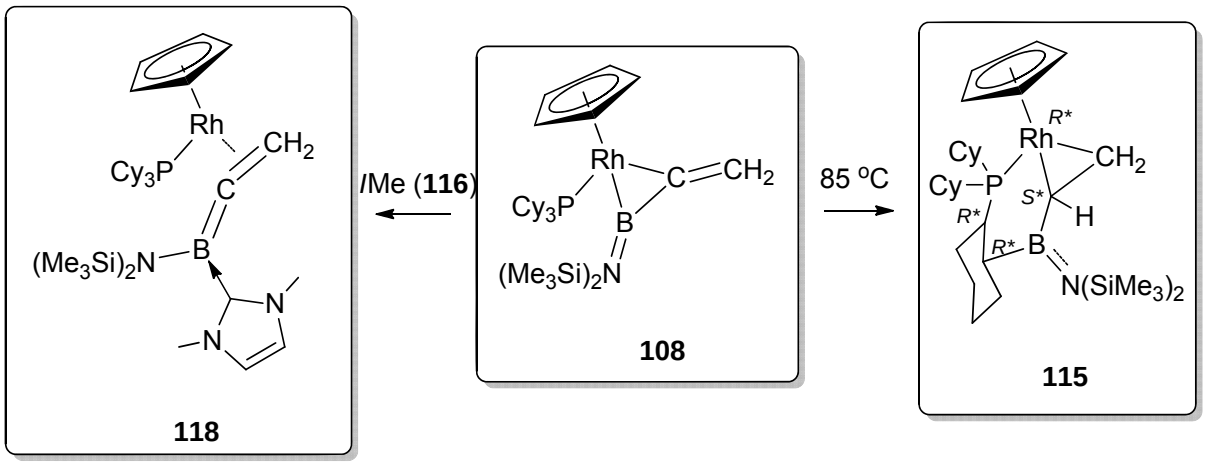

Abb. 87 Untersuchung der Reaktivität von 1-Aza-2-Borabutatrien Rhodium Komplexen.

Außerdem ist es in dieser Arbeit gelungen, den Eisen-Durylborylen-Komplex [$(PMe_3)(OC)_3Fe$=BDur] (**138**) in befriedigenden Ausbeuten, als ein seltenes Beispiel für eine Arylborylen-Spezies, zu synthetisieren (Abb. 88). Reaktivitätsuntersuchungen führten zum ersten Beispiel eines Metall-Base-stabilisierten Arylborylen-Komplexes. Die Umsetzung mit Benzophenon, einem ungesättigten und polaren Substrat, führte zu einer selektiven [2+2]-Cycloaddition, was darauf hindeutet, dass die Reaktivität der Arylborylen-Komplexe zwischen denen von Amino- und Alkylborylen-Komplexen liegt. Das Produkt der C-H-Aktivierung, das durch UV-Bestrahlung von einem Gemisch aus **138** und Naphthalin erhalten wurde, konnte mittels NMR-, IR- und EI-MS-Spektren bestätigt werden.

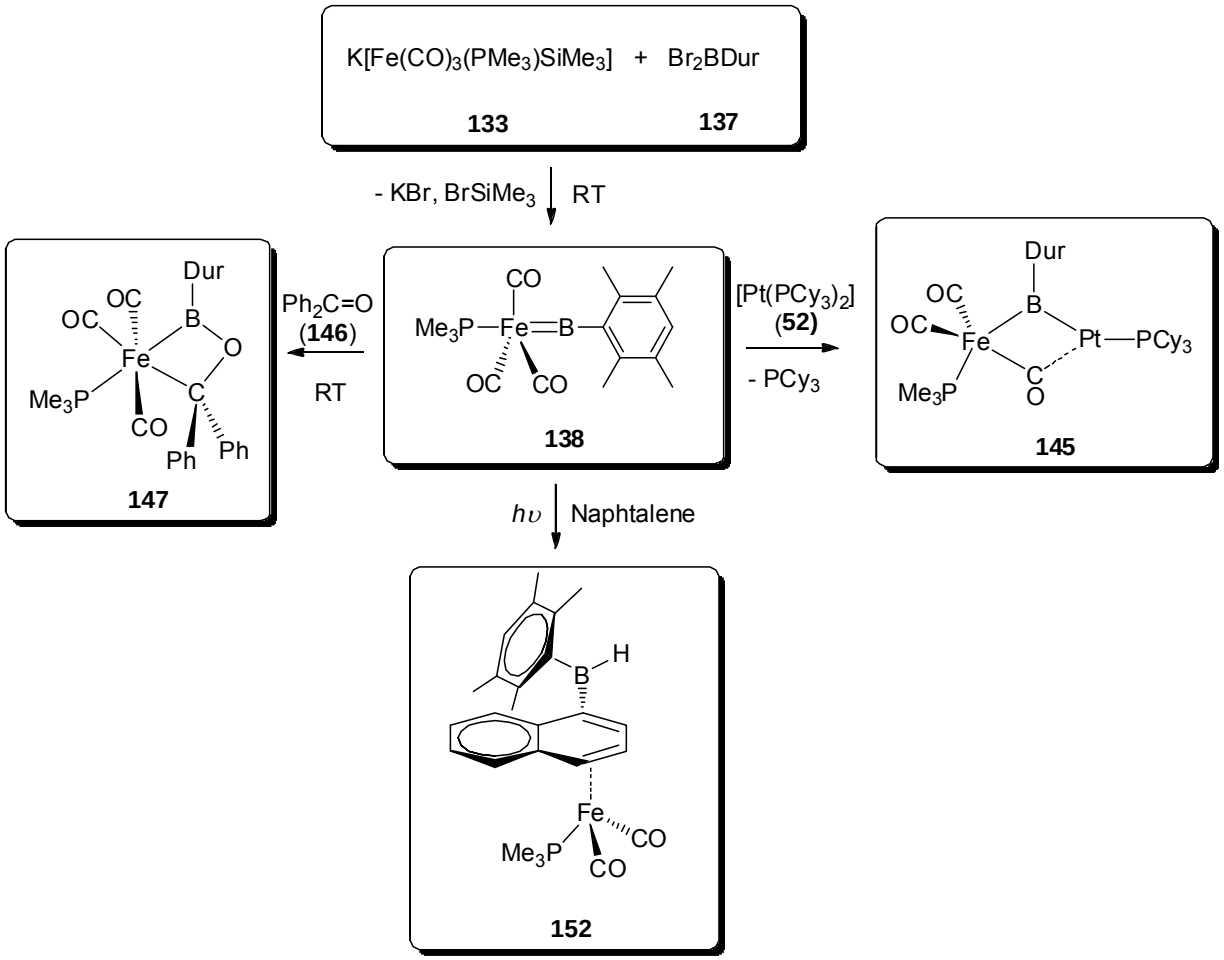

Abb. 88 Synthese und Reaktivität Untersuchung von [(PMe$_3$)(OC)$_3$Fe=BDur] (**138**).

Der carbonylreiche Durylborylen-Komplex [(PMe$_3$)(OC)$_3$Fe=BDur] (**138**) reagierte mit [(OC)$_5$Mo=BN(SiMe$_3$)$_2$] (**16**) unter einem Phosphan-Borylen-Austausch zum Eisen-Bis(borylen)-Komplex [(OC)$_3$Fe{BN(SiMe$_3$)$_2$}{BDur}] (**169**) (Abb. 89), der eine bemerkenswerte Neigung zur Borylen-Kupplung zeigte, was sowohl durch den kurzen B-B-Abstand als auch durch DFT-Rechnungen bestätigt wurde. Das Produkt der Umsetzung mit der metallorganischen Lewis-Base [Pt(PCy$_3$)$_2$] (**52**) stellt das erste Beispiel eines Bis(borylen)-Base-Addukts dar. Darüber hinaus konnte durch das Einstellen der Größe der acetylenischen Reste 1,4-Diboracyclohexadien- und die ersten 1,4-Dibora-1,3-Butadien-Komplexe in einer kontrollierten Weise durch Borylentransfer von einem Bis(borylen)-Komplex synthetisiert werden. Der beschriebene Bis(borylen)-Transfer zeigt daher ein großes Potenzial für die Synthese einer Vielzahl von bisher nicht zugänglichen Dibora-Heterocyclen.

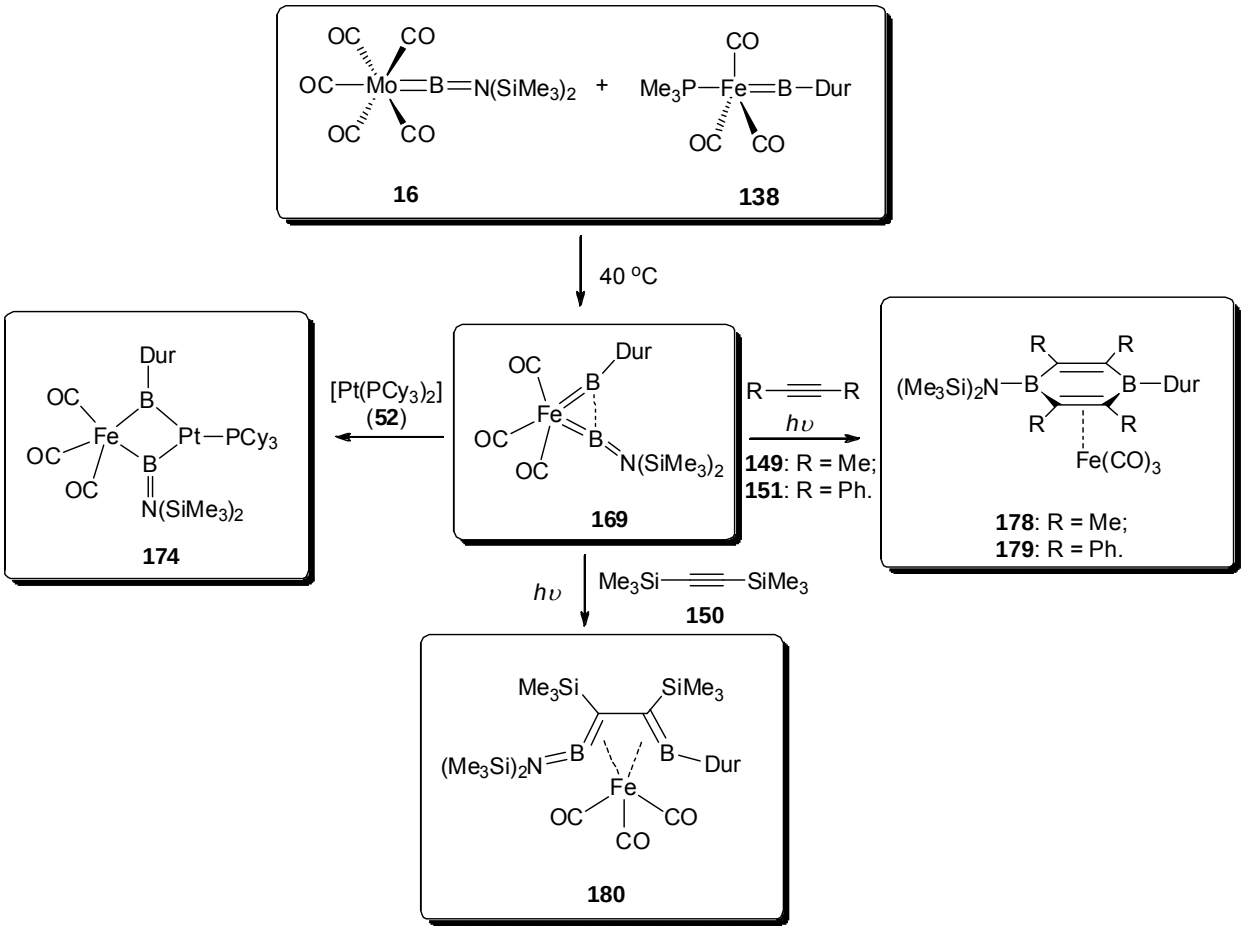

Abb. 89 Synthese und Reaktivität Untersuchung von **169**.

Schließlich wurde eine Fe-vermittelte Verkettung von Borylen-Einheiten sowohl experimentell als auch rechnerisch nachgewiesen (Abb. 90). Photolyse des einkernigen Bis(borylen)komplexes **169** führte zum zweikernigen Tetra(borylen)komplex **170** mit teilweise ausgebildeten B-B-Bindungen. Selektive Entfernung eines Eisen-Zentrums in **170** durch Anlegen einer CO-Atmosphäre unter thermischen Bedingungen führte zur Bildung von drei B-B-Bindungen, wodurch ein äusserst ungewöhnlicher, einkerniger Tetrabor-Komplex mit einer B_4-Kette erhalten wurde. DFT-Rechnungen bekräftigen, dass es sich beim Komplex um drei konventionelle B-B-σ-Bindungen handelt, die alle im "side-on"-σ-Modus an das Metall koordinieren, sowie dass eine Rückbindung von einem Metall-d_{z2}-Orbital zu den antibindenden B-B-Orbitalen vorliegt. Interessanterweise erfolgte durch Zugabe eines guten σ-Donor-Phosphan-Liganden die Insertion eines Carbonyl-Liganden in die Metall-Bor-Bindung unter gleichzeitiger Ausbildung einer B-B-Bindung, was zur Isolierung von **172** führte.

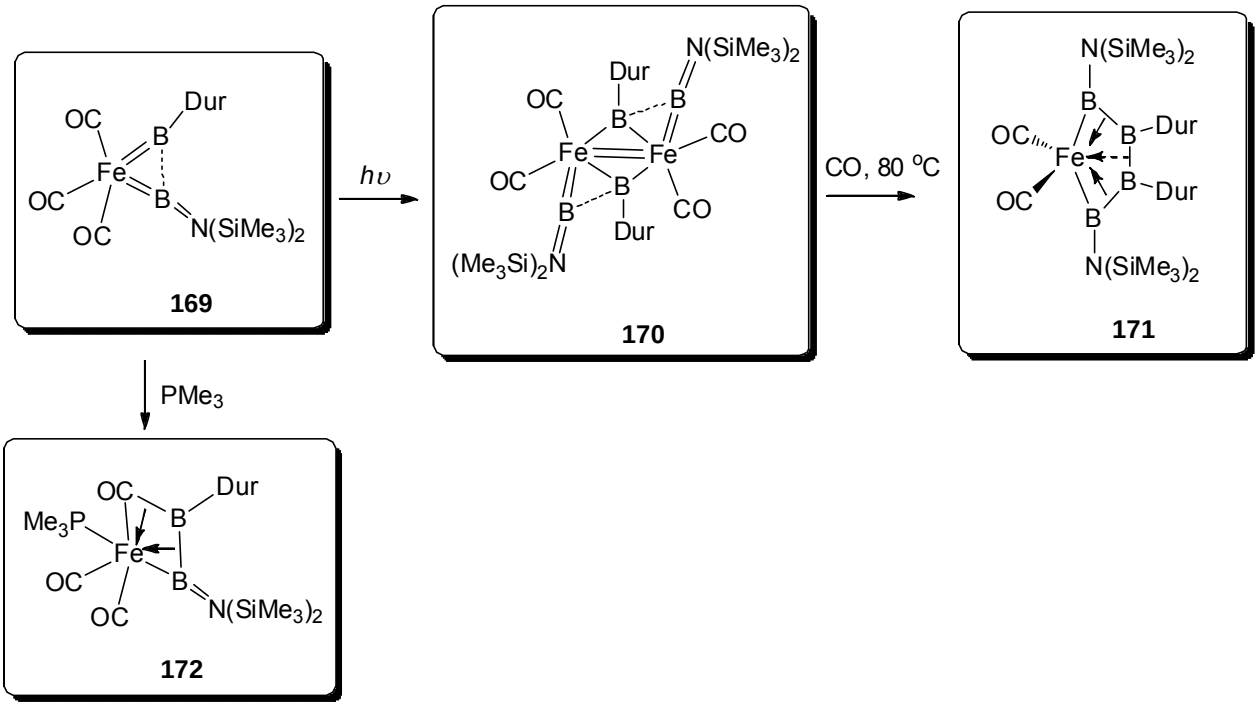

Abb. 90 Fe-vermittelte Borylen-Verkettung.

5 Experimental section

5.1 General

5.1.1 General considerations

All manipulations were conducted either under an atmosphere of dry argon or *in vacuo* using standard Schlenk line or glovebox techniques. Solvents were purified by distillation from Na/K alloy under dry argon immediately prior to use.

The light source was a Hg/Xe arc lamp (400-550 W) equipped with IR filters, irradiating at 210-600 nm. Large-scale experiments were performed in a 150-mL Schlenk flask equipped with a quartz cooling jacket into which a Hg lamp (125 W) was inserted vertically.

C_6D_6, THF-D8, Toluene-D8, CD_2Cl_2 and $CDCl_3$ was degassed by three freeze-pump-thaw cycles and stored over molecular sieves. NMR spectra were acquired on a Bruker Avance 500 (^{1}H: 500.1 MHz, ^{11}B: 160.4 MHz, ^{13}C: 125.7 MHz, ^{31}P: 202.4 MHz), Avance 200 (^{1}H: 200 MHz, ^{11}B: 64 MHz, ^{31}P: 81 MHz), Avance 400 (^{1}H: 400.1 MHz, ^{11}B: 128.4 MHz, ^{31}P: 162.0 MHz) or Varian Unity 500 (^{1}H: 499.834; ^{11}B: 160.364; ^{13}C: 125.697 MHz) NMR spectrometer. NMR spectra of isolated compounds were acquired on a Bruker Avance 500 NMR spectrometer. Routine NMR measurements were performed on a Bruker Avance 400 or Avance 200 NMR spectrometer. ^{1}H and ^{13}C{^{1}H} NMR spectra were referenced to external TMS *via* the residual protons of the solvent (^{1}H) or the solvent itself (^{13}C). ^{11}B NMR spectra were referenced to external $BF_3{\cdot}OEt_2$ and ^{31}P{^{1}H} NMR spectra to 85% H_3PO_4. NMR probe temperatures were calibrated using a MeOH standard for VT NMR spectroscopic studies.

Infrared data were acquired on a JASCO FT/IR-6200typeA apparatus. Microanalyses (C, H, N) were performed on an Elementar vario MICRO cube elemental analyzer. Mass spectra were recorded on Finnigan MAT-8200 (pos. electron ionization, 70 eV).

5.1.2 Starting materials

PMe_3 was used as a 0.10 mol/L solution in hexane. HCl was used as as a 0.24 mol/L solution in benzene.

The following starting materials were synthesized according to literature procedures:

$[(OC)_5M{=}BN(SiMe_3)_2]$ (M = Cr,[82] Mo[179]), $[Cp^*Fe(CO)_2(C{\equiv}CPh)]$[133],

$[CpFe(CO)_2(C{\equiv}CPh)]$[216], $[Cp^*Fe(CO)_2(C{\equiv}CSiMe_3)]$ (Synthesis[216], Spectrosopic data[217]), $[CpFe(CO)_2(C{\equiv}CSiMe_3)]$[216], $[1,4\text{-}\{Cp^*Fe(CO)_2C{\equiv}C\}_2\text{-}C_6H_4]$[218], $[CpFe(dppm)(C{\equiv}CSiMe_3)]$[216], $[CpFe(dppm)(C{\equiv}CPh)]$[216], $[Pt(PMe_3)_2Cl_2]$[219], $[Pt(P\textit{n}Bu_3)_2Cl_2]$[220], $[Pt(PEt_3)_2Cl_2]$[221], $[ClPt(PMe_3)_2(C{\equiv}CPh)]$[222], $[ClPt(P\textit{n}Bu_3)_2(C{\equiv}CPh)]$[223], $[1,4\text{-}\{ClPt(PEt_3)_2C{\equiv}C\}_2(C_6H_4)]$[224], *trans*-$[(PhCC)_2Pt(PEt_3)_2]$[225], $Na[CpFe(CO)_2]$[226], $[\{CpFe(CO)_2\}(BCl_2)]$[32], $[Cp(\textit{i}Pr_3P)Rh{=}C{=}CH_2]$[227], $[(OC)_4(Cy_3P)Mo\{BN(SiMe_3)_2\}]$[179], IMe[228], IMes[229], $[Fe(CO)_4(PMe_3)]$[230], $K[Fe(CO)_3(PMe_3)SiMe_3]$[231], $[Pt(PCy_3)_2]$[232], $[RhCl(C_8H_{14})_2]_2$[233].

5.2 Functionalization of transition metal alkynyl σ-complexes by borylene transfer

5.2.1 Borylene transfer to iron-alkynyl σ-complexes

5.2.1.1 Thermal reaction of $[(OC)_5Mo{=}BN(SiMe_3)_2]$ (**16**) with $[Cp^*Fe(CO)_2C{\equiv}CPh]$ (**64**)

In a Young NMR tube, a yellow solution of **16** (104 mg, 0.30 mmol) and **64** (120 mg, 0.30 mmol) in 2 ml of THF was heated in an oil bath at 80°C for 0.5 h. The volatile components were removed *in vacuo*, and the brown residue was extracted with 5 ml of hexane. The brown hexane solution was stored at –60°C overnight to separate $Mo(CO)_6$. The filtrate was stored at –60°C for 2 weeks to afford yellow crystals of **66** (98 mg, 63% yield). ^{1}H NMR: δ = 0.42 (s, 18H, $Si(CH_3)_3$), 1.42 (s, 15H, $C_5(CH_3)_5$), 7.09 (m, 1H, C*H-p* of C_6H_5), 7.31 (m, 2H, C*H-m* of C_6H_5), 7.47(m, 2H, C*H-o* of C_6H_5); $^{13}C\{^1H\}$ NMR: (*C* bonded to boron not detected), δ = 217.76 (s, *C*O), 143.67 (s, *C* of C_6H_5), 128.53 (s, *C*H-*m* of C_6H_5), 126.21 (s, *C*H-*o* of C_6H_5), 125.69 (s, *C*H-*p* of C_6H_5), 96.21 (s, *C* of $C_5(CH_3)_5$), 9.93 (s, *C*H_3 of $C_5(CH_3)_5$), 3.54 (s, $Si(CH_3)_3$); $^{11}B\{^1H\}$ NMR: δ = 36.1 (s). Elemental analysis calcd. [%] for $BC_{26}FeH_{38}NO_2Si_2$: C 60.12, H 7.37, N 2.70; found: C 59.96, H 7.35, N 2.94.

5.2.1.2 Thermal reaction of $[(OC)_5Mo{=}BN(SiMe_3)_2]$ (**16**) with $[Cp^*Fe(CO)_2C{\equiv}C(SiMe_3)]$ (**67**)

In a Young NMR tube, a solution of $[Cp^*Fe(CO)_2C{\equiv}C(SiMe_3)]$ (**67**) (33 mg, 0.1 mmol) and $[(OC)_5Mo{=}BN(SiMe_3)_2]$ (**16**) (40 mg, 0.1 mmol) in 1.5 ml THF was heated in an oil bath at 85°C, leading to a color change from yellow to deep brown. After 1 h heating: ^{1}H-NMR: δ = 0.38S(s), 0.36(s), 0.28(s), 0.22(s), 0.16(s); ^{11}B NMR: δ = 78 (bs). After 4 h heating: ^{11}B NMR: δ = 25(s), 44(s). After 4 h heating, ^{11}B NMR spectrum did not show any visible change and ^{1}H NMR spectrum revealed many more unassignable small peaks.

5.2.1.3 Reaction of $[(OC)_5Mo{=}BN(SiMe_3)_2]$ (**16**) with $[1,4\text{-}\{Cp^*Fe(CO)_2C{\equiv}C\}_2\text{-}C_6H_4]$ (**69**)

In a Young NMR tube, a solution of $[1,4\text{-}\{Cp^*Fe(CO)_2C{\equiv}C\}_2\text{-}C_6H_4]$ (**69**) (20 mg, 0.03 mmol) and $[(OC)_5Mo{=}BN(SiMe_3)_2]$ (**16**) (26 mg, 0.06 mmol) in 1.5 ml THF was heated in a oil bath at 85°C for 1 h. ^{11}B NMR: δ = 54(s), 17(s).

5.2.1.4 Reaction of $[(OC)_5M{=}BN(SiMe_3)_2]$ (**14**: M = Cr, **16**: M = Mo) with $[CpFe(dppm)C{\equiv}C(SiMe_3)]$ (**71**)

A solution of $[CpFe(dppm)C{\equiv}C(SiMe_3)]$ (**71**) (20 mg, 0.03 mmol) and $[(OC)_5Cr{=}BN(SiMe_3)_2]$ (**14**) (12 mg, 0.03 mmol) in 1.5 ml THF and a solution of $[CpFe(dppm)C{\equiv}C(SiMe_3)]$ (**71**) (20 mg, 0.03 mmol) and $[(OC)_5Mo{=}BN(SiMe_3)_2]$ (**16**) (14 mg, 0.03 mmol) in 1.5 ml THF were irradiated in NMR tube overnight respectively. ^{31}P NMR: δ = 43.3 (s, **71**); ^{11}B NMR: δ = 90 (bs, **14** or **16**)

In a Young NMR tube, a solution of $[CpFe(dppm)C{\equiv}C(SiMe_3)]$ (**73**) (20 mg, 0.03 mmol) and $[(OC)_5Mo{=}BN(SiMe_3)_2]$ (**16**) (14 mg, 0.03 mmol) in 1.5 ml THF was heated in an oil bath at 85^{o}C for 24 h.

^{11}B NMR: δ = 25 (bs); ^{31}P NMR: δ = 70.77(s), 69.80(s), 23.99(s), 23.02(s), 2.90(s).

5.2.1.5 Reaction of $[(OC)_5Mo{=}BN(SiMe_3)_2]$ (**16**) with $[Cp^*Fe(dppm)C{\equiv}CPh]$ (**73**)

In a Young NMR tube, a solution of $[Cp^*Fe(dppm)C{\equiv}CPh]$ (**73**) (20 mg, 0.03 mmol) and $[(OC)_5Mo{=}BN(SiMe_3)_2]$ (**16**) (12 mg, 0.03 mmol) in 1.5 ml THF was heated in an oil bath at 85°C for 2 d. ^{31}P NMR: δ = 41.80 (s, **73**); ^{11}B NMR: δ = 92 (bs, **16**).

5.2.2 Borylene transfer to platinum alkynyl σ-complexes

5.2.2.1 Reaction of $[(OC)_5Cr{=}BN(SiMe_3)_2]$ (**14**) with $[ClPt(PR_3)_2C{\equiv}CPh]$ (**84**: R = Me, **85**: R = *n*Bu)

In a 5 mm quartz NMR tube, a pale-yellow solution of $[(OC)_5Cr{=}BN(SiMe_3)_2]$ (**14**) (48 mg, 0.10 mmol) and $[ClPt(PMe_3)_2C{\equiv}CPh]$ (**84**) (36 mg, 0.10 mmol) in 1.5 mL of THF was irradiated for 7 h at room temperature. The volatile components were removed under vacuum,

and the brown residue was extracted with 8 mL of hexane. The light yellow filtrate was stored at –60°C overnight to yield colorless crystals of **86**. Evaporation of the filtrate afforded a second crop of analytically pure crystalline material (35 mg, 53%).
^{1}H NMR: δ = 0.46 (s, 18H, Si(C*H*$_3$)$_3$), 1.08 (m, 18 H, P(C*H*$_3$)$_3$), 8.39 (m, 2H, C*H*-*o* of C_6H_5), 7.36 (m, 2H, C*H*-*m* of C_6H_5), 7.18 (m, 1H, C*H*-*p* of C_6H_5); ^{13}C{^{1}H} NMR: (*C* bonded to boron not detected), 3.78 (s, Si(*C*H$_3$)$_3$), 13.60 (m, P(*C*H$_3$)$_3$), 129.28 (s, *C*-*i* of C_6H_5), 125.39 (s, *C*H-*p* of C_6H_5), 128.08 (s, *C*H-*p* or *C*H-*m* of C_6H_5), 128.23 (s, *C*H-*p* or *C*H-*m* of C_6H_5); ^{11}B{^{1}H} NMR: δ = 32.0(s); ^{31}P{^{1}H} NMR: δ = -16.23 ($^{1}J_{Pt, P}$ = 3377 Hz); elemental analysis (%) calcd. for $C_{20}H_{41}BNP_2Si_2ClPt$: C 36.67, H 6.31, N 2.14; found; C 36.68, H 6.32, N 2.44.

Likewise, in a 5 mm quartz NMR tube, a pale-yellow solution of [(OC)$_5$Cr=BN(SiMe$_3$)$_2$] (**14**) (15 mg, 0.04 mmol) and [ClPt(P*n*Bu$_3$)$_2$C≡CPh] (**85**) (30 mg, 0.04 mmol) in 1.5 mL of THF was irradiated for 30 h at room temperature. The volatile components were removed under vacuum, and the brown residue was extracted with 5 mL of hexane. The light yellow filtrate was stored at -70°C for several months, however yielded no crystals.
^{1}H NMR: δ = 0.50 (s, 18H, Si(C*H*$_3$)$_3$), 0.80-2.00 (m, 54 H, P*n*Bu$_3$), 8.39 (d, $^{3}J_{H-H}$ = 8.0 Hz, 2H, C*H*-*o* of C_6H_5), 7.41 (m, 2H, C*H*-*m* of C_6H_5), 7.19 (m, 1H, C*H*-*p* of C_6H_5); ^{11}B{^{1}H} NMR: δ = 34.9(s); ^{31}P{^{1}H} NMR: δ = 6.40 ($^{1}J_{Pt, P}$ = 2759 Hz)

5.2.2.2 Reaction of [(OC)$_5$Cr=BN(SiMe$_3$)$_2$] (**14**) with [1,4-{ClPt(PEt$_3$)$_2$C≡C}(C$_6$H$_4$)] (**88**)

In a 5 mm quartz NMR tube, a pale-yellow solution of [(OC)$_5$Cr=BN(SiMe$_3$)$_2$] (**14**) (15 mg, 0.04 mmol) and [1,4-{ClPt(PEt$_3$)$_2$C≡C}(C$_6$H$_4$)] (**88**) (22 mg, 0.02 mmol) in 1.5 mL of THF was irradiated for 9 h at room temperature. The volatile components were removed under vacuum, and the brown residue was extracted with 2 mL of hexane. After adding two drops of benzene, the light yellow filtrate was stored at –30°C overnight to remove Cr(CO)$_6$. The light yellow mother liquid was again dried under vacuum, extracted with 2 mL hexane, and stored at –30°C to yield light yellow crystals of **89** (10 mg, 34%).
^{1}H NMR: δ = 0.53 (s, 36H, Si(C*H*$_3$)$_3$), 1.67 (m, 24 H, C*H*$_2$ of PEt$_3$), 0.98 (m, 36H, C*H*$_3$ of PEt$_3$), 8.65 (s, 4H, C*H* of C$_6$H$_4$); ^{13}C{^{1}H} NMR: (Pt-*C*B not detected), 3.84 (s, Si(*C*H$_3$)$_3$), 8.38 (s, *C*H$_3$ of PEt$_3$), 15.47 (m, *C*H$_2$ of PEt$_3$), 129.16 (s, *C*H of C$_6$H$_4$), 133.92 (s, *C*-*i* of C$_6$H$_4$), 166.62 (C-*C*B, detected by HMBC NMR spectra); ^{11}B{^{1}H} NMR: δ = 34.0(bs); ^{31}P{^{1}H}

NMR: δ = 13.06 ($^{1}J_{Pt, P}$ = 2768 Hz); elemental analysis (%) calcd. for $B_2C_{46}Cl_2H_{100}N_2P_4Pt_2Si_4$: C 39.46, H 7.20, N 2.00; found; C 39.79, H 7.24, N 2.02.

5.2.2.3 Reaction of $[(OC)_5Cr{=}BN(SiMe_3)_2]$ (**14**) with *trans*-$[Pt(PEt_3)_2(C{\equiv}CPh)_2]$ (**91**)

In a 5 mm quartz NMR tube, a pale-yellow solution of $[(OC)_5Cr{=}BN(SiMe_3)_2]$ (**14**) (72 mg, 0.2 mmol) and $[Pt(PEt_3)_2(C{\equiv}CPh)_2]$ (**91**) (63 mg, 0.1 mmol) in 1.5 mL of THF was irradiated for 9 h at room temperature. The volatile components were removed under vacuum, and the brown residue was extracted with 4 mL of hexane. After adding two drops of benzene, the light yellow filtrate was stored at –30°C overnight to remove $Cr(CO)_6$. The light yellow mother liquid was again dried under vacuum, extracted with 2 mL hexane, and stored at –30°C to yield the mixture of **93** and **94** (1:1) in form of yellow crystals.
^{1}H NMR: δ = 0.57 (s, 36H, Si(C*H*$_3$)$_3$ of **93** or **94**), 0.59 (s, 36H, Si(C*H*$_3$)$_3$ of **93** or **94**), 1.41 (m, 24 H, C*H*$_2$ of PEt_3 in **93** and **94**), 0.72 (m, 36H, C*H*$_3$ of PEt_3 in **93** and **94**), 8.49 (m, 8H, C*H-o* of C_6H_5 in **93** and **94**), 7.49 (m, 8H, C*H-m* of C_6H_5 in **93** and **94**), 7.26 (m, 4H, C*H-p* of C_6H_5 in **93** and **94**); ^{11}B{^{1}H} NMR: δ = 37.3(bs); ^{31}P{^{1}H} NMR: δ = 5.93 ($^{1}J_{Pt, P}$ = 2761 Hz, **93** or **94**), 5.88 ($^{1}J_{Pt, P}$ = 2761 Hz, **93** or **94**).

5.3 Reactivity investigation of metal-substituted borirenes

5.3.1 Reversible iron-borirene-boryl transformation

5.3.1.1 Synthesis of [Cp*(OC)FeBN(SiMe$_3$)$_2$(η^2-CC)Ph] (**75**)

In a 5 mm quartz NMR tube, a pale yellow solution of [Cp*(OC)$_2$Fe{*cyclo*-BN(SiMe$_3$)$_2$C=C}Ph] (**66**) (80 mg, 0.15 mmol) in 1 ml of C_6D_6 was irradiated for 4 h at room temperature. During this period the NMR tube was degassed and filled with fresh argon every half an hour. The volatile components were removed *in vacuo*, and the deep red residue was extracted with hexane. The concentrated filtrate was stored at –30°C for several days to afford red crystals of **75** (54 mg, 71%).

^{1}H NMR: δ = 1.59 (s, 15H, C$_5$(C*H*$_3$)$_5$), 0.58 (bs, 9H, Si(C*H*$_3$)$_3$), 0.43 (bs, 9H, Si(C*H*$_3$)$_3$), 7.08 (m, 1H, C*H*-*p* of C_6H_5), 7.21 (m, 2H, C*H*-*m* of C_6H_5), 7.96(m, 2H, C*H*-*o* of C_6H_5); ^{13}C{^{1}H} NMR: (*C* of the alkyne ligand not detected), δ = 220.22 (s, *C*O), 133.08 (s, *C* of C_6H_5), 128.53 (s, *C*H-*m* of C_6H_5), 131.45 (s, *C*H-*o* of C_6H_5), 127.56 (s, *C*H-*p* of C_6H_5), 92.12 (s, *C* of C$_5$(CH$_3$)$_5$), 4.31 (bs, Si(*C*H$_3$)$_3$), 3.51 (bs, Si(*C*H$_3$)$_3$); ^{11}B{^{1}H} NMR: δ = 75.5; Elemental analysis calcd. [%] for BC$_{25}$FeH$_{38}$NOSi$_2$: C 61.10, H 7.79, N 2.85; found: C 61.23, H 7.92, N 3.20.

5.3.1.2 Synthesis of [Cp*(OC)$_2$FeBN(SiMe$_3$)$_2$CCPh] (**76**)

In a Young NMR tube, a deep red solution of [Cp*(OC)FeBN(SiMe$_3$)$_2$(η^2-CC)Ph] (**75**) (40 mg, 0.08 mmol) in 1 ml of C_6D_6 was degassed and refilled with dry CO gas. A gradual color change from deep red to golden-brown could be observed. After keeping the reaction mixture under CO for 2 h, the volatile components were removed *in vacuo*, and the brown residue was extracted with 1.5 ml of hexane. The brown hexane solution was stored at –70°C for a few days to afford yellow crystals of **76** (22 mg, 52% yield).

^{1}H NMR: δ = 0.68 (s, 18H, Si(C*H*$_3$)$_3$), 1.78 (s, 15H, C$_5$(C*H*$_3$)$_5$), 7.11 (m, 1H, C*H*-*p* of C_6H_5), 7.17 (m, 2H, C*H*-*m* of C_6H_5), 7.627(m, 2H, C*H*-*o* of C_6H_5); ^{13}C{^{1}H} NMR: (*C* of carbon-carbon triple bond not detected), δ = 218.08 (s, *C*O), 125.25 (s, *C*-*i* of C_6H_5), 128.83 (s, *C*H-*m* of C_6H_5), 130.55 (s, *C*H-*o* of C_6H_5), 128.16 (s, *C*H-*p* of C_6H_5), 96.84 (s, *C* of C$_5$(CH$_3$)$_5$), 9.99 (s, *C*H$_3$ of C$_5$(CH$_3$)$_5$), 5.12 (s, Si(*C*H$_3$)$_3$); ^{11}B{^{1}H} NMR: δ = 86.7 (s). Elemental analysis calcd. [%] for BC$_{26}$FeH$_{38}$NO$_2$Si$_2$: C 60.12, H 7.37, N 2.70; found: C 60.17, H 7.28, N 3.26.

5.3.1.3 Stepwise iron-boryl-borirene transformation

In a Young NMR tube, a tawny solution of **76** (20 mg, 0.04 mmol) in C_6D_6 under argon was heated in a oil bath at 80°C for 2 h, yielding a deep red solution constituted by **75** and a small amount of **66**, as indicated by ^{11}B- and ^{1}H-NMR spectroscopy. The reaction mixture was degassed and refilled with dry CO gas, brought again to 80°C for another 2 h, examined by multinuclear NMR spectroscopy, which indicated the formation of **66**.

5.3.1.4 Synthesis of [Cp*(OC)(Me_3P)Fe{*cyclo*-BN($SiMe_3$)$_2$C=C}Ph] (**77**)

In a Young NMR tube, a deep red solution of **75** (20 mg, 0.04 mmol) and PMe_3 (0.40 mL, c = 0.10 mol·L^{-1}, 0.04 mmol) in 1 ml of hexane was heated in a oil bath at 80°C for 1 h. The volatile components were removed *in vacuo*, and the brown residue was extracted with 1.5 ml of hexane. The brown hexane solution was stored at –70°C for several weeks to afford yellow crystals of **77** (15 mg, 65% yield).

^{1}H NMR: δ = 0.42 (s, 18H, Si(C*H*$_3$)$_3$), 1.55 (s, 15H, C$_5$(C*H*$_3$)$_5$), 0.97 (d, 15H, $^{2}J_{H\text{-}P}$ = 8.8 Hz, PMe_3), 7.06 (t, H, C*H*-*p* of C_6H_5), 7.29 (m, 4H, C*H*-*m* and C*H*-*o* of C_6H_5); ^{13}C{^{1}H} NMR: (*C* bonded to boron not detected), δ = 221.90 (d, $^{2}J_{C\text{-}P}$ = 35.0 Hz, *C*O), 147.51 (s, *C* of C_6H_5), 127.94 (s, *C*H-*m* of C_6H_5), 125.62 (s, *C*H-*o* of C_6H_5), 124.42 (s, *C*H-*p* of C_6H_5), 92.05 (s, *C* of C$_5$(CH$_3$)$_5$), 19.30 (d, $^{2}J_{C\text{-}P}$ = 26.1 Hz, *C* of PMe_3), 10.61 (s, *C*H$_3$ of C$_5$(CH$_3$)$_5$), 3.70 (s, Si(*C*H$_3$)$_3$); ^{11}B{^{1}H} NMR: δ = 38.4 (s); ^{31}P{^{1}H} NMR: δ = 35.39 (s). Elemental analysis calcd. [%] for $BC_{28}FeH_{47}NOPSi_2$: C 59.26, H 8.35, N 2.47; found: C 59.12, H 8.31, N 2.62.

5.3.2 Reaction of [Cp*(OC)$_2$Fe{μ-BN($SiMe_3$)$_2$C=C}Ph] (**66**) with HCl

A yellow solution of [Cp*(OC)$_2$Fe{μ-BN($SiMe_3$)$_2$C=C}Ph] (**66**) (30 mg, 0.06 mmol) in 3 mL of toluene was cooled to –70°C and treated with a benzene solution of HCl (0.24 mL, c = 0.24 mmol·mL^{-1}, 0.06 mmol). After warming to ambient temperature (ca. 1 h), all volatile components were removed *in vacuo*.

^{1}H NMR: δ = 8.99(s), 7.21-7.47(m), 1.26(s), 1.28(s), 1.37(s), 0.16(s), 0.32(s); ^{11}B NMR: δ = 45 (bs).

5.3.3 Platinum-borirene-boryl transformation

In a 5 mm quartz NMR tube, a pale-yellow solution of **86** (40 mg, 0.06 mmol) in 0.8 mL of C_6D_6 was irradiated for 4d at room temperature. The volatile components were removed under vacuum, and the yellow residue was extracted with 2 mL of hexane. The light yellow filtrate was concentrated to about 1 mL in volume, and stored at –30°C overnight to yield colorless crystals of **95**. Evaporation of the filtrate afforded a second crop of analytically pure crystalline material (26 mg, 65%).

^{1}H NMR: δ = 0.64 (s, 9 H, Si(CH_3)$_3$), 0.70 (s, 9 H, Si(CH_3)$_3$), 1.47 (m, 18 H, P(CH_3)$_3$), 7.60 (d, $^3J_{H\text{-}H}$ = 7.0 Hz, 2H, C*H*-*o* of C_6H_5), 7.17 (t, $^3J_{H\text{-}H}$ = 7.4 Hz, 2H, C*H*-*m* of C_6H_5), 7.12 (t, $^3J_{H\text{-}H}$ = 7.3 Hz, 1H, C*H*-*p* of C_6H_5); ^{13}C{^{1}H} NMR: δ = 5.34 (s, Si(*C*H$_3$)$_3$), 6.21 (s, Si(*C*H$_3$)$_3$), 43.66 (m, P(*C*H$_3$)$_3$), 125.48 (s, *C*-*i* of C_6H_5), 128.63 (s, *C*H-*p* of C_6H_5), 128.80 (s, *C*H-*m* of C_6H_5), 130.66 (s, *C*H-*o* of C_6H_5), B-*C*≡*C* not detected; ^{11}B{^{1}H} NMR: δ = 48.8 (s); ^{31}P{^{1}H} NMR: δ = -15.82 ($^1J_{Pt,P}$ = 3085 Hz); Elemental analysis (%) calcd. for $C_{20}H_{41}BNP_2Si_2ClPt$: C 36.67, H 6.31, N 2.14; found: C 37.65, H 6.35, N 2.99.

5.3.4 Reaction of platinum-boriren (**86**) with HCl

A pale yellow solution of **86** (50 mg, 0.076 mmol) in 3 mL of toluene was cooled to –70°C and treated with a benzene solution of HCl (0.32 mL, c = 0.24 mmol·mL^{-1}, 0.076 mmol). After warming to ambient temperature (ca. 1 h), the reaction mixture was filtered through a filter pipette in a glovebox and the filtrate evaporated to dryness. The pale yellow residue was extracted with 2 mL of hexane. After standing at ambient temperature for 1 h, the filtrate became turbid and was filtered again through a filter pipette, concentrated to about 1 mL in volume, and stored at –30°C overnight to yield colorless crystals of **96** (20 mg, 38%).

^{1}H NMR: δ = 0.28 (s, 18 H, Si(CH_3)$_3$), 1.05 (vt, $^2J_{P\text{-}H}$ + $^4J_{P\text{-}H}$ = 7.6 Hz, 18 H, P(CH_3)$_3$), 8.09 (dd, $^3J_{H\text{-}H}$ = 8.2 Hz, $^4J_{H\text{-}H}$ = 1.2 Hz, 2H, C*H*-*o* of C_6H_5), 7.21 (t, $^3J_{H\text{-}H}$ = 7.7 Hz, 2H, C*H*-*m* of C_6H_5), 7.07 (t, $^3J_{H\text{-}H}$ = 7.4 Hz, 1H, C*H*-*p* of C_6H_5), 9.77 (t, $^3J_{H\text{-}P}$ = 4.6 Hz, 1H, *H*C=C); ^{13}C{^{1}H} NMR:δ = 3.90 (s, Si(CH$_3$)$_3$), 13.19 (m, P(CH$_3$)$_3$), 147.58 (s, c-*i* of C_6H_5), 126.00 (s, CH-*p* of C_6H_5), 127.59 (s, CH-*m* of C_6H_5), 130.16 (s, CH-*o* of C_6H_5), 166.10 (t, $^2J_{P\text{-}C}$ = 9.1 Hz, Pt-CH), B-C=C not detected; ^{11}B{^{1}H} NMR: δ = 44.8 (s); ^{31}P{^{1}H} NMR: δ = -16.2 ($^1J_{Pt,P}$ = 2769 Hz); Elemental analysis (%) calcd. for $C_{20}H_{42}BNP_2Si_2Cl_2Pt$: C 34.74, H 6.12, N 2.02; found: C 34.73, H 5.69, N 2.24.

5.3.5 Reaction of platinum-borirene (**86**) with BBr_3

A pale yellow solution of **86** (50 mg, 0.076 mmol) in 3 mL of toluene was cooled to –70°C and treated with a hexane solution of BBr_3 (0.19 mL, c = 0.40 mmol·mL^{-1}, 0.076 mmol). After warming to ambient temperature (ca. 1 h), the reaction mixture was filtered through a filter pipette in a glovebox and the filtrate evaporated to dryness. The pale yellow residue was extracted with 2 mL of hexane. The filtrate was concentrated to about 1 mL in volume, and stored at –30°C overnight to yield colorless crystals of **98** (8 mg, 15%).

^{1}H NMR: δ = 0.47 (s, 18 H, Si(C*H*$_3$)$_3$), 1.13 (m, 18 H, P(C*H*$_3$)$_3$), 8.43 (dd, $^3J_{H\text{-}H}$ = 8.1 Hz, $^4J_{H\text{-}H}$ = 1.3 Hz, 2H, C*H*-*o* of C_6H_5), 7.37 (t, $^3J_{H\text{-}H}$ = 7.7 Hz, 2H, C*H*-*m* of C_6H_5), 7.20 (t, $^3J_{H\text{-}H}$ = 7.4 Hz, 1H, C*H*-*p* of C_6H_5); ^{13}C{^{1}H} NMR: δ = 2.39 (s, Si(*C*H$_3$)$_3$), 13.03 (m, P(*C*H$_3$)$_3$), 133.17 (s, *C*-*i* of C_6H_5), 127.25 (s, *C*H-*p* of C_6H_5), 127.34 (s, *C*H-*m* or *C*H-*o* of C_6H_5), 127.66 (s, *C*H-*o* or *C*H-*m* of C_6H_5), *C* bonded to boron not detected; ^{11}B{^{1}H} NMR: δ = 32.6 (s); ^{31}P{^{1}H} NMR: δ = -19.15 ($^1J_{Pt,P}$ = 2703 Hz); Elemental analysis (%) calcd. for $C_{20}H_{41}BBrNP_2PtSi_2$: C 34.34, H 5.91, N 2.00; found:C 35.40, H 6.08, N 2.01.

5.3.6 Attempt to synthesize chloroborirene by iron-boryl-borirene transformation

A 5 mL toluene suspension of NaC≡CPh (100 mg, 0.8 mmol) was added into 5 mL toluene solution of BCl_3 (2.5 mL, c = 0.40 mmol·mL^{-1}, 1 mmol) with stirring at –60°C. The reaction mixture was warmed slowly to ambient temperature (1 h). Excess BCl_3 was removed by the concentration of solvent *in vacuo* at 0°C. The formation of Cl_2B(C≡CPh) (**82**) was indicated by the peak at δ_B = 45 ppm in ^{11}B NMR spectrum. Additionally, a small amount of byproduct ClB(C≡CPh)$_2$ (δ_B = 42) was observed. The concentrated toluene solution was subsequently transferred to a 5 mL toluene suspension of [CpFe(CO)$_2$]Na (**81**) (140 mg, 0.7 mmol) with stirring at –60°C. After slow warming the reaction mixture to ambient temperature (2 h) and removing volatile components *in vacuo*, the brown residue was extracted with 1 mL C_6D_6. No signals were observed in ^{11}B NMR spectrum. ^{1}H NMR spectrum displayed a strong signal at δ_H = 4.23, indicating dimerization of the CpFe(CO)$_2$ fragment.

A toluene suspension of LiC≡CPh (**83**) (7 mg, 0.06 mmol) was added to a red solution of [Cp*Fe(CO)$_2$(BCl$_2$)] (**5**) (20 mg, 0.06 mmol) at –60°C. The reaction mixture was slowly warmed to ambient temperature, during which time the color changed from red to black. ^{11}B NMR spectrum displayed no signals. ^{1}H NMR spectrum revealed dimerization of the Cp*Fe(CO)$_2$ fragment (δ_H = 1.60).

5.4 Attempt to synthesize diazaboracyclopropane by borylene transfer

5.4.1 Reaction of $[(OC)_5Mo{=}BN(SiMe_3)_2]$ (**16**) with azobenzene (**100**)

In a Young NMR tube, a red solution of $[(OC)_5Mo{=}BN(SiMe_3)_2]$ (**16**) (112 mg, 0.30 mmol) and azobenzene (**100**) (50 mg, 0.3 mmol) in 2 ml of THF was heated in a oil bath at 80°C for 3 d. All volatile components were removed *in vacuo*. The resulting deep brown residue was dissolved in hexane (2 mL) and chromatographed with hexane on Al_2O_3 (neutral, activity grade V). A light orange fraction containing small amount of azobenzene **100** was eluted that was concentrated to ca. 1 mL *in vacuo*. Excess of azobenzene **100** was removed up storing the solution overnight at –78°C. The light yellow mother liquor was further concentrated to ca. 0.5 mL and stored at –78°C for one week. Triaminoborane **102** was obtained as colorless crytals (5 mg, 5%).

^{1}H NMR: δ = 0.21 (s, 18H, Si(C*H*$_3$)$_3$), 4.71 (bs, N*H*), 7.07 (m, 4H, C$_6$*H*$_5$), 6.85 (m, 6H, C$_6$*H*$_5$); ^{13}C{^{1}H} NMR: δ = 3.06 (s, Si(*C*H$_3$)$_3$), 121.08 (s, *C*$_6$H$_5$), 121.57 (s, *C*$_6$H$_5$), 129.38 (s, *C*$_6$H$_5$), 144.32 (s, *C*$_6$H$_5$); ^{11}B{^{1}H} NMR: δ = 25.7 (s).

The reaction was also carried out without solvent. In a Young NMR tube, $[(OC)_5Mo{=}BN(SiMe_3)_2]$ (**16**) (112 mg, 0.30 mmol) and azobenzene (**100**) (50 mg, 0.3 mmol) was mixed and melted at 85°C in a oil bath at 80°C. After 2 d, C_6D_6 was added into the Young NMR tube. Multinuclear NMR spectroscopy displayed all above mentioned signals for **102**.

5.4.2 Reaction of $[(OC)_5Mo{=}BN(SiMe_3)_2]$ (**16**) with 4-[(E)-(4-Methylphenyl)diazenyl]phenylamin (**103**)

In a Young NMR tube, a red solution of $[(OC)_5Mo{=}BN(SiMe_3)_2]$ (**16**) (96 mg, 0.24 mmol) and 4-[(E)-(4-Methylphenyl)diazenyl]phenylamin (**103**) (50 mg, 0.24 mmol) in 2 ml of THF was heated in a oil bath at 80°C for 36 h.

^{11}B-NMR: δ = 25.1(bs).

5.5 Synthesis of boracumulene complexes by borylene transfer

5.5.1 Reaction of $[(OC)_5Mo{=}BN(SiMe_3)_2]$ (**16**) with $[Cp(iPr_3P)Rh{=}C{=}CH_2]$ (**104**)

An orange-colored solution of $[(OC)_5Mo{=}BN(SiMe_3)_2]$ (**16**) (0.23 g, 0.56 mmol) and $[Cp(iPr_3P)Rh{=}C{=}CH_2]$ (**104**) (0.20 g, 0.56 mmol) in benzene (3 mL) was stirred at 40°C for 16 h. The solvent of the reaction mixture was then removed *in vacuo*. The resulting dark orange oily residue was dissolved in hexane (2 mL) and chromatographed with hexane on Al_2O_3 (neutral, activity grade V). A light yellow fraction was eluted that was concentrated to ca. 2 mL *in vacuo*. After storing the solution for 3 d at –78°C, the light yellow mother liquor was removed from the colorless precipitate. Removal of the solvent afforded complex **105** as an yellow air-sensitive oil (> 95% pure by multinuclear NMR spectroscopy, 191 mg, 65%).
^{1}H NMR: δ = 7.31 (dd, $^3J_{Rh-H}$ = 4.1 Hz, $^4J_{P-H}$ = 1.1 Hz, 1H, *exo-H*, C=CH$_2$), 6.48 (dd, $^3J_{Rh-H}$ = 2.9 Hz, $^4J_{P-H}$ = 2.2 Hz, 1H, *endo-H*, C=CH$_2$), 5.27 (s, 5H, C$_5H_5$), 1.83 (m, 3H, C*H* of P*i*Pr$_3$), 0.89 (m, 18H, C*H*$_3$ of P*i*Pr$_3$), 0.62 (s, 9H, *endo*-SiMe$_3$, N(SiMe$_3$)$_2$), 0.30 (s, 9H, *exo*-SiM$_3$, N(SiMe$_3$)$_2$); ^{13}C{^{1}H} NMR: δ = 166.06 (bs, *C*CH$_2$), 120.31 (dd, $^2J_{C-Rh}$ = $^3J_{C-P}$ = 3.9 Hz, C*C*H$_2$), 88.80 (dd, $^1J_{C-Rh}$ = $^2J_{C-P}$ = 2.2 Hz, *C*$_5$H$_5$), 5.09 (s, *endo*-Si(*C*H$_3$)$_3$), 4.87 (s, *exo*-Si(*C*H$_3$)$_3$), 24.84 (d, $^1J_{P-C}$ = 22.0 Hz, *C*H, *i*Pr), 20.29 (s, *C*H$_3$, *i*Pr); ^{11}B{^{1}H} NMR: δ = 67.9(s); ^{31}P{^{1}H} NMR: δ = 66.44 (d, $^1J_{Rh-P}$ = 202.5 Hz). EI MS: m/z: 525 [M$^+$].

5.5.2 Preparation of $[Cp(Cy_3P)Rh{=}C{=}CH_2]$ (**107**)

A solution of 300 mg (0.42 mmol) $[RhCl(C_8H_{14})_2]_2$ and 471 mg (1.68 mmol) PCy_3 was stirred in 20 mL benzene for 30 min, whereupon acetylene was bubbled through the solution till the purple color faded (ca. 15 s). The volatile components were removed under vacuum. The brown residue was treated with 88 mg (1.00 mmol) NaCp in THF and stirred overnight at room temperature. The solvent was removed under vacuum, and the residue was extracted with hexane and chromatographed on Al_2O_3 (neutral, activity grade V) with hexane. **107** was obtained as an air-sensitive analytically pure orange oil (204 mg, 51%).
^{1}H NMR: δ = 5.29 (s, 5H, C$_5H_5$), 2.75 (d, $^4J_{P-H}$ = 3.6 Hz, 2H, C=C*H*$_2$), 2.08-1.17 (m, 33H, PCy$_3$); ^{13}C{^{1}H} NMR: δ = 311.05 (dd, $^1J_{Rh-C}$ = 66.7 Hz, $^2J_{P-C}$ = 26.6 Hz, *C*=CH$_2$), 93.84 (dd, $^2J_{Rh-C}$ = 16.4 Hz, $^3J_{P-C}$ = 4.6 Hz, C=*C*H$_2$), 86.12 (dd, $^1J_{C-Rh}$ = $^2J_{C-P}$ = 2.7 Hz, *C*$_5$H$_5$), 36.60 (d, $^1J_{P-C}$ = 22.7 Hz, *C*^{1}, Cy), 30.37 (s, *C*^{3}, *C*^{5}, Cy), 28.04 (d, $^2J_{P-C}$ = 10.4 Hz, *C*^{2}, *C*^{6}, Cy), 27.06 (s,

C^4, Cy); $^{31}P\{^1H\}$ NMR: δ = 61.39 (d, $^1J_{Rh-P}$ = 208.0 Hz). Elemental analysis (%) calc. for $C_{25}H_{40}PRh$: C 63.29, H 8.50; found: C 63.00, H 8.14.

5.5.3 Reaction of $[(OC)_5Mo{=}BN(SiMe_3)_2]$ (**16**) with $[Cp(Cy_3P)Rh{=}C{=}CH_2]$ (**107**)

An orange-colored solution of $[(OC)_5Mo{=}BN(SiMe_3)_2]$ (**16**) (0.17 g, 0.42 mmol) and $[Cp(Cy_3P)Rh{=}C{=}CH_2]$ (**107**) (0.20 g, 0.42 mmol) in benzene (3 mL) was stirred at 40°C for 16 h. The solvent of the reaction mixture was then removed *in vacuo*. The resulting dark orange oily residue was dissolved in hexane (2 mL) and chromatographed with hexane on Al_2O_3 (neutral, activity grade V). A light yellow fraction was eluted that was concentrated to ca. 3 mL *in vacuo*. The solution was stored overnight at room temperature to yield pale yellow crystals of **108**. The filtrate was concentrated to ca. 1.5 mL and stored at –30°C for 3 d to afford a second crop of analytically pure crystalline material (157 mg, 58%).

^1H NMR: δ = 7.37 (d, $^3J_{Rh-H}$ = 3.5 Hz, 1H, *exo-H*, C=CH_2), 6.55 (d, $^3J_{Rh-H}$ = 2.9 Hz, 1H, *endo-H*, C=CH_2), 5.35 (s, 5H, C_5H_5), 1.96-1.11 (m, 33H, PCy_3), 0.64 (s, 9H, *endo*-$SiMe_3$, $N(SiMe_3)_2$), 0.33 (s, 9H, *exo*-$SiMe_3$, $N(SiMe_3)_2$); $^{13}C\{^1H\}$ NMR: δ = 166.18 (bs, *C*CH_2), 120.09 (dd, $^2J_{C-Rh}$ = $^3J_{C-P}$ = 4.3 Hz, C*C*H_2), 88.91 (dd, $^1J_{C-Rh}$ = $^2J_{C-P}$ = 2.2 Hz, C_5H_5), 4.78 (s, *endo*-Si(*C*H_3)$_3$), 3.22 (s, *exo*-Si(*C*H_3)$_3$), 35.31 (d, $^1J_{P-C}$ = 21.5 Hz, *C*^{1}, Cy), 30.20 (d, $^2J_{P-C}$ = 20.7 Hz, *C*^{2}, *C*^{6}, Cy), 27.85 (m, *C*^{3}, *C*^{5}, Cy), 26.89 (s, *C*^{4}, Cy); $^{11}B\{^1H\}$ NMR: δ = 68.7(s); $^{31}P\{^1H\}$ NMR: δ = 56.56 (d, $^1J_{Rh-P}$ = 201.9 Hz). Elemental analysis (%) calc. for $BC_{31}H_{58}NPRhSi_2$: C 57.67, H 9.05, N 2.17; found: C 57.81, H 9.04, N 2.08.

5.5.4 Synthesis of $[Cp(Cy_3P)Rh{=}C{=}CH(Me)]$ (**111**)

A solution of 200 mg (0.28 mmol) $[RhCl(C_8H_{14})_2]_2$ and 470 mg (1.7 mmol) PCy_3 was stirred in 20 mL benzene for 30 min, whereupon propyne was bubbled through the solution till the purple color faded (ca. 15 s). The volatile components were removed under vacuum. The brown residue was treated with 60 mg (0.68 mmol) NaCp in THF and stirred overnight at room temperature. The solvent was removed under vacuum, and the residue was extracted with hexane and chromatographed on Al_2O_3 (neutral, activity grade V) with hexane. **111** was obtained as an air-sensitive analytically pure orange oil (194 mg, 71%).

^1H NMR: δ = 5.30 (s, 5H, C_5H_5), 3.22 (m, 1H, C=C*H*Me), 1.91 (m, 3H, Me of C=CHMe), 2.00-1.15 (m, 33H, PCy_3); $^{13}C\{^1H\}$ NMR: δ = 85.77 (m, C_5H_5), 103.51 (dd, $^2J_{Rh-C}$ = 15.4 Hz, $^3J_{P-C}$ = 4.8 Hz, C=*C*HMe), 5.42 (d, $^3J_{Rh-C}$ = 3.1 Hz, Me of C=CHMe), 36.60 (d, $^1J_{P-C}$ = 22.7 Hz, *C*^{1}, Cy), 27.11 (d, $^3J_{P-C}$ = 1.1 Hz, *C*^{3}, *C*^{5}, Cy), 28.16 (d, $^2J_{P-C}$ = 10.6 Hz, *C*^{2}, *C*^{6}, Cy), 30.44 (s,

C[4], Cy), 310.63 (dd, $^{1}J_{Rh-C}$ = 66.4 Hz, $^{2}J_{P-C}$ = 26.1 Hz, *C*=CHMe),; $^{31}P\{^{1}H\}$ NMR: δ = 62.78 (d, $^{1}J_{Rh-P}$ = 209.3 Hz). Elemental analysis (%) calc. for $C_{26}H_{42}PRh$: C 63.93, H 8.67; found: C 63.07, H 8.57.

5.5.5 Reaction of $[(OC)_4(Cy_3P)Mo{=}BN(SiMe_3)_2]$ (**110**) with $[Cp(R_3P)Rh{=}C{=}CH_2]$ (**104**: R = *i*Pr, **107**: R = Cy)

In Young NMR tube, a solution of $[(OC)_4(Cy_3P)Mo{=}BN(SiMe_3)_2]$ (**110**) (30 mg, 0.05 mmol) and $[Cp(Cy_3P)Rh{=}C{=}CH_2]$ (**107**) (22 mg, 0.05 mmol) in benzene (3 mL) and a solution of $[(OC)_4(Cy_3P)Mo{=}BN(SiMe_3)_2]$ (**110**) (30 mg, 0.05 mmol) and $[Cp(iPr_3P)Rh{=}C{=}CH_2]$ (**104**) (16 mg, 0.05 mmol) in benzene (3 mL) were heated at 40°C for 16 h respectively. Multinuclear NMR spectroscopy revealed no expected reaction.

^{11}B NMR: δ = 92(bs, **110**); ^{31}P NMR: δ = 51.10(s, **110**), 61.39 (d, $^{1}J_{Rh-P}$ = 208.0 Hz, **107**), 73.48 (d, $^{1}J_{Rh-P}$ = 209.0 Hz, **104**).

5.5.6 Reaction of $[(OC)_5Mo{=}BN(SiMe_3)_2]$ (**16**) with $[Cp(Cy_3P)Rh{=}C{=}CHMe]$ (**111**)

In a Young NMR tube, an orange-colored solution of $[(OC)_5Mo{=}BN(SiMe_3)_2]$ (**16**) (80 g, 0.20 mmol) and $[Cp(Cy_3P)Rh{=}C{=}CH(Me)]$ (**111**) (96 mg, 0.20 mmol) in benzene (1.5 mL) was heated in a oil bath at 40°C for 16 h. The solvent of the reaction mixture was then removed *in vacuo*. The resulting dark orange oily residue was dissolved in hexane (2 mL) and chromatographed with hexane on Al_2O_3 (neutral, activity grade V). A light yellow fraction was eluted that was concentrated to ca. 3 mL *in vacuo*. The solution was stored overnight at room temperature to yield pale yellow crystals of **112** (15 mg, 11%). Removing the solvent of mother liquor *in vacuo* afforded mixture of **112** and **113**.

NMR spectroscopic data of **112**: ^{1}H NMR: δ = 6.72 (m, 1H, *endo-H*, C=C*H*Me), 5.343 (s, 5H, C_5H_5), 2.08 (dd, $^{3}J_{H-H}$ = 6.9 Hz, $^{4}J_{Rh-H}$ = 1.7 Hz, *exo*-Me of C=CHMe), 1.94-1.08 (m, 33H, PCy_3), 0.63 (s, 9H, *endo*-$SiMe_3$, $N(SiMe_3)_2$), 0.35 (s, 9H, *exo*-$SiMe_3$, $N(SiMe_3)_2$); $^{13}C\{^{1}H\}$ NMR: δ = 149.0 (bs, *C*CHMe), 130.33 (m, C*C*HMe), 88.73 (m, C_5H_5), 5.11 (s, *endo*-$Si(CH_3)_3$), 3.76 (s, *exo*-$Si(CH_3)_3$), 30.0 (m, CH_2 of Cy), 28.1 (m, CH_2 of Cy), 26.99 (s, CH_2 of Cy), 34.84 (d, $^{1}J_{P-C}$ = 21.3 Hz, *C*[1], Cy); $^{11}B\{^{1}H\}$ NMR: δ = 67.7(bs); $^{31}P\{^{1}H\}$ NMR: δ = 56.61 (d, $^{1}J_{Rh-P}$ = 206.2 Hz).

In a Young NMR tube, above isolated **112** (10 mg, 0.015 mmol) was dissolved in C_6D_6 and stored at ambient temperature overnight. Multinuclear NMR spectroscopy revealed the presence of **112** and **113** in a ratio of ca. 2:1.

NMR spectroscopic data of **113**: ^{1}H NMR: δ = 7.55 (m, 1H, *exo-H*, C=C*H*Me), 5.337 (s, 5H, C_5H_5), 2.29 (d, $^3J_{H-H}$ = 6.3 Hz, 3H, *endo*-Me of C=CHMe), 1.94-1.08 (m, 33H, PCy_3), 0.65 (s, 9H, *endo*-$SiMe_3$, $N(SiMe_3)_2$), 0.35 (s, 9H, *exo*-$SiMe_3$, $N(SiMe_3)_2$); $^{13}C\{^1H\}$ NMR: δ = 149.0 (bs, *C*CHMe), 127.42 (m, C*C*HMe), 88.42 (m, C_5H_5), 4.97 (s, *endo*-$Si(CH_3)_3$), 3.60 (s, *exo*-$Si(CH_3)_3$), 30.4 (m, CH_2 of Cy), 28.0 (m, CH_2 of Cy), 26.94 (s, CH_2 of Cy), 36.57 (d, $^1J_{P-C}$ = 20.4 Hz, C^1, Cy); $^{11}B\{^1H\}$ NMR: δ = 67.7(bs); $^{31}P\{^1H\}$ NMR: δ = 58.28 (d, $^1J_{Rh-P}$ = 205.1 Hz).

5.5.7 C-H activation by B=C double bond

In a Young NMR tube, a light yellow solution of **108** (20 mg, 0.03 mmol) in C_6D_6 (0.8 mL) was heated in an oil bath at 85°C for 2 weeks. The volatile components were removed in vacuo, and the yellow residue was extracted with 1 mL hexane. The yellow hexane solution was stored at room temperature to afford yellow crystals of **115** (14 mg, 70%).

^{1}H NMR: δ = 5.15 (s, 5H, C_5H_5), 3.17 (d, 1H, H of olefinic CH_2 *cis* to $BN(SiMe_3)_2$, $^3J_{H-H}$ = 12.1 Hz), 2.99 (dd, 1H, H of olefinic BC*H*, $^3J_{H-H}$ = 12.1 Hz), 1.88 (dd, 1H, H of olefinic CH_2 *trans* to $BN(SiMe_3)_2$, $^3J_{H-H}$ = 12.1 Hz, $^3J_{P-H}$ = 7.5 Hz), 2.31 (m, 1H, Cy), 2.17 (m, 1H, Cy), 2.01 (m, 1H, Cy), 0.83 (m, 1H, PCHC*H*B), 1.81-0.80 (m, 28H, Cy), 0.50 (s, 9H, $N(SiMe_3)_2$), 0.45 (s, 9H, $N(SiMe_3)_2$); $^{13}C\{^1H\}$ NMR: δ = 5.37 (s, $Si(CH_3)_3$), 5.07 (s, $Si(CH_3)_3$), 85.60 (dd, $^1J_{C-Rh}$ or $^2J_{C-P}$ = 2.4 Hz, $^1J_{C-Rh}$ or $^2J_{C-P}$ = 3.6 Hz, C_5H_5), 34.26 (s, olefinic CH_2), 47.70 (bs, olefinic *C*HB), 38.55 (bs, PCH*C*HB), 34.49-34.21 (m, *C*H of Cy), 31.93-26.65 (m, CH_2 of Cy); $^{11}B\{^1H\}$ NMR: δ = 42.7; $^{31}P\{^1H\}$ NMR: δ = 74.25 (d, $^1J_{Rh-P}$ = 187.8 Hz). Elemental analysis (%) calc. for $BC_{34}H_{65}NPRhSi_2$: C 59.29, H 9.51, N 2.03; found: C 59.38, H 9.44, N 2.02.

5.5.8 Reaction of [CpRh(PCy_3){(B,C-η^2)-$(SiMe_3)_2N$=B=C=CH_2)}] (**108**) with *I*Me (**116**)

A toluene solution of IMe (**116**) (0.09 mL, c = 0.36 mmol·mL^{-1}, 0.03 mmol) was added *via* syringe to a yellow solution of [CpRh(PCy_3){(B,C-η^2)-$(SiMe_3)_2N$=B=C=CH_2)}] (**108**) 20 mg, 0.03 mmol) in 1.5 mL toluene at ambient temperature. The color turned immediately deep red. The reaction solution was concentrated to ca. 0.2 mL *in vacuo*, layered with ca. 0.4 mL

hexane and stored at –30°C for 2 weeks. **118** was obtained as deep red crystals (6 mg, 27%). Due to the instability of **118** in solution at ambient temperature, NMR experiments were carried out at –30°C.

^{1}H NMR: δ = 3.55 (m, 1H, *endo-H* of olefinic CH_2), 2.58 (m, 1H, *exo-H* of olefinic CH_2), 5.02 (s, 5H, C_5H_5), 2.15-1.15 (m, 33H, PCy_3), 0.51 (bs, 9H, CH_3 of $N(SiMe_3)_2$), 0.14 (bs, 9H, CH_3 of $N(SiMe_3)_2$), 4.15 (bs, 3H, CH_3 of IMe), 3.21 (bs, 3H, CH_3 of IMe), 5.58 (bs, 2H, C*H* of IMe); ^{13}C{^{1}H} NMR: boron-bound carbons were not detected, δ = 5.05 (bs, Si(CH_3)$_3$), 3.85 (bs, Si(CH_3)$_3$), 86.35 (s, C_5H_5), 23.41 (s, olefinic CH_2), 38.04 (bs, CH_3 of IMe), 36.31 (bs, CH_3 of IMe), 119.40 (bs, *C*H of IMe), 30.73-27.33 (m, CH_2 of Cy), 32.34 (s, *C*H of Cy); ^{11}B{^{1}H} NMR: δ = 16.3(bs); ^{31}P{^{1}H} NMR: δ = 55.39 (d, $^{1}J_{Rh-P}$ = 209.0 Hz). Elemental analysis (%) calc. for $BC_{36}H_{66}N_3PRhSi_2$: C 58.29, H 8.97, N 5.67; found: C 57.71, H 8.70, N 5.78.

5.6 Reductive elimination of borylene ligands

5.6.1 Reaction of $[(OC)_5M{=}BN(SiMe_3)_2]$ (**14**: M = Cr, **16**: M = Mo) with KC_8

KC_8 (27 mg, 0.2 mmol) was added into a solution of $[(OC)_5Cr{=}BN(SiMe_3)_2]$ (**14**) (36 mg, 0.1 mmol) in 1.5 mL THF-D_8 at ambient temperature. Whereupon the black suspension was stirred for 5 min at ambient temperature and filtered through a filter pipette in a glovebox. ^{1}H NMR: δ = -0.03 (s, 9H), 0.06 (s, 9H); ^{11}B NMR: δ = 48 (bs).

18-Crown-6 (52 mg, 0.2 mmol) was then added to the brown filtrate that was concentrated to ca. 1 mL. The mixture was aubsequently layered with ca. 0.5 mL haxane and stored at –30°C for 2 d. $[Cr_2(CO)_{10}]K_2{\cdot}(18\text{-crown-}6)_2{\cdot}(THF)_2$ was obained as colorless crystals.

The same procedure was applied for the reaction of $[(OC)_5Mo{=}BN(SiMe_3)_2]$ (**16**) (40 mg, 0.1 mmol) with KC_8 (27 mg, 0.2 mmol) and 18-Crown-6 (52 mg, 0.2 mmol).

5.6.2 Reaction of $[(OC)_4(Cy_3P)Cr{=}BN(SiMe_3)_2]$ (**132**) with KC_8

KC_8 (27 mg, 0.2 mmol) was added into 1.5 mL THF solution of $[(OC)_4(Cy_3P)Cr{=}BN(SiMe_3)_2]$ (**132**) (62 mg, 0.1 mmol) in Young NMR tube at ambient temperature. Multinuclear NMR spectra revealed merely gradual weakening of peaks for **132**.

5.7 Synthesis of novel iron-arylborylene complexes

5.7.1 Synthesis of X_2BDur (**134**: X = Cl, **137**: X = Br)

The colorless DurLi (9.47 g, 67.57 mmol) was suspended in hexane (200 mL) at –70°C. BBr_3 (16.93 g, 6.4 mL, 67.57 mmol) was added dropwise by a syringe. The reaction mixture was allowed to warm to ambient temperature very slowly. After overnight stirring, the colorless suspension was filtered. The colorless residue was extracted with warm hexane (3 x 50 mL). All volatile materials were removed under high vacuum then. **137** was obtained as colorless crystalline solide (12.10 g, 59%).

^{1}H NMR: δ = 1.90 (s, 6H, Me of Dur), 2.07 (s, 6H, Me of Dur), 6.75 (s, 1H, *p*-H of Dur); ^{11}B{^{1}H} NMR: δ = 62.68 (s).

The same synthetic procedure was applied for preparation of Cl_2BDur (**134**). Starting materials: DurLi (4.3 g, 30.7 mmol), hexane solution of BCl_3 (15.4 mL, c = 2 mmol·mL^{-1}, 30.7 mmol). Yield: 4.42 g, 67%.

^{1}H NMR: δ = 1.91 (s, 6H, Me of Dur), 2.02 (s, 6H, Me of Dur), 6.77 (s, 1H, *p*-H of Dur); ^{11}B{^{1}H} NMR: δ = 61.52 (s).

5.7.2 Reaction of K[$(OC)_3(Me_3P)FeSiMe_3$] (**133**) mit Cl_2BDur (**134**)

A toluene solution (30 mL) of Cl_2BDur (**134**) (42 mg, 0.20 mmol) was added to a grey-colored suspension of K[$(CO)_3(PMe_3)Fe(SiMe_3)$] (**133**) (66 mg, 0.20 mmol) in hexane (3 mL) at RT. The reaction mixture was stirred for 2 h at ambient temperature and was subsequently filtered. All volatile components were removed in vacuo. The pale brown residue was extracted with ca. 1.5 mL hexane and stored at –30°C overnight, yielding **135** as colorless crystals (46 mg, 49% yield).

^{1}H NMR: δ = 6.87 (s, 1H, *p-H* of Dur), 2.30 (bs, 6H, Me of Dur), 2.10 (s, 6H, Me of Dur), 0.81 (m, 9H, PMe_3), 0.65 (s, 9H, $SiMe_3$); ^{11}B{^{1}H} NMR: δ = 114.2 (bs); ^{31}P{^{1}H} NMR: δ = 2.45 (s); elemental analysis (%) calcd. for $BC_{19}ClFeH_{31}O_3PSi$: C 48.70, H 6.67; found: C 48.64, H 6.75.

5.7.3 Reaction of K[$(OC)_3(Me_3P)FeSiMe_3$] (**133**) with Br_2BDur (**137**)

In a centrifuge schlenk, a hexane solution (30 mL) of Br_2BDur (**137**) (936 mg, 3.08 mmol) was added to a grey-colored suspension of $K[(OC)_3(Me_3P)FeSiMe_3]$ (**133**) (1 g, 3.05 mmol) in hexane (30 mL) at ambient temperature. The reaction mixture was stirred for 1 h at ambient temperature and was subsequently centrifuged. The obtained yellow hexane solution containing **138** was concentrated to ca. 20 mL and stored at –30°C overnight, yielding **138** as yellow crystals (666 mg, 61% yield).

^{1}H NMR: δ = 6.78 (s, 1H, *p*-H of Dur), 2.71 (s, 6H, Me of Dur), 1.87 (s, 6H, Me of Dur), 1.10 (d, $^2J_{H-P}$ = 9.24 Hz, 9H, PMe_3); $^{13}C\{^1H\}$ NMR: signal for boron-bound carbon was not detected, δ = 216.26 (d, $^2J_{C-P}$ = 23.33 Hz, *C*O), 18.71 (s, *C*H_3 of Dur), 18.97 (s, *C*H_3 of Dur), 20.32 (d, $^1J_{P-C}$ = 28.60 Hz, P(*C*H_3)$_3$), 137.19 (s, *p*-*C*H of Dur), 134.11 (s, *C*CH_3 of Dur), 140.49 (s, *C*CH_3 of Dur); $^{11}B\{^1H\}$ NMR: δ = 145.67 (bs); $^{31}P\{^1H\}$ NMR: δ = 17.63 (s); elemental analysis (%) calcd. for $C_{16}H_{22}BFeO_3P$: C 53.39, H 6.16; found: C 53.43, H 6.03.

5.8 Reactivity investigation of iron-arylborylene complexes

5.8.1 Reaction of $[(OC)_3(Me_3P)Fe{=}BDur]$ (**138**) with $[Pt(PCy_3)_2]$ (**52**)

Compound $[Pt(PCy_3)_2]$ (**52**) (42 mg, 0.056 mmol) was added to a solution of $[(OC)_3(Me_3P)Fe{=}BDur]$ (**138**) (20 mg, 0.056 mmol) in 0.4 mL toluene. The color of the solution immediately changed from yellow to deep red. The solution was concentrated to ca. 0.1 mL, layered with 0.3 mL hexane, stored at –35°C, yielding **145** as deep red crystals (35 mg, 75% yield).

^{1}H NMR: δ = 6.86 (s, 1H, *p*-H of Dur), 2.84 (s, 6H, Me of Dur), 2.11 (s, 6H, Me of Dur), 1.37 (d, $^2J_{H\text{-}P}$ = 9.56 Hz, 9H, PMe_3), 1.01-1.87 (m, 33H, Cy); $^{13}C\{^1H\}$ NMR: signal for boron-bound carbon was not detected, δ = 220.20 (m, *C*O), 19.71 (s, *C*H_3 of Dur), 19.48 (s, *C*H_3 of Dur), 19.64 (d, $^1J_{P\text{-}C}$ = 30.61 Hz, P(*C*H_3)$_3$), 133.56 (s, *p*-*C*H of Dur), 132.98 (s, *C*CH_3 of Dur), 140.49 (s, *C*CH_3 of Dur), 27.51 (d, $^2J_{C\text{-}P}$ = 11.45 Hz, $C_{2,6}$ of Cy), 30.72 (d, $^3J_{C\text{-}P}$ = 1.17 Hz, $C_{3,5}$ of Cy), 26.28 (d, $^4J_{C\text{-}P}$ = 1.08 Hz, C_4 of Cy), 35.03 (d, $^1J_{C\text{-}P}$ = 25.34 Hz, C_1 of Cy); $^{11}B\{^1H\}$ NMR: δ = 125.2 (bs); $^{31}P\{^1H\}$ NMR: δ = 66.84 (d, $^3J_{P\text{-}P}$ = 14.56 Hz, $^1J_{Pt\text{-}P}$ = 4964.38 Hz, Pt-*P*), 36.10 (d, $^3J_{P\text{-}P}$ = 14.56 Hz, Fe-*P*); elemental analysis (%) calcd. For $BC_{34}FeH_{55}O_3P_2Pt \cdot (C_6H_5CH_3)_{0.5}$: C 51.09, H 6.75; found: C 51.31, H 7.23.

5.8.2 Reaction of $[(OC)_3(Me_3P)Fe{=}BDur]$ (**138**) with benzophenone (**146**)

Benzophenoe (**146**) was added to a solution of **138** (30 mg, 0.083 mmol) in 0.4 mL toluene. The color of the solution immediately changed from yellow to pale yellow. The solution was concentrated to ca. 0.1 mL, layered with 0.3 mL hexane, stored at –35°C, yielding **147** as colorless crystals (52 mg, 85% yield).

^{1}H NMR: δ = 0.57 (d, $^2J_{H\text{-}P}$ = 8.94 Hz, 9H, PMe_3), 6.86 (s, 1H, *p*-*H* of Dur), 2.39 (s, 6H, Me of Dur), 2.07 (s, 6H, Me of Dur), 8.13 (d, 4H, $^3J_{H\text{-}H}$ = 7.55 Hz, *o*-*H* of Ph), 7.31 (t, 4H, $^3J_{H\text{-}H}$ = 7.59 Hz, *m*-*H* of Ph), 6.99 (t, 2H, $^3J_{H\text{-}H}$ = 7.50 Hz, *p*-*H* of Ph); $^{13}C\{^1H\}$ NMR: signal for boron-bound carbon was not detected, δ = 212.02 (d, $^2J_{C\text{-}P}$ = 23.20 Hz, *C*O), 20.32 (s, *C*H_3 of Dur), 19.64 (s, *C*H_3 of Dur), 18.41 (d, $^1J_{P\text{-}C}$ = 28.51Hz, P(*C*H_3)$_3$), 131.90 (s, *p*-*C*H of Dur), 133.71 (s, *C*CH_3 of Dur), 133.86 (s, *C*CH_3 of Dur), 124.91 (s, *p*-*C*H of Ph), 125.00 (s, *o*-*C*H of Ph), 128.42 (s, *m*-*C*H of Ph), 129.27 (s, *C* of Ph), 155.13 (s, Fe-*C*-O-B); $^{11}B\{^1H\}$ NMR: δ = 72.8 (bs); $^{31}P\{^1H\}$ NMR: δ = 12.42 (s); elemental analysis (%) calcd. For $BC_{29}FeH_{32}O_4P$: C 64.24, H 5.95; found C 64.28, H 5.98.

5.8.3 Reaction of $[(OC)_3(Me_3P)Fe{=}BDur]$ (**138**) with alkynes and metal alkynyl σ-complexes

In Young NMR tube, a 1.5 mL hexane or C_6D_6 solution of $[(OC)_3(Me_3P)Fe{=}BDur]$ (**138**) (10 mg, 0.03 mmol) with euqimolar amount of 3-hexine (**148**) (2.3 mg, 0.03 mmol) or 2-butine (**149)** (0.3 mL hexane solution, c = 0.1 $mmol{\cdot}mL^{-1}$, 0.03 mmol) or bistrimethylsilylacetylene (**150**) (5 mg, 0.03 mmol) or diphenylacetylene (**151**) (5 mg, 0.03 mmol) or $[Cp^*Fe(CO)_2C{\equiv}CPh]$ (**64**) (10 mg, 0.03 mmol) or $[Cl(Me_3P)_2PtC{\equiv}CPh]$ (**84**) (15 mg, 0.03 mmol) was irradiated at ambient temperature or heated at 80°C (except for **64**). Both ^1H and ^{11}B NMR spectra revealed merely gradual weakening of signals for **138**.

5.8.4 Reaction of $[(OC)_3(Me_3P)Fe{=}BDur]$ (**138**) with naphtalene

In a Young NMR tube, a 1.5 mL C_6D_6 solution of $[(OC)_3(Me_3P)Fe{=}BDur]$ (**138**) (18 mg, 0.05 mmol) with naphtalene (6 mg, 0.05 mmol) was irradiated at ambient temperature for 16 h. All volatile components were removed *in vacuo*. The brown residue was extracted with 0.5 mL hexane and stored at –30°C overnight, leading to yellow precipitate, which was subsequently extracted with 0.5 mL hexane. Slow evaporation of the obtained pale yellow solution at ambient temperature afforded **152** as fibrous crystalline solids.

^1H NMR: δ = 7.04 (s, 1H, *p-H* of Dur), 2.30 (s, 6H, *m*-Me of Dur), 2.64 (s, 6H, *o*-Me of Dur), 3.06 (bs, 1H, B*H*), 5.87 (d, 1H, $^3J_{H\text{-}H}$ = 9.6 Hz, C^2-*H*), 5.18 (bs, 1H, C^3-*H*), 3.89 (bs, 1H, C^4-*H*), 0.77 ($^2J_{H\text{-}P}$ = 7.4 Hz, 9H, PMe_3), 6.62-6.70 (m, 4H, $C^{6,7,8,9}$-*H*); $^{11}B\{^1H\}$ NMR: δ = 29.8 (bs); $^{13}C\{^1H\}$ NMR: δ = 18.0 (bs, *C*H_3 of PMe_3), 20.93 (s, *m*-Me of Dur), 22.01 (bs, *o*-Me of Dur), 131.49 (s, *C*H of Dur), 133.31 (s, *C*Me of Dur), 138.86 (s, *C*Me of Dur), 143.1 (bs, B*C* of Dur, detected by HMBC NMR), 100.8 (bs, C^2-H, detected by HMQC NMR), 111.0 (bs, C^3-H, detected by HMQC NMR), 79.3 (bs, C^4-H, detected by HMQC NMR), 126.25, 126.09, 125.70, 122.51 (s, $C^{6,7,8,9}$-H), 154.0 (bs, C^5 or C^{10}, detected by HMBC NMR), 227.6 (bs, *C*O);$^{31}P\{^1H\}$ NMR: δ = 23.2 (bs); IR (solid): 1990(s, C≡O), 1942 cm^{-1} (s, C≡O); EI MS: m/z: 460 [M^+].

5.9 Catenation of borylene-units in the coordinationsphere of iron

5.9.1 Synthesis of [(OC)$_3$Fe(BDur){BN(SiMe$_3$)$_2$}] (**169**)

A pale yellow hexane solution (8 mL) of **138** (120 mg, 0.33 mmol) and [(OC)$_5$Mo=BN(SiMe$_3$)$_2$] (**16**) (114 mg, 0.280 mmol) was stirred for 8 h at 40°C. The obtained deep red reaction solution was concentrated to ca. 3 mL and stored at –72°C overnight. The obtained deep red precipitate was extracted with 3 mL hexane and stored at –30°C overnight, yielding spectroscopically pure **169** as well as crystals suitable for X-ray analysis (64 mg, 50%). As slow decomposition of **169** in aromatic solvents was observed, NMR measurements were performed at –30°C.

^{1}H NMR: δ = 7.00 (s, 1H, *p*-H of Dur), 2.54 (s, 6H, Me of Dur), 2.08 (s, 6H, Me of Dur), 0.13 (s, 18H, SiMe$_3$); ^{13}C{^{1}H} NMR: signal for boron-bound carbon was not detected, δ = 215.69 (s, *C*O), 19.44 (s, *C*H$_3$ of Dur), 19.46 (s, *C*H$_3$ of Dur), 2.30 (s, *C*H$_3$ of SiMe$_3$), 136.11 (s, *p*-*C*H of Dur), 139.09 (s, *C*CH$_3$ of Dur), 133.95 (s, *C*CH$_3$ of Dur); ^{11}B{^{1}H} NMR: δ = 129 (bs, *B*C), 78 (bs, *B*N). IR (solid): 2000 (w, C≡O), 1923 cm^{-1} (s, C≡O); Elemental analysis calcd. [%] for $C_{19}H_{31}B_2FeNO_3Si_2$: C 50.14, H 6.86, N 3.08; found: C 50.14, H 6.92, N 2.92.

5.9.2 Photolysis of [(OC)$_3$Fe(BDur){BN(SiMe$_3$)$_2$}] (**169**)

A deep red hexane solution (5 mL) of [(OC)$_3$Fe(BDur){BN(SiMe$_3$)$_2$}] (**169**) (40 mg, 0.088 mmol) was irradiated with stirring for 2 d, yielding a suspension which was subsequently centrifuged in a centrifuge Schlenk flask. **170** was obtained as spectroscopically pure black solid (23 mg, 60%). Crystals suitable for X-ray analysis were obtained upon irradiation of a hexane solution of **169** in an NMR tube.

^{1}H NMR: δ = 7.02 (s, 2H, *p*-H of Dur), 2.23 (s, 12H, Me of Dur), 1.94 (s, 12H, Me of Dur), 0.01 (s, 36H, SiMe$_3$); ^{13}C{^{1}H} NMR: signal for boron-bound carbon was not detected, δ = 214.95 (s, *C*O), 18.38 (s, *C*H$_3$ of Dur), 17.76 (s, *C*H$_3$ of Dur), 0.00 (s, *C*H$_3$ of SiMe$_3$), 129.35 (s, *p*-*C*H of Dur), 129.16 (s, *C*CH$_3$ of Dur), 131.73 (s, *C*CH$_3$ of Dur); ^{11}B{^{1}H} NMR: δ = 140 (bs, *B*C), 86 (bs, *B*N). IR (solid): 1959 (w, C≡O), 1921 cm^{-1} (m, C≡O); Elemental analysis calcd. [%] for $C_{36}H_{62}B_4Fe_2N_2O_4Si_4$: C 50.62, H 7.32, N 3.28; found: C 51.10, H 7.39, N 3.32.

5.9.3 Synthesis of [(OC)$_2$Fe({BN(SiMe$_3$)$_2$}$_2${BDur}$_2$)] (**171**)

A suspension of **170** (20 mg, 0.023 mmol) in hexane (4 mL) was stirred at 80°C under CO atmosphere (ca. 1.2 atm) for 2 h, yielding a orange solution, which was then concentrated to ca. 1 mL and stored at –30°C overnight, yielding **171** as orange crystals (7 mg, 80%). ^{1}H NMR: δ = 6.74 (s, 2H, *p*-H of Dur), 2.08 (s, 12H, Me of Dur), 2.02 (s, 12H, Me of Dur), 0.23 (s, 36H, $SiMe_3$); $^{13}C\{^{1}H\}$ NMR: signal for boron-bound carbon was not detected, δ = 214.91 (s, *C*O), 21.96 (s, *C*H_3 of Dur), 20.00 (s, *C*H_3 of Dur), 2.73 (s, *C*H_3 of $SiMe_3$), 130.65 (s, *p*-*C*H of Dur), 133.38 (s, *C*CH_3 of Dur), 131.98 (s, *C*CH_3 of Dur); $^{11}B\{^{1}H\}$ NMR: δ = 83 (s), 76 (s). IR (solid): 1981 (m, C≡O), 1934 cm^{-1} (m, C≡O); Elemental analysis calcd. [%] for $C_{34}H_{62}B_4FeN_2O_2Si_4$: C 55.01, H 8.42, N 3.77; found: C 55.22, H 8.27, N 3.86.

5.10 Reactivity of iron-bis(borylene) complexes

5.10.1 Reaction of $[(OC)_3Fe(BDur)\{BN(SiMe_3)_2\}]$ (**169**) with $[Pt(PCy_3)_2]$ (**52**)

Compound $[Pt(PCy_3)_2]$ (**52**) (38 mg, 0.05 mmol) was added to a solution of $[(OC)_3Fe(BDur)\{BN(SiMe_3)_2\}]$ (**169**) (23 mg, 0.05 mmol) in 1 mL hexane. The color of the solution immediately changed from red to deep brown. The solution was concentrated to ca. 0.5 mL, stored at –35°C overnight, yielding **174** as brown crystals (33 mg, 71% yield).
^{1}H NMR: δ = 6.83 (s, 1H, *p*-H of Dur), 2.64 (s, 6H, Me of Dur), 2.06 (s, 6H, Me of Dur), 0.47 (s, 18H, $SiMe_3$), 1.01-1.87 (m, 33H, Cy); $^{13}C\{^1H\}$ NMR: signal for boron-bound carbon was not detected, δ = 218.93 (s, *C*O), 218.90 (s, *C*O), 19.80 (s, *C*H_3 of Dur), 19.55 (s, *C*H_3 of Dur), 2.23 (s, $SiMe_3$), 132.99 (s, *p*-*C*H of Dur), 134.38 (s, *C*CH_3 of Dur), 133.62 (s, *C*CH_3 of Dur), 30.61 (s, *C*H_2 of Cy), 27.57 (d, $^2J_{C\text{-}P}$ = 11.2 Hz, *C*H_2 of Cy), 26.21 (bs, *C*H_2 of Cy), 35.22 (d, $^1J_{C\text{-}P}$ = 22.8 Hz, *C*H of Cy); $^{11}B\{^1H\}$ NMR: δ = 121.8(bs), 97.6 (bs); $^{31}P\{^1H\}$ NMR: δ = 74.39 (d, $^1J_{Pt\text{-}P}$ = 4021.6 Hz); elemental analysis (%) calcd. For $B_2C_{37}FeH_{64}NO_3PPtSi_2$: C 47.75, H 6.93, N 1.51; found: C 47.81, H 7.14, N 1.47.

5.10.2 Reaction of $[(OC)_3Fe(BDur)\{BN(SiMe_3)_2\}]$ (**169**) with BCl_3

BCl_3 (0.33 mL hexane solution, c = 0.2 mmol·mL^{-1}, 0.07 mmol) was added into a red suspension of $[(OC)_3Fe(BDur)\{BN(SiMe_3)_2\}]$ (**169**) (30 mg, 0.07 mmol) in 2 mL hexane at –70°C. After 1 h stirring at low temperature, a pale yellow solution was yielded. All volatile components were removed *in vacuo* at –30°C. The yellow residue was extracted with 0.5 mL hexane at ambient temperature in a glovebox, whereupon the hexane solution turned from pale yellow to deep green gradually. After storing the green solution at –35°C for 1 week, deep green single crystals of **177** suitable for X-ray diffraction analysis were obtained.
^{11}B NMR spectrum for the green solution: δ = 149(bs), 113(bs), 108(bs), 72(bs), 42(s), 41(s).

5.10.3 Reaction of $[(OC)_3Fe(BDur)\{BN(SiMe_3)_2\}]$ (**169**) with 2-butyne (**149**)

In a Young NMR tube, a deep red hexane solution (1.5 mL) of $[(OC)_3Fe(BDur)\{BN(SiMe_3)_2\}]$ (**169**) (40 mg, 0.09mmol) and 2-butyne (**149**) (0.22 mL hexane solution, c = 0.8 mmol·mL^{-1}, 0.18 mmol) was irradiated for 24 h, yielding a brown

suspension which was subsequently filtered and concentrated to ca. 0.5 mL and stored at –35°C for one week. **178** was obtained as yellow crystals (12 mg, 12%).

^{1}H NMR: δ = 7.04 (s, 1H, *p*-H of Dur), 2.71 (s, 3H, Me of Dur), 2.78 (s, 3H, Me of Dur), 2.23 (s, 3H, Me of Dur), 2.10 (s, 3H, Me of Dur), 0.55 (s, 9H, $SiMe_3$), 0.19 (s, 9H, $SiMe_3$), 1.63 (s, 3H, BCC*H*3), 1.45 (s, 3H, BCC*H*3); ^{13}C{^{1}H} NMR: *C-i* of Dur bound to boron was not detected, δ = 212.02 (s, *C*O), 23.14 (s, *C*H_3 of Dur), 20.87 (s, *C*H_3 of Dur), 20.36 (s, *C*H_3 of Dur), 20.04 (s, *C*H_3 of Dur), 5.34 (s, $SiMe_3$), 4.56 (s, $SiMe_3$), 131.22 (s, *p-C*H of Dur), 136.45 (s, *C*CH_3 of Dur), 134.90 (s, *C*CH_3 of Dur), 133.97 (s, *C*CH_3 of Dur), 133.35 (s, *C*CH_3 of Dur), 18.60 (s, BC*C*H_3), 17.44 (s, BC*C*H_3), 118.49 (bs, B*C*CH_3), 115.84 (bs, B*C*CH_3); ^{11}B{^{1}H} NMR: δ = 27.4 (bs), 25.2 (bs); elemental analysis (%) calcd. For $C_{27}H_{43}B_2FeNO_3Si_2$: C 57.57, H 7.69, N 2.49; found: C 58.30, H 8.19, N 2.49.

5.10.4 Reaction of [(OC)$_3$Fe(BDur){BN(SiMe$_3$)$_2$}] (**169**) with diphenylacetylene (**151**)

In a Young NMR tube, a deep red hexane solution (1.5 mL) of [(OC)$_3$Fe(BDur){BN(SiMe$_3$)$_2$}] (**169**) (40 mg, 0.09mmol) and diphenylacetylene (**151**) (32 mg, 0.18 mmol) was irradiated for 3 d, yielding a brown suspension which was subsequently filtered and concentrated to ca. 0.5 mL and stored at –35°C for one week. **179** was obtained as orange crystals (24 mg, 34%).

^{1}H NMR: δ = 6.72 (s, 1H, *p*-H of Dur), 2.42 (s, 3H, Me of Dur), 2.29 (s, 3H, Me of Dur), 1.98 (s, 3H, Me of Dur), 1.97 (s, 3H, Me of Dur), 0.30 (s, 9H, $SiMe_3$), 0.03 (s, 9H, $SiMe_3$), 7.27 (m, 4H, Ph), 6.86-6.95 (m, 10H, Ph), 6.61-6.66 (m, 6H, Ph); ^{13}C{^{1}H} NMR: δ = 211.70 (s, *C*O), 22.37 (s, *C*H_3 of Dur), 21.50 (s, *C*H_3 of Dur), 20.74 (s, *C*H_3 of Dur), 20.08 (s, *C*H_3 of Dur), 6.04 (s, $SiMe_3$), 4.84 (s, $SiMe_3$), 131.04 (s, *p-C*H of Dur), 131.59 (s, *C*CH_3 of Dur), 132.69 (s, *C*CH_3 of Dur), 134.81 (s, *C*CH_3 of Dur), 135.78 (s, *C*CH_3 of Dur), 143.1 (bs, *C-i* of Dur), 141.13 (s, *C-i* of Ph), 140.22 (s, *C-i* of Ph), 132,64, 131.59, 127.43, 126.57, 126.46, 126.19 (s, *C*H of Ph), 113.9 (bs, B*C*Ph); ^{11}B{^{1}H} NMR: δ = 34.8 (bs), 25.7 (bs); elemental analysis (%) calcd. For $C_{47}H_{51}B_2FeNO_3Si_2$: C 69.56, H 6.33, N 1.73; found: C 69.72, H 6.36, N 1.58.

5.10.5 Reaction of [(OC)$_3$Fe(BDur){BN(SiMe$_3$)$_2$}] (**169**) with bis(trimethylsilyl)acetylene (**150**)

In a Young NMR tube, a deep red hexane solution (1.5 mL) of [(OC)$_3$Fe(BDur){BN(SiMe$_3$)$_2$}] (**169**) (36 mg, 0.08 mmol) and bis(trimethylsilyl)acetylene (**150**) (14 mg, 0.08 mmol) was irradiated for 2 d, yielding a brown suspension which was subsequently filtered and concentrated to ca. 0.5 mL and stored at –35°C for one week. **180** was obtained as orange crystals (10 mg, 20%).

^{1}H NMR: δ = 6.88 (s, 1H, *p*-H of Dur), 2.98 (s, 3H, Me of Dur), 2.07 (s, 3H, Me of Dur), 2.00 (s, 3H, Me of Dur), 1.74 (s, 3H, Me of Dur), 0.31 (s, 9H, N(SiMe$_3$)$_2$), 0.13 (s, 9H, N(SiMe$_3$)$_2$), 0.49 (s, 9H, CSiMe$_3$), 0.27 (s, 9H, CSiMe$_3$); ^{13}C{^{1}H} NMR: δ = 219.74 (bs, *C*O), 217.69 (bs, *C*O), 214.40 (bs, *C*O), 22.78 (s, *C*H$_3$ of Dur), 22.25 (s, *C*H$_3$ of Dur), 20.13 (s, *C*H$_3$ of Dur), 19.83 (s, *C*H$_3$ of Dur), 4.41 (s, N(SiMe$_3$)$_2$), 3.57 (s, N(SiMe$_3$)$_2$), 131.41 (s, *p*-*C*H of Dur), 134.02 (s, *C*CH$_3$ of Dur), 134.68 (s, *C*CH$_3$ of Dur), 135.24 (s, *C*CH$_3$ of Dur), 139.10 (s, *C*CH$_3$ of Dur), 3.29 (s, SiMe$_3$), 2.01 (s, SiMe$_3$), 56.4, 72.5 (detected by HMBC NMR, *C*SiMe$_3$); ^{11}B{^{1}H} NMR: δ = 92.3 (bs), 58.1 (bs); elemental analysis (%) calcd. For $C_{27}H_{49}B_2FeNO_3Si_4$: C 51.85, H 7.90, N 2.24; found: C 51.98, H 7.94, N 2.22.

5.11 Computational details

The Gaussian03 program[235] was used for geometry optimizations and frequency calculations at the OLYP/TZVP[236,237] level, CAM-B3LYP/6-311+G*[238-245] was used for the $(OC)_3Fe\{(Me_3Si)_2NB{=}BDur\}^{-1}$ system using Gaussian09[246]. Spin-restricted calculations were performed by constraining the projection of the total electronic spin along a reference axis to zero. Frequency calculations were conducted to determine if each stationary point corresponds to a minimum. The Jmol[247] programs were used for vizualisation purposes.

6 Crystal structure analysis

6.1 General

The crystal data were collected on a Bruker X8APEX diffractometer with a CCD area detector and multi-layer mirror monochromated $Mo_{K\alpha}$ radiation. The structure was solved using direct methods, refined with the Shelx software package (G. Sheldrick, *Acta Cryst.*, **2008**, *A64*, 112–122) and expanded using Fourier techniques. All non-hydrogen atoms were refined anisotropically. Hydrogen atoms were included in structure factors calculations. All hydrogen atoms were assigned to idealised geometric positions. Crystallographic data have been deposited with the Cambridge Crystallographic Data Center. These data can be obtained free of charge from The Cambridge Crystallographic Data Centre *via* www.ccdc.cam.ac.uk/data_request/cif.

6.2 Crystal data and parameters of the structure determinations

	66	**75**	**76**
Empirical formula	$C_{26}H_{38}BFeNO_2Si_2$	$C_{25}H_{38}BFeNOSi_2$	$C_{26}H_{38}BFeNO_2Si_2$
Formula weight ($g \cdot mol^{-1}$)	519.41	491.40	519.41
Temperature (K)	233(2)	100(2)	100(2)
Radiation, λ (Å)	$Mo_{K\alpha}$ 0.71073	$Mo_{K\alpha}$ 0.71073	$Mo_{K\alpha}$ 0.71073
Crystal system	Monoclinic	Triclinic	Orthorhombic
Space group	P2(1)/c	*P*-1	*Pbca*
a (Å)	15.9329(4)	7.2055(8)	8.0512(7)
b (Å)	8.3475(3)	19.729(2)	18.0246(14)
c (Å)	22.8808(7)	19.868(2)	38.492(3)
α (°)	90.00	71.520(5)	90.00
β (°)	110.2980(10)	83.681(5)	90.00
γ (°)	90.00	85.313(5)	90.00
Volume ($Å^3$)	2854.17(15)	2659.2(5)	5586.0(8)
Z	4	4	8
Calculated density ($Mg \cdot m^{-3}$)	1.209	1.227	1.235
Absorbtion coefficient (mm^{-1})	0.634	0.674	0.648
F(000)	1104	1048	2208
Theta range for collection	1.36 to 28.33°	1.76 to 26.79°	2.12 to 27.64°
Reflections collected	238158	118503	147965
Independent reflections	7105	11191	6425
Minimum/maximum transmission	0.8475/0.8890	0.8443/0.9235	0.9205/0.9683
Refinement method	Full-matrix least-squares on F^2	Full-matrix least-squares on F^2	Full-matrix least-squares on F^2
Data / parameters / restrains	7105 / 309 / 0	11191 / 581 / 0	6425 / 309 / 0
Goodness-of-fit on F^2	1.163	1.043	1.237
Final R indices [I>2σ(I)]	$R_1 = 0.0286$, $wR^2 = 0.0859$	$R_1 = 0.0300$, $wR^2 = 0.0791$	$R_1 = 0.0359$, $wR^2 = 0.0802$
R indices (all data)	$R_1 = 0.0377$, $wR^2 = 0.0998$	$R_1 = 0.0346$, $wR^2 = 0.0826$	$R_1 = 0.0478$, $wR^2 = 0.0857$
Maximum/minimum residual electron density ($e \cdot Å^{-3}$)	0.462 / –0.567	0.642 / –0.381	0.379 / –0.419

	77	**86**	**89**
Empirical formula	$C_{28}H_{47}BFeNOPSi_2$	$C_{20}H_{41}BClNP_2PtSi_2$	$C_{46}H_{100}B_2Cl_2N_2P_4Pt_2Si_4$
Formula weight ($g \cdot mol^{-1}$)	567.48	655.01	1400.22
Temperature (K)	100(2)	100(2)	100(2)
Radiation, λ (Å)	$Mo_{K\alpha}$ 0.71073	$Mo_{K\alpha}$ 0.71073	$Mo_{K\alpha}$ 0.71073
Crystal system	Triclinic	Monoclinic	Monoclinic
Space group	P-1	$P2_1/c$	$P2_1/c$
a (Å)	8.9941(5)	13.670(4)	20.2828(19)
b (Å)	11.8876(6)	19.510(6)	15.9618(17)
c (Å)	15.4367(8)	21.795(6)	22.002(2)
α (°)	92.142(2)	90.00	90.00
β (°)	98.880(2)	92.514(12)	116.677(4)
γ (°)	109.052(2)	90.00	90.00
Volume ($Å^3$)	1534.54(14)	5807(3)	6364.9(11)
Z	2	8	4
Calculated density ($Mg \cdot m^{-3}$)	1.228	1.498	1.461
Absorbtion coefficient (mm^{-1})	0.643	5.125	4.681
F(000)	608	2608	2824
Theta range for collection	1.34 to 26.38°	1.40 to 28.33°	1.64 to 26.47°
Reflections collected	31401	359242	70945
Independent reflections	6248	14305	12966
Minimum/maximum transmission	0.6991/0.9385	0.4125/0.6556	0.6469/0.7454
Refinement method	Full-matrix least-squares on F^2	Full-matrix least-squares on F^2	Full-matrix least-squares on F^2
Data / parameters / restrains	6248 / 330 / 0	14305 / 529 / 0	12966 / 592 / 669
Goodness-of-fit on F^2	1.050	1.322	1.016
Final R indices [I>2σ(I)]	$R_1 = 0.0306$, $wR^2 = 0.0804$	$R_1 = 0.0340$, $wR^2 = 0.0905$	$R_1 = 0.0450$, $wR^2 = 0.0955$
R indices (all data)	$R_1 = 0.0343$, $wR^2 = 0.0833$	$R_1 = 0.0360$, $wR^2 = 0.0912$	$R_1 = 0.0809$, $wR^2 = 0.1092$
Maximum/minimum residual electron density ($e \cdot Å^{-3}$)	0.989 / –0.409	2.345 / –2.146	1.853 / –1.560

	95	**96**	**98**
Empirical formula	$C_{23}H_{48}BClNP_2PtSi_2$	$C_{20}H_{42}BCl_2NP_2PtSi_2$	$C_{20}H_{41}BBrNP_2PtSi_2$
Formula weight ($g \cdot mol^{-1}$)	698.09	691.47	699.47
Temperature (K)	100(2)	100(2)	100(2)
Radiation, λ (Å)	$Mo_{K\alpha}$ 0.71073	$Mo_{K\alpha}$ 0.71073	$Mo_{K\alpha}$ 0.71073
Crystal system	Monoclinic	Monoclinic	Monoclinic
Space group	$P2_1/c$	P2(1)/c	$P2_1/n$
a (Å)	9.4809(6)	16.3309(9)	8.9084(5)
b (Å)	9.6771(6)	9.2064(5)	21.5491(11)
c (Å)	33.348(2)	39.750(2)	15.4872(8)
α (°)	90.00	90.00	90.00
β (°)	91.352(3)	91.016(3)	106.388(2)
γ (°)	90.00	90.00	90.00
Volume ($Å^3$)	3058.7(3)	5975.4(6)	2852.3(3)
Z	4	8	4
Calculated density ($Mg \cdot m^{-3}$)	1.516	1.537	1.629
Absorbtion coefficient (mm^{-1})	4.870	5.071	6.524
F(000)	1404	2752	1376
Theta range for collection	2.15 to 26.39°	1.60 to 27.16°	1.66 to 28.36°
Reflections collected	74731	33669	41868
Independent reflections	6243	12819	7106
Minimum/maximum transmission	0.5577/0.7454	0.3884/0.9054	0.2450/0.4034
Refinement method	Full-matrix least-squares on F^2	Full-matrix least-squares on F^2	Full-matrix least-squares on F^2
Data / parameters / restrains	6243 / 303 / 219	12819 / 547 / 0	7106 / 265 / 0
Goodness-of-fit on F^2	1.224	1.153	1.044
Final R indices [I>2σ(I)]	$R_1 = 0.0469$, $wR^2 = 0.1115$	$R_1 = 0.0516$, $wR^2 = 0.1062$	$R_1 = 0.0210$, $wR^2 = 0.0461$
R indices (all data)	$R_1 = 0.0490$, $wR^2 = 0.1127$	$R_1 = 0.0719$, $wR^2 = 0.1130$	$R_1 = 0.0262$, $wR^2 = 0.0481$
Maximum/minimum residual electron density ($e \cdot Å^{-3}$)	2.922 / –3.457	2.657 / –4.510	2.080 / –1.062

	107	**108**	**111**
Empirical formula	$C_{25}H_{40}PRh$	$C_{31}H_{58}BNPRhSi_2$	$C_{26}H_{42}PRh$
Formula weight ($g \cdot mol^{-1}$)	474.45	645.65	488.48
Temperature (K)	103(2)	100(2)	103(2)
Radiation, λ (Å)	$Mo_{K\alpha}$ 0.71073	$Mo_{K\alpha}$ 0.71073	$Mo_{K\alpha}$ 0.71073
Crystal system	Triclinic	Monoclinic	Triclinic
Space group	*P*-1	$P2_1/c$	*P*-1
a (Å)	10.1676(9)	9.9520(8)	10.1944(7)
b (Å)	10.5044(10)	19.6336(14)	10.4550(7)
c (Å)	11.6368(12)	17.3567(14)	11.9785(7)
α (°)	75.475(4)	90.00	72.796(3)
β (°)	79.579(4)	94.548(3)	80.745(3)
γ (°)	84.859(4)	90.00	84.715(3)
Volume ($Å^3$)	1182.0(2)	3380.7(5)	1202.36(14)
Z	2	4	2
Calculated density ($Mg \cdot m^{-3}$)	1.333	1.269	1.349
Absorbtion coefficient (mm^{-1})	0.797	0.644	0.786
F(000)	500	1376	516
Theta range for collection	1.83 to 28.28°	1.57 to 26.03°	2.03 to 26.06°
Reflections collected	38209	52568	65757
Independent reflections	5803	6653	4709
Minimum/maximum transmission	0.5885/0.7457	0.6643/0.7460	0.6681/0.7453
Refinement method	Full-matrix least-squares on F^2	Full-matrix least-squares on F^2	Full-matrix least-squares on F^2
Data / parameters / restrains	5803 / 194 / 64	6653 / 339 / 0	4709 / 252 / 127
Goodness-of-fit on F^2	1.038	1.181	3.579
Final R indices [I>2σ(I)]	$R_1 = 0.0373$, $wR^2 = 0.0867$	$R_1 = 0.0845$, $wR^2 = 0.1921$	$R_1 = 0.0290$, $wR^2 = 0.0970$
R indices (all data)	$R_1 = 0.0425$, $wR^2 = 0.0900$	$R_1 = 0.0874$, $wR^2 = 0.1934$	$R_1 = 0.0304$, $wR^2 = 0.0977$
Maximum/minimum residual electron density ($e \cdot Å^{-3}$)	1.201 / –1.453	1.642 / –1.844	1.419 / –1.187

	112	**115**	**118**
Empirical formula	$C_{32}H_{60}BNPRhSi_2$	$C_{34}H_{64}BNPRhSi_2$	$C_{36}H_{66}BN_3PRhSi_2$
Formula weight ($g \cdot mol^{-1}$)	659.68	687.73	741.79
Temperature (K)	100(2)	100(2)	100(2)
Radiation, λ (Å)	$Mo_{K\alpha}$ 0.71073	$Mo_{K\alpha}$ 0.71073	$Mo_{K\alpha}$ 0.71073
Crystal system	Monoclinic	Triclinic	Triclinic
Space group	*C*2/*c*	*P*-1	*P*-1
a (Å)	42.086(2)	11.4506(13)	10.6199(17)
b (Å)	8.8183(4)	17.092(2)	13.047(2)
c (Å)	18.5006(9)	19.724(2)	15.053(2)
α (°)	90.00	76.412(8)	75.854(7)
β (°)	97.114(2)	89.872(6)	86.561(7)
γ (°)	90.00	73.661(5)	76.536(7)
Volume ($Å^3$)	6813.3(6)	3592.2(7)	1966.9(5)
Z	8	4	2
Calculated density ($Mg \cdot m^{-3}$)	1.286	1.272	1.253
Absorbtion coefficient (mm^{-1})	0.640	0.610	0.563
F(000)	2816	1472	792
Theta range for collection	0.98 to 26.03°	1.28 to 26.49°	1.40 to 28.38°
Reflections collected	6760	14564	154010
Independent reflections	6803	14564	9329
Minimum/maximum transmission	0.657454/0.745313	0.391729/0.745374	0.7000/0.7457
Refinement method	Full-matrix least-squares on F^2	Full-matrix least-squares on F^2	Full-matrix least-squares on F^2
Data / parameters / restrains	6803 / 351 / 0	14564 / 787 / 180	9329 / 442 / 72
Goodness-of-fit on F^2	1.142	1.061	1.047
Final R indices [I>2σ(I)]	$R_1 = 0.0502$, $wR^2 = 0.1099$	$R_1 = 0.0513$, $wR^2 = 0.1218$	$R_1 = 0.0315$, $wR^2 = 0.0767$
R indices (all data)	$R_1 = 0.0556$, $wR^2 = 0.1123$	$R_1 = 0.0684$, $wR^2 = 0.1354$	$R_1 = 0.0415$, $wR^2 = 0.0931$
Maximum/minimum residual electron density ($e \cdot Å^{-3}$)	2.293 / –1.260	1.844 / –0.901	2.134 / –0.802

	135	**138**	**145**
Empirical formula	$C_{19}H_{31}BClFeO_3PSi$	$C_{16}H_{22}BFeO_3P$	$C_{75}H_{118}B_2Fe_2O_6P_4Pt_2$
Formula weight ($g \cdot mol^{-1}$)	468.61	359.97	1763.07
Temperature (K)	99(2)	103(2)	100(2)
Radiation, λ (Å)	$Mo_{K\alpha}$ 0.71073	$Mo_{K\alpha}$ 0.71073	$Mo_{K\alpha}$ 0.71073
Crystal system	Monoclinic	Monoclinic	Triclinic
Space group	$P2_1/n$	$P2_1/c$	P-1
a (Å)	8.6064(4)	8.7378(6)	8.9521(5)
b (Å)	18.2514(10)	12.5147(8)	10.0878(6)
c (Å)	14.9970(8)	16.5294(10)	22.4284(14)
α (°)	90.00	90.00	97.278(4)
β (°)	91.994(2)	99.597(3)	95.272(4)
γ (°)	90.00	90.00	107.887(3)
Volume ($Å^3$)	2354.3(2)	1782.2(2)	1893.57(19)
Z	4	4	1
Calculated density ($Mg \cdot m^{-3}$)	1.322	1.342	1.546
Absorbtion coefficient (mm^{-1})	0.889	0.943	4.191
F(000)	984	752	894
Theta range for collection	1.76 to 27.14°	2.05 to 30.54°	2.20 to 25.99°
Reflections collected	43505	82607	55524
Independent reflections	5175	5191	7363
Minimum/maximum transmission	0.6265/0.7455	0.6662/0.7461	0.5686/0.7453
Refinement method	Full-matrix least-squares on F^2	Full-matrix least-squares on F^2	Full-matrix least-squares on F^2
Data / parameters / restrains	5175 / 254 / 0	5191 / 206 / 0	7363 / 401 / 0
Goodness-of-fit on F^2	1.175	1.047	1.168
Final R indices [I>2σ(I)]	$R_1 = 0.0270$, $wR^2 = 0.0785$	$R_1 = 0.0243$, $wR^2 = 0.0620$	$R_1 = 0.0256$, $wR^2 = 0.0698$
R indices (all data)	$R_1 = 0.0358$, $wR^2 = 0.0869$	$R_1 = 0.0304$, $wR^2 = 0.0648$	$R_1 = 0.0267$, $wR^2 = 0.0703$
Maximum/minimum residual electron density ($e \cdot Å^{-3}$)	0.448 / –0.399	0.394 / –0.212	1.775 / –1.133

	147	**169**	**170**
Empirical formula	$C_{29}H_{32}BFeO_4P$	$C_{19}H_{31}B_2FeNO_3Si_2$	$C_{36}H_{62}B_4Fe_2N_2O_4Si_4$
Formula weight ($g \cdot mol^{-1}$)	542.18	455.10	854.18
Temperature (K)	100(2)	100(2)	100(2)
Radiation, λ (Å)	$Mo_{K\alpha}$ 0.71073	$Mo_{K\alpha}$ 0.71073	$Mo_{K\alpha}$ 0.71073
Crystal system	Triclinic	Triclinic	Monoclinic
Space group	*P*-1	*P*-1	*C*2/*c*
a (Å)	9.1705(8)	8.7118(3)	27.394(4)
b (Å)	16.2856(16)	9.6694(3)	9.3733(13)
c (Å)	18.7869(17)	16.1522(6)	21.725(3)
α (°)	79.362(4)	91.546(2)	90.00
β (°)	89.368(4)	96.857(2)	126.076(4)
γ (°)	84.646(4)	116.7720(10)	90.00
Volume ($Å^3$)	2745.5(4)	1201.07(7)	4508.7(10)
Z	4	2	4
Calculated density ($Mg \cdot m^{-3}$)	1.312	1.258	1.258
Absorbtion coefficient (mm^{-1})	0.640	0.746	0.787
F(000)	1136	480	1808
Theta range for collection	1.10 to 30.53°	1.28 to 28.35°	1.84 to 25.99°
Reflections collected	163239	29160	28406
Independent reflections	14709	5915	4406
Minimum/maximum transmission	0.6935/0.7461	0.6689/0.7457	0.6244/0.7453
Refinement method	Full-matrix least-squares on F^2	Full-matrix least-squares on F^2	Full-matrix least-squares on F^2
Data / parameters / restrains	14709 / 663 / 0	5915 / 263 / 0	4406 / 245 / 0
Goodness-of-fit on F^2	1.029	1.017	1.041
Final R indices [I>2σ(I)]	$R_1 = 0.0318$, $wR^2 = 0.0741$	$R_1 = 0.0351$, $wR^2 = 0.0761$	$R_1 = 0.0274$, $wR^2 = 0.0667$
R indices (all data)	$R_1 = 0.0442$, $wR^2 = 0.0797$	$R_1 = 0.0537$, $wR^2 = 0.0825$	$R_1 = 0.0358$, $wR^2 = 0.0711$
Maximum/minimum residual electron density ($e \cdot Å^{-3}$)	0.603 / –0.323	0.492 / –0.267	0.380 / –0.256

	171	**172**	**174**
Empirical formula	$C_{34}H_{62}B_4FeN_2O_2Si_4$	$C_{22}H_{40}B_2FeNO_3PSi_2$	$C_{37}H_{64}B_2FeNO_3PPtSi_2$
Formula weight ($g \cdot mol^{-1}$)	742.31	531.17	930.60
Temperature (K)	100(2)	100(2)	100(2)
Radiation, λ (Å)	$Mo_{K\alpha}$ 0.71073	$Mo_{K\alpha}$ 0.71073	$Mo_{K\alpha}$ 0.71073
Crystal system	Triclinic	Triclinic	Monoclinic
Space group	*P*-1	*P*-1	$P2_1/c$
a (Å)	9.1423(5)	8.4379(4)	21.750(16)
b (Å)	13.2797(8)	17.9889(9)	12.337(9)
c (Å)	18.3330(11)	21.0632(11)	15.479(12)
α (°)	81.242(2)	114.833(2)	90.00
β (°)	86.113(2)	94.235(3)	94.824(15)
γ (°)	78.661(2)	91.668(3)	90.00
Volume ($Å^3$)	2155.2(2)	2887.2(2)	4139(5)
Z	2	4	4
Calculated density ($Mg \cdot m^{-3}$)	1.144	1.222	1.493
Absorbtion coefficient (mm^{-1})	0.491	0.683	3.858
F(000)	796	1128	1896
Theta range for collection	1.12 to 26.37°	1.07 to 28.36°	0.94 to 26.78°
Reflections collected	8589	71976	43855
Independent reflections	8589	14102	8727
Minimum/maximum transmission	0.8660/1.0000	0.6129/0.7457	0.5480/0.7454
Refinement method	Full-matrix least-squares on F^2	Full-matrix least-squares on F^2	Full-matrix least-squares on F^2
Data / parameters / restrains	8589 / 445 / 0	14102 / 603 / 0	8727 / 443 / 0
Goodness-of-fit on F^2	1.153	1.020	1.013
Final R indices [I>2σ(I)]	$R_1 = 0.0575$, $wR^2 = 0.1378$	$R_1 = 0.0509$, $wR^2 = 0.1167$	$R_1 = 0.0267$, $wR^2 = 0.0532$
R indices (all data)	$R_1 = 0.0701$, $wR^2 = 0.1421$	$R_1 = 0.0921$, $wR^2 = 0.1350$	$R_1 = 0.0370$, $wR^2 = 0.0567$
Maximum/minimum residual electron density ($e \cdot Å^{-3}$)	0.692 / –0.728	0.941 / –0.559	0.836 / –0.830

	177	**178**	**179**
Empirical formula	$C_{25}H_{38}B_2Fe_2NO_6Si_2$	$C_{27}H_{43}B_2FeNO_3Si_2$	$C_{47}H_{51}B_2FeNO_3Si_2$
Formula weight ($g \cdot mol^{-1}$)	638.06	563.27	811.54
Temperature (K)	100(2)	100(2)	100(2)
Radiation, λ (Å)	$Mo_{K\alpha}$ 0.71073	$Mo_{K\alpha}$ 0.71073	$Mo_{K\alpha}$ 0.71073
Crystal system	Monoclinic	Triclinic	Monoclinic
Space group	$P2_1/n$	P-1	$P2_1/n$
a (Å)	15.5507(7)	12.8085(19)	8.9760(6)
b (Å)	12.1492(6)	15.140(2)	20.9580(16)
c (Å)	16.7976(9)	17.610(3)	23.0805(17)
α (°)	90.00	100.019(8)	90.00
β (°)	97.604(2)	106.025(7)	96.827(3)
γ (°)	90.00	107.003(7)	90.00
Volume ($Å^3$)	3145.6(3)	3015.8(8)	4311.1(5)
Z	4	4	4
Calculated density ($Mg \cdot m^{-3}$)	1.347	1.241	1.250
Absorbtion coefficient (mm^{-1})	1.035	0.607	0.447
F(000)	1332	1200	1712
Theta range for collection	1.68 to 26.81°	1.25 to 26.44°	1.32 to 26.37°
Reflections collected	164986	55198	135999
Independent reflections	6701	12054	8823
Minimum/maximum transmission	0.6712/0.7454	0.5111/0.7454	0.6437/0.7454
Refinement method	Full-matrix least-squares on F^2	Full-matrix least-squares on F^2	Full-matrix least-squares on F^2
Data / parameters / restrains	6701 / 353 / 0	12054 / 677 / 0	8823 / 515 / 204
Goodness-of-fit on F^2	1.040	1.093	1.091
Final R indices [I>2σ(I)]	$R_1 = 0.0226$, $wR^2 = 0.0598$	$R_1 = 0.0586$, $wR^2 = 0.1407$	$R_1 = 0.0328$, $wR^2 = 0.0784$
R indices (all data)	$R_1 = 0.0266$, $wR^2 = 0.0626$	$R_1 = 0.1122$, $wR^2 = 0.1782$	$R_1 = 0.0462$, $wR^2 = 0.0889$
Maximum/minimum residual electron density ($e \cdot Å^{-3}$)	0.870 / –0.356	1.308 / –0.725	0.896 / –0.343

	180
Empirical formula	$C_{27}H_{49}B_2FeNO_3Si_4$
Formula weight ($g \cdot mol^{-1}$)	625.50
Temperature (K)	100(2)
Radiation, λ (Å)	$Mo_{K\alpha}$ 0.71073
Crystal system	Monoclinic
Space group	$P2_1/c$
a (Å)	18.980(8)
b (Å)	11.129(8)
c (Å)	17.387(7)
α (°)	90.00
β (°)	109.104(14)
γ (°)	90.00
Volume ($Å^3$)	3470(3)
Z	4
Calculated density ($Mg \cdot m^{-3}$)	1.197
Absorbtion coefficient (mm^{-1})	0.600
F(000)	1336
Theta range for collection	1.14 to 26.79°
Reflections collected	56960
Independent reflections	7359
Minimum/maximum transmission	0.5619/0.7454
Refinement method	Full-matrix least-squares on F^2
Data / parameters / restrains	7359 / 359 / 0
Goodness-of-fit on F^2	1.036
Final R indices [I>2σ(I)]	$R_1 = 0.0562$, $wR^2 = 0.1386$
R indices (all data)	$R_1 = 0.0887$, $wR^2 = 0.1577$
Maximum/minimum residual electron density ($e \cdot Å^{-3}$)	1.113 / –1.010

7 Bibliography

[1] A. Ludi, *J. Chem. Educ.* **1981**, *58*, 1013.

[2] E. Frankland, *Justus Liebigs Ann. Chem.* **1849**, 171.

[3] T. D. Tilley in *Chemistry of Organic Silicon Compounds, Vol. 2* (Eds.: S. W. Patai, Z. Rappoport), Wiley, New York, **1989**, pp. 1415.

[4] U. Schubert, *Transition Met. Chem.* **1991**, *16*, 136.

[5] C. Zybill, H. Handwerker, H. Friedrich, *Adv. Organomet. Chem.* **1994**, *36*, 229.

[6] P. D. Lickiss, *Chem. Soc. Rev.* **1992**, *21*, 271.

[7] R. A. Fischer, J. Weiss, *Angew. Chem. Int. Ed.* **1999**, *38*, 2830.

[8] H. Nöth, G. Schmid, *Angew. Chem. Int. Ed.* **1963**, *2*, 623.

[9] R. T. Baker, D. W. Ovenall, J. C. Calabrese, S. A. Westcott, N. J. Taylor, I. D. Williams, und T. B. Marder, *J.Am.Chem.Soc.* **1990**, *112*, 9399.

[10] J. R. Knorr, J. S. Merola, *Organometallics* **1990**, *9*, 3008.

[11] X. Wang, B. O. Roos, L. Andrews, *Angew.Chem. Int. Ed.* **2010**, *49*, 157.

[12] D. Männig, H. Nöth, *Angew. Chem. Int. Ed. Engl.* **1985**, *24*, 878.

[13] D. Vidovic, G. A. Pierce, S. Aldridge, *Chem. Commun.* **2009**, 1157.

[14] D. F. Shriver, *J. Am. Chem. Soc.* **1963**, *85*, 3509.

[15] H. Braunschweig, T. Wagner, *Chem. Ber.* **1994**, *127*, 1613.

[16] H. Braunschweig, T. Wagner, *Zeitschrift fuer Naturforschung, B: Chemical Sciences* **1996**, *51*, 1618.

[17] H. Braunschweig, C. Kollann, *Zeitschrift fuer Naturforschung, B: Chemical Sciences* **1999**, *54*, 839.

[18] K. B. Gilbert, S. K. Boocock, S. G. Shore, in *Comprehensive Organometallic Chemistry*; E. W. Abel, F. G. A. Stone, G. Wilkinson, Eds.; Pergamon: Oxford, **1982**; *Vol. 6*, p 880.

[19] J. M. Burlitch, J. H. Burk, M. E. Leonowicz, R. E. Hughes, *Inorg. Chem.* **1979**, *18*, 1702.

[20] M. R. S. Foreman, A. F. Hill, A. J. P. White, D. J. Williams, *Organometallics* **2004**, *23*, 913.

[21] D. J. Mihalcik, J. L. White, J. M. Tanski, L. N. Zakharov, G. P. A. Yap, C. D. Incarvito, A. L. Rheingold, D. Rabinovich, *Dalton Trans.* **2004**, 1626.

[22] I. R. Crossley, M. R. S. Foreman, A. F. Hill, A. J. P. White, D. J. Williams, *Chem. Commu.* **2005**, 221.

[23] I. R. Crossley, A. F. Hill, A. C. Willis, *Organometallics* **2005**, *24*, 1062.

[24] M. Sircoglou, S. Bontemps, G. Bouhadir, N. Saffon, K. Miqueu, W. Gu, M. Mercy, C. H. Chen, B. M. Foxman, L. Maron, O. V. Ozerov, D. Bourissou, *J. Am. Chem. Soc.* **2008**, *130*, 16729.

[25] I. R. Crossley, A. F. Hill, *Organometallics* **2004**, *23*, 5656.

[26] S. Bontemps, G. Bouhadir, W. Gu, M. Mercy, C. H. Chen, B. M. Foxman, L. Maron, O. V. Ozerov, D. Bourissou, *Angew. Chem. Int. Ed.* **2008**, *47*, 1481.

[27] D. G. Musaev, K. Morokuma, *J. Phys. Chem.* **1996**, *100*, 6509.

[28] A. A. Dickinson, D. J. Willock, R. J. Calder, S. Aldridge, *Organometallics* **2002**, *21*, 1146.

[29] T. R. Cundari, Y. Zhao, *Inorg. Chim. Acta* **2003**, *345*, 70.

[30] K. C. Lam, W. H. Lam, Z. Lin, T. B. Marder, N. C. Norman, *Inorg. Chem.* **2004**, *43*, 2541.

[31] H. Braunschweig, K. Radacki, F. Seeler, G. R. Whittell, *Organometallics* **2004**, *23*, 4178.

[32] H. Braunschweig, K. Radacki, F. Seeler, G. R. Whittell, *Organometallics* **2006**, *25*, 4605.

[33] Y. Segawa, M. Yamashita, K. Nozaki, *Science* **2006**, *314*, 113.

[34] Y. Segawa, Y. Suzuki, M. Yamashita, K. Nozaki, *J. Am. Chem. Soc.* **2008**, *130*, 16069.

[35] M. Yamashita, Y. Suzuki, Y. Segawa, K. Nozaki, *J. Am. Chem. Soc.* **2007**, *129*, 9570.

[36] T. Kajiwara, T. Terabayashi, M. Yamashita, K. Nozaki, *Angew. Chem. Int. Ed.* **2008**, *47*, 6606.

[37] Y. Segawa, M. Yamashita, K. Nozaki, *Angew. Chem. Int. Ed.* **2007**,*46*, 6710.

[38] T. Terabayashi, T. Kajiwara, M. Yamashita, K. Nozaki, *J. Am. Chem. Soc.* **2009**, *131*, 14162.

[39] T. B. Marder, N. C. Norman, *Top. Catal.* **1998**, *5*, 63.

[40] T. Ishiyama, N. Matsuda, N. Miyaura, A. Suzuki, *J. Am. Chem. Soc.* **1993**, *115*, 11018.

[41] C. N. Iverson M. R. Smith, *J.Am.Chem.Soc.* **1995**, *117*, 4403.

[42] C. N. Iverson und M. R. Smith, III, *Organometallics* **1996**, *15*, 5155.

[43] G. Lesley, P. Nguyen, N. J. Taylor, T. B. Marder, A. J. Scott, W. Clegg, N. C. Norman, *Organometallics* **1996**, *15*, 5137.

[44] T. Ishiyama, N. Matsuda, M. Murata, F. Ozawa, A. Suzuki, N. Miyaura, *Organometallics* **1996**, *15*, 713.

[45] T. Ishiyama, M. Yamamoto, N. Miyaura, *Chem. Commun.* **1996**, 2073.

[46] T. Ishiyama, N. Miyaura, *J. Organomet. Chem.* **2000**, *611*, 392.

[47] C. J. Adams, R. A. Baber, A. S. Batsanov, G. Bramham, J. P. H. Charmant, M. F. Haddow, J. A. K. Howard, W. H. Lam, Z. Lin, T. B. Marder, N. C. Norman, A. G. Orpen, *Dalton Trans.* **2006**, 1370.

[48] H. E. Burks, S. Liu, J. P. Morken, *J. Am. Chem. Soc.* **2007**, *129*, 8766.

[49] H. Braunschweig, T. Kupfer, M. Lutz, K. Radacki, F. Seeler, R. Sigritz, *Angew. Chem. Int. Ed.* **2006**, *45*, 8048.

[50] H. Braunschweig, T. Kupfer, *J. Am. Chem. Soc.* **2008**, *130*, 4242.

[51] K. Kawamura, J. F. Hartwig, *J. Am. Chem. Soc.* **2001**, *123*, 8422.

[52] H. Chen, S. Schlecht, T. C. Semple, J. F. Hartwig, *Science* **2000**, *287*, 1995.

[53] T. Braun, M. A. Salomon, K. Altenhoner, M. Teltewskoi, S. Hinze, *Angew. Chem. Int. Ed.* **2009**, *48*, 1818.

[54] Y. Segawa, M. Yamashita, K. Nozaki, *J. Am. Chem. Soc.* **2009**, *131*, 9201.

[55] Y. Segawa, M. Yamashita, K. Nozaki, *Organometallics* **2009**, *28*, 6234.

[56] P. L. Timms, *J. Am. Chem. Soc.* **1967**, *89*, 1629.

[57] P. L. Timms, *Acc. Chem. Res.* **1973,** *6*, 118.

[58] B. Pachaly, R. West, *Angew. Chem. Int. Ed. Engl.* **1984**, *23*, 454.

[59] H. Braunschweig, *Angew. Chem. Int. Ed.* **1998**, *37*, 1786.

[60] H. Braunschweig, M. Colling, *J. Organomet. Chem.* **2000**, *614–615*, 18.

[61] H. Braunschweig, M. Colling, *Coord. Chem. Rev.* **2001**, *223*, 1.

[62] H. Braunschweig, M. Colling, *Eur. J. Inorg. Chem.* **2003**, 393.

[63] H. Braunschweig, *Adv. Organomet. Chem.* **2004**, *51*, 163.

[64] H. Braunschweig, G. R. Whittell, *Chem. Eur. J.* **2005**, *11*, 6128.

[65] H. Braunschweig, D. Rais, *Heteroatom Chem.* **2005**, *16*, 566.

[66] H. Braunschweig, C. Kollann, D. Rais, *Angew. Chem. Int. Ed.* **2006**, *45*, 5254.

[67] C. E. Anderson, H. Braunschweig, R. D. Dewhurst, *Organometallics* **2008**, *27*, 6381.

[68] B. Wrackmeyer, *Angew. Chem. Int. Ed.* **1999**, *38*, 771.

[69] S. Aldridge, D. L. Coombs, *Coord. Chem. Rev.* **2004**, *248*, 535.

[70] D. Vidovic, G. A. Pierce, S. Aldridge, *Chem. Commun.* **2009**, 1157.

[71] U. Radius, F. M. Bickelhaupt, A. W. Ehlers, N. Goldberg, R. Hoffmann, *Inorg. Chem.* **1998**, *37*, 1080.

[72] C. L. B. Macdonald, A. H. Cowley, *J. Am. Chem. Soc.* **1999**, *121*, 12113.

[73] J. Uddin, C. Boehme, G. Frenking, *Organometallics* **2000**, *19*, 571.

[74] Y. Chen, G. Frenking, *Dalton Trans.* **2001**, 434.

[75] J. Uddin, G. Frenking, *J. Am. Chem. Soc.* **2001**, *123*, 1683.

[76] C. Boehme, J. Uddin, G. Frenking, *Coord. Chem. Rev.* **2000**, *197*, 249.

[77] L. Xu, Q.-S. Li, Y. Xie, R. B. King, H. F. Schaefer, *Inorg. Chem.* **2010**, *49*, 1046.

[78] K. K. Pandey, D. G. Musaev, *Organometallics* **2010**, *29*, 142.

[79] A. W. Ehlers, E. J. Baerends, F. M. Bickelhaupt, U. Radius, *Chem.-Eur. J.* **1998**, *4*, 210.

[80] A. H. Cowley, V. Lomelí, A. Voigt, *J. Am. Chem. Soc.* **1998**, *120*, 6401.

[81] D. Vidovic, M. Findlater, G. Reeske, A. H. Cowley, *Chem. Commun.* **2006**, 3786.

[82] H. Braunschweig, C. Kollann, U. Englert, *Angew. Chem. Int. Ed.* **1998**, *37*, 3179.

[83] H. Braunschweig, M. Colling, C. Kollann, K. Merz, K. Radacki, *Angew. Chem. Int. Ed.* **2001**, *38*, 4198.

[84] D. L. Coombs, S. Aldridge, C. Jones, D. J. Willock, *J. Am. Chem. Soc.* **2003**, *125*, 6356.

[85] D. L. Coombs, S. Aldridge, A. Rossin, C. Jones, D. J. Willock, *Organometallics* **2004**, *23*, 2911.

[86] G. A. Pierce, D. Vidovic, D. L. Kays, N. D. Coombs, A. L. Thompson, E. D. Jemmis, S. De, und S. Aldridge, *Organometallics* **2009**, *28*, 2947.

[87] D. L. Kays, J. K. Day, L. L. Ooi, S. Aldridge, *Angew.Chem.Int.Ed.* **2005**, *44*, 7457.

[88] H. Braunschweig, K. Radacki, D. Rais, D. Scheschkewitz, *Angew. Chem. Int. Ed.* **2005**, *44*, 5651.

[89] H. Braunschweig, K. Radacki, K. Uttinger, *Organometallics* **2008**, *27*, 6005.

[90] H. Braunschweig, K. Radacki, K. Uttinger, *Angew. Chem. Int. Ed.* **2007**, *46*, 3979.

[91] G. Alcaraz, U. Helmstedt, E. Clot, L. Vendier, S. Sabo-Etienne, *J. Am. Chem. Soc.* **2008**, *130*, 12878.

[92] H. Braunschweig, R. D. Dewhurst, *Angew. Chem. Int. Ed.* **2009**, *48*, 1893.

[93] H. Braunschweig, M. Burzler, U. Flierler, J. Henn, D. Leusser, H. Ott, D. Stalke, *Angew. Chem. Int. Ed.* **2008**, *47*, 4321.

[94] K. Götz, M. Kaupp, H. Braunschweig, D. Stalke, *Chem. Eur J.* **2009**, *15*, 623.

[95] P. Bissinger, H. Braunschweig, F. Seeler, *Organometallics* **2007**, *26*, 4700.

[96] H. Braunschweig, C. Kollann, U. Englert, *Eur. J. Inorg. Chem.* **1998**, 465.

[97] H. Braunschweig, C. Kollann, K. W. Klinkhammer, *Eur. J. Inorg. Chem.* **1999**, 1523.

[98] S. Aldridge, D. L. Coombs, C. Jones, *Chem. Commun.* **2002**, 856.

[99] S. Aldridge, D. L. Coombs, C. Jones, *J. Chem. Soc., Dalton Trans.* **2002**, 3851.

[100] D. L. Kays (née Coombs), A. Rossin, J. K. Day, L.-L. Ooi, S. Aldridge, *Dalton Trans.* **2006**, 399.

[101] D. L. Coombs, S. Aldridge, S. J. Coles, M. B. Hursthouse, *Organometallics* **2003**, *22*, 4213.

[102] H. Braunschweig, M. Colling, C. Hu, K. Radacki, *Angew. Chem. Int. Ed.* **2003**, *42*, 205.

[103] H. Braunschweig, M. Colling, C. Kollann, B. Neumann, H.-G. Stammler, *Angew. Chem. Int. Ed.* **2001**, *40*, 2298.

[104] H. Braunschweig, M. Forster, F. Seeler, *Chem. Eur. J.* **2009**, *15*, 469.

[105] H. Braunschweig, M. Forster, K. Radacki, F. Seeler, G. Whittell, *Angew. Chem. Int. Ed.* **2007**, *46*, 5212.

[106] H. Braunschweig, M. Forster, T. Kupfer, F. Seeler, *Angew. Chem. Int. Ed.* **2008**, *47*, 5981.

[107] H. Braunschweig, M. Forster, K. Radacki, *Angew. Chem. Int. Ed.* **2006**, *45*, 2132.

[108] S. Bertsch, H. Braunschweig, B. Christ, M. Forster, K. Schwab, K. Radacki, *Angew. Chem. Int. Ed.* **2010**, *49*, 9517.

[109] M. E. Volpin, Y. D. Koreshkov, V. G. Dulova, D. N. Kursanov, *Tetrahedron* **1962**, *18*, 107.

[110] For INDO calculations, see: C. U. Pittman, A. Kress, T. B. Patterson, P. Walton, L. D. Kispert, *J. Org. Chem.* **1974**,*39*, 373.

[111] N. L. Allinger, J. H. Siefert, *J. Am. Chem. Soc.* **1975**, *97*, 752.

[112] For ab initio calculations, see: K. Krogh-Jespersen, D. Cremer, J. D. Dill, J. A. Pople, P. v. R. Schleyer, *J. Am. Chem. Soc.* **1981**, *103*, 2589.

[113] C. Pues, A. Berndt, *Angew. Chem. Int. Ed. Engl.* **1984**, *23*, 313.

[114] J. J. Eisch, B. Shafii, A. L. Rheingold, *J. Am. Chem. Soc.* **1987**, *109*, 2526.

[115] J. J. Eisch, B. Shafii, J. D. Odom, A. L. Rheingold, *J. Am. Chem. Soc.* **1990**, *112*, 1847.

[116] H. Braunschweig, T. Herbst, D. Rais, F. Seeler, *Angew. Chem. Int. Ed.* **2005**, *44*, 7461.

[117] H. Braunschweig, T. Herbst, D. Rais, S. Ghosh, T. Kupfer, K. Radacki, A. Crawford, R. Ward, T. Marder, I. Fernández, G. Frenking, *J. Am. Chem. Soc.* **2009**, *131*, 8989.

[118] N. Matsumi, Y. Chujo, In *Contemporary Boron Chemistry, Spec. Publ. No. 253*; M. G. Davidson, A. K. Hughes, T. B. Marder, K. Wade, Eds.; Royal Society of Chemistry: Cambridge, **2000**; p 51.

[119] C. D. Entwistle, T. B. Marder, *Angew. Chem. Int. Ed.* **2002**, *41*, 2927.

[120] F. J. Jäckle, *Inorg. Organomet. Polym. Mater.* **2005**, *15*, 293.

[121] D. *Gabel*, In *Science of Synthesis: Houben-Weyl Methods of Molecular Transformation*; D. Kaufmann, D. S. Matteson, Eds.; Verlag G. T. Thieme: Stuttgart, **2005**; *Vol. 6*, p 1277.

[122] H. Braunschweig, R. D. Dewhurst, T. Herbst, K. Radacki, *Angew. Chem. Int. Ed.* **2008**, *47*, 5978.

[123] G. A. Molander, C. R. Bernardi, *J. Org. Chem.* **2002**, *67*, 8424-8429.

[124] J. H. Kirchhoff, M. R. Netherton, I. D. Hills, G. C. Fu, *J. Am. Chem. Soc.* **2002**, *124*, 13662.

[125] M. Shimizu, C. Nakamaki, K. Shimono, M. Schelper, T. Kurahashi, T. Hiyama, *J. Am. Chem. Soc.* **2005**, *127*, 12506.

[126] H. Braunschweig, M. Burzler, K. Radacki, F. Seeler, *Angew. Chem. Int. Ed.* **2007**, *46*, 8071.

[127] S. Aldridge, C. Jones, T. Gans-Eichler, A. Stasch, D. L. Kays, N. D. Coombs, D. J. Willock, *Angew. Chem. Int. Ed.* **2006**, *45*, 6118.

[128] H. Braunschweig, D. Rais, K. Uttinger, *Angew. Chem. Int. Ed.* **2005**, *44*, 3763.

[129] H. Braunschweig, K. Radacki, D. Rais, K. Uttinger, *Organometallics* **2006**, *25*, 5159.

[130] H. Braunschweig, K. Radacki, K. Uttinger, *Eur. J. Inorg. Chem.* **2007**, 4350.

[131] G. A. Pierce, S. Aldridge, C. Jones, T. Gans-Eichler, A. Stasch, N. D. Coombs, D. J. Willock, *Angew. Chem. Int. Ed.* **2007**, *46*, 2043.

[132] G. A. Pierce, N. D. Coombs, D. J. Willock, J. K. Day, A. Stasch, S. Aldridge, *Dalton Trans.* **2007**, 4405.

[133] M. Akita, M. Terada, S. Oyama, Y. Morooka, *Organometallics***1990**, *9*, 816.

[134] H. Braunschweig, B. Ganter, M. Koster, T. Wagner, *Chem. Ber.* **1996**, *129*, 1099.

[135] H. Braunschweig, C. Kollann, M. Müller, *Eur. J. Inorg. Chem.* **1998**, 291.

[136] H. Braunschweig, M. Colling, C. Kollann, U. Englert, *J. Chem. Soc., Dalton Trans.* **2002**, 2289.

[137] R. G. Ball, M. R. Burke, J. Takats, *Organometallics* **1987**, *6*, 1918.

[138] H. Feulner, N. Metzler, H. Nöth, *J. Organomet. Chem.* **1995**, *489*, 51.

[139] H. Braunschweig, T. Herbst, K. Radacki, G. Frenking, M. A. Celik, *Chem. Eur. J.* **2009**, *15*, 12099.

[140] C. Brown, R. H. Cragg, T. J. Miller, D. O. Smith, *J. Organomet. Chem.* **1983**, *244*, 209.

[141] K. Sünkel, U. Birk, C. Robl, *Organometallics* **1994**, *13*, 1679.

[142] C.-Y. Wong, C.-M. Che, M. C. W. Chan, J. Han, K.-H. Leung, L. D. Philips, K.-Y. Wong, N. Zhu, *J. Am. Chem. Soc.* **2005**, *127*, 13997;

[143] L. A. Emmert, W. Choi, J. A. Marshall, J. Yang, L. A. Meyer, J. A. Brozik, *J. Phys. Chem. A* **2003**, *107*, 11340;

[144] E. R. Batista, R. L. Martin, *J. Phys. Chem. A* **2005**, *109*, 9856;

[145] T.M. Cooper, D. M. Krein, A. R. Burke, D. G. McLean, J. E. Rogers, J. E. Stagle, *J. Phys. Chem. A* **2006**, *110*, 13370.

[146] D. Curtis, M. J. G. Lesley, N. C. Norman, A. G. Orpen, J. Starbuck, *J. Chem. Soc., Dalton Trans.*, **1999**, 1687.

[147] H. Braunschweig, K. Radacki, D. Rais, F. Seeler, *Organometallics*, **2004**, *23*, 5545.

[148] H. Braunschweig, P. Brenner, A. Müller, K. Radacki, D. Rais, K. Uttinger, *Chem. Eur. J.* **2007**, *13*, 7171.

[149] F. Dirschl, W. Nöth, W. Wagner, *J. Chem. Soc., Chem. Commun.* **1984**, 1533

[150] U. Klingebiel, Angew*. Chem.* **1984**, *96*, 807

[151] R. Boese, U. Klingebiel, *J. Organom. Chem*. **1986**, *306*, 295.

[152] G. Gustavson, N. Demjanov, *J. Prakt. Chem.* **1888**, *38*, 201.

[153] L. M. Morton, A. A. Noyes, *Am. Chem. J.* **1888**, *10*, 430.

[154] N. Suzuki, D. Hashizume, *Coord. Chem. Rev.* **2010**, *254*, 1307.

[155] N. Suzuki, M. Nishiura, Y. Wakatsuki, *Science* **2002**, *295*, 660.

[156] R. P. Hughes, R. B. Laritchev, L. N. Zakharov, A. L. Rheingold, J*. Am. Chem. Soc.* **2004**, *126*, 2308.

[157] F. A. Akkerman, D. Lentz, *Angew. Chem. Int. Ed.* **2007**, *46*, 4902.

[158] C. D. Entwistle, T. B. Marder, *Angew. Chem. Int. Ed.* **2002**, *41*, 2927.

[159] F. Jäkle, *J. Inorg. Organomet. Polym. Mater.* **2005**, *15*, 293.

[160] B. Glaser, H. Nöth, *Angew. Chem. Int. Ed.* **1985**, *24*, 416.

[161] R. Boese, P. Paetzold, A. Tapper, *Chem. Ber.* **1987**, *120*, 1069.

[162] B. Glaser, E. Hanecker, H. Nöth, H. Wagner, *Chem. Ber.* **1987**, *120*, 659.

[163] N. Metzler, H. Nöth, *Chem. Ber.* **1995**, *128*, 711.

[164] M. E. Volpin, Y. D. Koreshkov, V. G. Dulova, D. N. Kursanov, *Tetrahedron* **1962**, *18*, 107.

[165] For INDO calculations, see: C. U. Pittman, A. Kress, T. B. Patterson, P. Walton, L. D. Kispert, *J. Org. Chem.* **1974**, *39*, 373.

[166] N. L. Allinger, J. H. Siefert, *J. Am. Chem. Soc.* **1975**, *97*, 752.

[167] For ab-initio calculations, see: K. Krogh-Jespersen, D. Cremer, J. D. Dill, J. A. Pople, P. von R. Schleyer, *J. Am. Chem. Soc.* **1981**, *103*, 2589.

[168] T. E. Bitterwolf, *Inorg. Chim. Acta* **1986**, *122*, 175.

[169] C. Brown, R. H. Cragg, T. J. Miller, D. O. Smith, *J. Organomet. Chem.* **1983**, *244*, 209.

[170] H. Braunschweig, M. Burzler, T. Kupfer, K. Radacki, F. Seeler, *Angew. Chem. Int. Ed.* **2007**, *46*, 7785.

[171] P. Bissinger, H. Braunschweig, K. Kraft, T. Kupfer, *Angew. Chem. Int. Ed.* **2011**, *50*, 4704.

[172] R. Kinjo, B. Donnadieu, M. A. Celik, G. Frenking, G. Bertrand, *Science*, **2011**, *333*, 610.

[173] J. M. Maher, R. P. Beatty, N. J. Cooper, *Organometallics* **1985**, *4*, 1354.

[174] P. Paetzold *Adv. Inorg. Chem* **1987**, *31*, 123.

[175] H. Nöth Angew*. Chem. Int. Ed. Engl.* **1988**, *27*, 1603.

[176] P. Paetzold, C. Von Plotho, G. Schmid, R. Boese, B. Schrader, D. Bougeard, U. Pfeiffer, R. Gleiter, W. Schaefer, *Chem. Ber.* **1984**, *117*, 1089.

[177] H. C. Brown, B. Nazer, J. S. Cha, J. A. Sikorski, *J. Org. Chem.* **1986**, *51* , 5264.

[178] J. K. Ruff, W. J. Schlientz, *Inorg. Synth.* **1974**, *15*, 84.

[179] B. Blank, H. Braunschweig, M. Colling-Hendelkens, C. Kollann, K. Radacki, D. Rais, K. Uttinger, G. Whittell, *Chem. Eur. J.* **2007**, *13*, 4770.

[180] G. Bellachioma, G. Cardaci, A. Macchiono, G. Reichenbach, *J. Organomet. Chem.* **1990**, *391*, 367.

[181] H. Braunschweig, K. Kraft, S. Östreicher, K. Radacki, F. Seeler, *Chem. Eur. J.* **2010**, *16*, 10635.

[182] H. Braunschweig, K. Radacki, D. Rais, G. R. Whittell, *Angew. Chem. Int. Ed.* **2005**, *44*, 1192.

[183] H. Braunschweig, C. Burschka, M. Burzler, S. Metz, K. Radacki, *Angew. Chem. Int. Ed.* **2006**, *45*, 4352.

[184] H. Braunschweig, K. Radacki, D. Rais, F. Seeler, *Angew. Chem. Int. Ed.* **2006**, *45*, 1066.

[185] H. Braunschweig, K. Radacki, D. Rais, F. Seeler, K. Uttinger, *J. Am. Chem. Soc.* **2005**, *127*, 1386.

[186] N. R. Pace, *Proc. Natl. Acad. Sci.* **2001**, *98*, 805.

[187] J. E. Huheey, E. A. Keiter, R. L. Keiter, *Inorganic Chemistry* (Harper, New York, ed. 4, **1995**).

[188] R. D. Miller, J. Michl, *Chem. Rev.* **1989**, *107*, 1359.

[189] M. Atoji, W. N. Lipscomb, *J. Chem. Phys.* **1953**, *21*, 172.

[190] M. Atoji, W. N. Lipscomb, *Acta Crystallogr.* **1953**, *6*, 547.

[191] T. Davan, J. A. Morrison, *J. Chem. Soc., Chem. Commun.* **1981**, 250.

[192] G. Urry, A. G. Garrett, H. I. Schlesinger, *Inorg. Chem.* **1963**, *2*, 396.

[193] M. Baudler, K. Rockstein, W. Oehlert, *Chem. Ber.* **1991**, *124*, 1149.

[194] C.-J. Maier, H. Pritzkow, W. Siebert, *Angew. Chem. Int. Ed.* **1999**, *38*, 1666.

[195] K. H. Hermannsdörfer, E. Matejčikova, H. Nöth, *Chem. Ber.* **1970**, *103*, 516.

[196] H. Nöth, H. Pommerening, *Angew. Chem. Int. Ed.* **1980**, *19*, 482.

[197] H. Klusik, A. Berndt, *J. Organomet. Chem.* **1982**, *234*, C17.

[198] A. Papakondylis, E. Miliordos, A. Mavridis, *J. Phys. Chem. A* **2004**, *108*, 4335.

[199] H. Braunschweig, R. D. Dewhurst, A. Schneider, *Chem. Rev.* **2010**, *110*, 3924.

[200] P. Bissinger, H. Braunschweig, A. Damme, R. D. Dewhurst, T. Kupfer, K. Radacki, K. Wagner, *J. Am. Chem. Soc.* **2011**, *133*, 19044.

[201] H. Braunschweig, M. Colling, C. Hu, K. Radacki, *Angew. Chem. Int. Ed.* **2002**, *39*, 1359.

[202] L. Xu, Q. Li, R. B. King, H. F. Schaefer III, *Organometallics* **2011**, *30*, 5084.

[203] M. Poliakoff, J. J. Turner, *J. Chem. Soc*. **1971**, *A* 2403.

[204] S. C. Fletcher, M. Poliakoff, J. J. Turner, *Inorg. Chem*. **1986**, *25*, 3597.

[205] S. Fedrigo, T. L. Haslett, M. Moskovits, *J. Am. Chem. Soc*. **1996**, *118*, 5083.

[206] F. A. Cotton, M. J. Troup, *J. Chem. Soc., Dalton Trans*. **1974**, 800.

[207] P. L. Timms, *J. Am. Chem. Soc.* **1968**, *90*, 4585.

[208] S. M. Van der Kerk, A. L. M. Van Eekeren, G. J. M. Van der Kerk, *J. Organomet. Chem.* **1980**, *190*, C8.

[209] G. E. Herberich, B. Hessner, *J. Organomet. Chem.* **1978**, *161*, C36.

[210] P. Bineer. *Tetrahedron Lett.* **1966**, 2675.

[211] B. Wrackmeyer, G. Kehr, *Polyhedron*, **1991**, *10*, 1497.

[212] G. E. kerberich, B. Hessner, **S.** Beswetherik, J. A. K. Howard, P. Woodward, *J. Organormet. Chem.* **1980**, *192*, 421.

[213] K.-F. Wörner, W. Siebert, *Z. Naturforsch., Teil* B **1989**, *44*, 1211.

[214] P. S. Maddren , A. Modinos, P. L. Timms, P. Woodward, *J. Chem. Soc., Dalton Trans.* **1975**, 1272.

[215] S. L. Ingham, S. W. Magennis, *J. Organomet. Chem.* **1999**, *574*, 302.

[216] M. P. Gamasa, J. Gimeno, E. Lastra, *J. Organomet. Chem.* **1991**, *405*, 333.

[217] J. Kiesewetter, G. Poignant, V. Guerchais, *J. Organomet. Chem.* **2000**, *595*, 81.

[218] L.-K. Liu, K.-Y. Chang, Y.-S. Wen, *J. Chem. Soc., Dalton Trans.* **1998**, 741.

[219] J. G. Evans, P. L. Goggin, R. J. Goodfellow, J. G. Smith, *J. Chem. Soc. (A)* **1968**, *2*, 464.

[220] C.-Y. Hus, B. T. Leshner, M. Orchin, *Inorg. Synth.* **1979**, *19*, 114.

[221] E. Matern, J. Pikies, G. Fritz, *Z. Anorg. Allg. Chem.* **2000**, *626*, 2136.

[222] K. H.-Blusac, M. R. Pinto, C. Tan, K. S. Schanze, *J. Am. Chem. Soc.* **2004**, *126*,14964.

[223] Y. Liu, S. Jiang, K. Glusac, D. H. Powell, D. F. Anderson, K. S. Schanze, *J. Am. Chem. Soc.* **2002**, *124*, 12412.

[224] R. Nast, J. Moritz, *J. Organomet. Chem.* **1976**, *117*, 81.

[225] K. Gagnon, S. M. Aly, A. Brisach-Wittmeyer, D. Bellows, J,-F. Bérubé, L. Caron, A. S. Adb-El-Aziz, D. Fortin, P. D. Harvey, *Organometallics*, **2008**, *27*, 2201.

[226] K. M. Waltz, C. N. Muhoro, J. F. Hartwig, *Organometallics* **1999**, *18*, 3383.

[227] H. Werner, J. Wolf, F. J. Garcia Alonso, *J. Organomet. Chem.* **1987**, *336*, 397.

[228] T. Schaub, M. Backes, U. Radius, *Organometallics* **2006**, *25*, 4196.

[229] A. J. Arduengo, III, R. Krafczyk, R. Schmutzler, *Tetrahedron* **1999**, *51*,14523.

[230] W. Strohmeier, F.-J. Müller, *Chem. Ber.* **1969**, *102*, 3613.

[231] G. Reinhard, B. Hirle, U. Schubert, *J. Organomet. Chem.* 1992, *427*, 173.

[232] T. Yoshida, S. Otsuka, *Inorg. Synth.* **1990**, *28*, 113.

[233] A. Van der Ent, A. L. Onderdelinden, *Inorg. Synth.* **1990**, *28*, 90.

[234] N. J. Long, C. K. Williams, *Angew. Chem. Int. Ed.* **2003**, *42*, 2586.

[235] M. J. Frisch, G. W. Trucks, H. B. Schlegel, G. E. Scuseria, M. A. Robb, J. R. Cheeseman, J. A. Montgomery, Jr., T. Vreven, K. N. Kudin, J. C. Burant, J. M. Millam, S. S. Iyengar, J. Tomasi, V. Barone, B. Mennucci, M. Cossi, G. Scalmani, N. Rega, G. A. Petersson, H. Nakatsuji, M. Hada, M. Ehara, K. Toyota, R. Fukuda, J. Hasegawa, M. Ishida, T. Nakajima, Y. Honda, O. Kitao, H. Nakai, M. Klene, X. Li, J. E. Knox, H. P. Hratchian, J. B. Cross, V. Bakken, C. Adamo, J. Jaramillo, R. Gomperts, R. E. Stratmann, O. Yazyev, A. J. Austin, R. Cammi, C. Pomelli, J. W. Ochterski, P. Y. Ayala, K. Morokuma, G. A. Voth, P. Salvador, J. J. Dannenberg, V. G. Zakrzewski, S. Dapprich, A. D. Daniels, M. C. Strain, O. Farkas, D. K. Malick, A. D. Rabuck, K. Raghavachari, J. B. Foresman, J. V. Ortiz, Q. Cui, A. G. Baboul, S. Clifford, J. Cioslowski, B. B. Stefanov, G. Liu, A. Liashenko, P. Piskorz, I. Komaromi, R. L. Martin, D. J. Fox, T. Keith, M. A. Al-Laham, C. Y. Peng, A. Nanayakkara, M. Challacombe, P. M. W. Gill, B. Johnson, W. Chen, M. W. Wong, C. Gonzalez, and J. A. Pople. Gaussian 03, Revision E.01. Gaussian, Inc., Wallingford, CT, 2004.

[236] N. C. Handy, A. J. Cohen, *Mol. Phys.* **2001**, *99*, 403.

[237] A. Schaefer, C. Huber, R. Ahlrichs. *J. Chem. Phys.* **1994**, *100*, 5829.

[238] T. Yanai, D. Tew, N. Handy, *Chem. Phys. Lett.* **2004**, *393*, 51.

[239] A. D. McLean and G. S. Chandler, *J. Chem. Phys.* **1980**, *72*, 5639.

[240] R. Krishnan, J. S. Binkley, R. Seeger, J. A. Pople, *J. Chem. Phys.* **1980**, *72*, 650.

[241] A. J. H. Wachters, *J. Chem. Phys.* **1970**, *52*,1033.

[242] P. J. Hay. *J. Chem. Phys.* **1977**, *66*, 4377.

[243] K. Raghavachari, G. W. Trucks, *J. Chem. Phys.* **1989**, *91*, 1062.

[244] T. Clark, J. Chandrasekhar, G. W. Spitznagel, P. v. R. Schleyer, *J. Comp. Chem.* **1983**, *4*, 294.

[245] M. J. Frisch, J. A. Pople, J. S. Binkley, *J. Chem. Phys.* **1984,** *80*, 80.

[246] M. J. Frisch, G. W. Trucks, H. B. Schlegel, G. E. Scuseria, M. A. Robb, J. R. Cheeseman, G. Scalmani, V. Barone, B. Mennucci, G. A. Petersson, H. Nakatsuji, M. Caricato, X. Li, H. P. Hratchian, A. F. Izmaylov, J. Bloino, G. Zheng, J. L. Sonnenberg, M. Hada, M. Ehara, K. Toyota, R. Fukuda, J. Hasegawa, M. Ishida, T. Nakajima, Y. Honda, O. Kitao, H. Nakai, T. Vreven, J. A. Montgomery, Jr., J. E. Peralta, F. Ogliaro, M. Bearpark, J. J. Heyd, E. Brothers, K. N. Kudin, V. N. Staroverov, T. Keith, R. Kobayashi, J. Normand, K. Raghavachari, A. Rendell, J. C. Burant, S. S. Iyengar, J. Tomasi, M. Cossi, N. Rega, J. M. Millam, M. Klene, J. E. Knox, J. B. Cross, V. Bakken, C. Adamo, J. Jaramillo, R. Gomperts, R. E. Stratmann, O. Yazyev, A. J. Austin, R. Cammi, C. Pomelli, J. W. Ochterski, R. L. Martin, K. Morokuma, V. G. Zakrzewski, G. A. Voth, P. Salvador, J. J. Dannenberg, S. Dapprich, A. D. Daniels, O. Farkas, J. B. Foresman, J. V. Ortiz, J. Cioslowski, , and D. J. Fox. Gaussian 09, Revision B.01. Gaussian, Inc., Wallingford, CT, 2004.

[247] Jmol: an open-source Java viewer for chemical structures in 3D. http://www.jmol.org/.

[248] H. Braunschweig, T. Wagner, *Angew. Chem. Int. Ed.* **1995**, *34*, 825.